

Atomic Scale Investigations of the Thermal and Electron Induced Chemistry of Small Molecules on Pt(111) as Revealed by Scanning Tunneling Microscopy

by

Todd Charles Schwendemann

Humboldt, IA

B.S. Buena Vista University, 1996

M.A. University of South Dakota, 2005

A Dissertation presented to the Graduate Faculty
of the University of Virginia in Candidacy for the Degree of
Doctor of Philosophy

Department of Chemistry

University of Virginia

January, 2006

The image shows four handwritten signatures in black ink, each above a horizontal line. From top to bottom, the signatures are: "James M. Sikkema", "John W. Moore", "Lester Andrews", and "Fred Richard". The signatures are cursive and appear to be in ink.

Abstract

ATOMIC SCALE INVESTIGATIONS OF THE THERMAL AND ELECTRON INDUCED CHEMISTRY OF SMALL MOLECULES ON Pt(111) AS REVEALED BY SCANNING TUNNELING MICROSCOPY

by

Todd Charles Schwendemann
Doctor of Philosophy in Chemistry
University of Virginia
Professor A. I. Harrison, Advisor

Scanning tunneling microscopy (STM) was used to investigate the behavior of some catalytically and/or photochemically active small molecules interacting with a reactive transition metal surface. STM provides opportunities to gather positional and spectroscopic information about single molecules rather than having to average over an ensemble of molecules as is customary with traditional surface science techniques. Atomic scale investigation of CH₃Br, CO₂, N₂ and CH₄ adsorbed onto a Pt(111) surface were made under ultra high vacuum (UHV) conditions using a home built variable temperature scanning tunneling microscope capable of imaging over a surface temperature range from 18 K to 400 K. By cooling molecules on the surface to sufficiently low temperatures thermal diffusion could be quenched and individual molecules could be imaged by STM. It was found that the CH₃Br monolayer forms a ferroelectric (6 x 3) lattice, with Br end next to the surface and dipoles oriented along the surface normal. CH₃Br in this well-ordered monolayer occupies top and three-fold hollow adsorption sites. Infrared spectroscopy shows an exceptionally sharp (3 cm⁻¹ fwhm) and symmetric splitting of the v₂ vibrational mode that is related to the monolayer structure. CO₂ on Pt(111) formed two stable structures depending on the coverage and method of

preparation. Whereas a thermodynamically stable (3 x 3) structure containing both vertically and horizontally oriented molecules could be formed under high temperature dosing conditions and at low coverages, a stressed (5 x 3) lattice was formed after dosing multilayers at low temperature. A (2 x 2) N₂ structure was imaged on Pt(111) at 23 K. Finally, CH₄ was imaged and then photodissociated with a 193 nm ArF laser light to produce the first STM images of methyl radicals on a transition metal surface. The goal of this work has been to better define the microscopic interactions of small molecules at a catalytic surface as a prerequisite to understanding their thermal and photochemical reactivity.

To my wife,

Jennifer Paul Schwendemann

Who put up with many years of long days, and stuck with me through more than a couple
years of saying “Yes, I should be done this year”.

and to my new daughter,

Katherine Alexis Schwendemann

who is a great motivation for finishing my life as a student.

CONTENTS

List of Figures	viii
Acknowledgements	xii
1 Introduction	1
1.1 Catalyst	1
1.2 Single Crystal Metal Surfaces	2
1.3 Catalysis on Surfaces	4
1.4 STM History	6
1.5 Basic STM Operation	6
1.6 Theory of Tunneling	8
1.7 Capabilities and Limitations of STM	11
1.8 Vibration Damping	12
1.9 Design Considerations of an STM	15
Chapter 1 References	18
2 Instruments and Techniques	19
2.1 Overview	19
2.2 UHV Chamber and Conditions	22
2.3 Cooling and Temperature Control	26
2.4 Sample Holder and Manipulator	28
2.5 Crystal Mounts	33
2.6 Vibration Isolation of the STM	36
2.7 Cleaning of the Pt(111) Crystal	40
2.8 Instruments	42
2.8.1 Mass Spectroscopy	42
2.8.2 Auger Electron Spectroscopy	48
2.8.3 Low Energy Electron Diffraction	53
2.9 ArF Excimer Laser	54
2.10 Alkali and Halogen Dosers	61
Chapter 2 References	78
3 STM Operation, Design, Constructions and Tips	79
3.1 SMP-32 Program Description and Operation	79
3.2 RHK SPM-100 and Associated Electronics	97
3.3 Calibration of the Piezoelectric	119

3.3.1	X & Y Calibration	119
3.3.2	Vertical Calibration of Scan Piezoelectric	121
3.4	STM Noise	122
3.4.1	Mechanical Noise	123
3.4.2	Electrical Noise	123
3.4.3	How to Look for Noise	129
3.5	Beetle STM Construction	135
3.5.1	Etching the Piezoelectric Tubes	138
3.5.2	Beetle Type STM Assembly	146
3.5.3	Wiring a Beetle STM	158
3.6	STM Tip Creation	182
3.6.1	Introduction / Background	182
3.6.2	Tip and Tip Preparation Terminology	192
3.6.3	Coarse Etching	193
3.6.4	Fine Polishing	199
3.6.5	Judging Tip Sharpness	204
3.6.6	STM Tip Storage	206
3.6.7	DC Etching	206
3.6.8	Ambient Condition Cleaning of STM Tips	209
3.6.9	Tip Cleaning Methods within the Chamber	209
3.7	Field Emission	214
3.8	MatLab Code and Instructions	224
	Chapter 3 References	236
4	CH₃Br Structures on Pt(111): Ferroelectric Self Assembly of Dipolar and Weakly Adsorbed Molecules	237
4.1	Introduction	237
4.2	Experimental	240
4.3	Results and Discussion	242
4.3.1	Thermal Programmed Desorption	242
4.3.2	Molecular Orientation within the CH ₃ Br Monolayer	244
4.3.2a	Scanning Tunneling Microscopy	244
4.3.2b	Reflection Adsorption Infrared Spectroscopy	246
4.3.3	Structure of the (6 x 3) CH ₃ Br Monolayer	250
4.3.4	Submonolayer CH ₃ Br Structures	253
4.4	Conclusions	258
	Chapter 4 References	259
5	STM Analysis of CO₂ Adsorption on Pt(111)	260
5.1	Introduction	260
5.2	Experimental	262
5.3	Results and Discussion	263

5.3.1	RAIRS	264
5.3.2	STM Images	267
5.3.3	Low Temperature Dose	281
5.3.4	High Temperature Dose Full Coverage	285
5.4	Summary	287
	Chapter 5 References	289
6	Atomic Resolution Imaging of Methane and Methyl Radical	290
6.1	Introduction	290
6.2	Experimental	292
6.3	Result and Discussion	293
6.3.1	Methane Adsorption	293
6.3.2	Methyl Radical Formation and Imaging	299
6.4	Conclusion	305
	Chapter 6 References	306
7	Identification of Photoactive Diatomic Nitrogen Adsorbates	307
7.1	Introduction	307
7.2	Experimental	309
7.3	Results and Discussion	309
7.4	Conclusions	320
	Chapter 7 References	320
8	Future Experiments	321
	Chapter 8 References	324
Appendix		
A	Mass Spectrometer Emission Control Testing	325
B	Materials List for STM Head Construction	328
C	Short Explanation of the DC Tip Etching Box	330
D	Ion Pump Reconstruction / Operation	334
E	Bakeout Procedure	345
F	Isothermal Single Tube STM Design	353
G	SPM-32 Parameter File Settings	379

LIST OF FIGURES

Chapter 1

Figure 1	Pt(111) hexagonal lattice.....	3
Figure 2	STM Operation Schematic.....	7
Figure 3	Single Stage Vibration Dampening System.....	14
Figure 4	Vibration transfer vs. Frequency.....	15

Chapter 2

Figure 1	STM UHV Chamber Diagram.....	21
Figure 2	Image of the Manipulator.....	28
Figure 3	Image of the Manipulator Linear Translation Stage	31
Figure 4	Vibration Dampening of the Manipulator.....	32
Figure 5	Molybdenum Crystal Mount.....	33
Figure 6	New Sandwich Crystal Mount.....	34
Figure 7	Image of the Pt(111) surface.....	39
Figure 8	RGA Spectrum of the Chamber.....	43
Figure 9	Thermal Desorption Spectrum of Oxygen.....	44
Figure 10	Auger Electron Spectrometer Instrument.....	48
Figure 11	AES Ionization Diagram.....	49
Figure 12	Auger Electron States.....	50
Figure 13	AES Electron Energy Filtering.....	51
Figure 14	Differential AES of the Pt(111) crystal.....	52
Figure 15	LEED image of the Pt(111) crystal.....	53
Figure 16	Screen Capture of Laser Operation Program.....	57
Figure 17	Excimer Laser Setup.....	60
Figure 18	Early Image of the Br Covered Surface.....	61
Figure 19	Cs Doser.....	65

Chapter 3

Figure 1	IVP family of Pre-Amps.....	98
Figure 2	RHK SPM-100 Electronics.....	100
Figure 3	High Voltage Piezo Drive Board.....	102
Figure 4	Inside the SPM-100.....	104
Figure 5	Front Panel of the SPM-100.....	105
Figure 6	Rear Panel of the SPM-100.....	112
Figure 7	The PPC-100.....	117
Figure 8	Coordinate directions for the STM piezos.....	118
Figure 9	Ground Loop Problem.....	126

Figure 10	Correct Grounding (No Ground Loops).....	127
Figure 11	Grounding Diagram for the STM UHV Chamber.....	128
Figure 12	Noise Power Spectrum of the STM.....	129
Figure 13	Etching Mandrel,Rings and Flats.....	139
Figure 14	Etching Ring Guide.....	141
Figure 15	Making Quadrant Cuts in Microshield.....	143
Figure 16	Macor Tip Tube Holder.....	146
Figure 17	STM Head Design.....	148
Figure 18	Assembly Jig for Beetle STM.....	152
Figure 19	Piezo Tube Electrode Configuration.....	159
Figure 20	Piezo Movement Voltage Sequence.....	164
Figure 21	Beetle Quadrants with only Radial movement	165
Figure 22	Beetle Quadrants with X-Y axis	165
Figure 23	Approach Waveform Quadrant Guide.....	169
Figure 24	STM Head Wiring.....	173
Figure 25	Teflon Ring Wiring.....	175
Figure 26	Wiring from SPM-100 to STM.....	178
Figure 27	STM UHV Flange.....	179
Figure 28	STM Support Stalk.....	180
Figure 29	Electrical Isolation of STM Stalk from Flange.....	182
Figure 30	Theoretical Tip Structures.....	185
Figure 31	Tunneling from a Curved Tip.....	186
Figure 32	SEM Scans of at tip being milled by a FIB.....	189
Figure 33	Tip Terminology.....	192
Figure 34	STM Tip Etching Set-up.....	195
Figure 35	STM Tip Etching Beaker.....	197
Figure 36	Tip Micropolisher and Microscope.....	198
Figure 37	Judging Tip Sharpness in an Optical Microscope.....	205
Figure 38	DC Tip Etching Schematic.....	206
Figure 39	I/Z Spectra of Good and Bad Tip Crash.....	213
Figure 40	Theoretically Generated Image of MeBr on Pt(111).....	228
Figure 41	Selecting Image Coordinates.....	230
Figure 42	Overlay of a Pt(111) lattice on an Image.....	231

Chapter 4

Figure 1	TPD of Methyl Bromide Anneal an Unannealed.....	243
Figure 2	Monolayer of MeBr with Defects.....	246
Figure 3	RAIRS Spectra with Sharp symmetric modes.....	248
Figure 4	High Resolution Image of the MeBr (6 x 3) Lattice.....	251
Figure 5	Model of MeBr on Pt(111) showing (6 x 3) Lattice	252
Figure 6	(6 x 3) Lattice Showing Round and Oblong Holes.....	253
Figure 7	Sub Monolayer Coverage with a Square Lattice.....	254
Figure 8	Fractal Ordering seen in Submonolayer Coverage.....	255
Figure 9	Local Higher Coverage of MeBr in rows.....	257

Chapter 5

Figure 1	TPD Spectra of CO ₂ as a function of Dose.....	264
Figure 2	RAIRS Spectra of CO ₂ as a Function of Annealing	266
Figure 3	Islanding of Carbon Dioxide Image.....	267
Figure 4	Graph of Dosing Temperature Range.....	268
Figure 5	High Temperature Dosing Scheme.....	269
Figure 6	3 x 3 Lattice of Carbon Dioxide.....	270
Figure 7	3 x 3 Lattice with Pt(111) overlay on top.....	272
Figure 8	CO ₂ Singletons on the surface.....	273
Figure 9	Line Scan of the 3 x 3 lattice.....	274
Figure 10	IR Frequency Shift vs. Coverage.....	275
Figure 11	Multiple Lattice arrangements of CO ₂	276
Figure 12	Theoretical Image of the 3 x3 Lattice.....	277
Figure 13	Line Scans Showing Vertical CO ₂ Off Center.....	279
Figure 14	3 x 3 Lattice missing vertical molecules.....	280
Figure 15	Dose and Anneal Covered Surface.....	281
Figure 16	5 x 3 Lattice of CO ₂ with Pt(111) overlay.....	282
Figure 17	Full Coverage CO ₂ with High Temperature Dose.....	285
Figure 18	Large Scale image of Full Coverage.....	286

Chapter 6

Figure 1	TPD Spectrum of the Methane molecule.....	294
Figure 2	Multiple Images of Methane Covered Surfaces.....	295
Figure 3	Ordered ($\sqrt{3} \times \sqrt{3}$ R30) of Methane on Pt(111).....	296
Figure 4	Large Scale image of Methane Covered Surface.....	297
Figure 5	Line Scan of Methane Covered Surface.....	297
Figure 6	Theoretical ($\sqrt{3} \times \sqrt{3}$ R30) Methane Surface.....	298
Figure 7	Methane Surface with Pt(111) overlay.....	299
Figure 8	High Resolution Image of Methyl Radicals.....	300
Figure 9	Larger Methyl Radical Covered Surface.....	301
Figure 10	Theoretical Methyl Radical Surface with Overlay.....	303
Figure 11	Alignment of Methyl Radical on the Surface.....	304
Figure 12	TPD of Methyl covered Surface Post Imaging.....	305

Chapter 7

Figure 1	TPD Spectra of Nitrogen Covered Surface.....	310
Figure 2	N ₂ Stuck to Top Side of Step Edge.....	312
Figure 3	Line Scan of N2 on a Step Edge.....	313
Figure 4	2 x 2 island of Nitrogen on Lower side of the Step.....	315
Figure 5	Line Scan Across Nitrogen Island.....	316

Figure 6	Previous theoretical Nitrogen Pinwheel Structure.....	317
Figure 7	Nitrogen 2 x 2 with Pt(111) overlay.....	318
Figure 8	Theoretical image of Nitrogen 2 x 2 Lattice.....	319
Chapter 8		
Figure 1	STM Induced Dissociation of MeBr.....	322

Acknowledgements

There are many people who helped and encouraged me along the way in pursuit of my degree. I would like to thank first and foremost my wife, who continued to support me all through my graduate experience at UVA and was there for me whenever I was upset or discouraged. I would also like to thank my parents Lyle and Pat Schwendemann, who always thought an education was extremely important and encouraged me to go to college and beyond (maybe not 13 year post-high school, but still very encouraging.)

Much Thanks to all of my lab mates, whom help make grad life tolerable with the helpful discussions of chemical systems with Alex Bukoski, and trying to find solutions for fixing most of the equipment in lab with Rob Zehr and Indraneel Somanta, the laughing at some good humor with everyone in the lab and the commiserating with Rob when it seemed nothing was working right. Also, I would like to thank my Advisor Dr. Ian Harrison for always being upbeat and excited about whatever we were doing, I especially needed this when it seemed like nothing was going right and after a “short” talk with Ian I was always reenergized and ready to tackle the problem again.

A big thanks has to be said to all the guys in the machine shop, who continually made the small intricate pieces that had to be machined precisely, usually out of some unmachineable exotic material, but they always got it done. Thank you, Harvey Sugerman in the electronic lab. For without Harvey, all of the PHI equipment would have died years ago and the lab would have about two surface science instruments working at any given time. Another big thanks has to go to Willie Shoop in the Glass shop. Willie always had the neatest toys that help make the Harrison lab continue to run, like a dentist drill for putting holes in sapphire, and was always a great source of information and ideas on solving problems in the lab.

I would like to thank all of the professors at UVA that helped to answer question in my research along the way. I would especially like to thank my committee members for their help and encouragement.

The last people that I would like to thank are Dr. Charles Slagle, and Dr. Mary Berry. Dr. Slagle was always supportive and a tremendous influence on me while in my undergrad studies. We traveled the world together and he always had an interest and knowledge of a great many things in, as well as out of chemistry, and he set me down the path of studying physical chemistry. Although I spent the shortest amount of time in my academic career under the tutelage of Dr. Berry, She is one of the greatest influences in my life. She helped me understand much of physical chemistry and laid down a basis for good scientific discovery, without her I certainly wouldn’t be here today defending for a doctorate degree in chemistry. All I can say to her and all the other people here is Thank You!

Also to my friends and family who would always ask “When are you going to be done?” (You know who you are) I can now say... “I’m finally done!”

CHAPTER 1

INTRODUCTION

Definition of catalyst:

A substance that is added to a chemical reaction in small amounts that increases the rate of that reaction without itself being altered or consumed in the process.¹

Catalysis, although recently defined in scientific terms (1835 by Berzélius), has been an important process in human history for thousands of years. One of the first known human instigated catalytic processes started with the formation of soap over 2000 years ago. The process was developed by the Gallics, and later described in written form by the Romans. In the 1800's, Chevreul² showed the formation of soap to be an alkali promoted reaction where animal fat has its glycerides cleaved to release a fatty acid (soap) and glycerin. Today, because of the study of catalysis, the world is a vastly different place than if catalysis didn't exist. Examples of catalytic reactions of current importance range from the cracking of crude oil to gasoline,³ and the Haber process^{4,5} which makes ammonia out of N₂ and H₂ for the fertilizer that currently supports 2.4 billion lives beyond what the earth could otherwise sustain.⁴

The study of catalysis is split into two main types, homogenous and heterogeneous catalysis. The differences between the two types are: in heterogeneous

catalysis, the catalyst is in a different phase than the reactants (i.e., a solid catalyst added to a liquid reaction), vs. homogenous catalysis, where the catalyst and the reactants are in the same phase. In the Harrison lab, we study reactions of gases on single crystal transition metal surface that are relevant to heterogeneous catalysis.

Since, a true catalytic process can be a complex process involving many reactive steps, we attempt to achieve a fundamental understanding of catalysis by simplifying the process and try to study one reactive step, preferably the rate limiting one. To reduce the number of variables we use a single crystal metal surface cut to a specific orientation (in these studies Pt(111)) to expose a limited and known number of surface adsorption sites. Additionally, we use ultra high vacuum (UHV) chambers to ensure the gas/surface system under study remains clean and contain only the atoms/molecules that we are interested in studying.

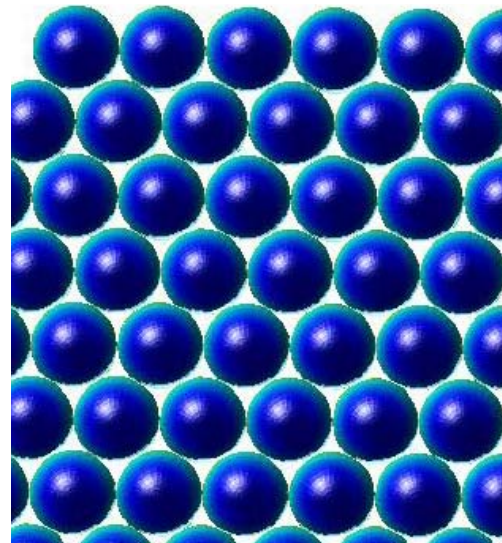
The research that is described in this dissertation utilizes a scanning tunneling microscope (STM) to give a microscopically detailed picture of CH₃Br, CO₂, and CH₄ adsorption on a Pt(111) surface. It relates their structural arrangement to the ensemble averaged knowledge of their dissociation, adsorption, and desorption behavior collected from a variety of photochemical and surface science techniques. Additionally, an initial structural study of adsorbed N₂ is described.

1.2 SINGLE CRYSTAL METAL SURFACE:

Platinum is a very important catalytic metal and its (111) face is what we have chosen to study. Platinum is a face centered cubic crystal that when cut along the Miller indices of 1,1,1 will form a hexagonally closed packed surface (Figure 1) that has a DFT

calculated inter-atom spacing of 2.81 Angstroms,⁶ and an experimentally measured spacing of 2.78 Angstroms. Small molecules on the hexagonal close packed platinum surface typically adsorb in one of four high symmetry locations depending on their interaction with the metal surface.⁷ These adsorption sites are 1) top, 2) bridge, and 3) three fold hollow sites which are further divided into face centered cubic (fcc) and hexagonally close packed (hcp) three fold hollow sites (3fh). Molecules on top sites sit directly on a platinum atom. Molecules that sit at bridge sites are in between two Pt atoms and are therefore shared by two Pt atoms. The three fold hollow site is in between three Pt atoms, but whether the molecule occupies a fcc or a hcp three fold hollow site is determined by the 2nd and 3rd layers of platinum atoms, the fcc 3fh sites have a Pt atom directly below them in the 2nd layer of platinum atoms. The hcp 3fh sites have a Pt atom directly below them in the 3rd layer of platinum atoms because of the fcc “ABC” packing. Because the distinction between these two 3fh sites beneath the fcc(111) surface is dependent on atoms farther away than other platinum atoms in the surface plane, there is typically very little distinction in molecular adsorption energies between the 3fh sites and they can typically be grouped together as a single “three fold hollow” adsorption site.

Figure 1 Theoretical structure of a hexagonally closed packed crystal face showing the 111 face of a fcc crystal.



1.3 CATALYSIS ON SURFACES:

There are many possible crystallographic faces that a crystal can present for catalysis, and each face has different characteristics for molecular adsorption/diffusion/desorption and reaction. Professor Gwathmey at the University of Virginia was among the first to demonstrate and detail the rates at which catalytic processes vary with the crystallographic plane exposed.⁸ The principles that he described from his studies are still in use today. Many companies and research groups utilize his ideas to create catalysts that present the most active face for the particular reaction of their interest. Typically, the most catalytically relevant plane for platinum is the most stable and abundant (111) face and for that reason it is the one we study.

Catalysis of the gas-surface interface is important to sustaining human life as we know it. For example, the Haber ammonia synthesis process reacts N₂ and H₂ gases over an alkali metal promoted Fe or Ru supported catalyst to produce the ammonia that is the precursor to fertilizer. This is one of many heterogeneously catalyzed reactions that sustain our way of life. One of the early reactions on a platinum surface that provided light and a means to light fires in the early 19th century is the ignition of hydrogen gas under ambient conditions when flowed over a platinum sponge. This was observed by Döbereiner in 1823, and was the basis for the Döbereiner lamp.⁹

Surface chemistry, surface physics and catalysis were intensively studied over the last century, but it was the advent of ultra high vacuum technology in the 1960's which allowed chemically clean crystal surfaces to be prepared that resembled ideal surfaces.¹⁰ That allowed for rapid scientific progress.

Following the production and relatively easy maintenance of UHV, came the development of many surface analytic techniques. These techniques include low energy electron diffraction (LEED), Auger electron spectroscopy (AES), X-ray photoelectron spectroscopy (XPS), reflection adsorption infrared spectroscopy (RAIRS), thermal program desorption (TPD), field ion microscopy (FIM), scanning electron microscopy (SEM), atomic force microscopy (AFM), and the focus of the work presented here, scanning tunneling microscopy (STM).

All of the techniques named above with the exception of FIM, AFM and STM, are techniques that produce data by averaging over macroscopic regions of the crystal. While LEED can provide sub-angstrom spatial information about atomic arrangements on surfaces, as a diffraction technique with an electron beam diameter of greater than 5 nm, it still averages over a multi nanometer area.¹¹ Hence, LEED is an indirect measurement not sensitive to single atom defects, and is unable to determine whether a particular atom/molecule is bound to a step edge or terrace site. The two instruments that are capable of examining single atom interactions with a surface are FIM and STM (discounting AFM except under extraordinary circumstances). FIM has a limited usefulness as a tool for general analysis of adsorbate dynamics due to the limited number of substrate/adsorbate systems that can withstand, and are unperturbed by, the very high electric fields needed for FIM.¹² STM is a very versatile technique that can probe the dynamics and interactions of virtually any conductive adsorbate/substrate system.

1.4 STM HISTORY:

The scanning tunneling microscope was invented by Binning and Rohrer,¹³ and in 1983 the first real space atomic resolution image of a Si(111) 7 x 7 crystal lattice was published by Binning, Rohrer, Gerber and Weibel.¹⁴ This key paper signaled the new opportunity to visualize surfaces at the atomic scale level of detail. The new STM technique was unlike any previous surface analysis instrument, because it offered the ability to study both ordered and disordered surfaces with resolution of single atoms and defects in a real space image. Binning and Rohrer were awarded the Nobel Prize for Physics in 1986, and the STM has been adapted to study all types of conductive surfaces under conditions that range from millikelvin temperatures,¹⁵ to UHV,^{16,17} high pressures,¹⁸ and under high magnetic fields.¹⁹ Interestingly, the basic design of the STM derived from Dr. Young's work at NIST on a scanning field emission microscope called the topografiner.²⁰ Binning and Rohrer's genius was to combine Dr. Young's work with some brilliant insight into the quantum mechanics of electron tunneling, to develop the topografiner into an STM that could resolve individual atoms.

1.5 BASIC STM OPERATION:

The scanning tunneling microscope utilizes an atomically sharp tip that is rastered across a flat conductive surface. A biasing voltage potential applied between the tip and sample induces a current to flow (Figure 2). The current flow is measured as a function of the X-Y location and bias voltage. The STM can operate in one of two modes: a constant height mode or a constant current mode. The constant height mode is typically used only under conditions where the surface is very flat (i.e., no step edges or protrusion of large

adsorbates) or when very high scan speeds are required. In constant height mode, the voltages applied to the scan piezo are kept constant and the fluctuation of current as a function of tip position is recorded to generate an image. In the constant current mode, the tunneling current is measured and a feedback circuit adjusts the voltage applied to the Z-scan piezo to move the tip in or out from the surface in order to maintain a set current. The voltage applied to the Z-scan piezo that is required to keep the current constant during x-y rastering is recorded to produce an image of the surface. Because the tip height is adjusted during operation in the constant current mode

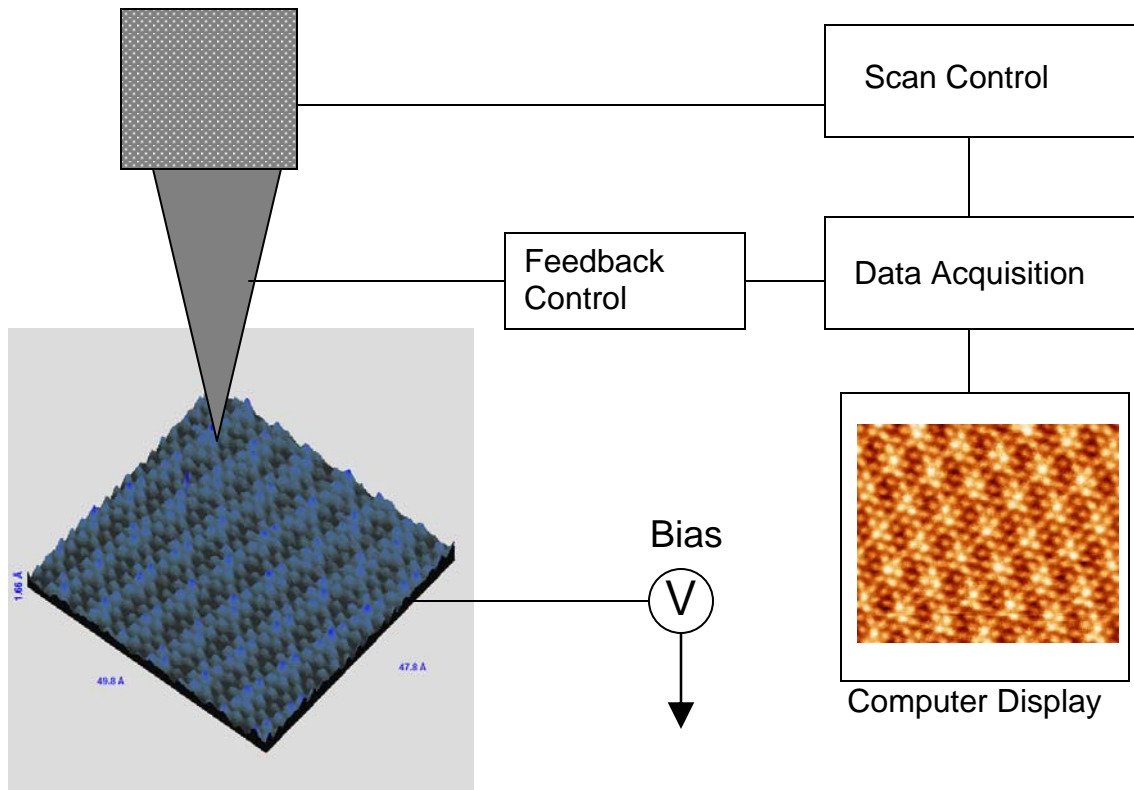


Figure 2 Schematic diagram of STM operation and components.

mode, the scan speeds are not as fast as those possible in the constant height mode. However, there is much less chance of crashing the tip into something on the surface because the tip will be moved away from a large protrusion. In constant current mode

scanning, the tip might run right into the surface protrusion. This makes the constant current mode the most widely used method of operation unless very high scan speeds are required (e.g., to follow molecular diffusion or to eliminate low frequency noise).

Our Besocke²¹ (beetle) STM operated with RHK electronics holds the tunneling tip at a virtual ground and applies a voltage bias to the Pt(111) crystal. The beetle STM consists of a scan tube that houses the tunneling tip and three outer piezo tubes used for coarse approach to move the tip into tunneling range (e.g. Z = 10 Å, I = 100 pA, V_B = 100 mV crystal bias). The scan piezo is divided into four outer quadrants which are assigned as +/- X and +/- Y. In addition, a reference ground is applied to the interior of the scan piezo, which means that the Z-scan adjust of the scan piezo is applied symmetrically to both its X and Y quadrants.

1.6 THEORY OF TUNNELING:

The most common mode of STM measurement is called “topography”, where people assign voltage changes made to maintain a constant tunneling current as height changes on the surface. However, in the context of STM the exact height of a tip above a surface is somewhat unclear. A general treatment of electron tunneling through a vacuum shows that the potential in the vacuum region acts as a barrier to electron flow (i.e., the gap between surface and tip). In the limit of a 1-D weak electron transmission, the solution to the Schrodinger equation for the wave function after electron transmission across a rectangular barrier is

$$\Psi = e^{-\kappa z} \quad (1.1)$$

where κ is a function of the energy of the state E and potential barrier height V_B inside the vacuum.

$$\kappa = \sqrt{\frac{2m(V_B - E)}{\hbar^2}} \quad (1.2)$$

In the simplest case, κ is just an adjusted work function of the surface and the tunneling current decays exponentially with the tip to surface distance, z .

$$I \propto e^{-2\kappa z} \quad (1.3)$$

In this very simplified approximation, if the local work function across the crystal is constant, then the image observed is only a function of z . If the average (presumed locally constant here) work function for the metal surface is ≈ 4.5 V then the value of 2κ would be $\approx 2 \text{ \AA}^{-1}$, giving nearly an order of magnitude change in tunneling current for a 1 \AA change in tip to surface separation.

The above explanation shows that the topographical images are mostly a function of the tip height and that because of the exponential dependence of the tunneling current on tip to sample distance, the tip can resolve very small changes in the height of the surface, and also that the tip must be held very close to the surface, typically a nanometer or less.

More rigorous explanations of how the tunneling current depends on the tip height and barrier conditions has been described by Bardeen,²² Tersof-Hammon²³ and Lang.²⁴ In these tunneling models, the tip and sample are treated as two separate entities with their local density of states slightly overlapping in space. Time dependent perturbation theory is then used to calculate the rate of electron transfer between the tip and sample

systems. Assuming that the tunneling process is an elastic (energy conserving) tunneling process the current depends on the density of states of each system:

$$I = I_{\text{sample} \rightarrow \text{tip}} - I_{\text{tip} \rightarrow \text{sample}} \quad (1.4)$$

$$I = \frac{4\pi e}{\hbar} \int_{-\infty}^{\infty} |M|^2 \rho_s(E_s) \rho_t(E_t) \{ f(E_s)[1-f(E_t)] - f(E_t)[1-f(E_s)] \} d\varepsilon \quad (1.5)$$

Where e is the charge on an electron, \hbar is Planks constant, and $|M|$ is the matrix element for tunneling. ρ is the density of states of the sample s or tip t , and f is the Fermi function,

$$f(E) = \left\{ 1 + e^{\left[\frac{E-E_F}{k_B T} \right]} \right\}^{-1} \quad (1.6)$$

where E_F is the Fermi energy, k_B is Boltzmann's constant and T is the temperature. Therefore, the probability of current flow depends on the electron leaving a filled state on either the sample or tip and entering an empty state on the opposing surface.

When energy is conserved in the tunneling process E_s and E_t have to describe states of equal energy. But when a bias voltage is applied to the system the energies of the sample have to be described relative to the Fermi level defined with a 0 bias voltage connection. Therefore with a bias voltage V the energies become $E_s=\varepsilon-eV$ and $E_t=\varepsilon$, which makes the tunneling current

$$I(V, z) = \frac{4\pi e}{\hbar} \int_{-\infty}^{\infty} |M(z)|^2 \rho_s(\varepsilon - eV) \rho_t(\varepsilon) [f(\varepsilon - eV) - f(\varepsilon)] d\varepsilon \quad (1.7)$$

1.7 CAPABILITIES AND LIMITATIONS OF STM:

The STM is uniquely qualified to probe surfaces on the atomic scale because of its very high resolution abilities. Beyond atomic spatial resolution, STM can be an extremely versatile spectroscopic tool. STMs have been used to study spectroscopic detail of metals,^{25,26} semiconductor,²⁷ superconductors²⁸ and even thin non-conducting oxides on a conductive substrate.²⁹ A surprising feature of STM is that it does not require vacuum conditions. Because of the very close proximity of tunneling tip and surface, electrons are not scattered by the intervening air, or even liquid. Therefore STM can be used in UHV conditions,³⁰ atmospheric pressures and higher,³¹ or even in liquid environments.³² The STM can also be used over a wide temperature range, from a few miliKelvin¹⁵ to a thousand degrees Kelvin.³³ It also operates under high magnetic fields.¹⁹

The number of different conditions that the STM can be used under is amazing. However, no one STM design will work for all situations. Specialized STMs are required for different environmental conditions and kinds of experiments. Some interesting feats accomplished by STM include the assembly of atomic scale structures,³⁴ single molecule vibrational spectroscopy,³⁵ energy filtering of the surface,³⁶ and probing of local work function measurements.³⁷

However, because images collected by STM are a combination of the electronic local density of states and the topology of the surface, a straight forward interpretation of the collected STM images is difficult. Perhaps, the biggest deficiency of the STM technique is its inability to chemically identify atoms or molecules. Therefore, to compliment the use of an STM many other techniques are useful to determine the initial

and final chemical conditions of the surface. Such techniques include: AES, RAIRS, XPS and TPD. Even though the STM was not designed for chemical identification of adsorbate molecules, a few groups are developing new spectroscopic techniques to identify adsorbed atoms or molecules. Dr. Moller at the University of Essen developed a method known as thermovoltage spectroscopy that can generate limited chemical information of the adsorbates.³⁸ Currently the most interesting method of chemical identification by STM was developed by Dr. Wilson Ho who uses inelastic tunneling of the electrons from the STM to stimulate a vibrational loss or gain in the molecule between the tip and sample.³⁵ In doing so, the vibrational characteristics of the molecule can be monitored with sub-angstrom spatial resolution.

1.8 VIBRATION DAMPENING EQUATIONS AND STAGES:

Elimination and reduction of vibrations that couple into the STM tip to surface junction is key to the production of high resolution images. Measurement of low corrugation surfaces, such as the Pt(111) lattice with a 0.02 Å corrugation, need very high vibrational stability. Therefore the aim of vibration reduction is to keep the tip to surface distance stable to a length of 0.01Å, or better, over the duration of an STM image acquisition (e.g., 1 min.)

Many stages of vibration isolation are used in the current generation of STMs. A combination of large mass and low resonance frequency of our UHV system coupled with a small mass and high resonance frequency of the STM provides adequate vibrational isolation to achieve atomic resolution of the Pt(111) lattice.

A true theoretical analysis of the vibrations of the STM system would require six degrees of freedom to describe the complete relative motions for each component. In practice this becomes very difficult, and so it is assumed that the vibrations in the floor are motions in the vertical direction only and the system is composed of just a few rigid components.

The equation of motion of a mass coupled to the floor is

$$m\ddot{x} + b(\dot{x} - \dot{x}') + k(x - x') = 0 \quad (1.8)$$

where x is the vertical position and b is the dampening factor, k is the spring constant and x' is the equilibrium vertical displacement. The resonance frequency and dampening are

$$\omega_0 = \sqrt{\frac{k}{m}} \quad (1.9)$$

$$\gamma = \frac{b}{2m} \quad (1.10)$$

Substituting Eqs. (1.9) and (1.10) into Eqs. (1.8) yields

$$\ddot{x} + 2\gamma(\dot{x} - \dot{x}') + \omega_0^2(x - x') = 0 \quad (1.11)$$

Assuming sinusoidal vibrations, Park and Barret³⁹ show that the Laplace transform of equation (1.11) is

$$|T_1(\omega)| = \left| \frac{x_0 - x'_0}{x'_0} \right| = \left| \frac{\omega^2}{\omega_0^2 - \omega^2 + 2i\gamma\omega} \right| \quad (1.12)$$

Which is the transfer function describing the response of the tunneling gap to external vibration. The analysis of the transfer function shows that for a high resonant frequency system of 5 kHz, the response of the tunneling gap decreases 100 times for a 10 times

reduction in driving vibration frequency. So, for low frequency vibrations at 5 Hz the gap response is 10^{-6} less. If a typical floor vibration of 1000 \AA occurs, its affect on the tunneling gap would be on the order of $.01 \text{ \AA}$ (see Figure 4).

The above analysis is appropriate for the single stage dampening system shown schematically in Figure 3. A real STM employs many different stages of dampening that would start to include more spring and motion components in the initial equation of motion and has been described well by Okano.⁴⁰

Figure 3 A diagram of a single stage vibration dampening system.

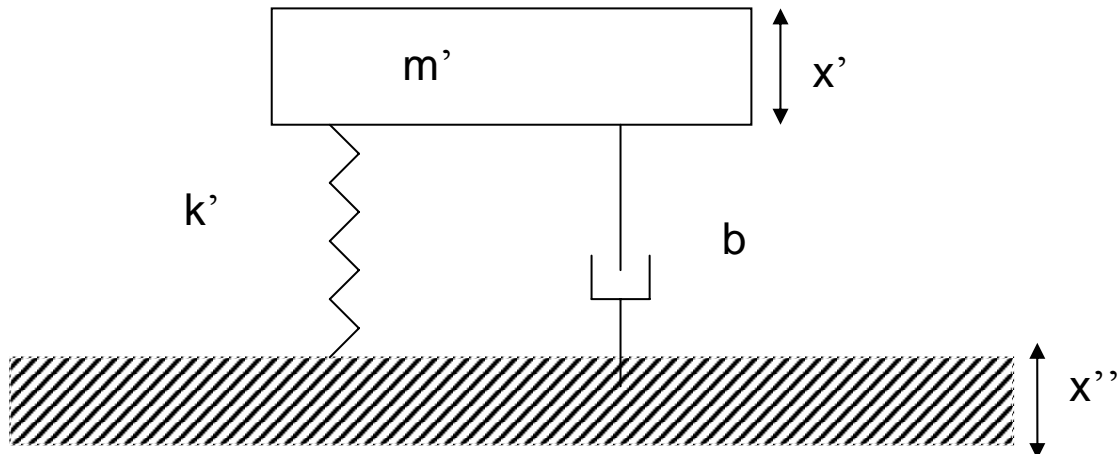
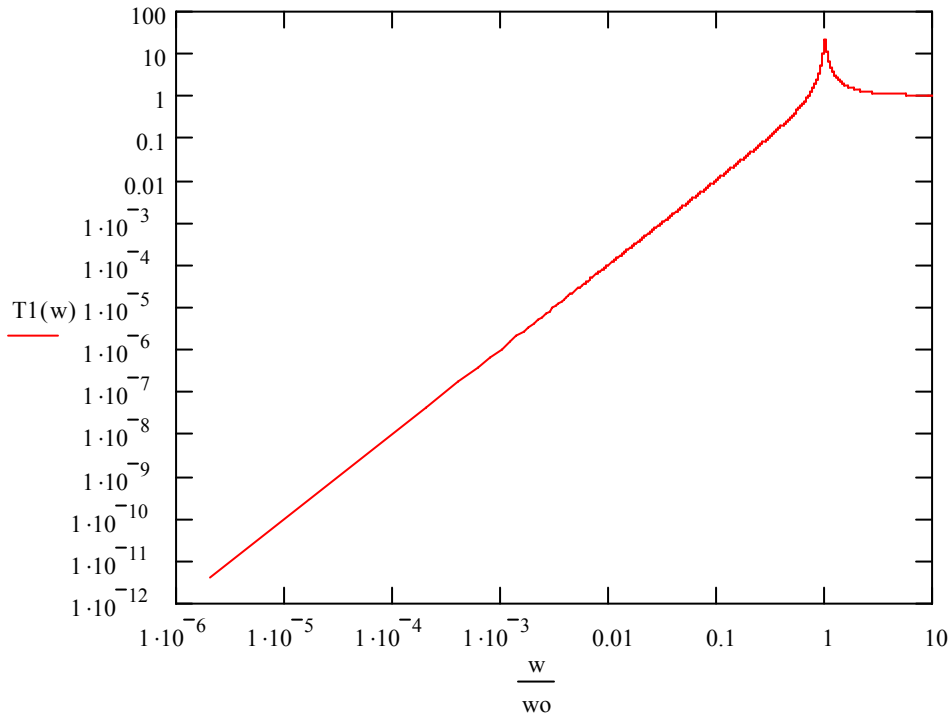


Figure 4 A representation of the frequency response of a single stage dampening with a resonant frequency of 5 kHz and a dampening of $\gamma = 0.025\omega_0$



1.9 DESIGN CONSIDERATIONS FOR AN STM:

As described above, an STM can be used in a variety of ways, but to make the most out of the STM technique one must consider what experiments are going to be performed using your STM. A few things to consider is size of the system, whether thermal drift is a problem, the need or desire to move macroscopic distances across the sample, whether the STM has to be retracted and approached to the same location on the sample, the ability to exchange tips, and, of course, the most important noise factor is your systems vibrational resonant frequency. While a detailed explanation of all the different STMs developed is well beyond the scope of this dissertation the advantages and disadvantages of a few systems will be described here.

Our Besocke²¹ STM was chosen for its ease of approach, good thermal stability, high resonant frequencies, and its ability to macroscopically move across the crystal. Some of the advantages that are associated with the Besocke style can also be disadvantages, such as: the small size of the scanner to keep a high resonance frequency limits the size of the sample, and the macroscopic movement across the sample. Also the coarse approach is very small (≈ 0.001 of an inch) requiring a fine adjustment to the tip position within the STM, making tip exchange very difficult. The thermal stability of the STM is based on the symmetric construction of the head, so all thermal expansion or contraction for the head is supposed to be uniform. However, a perfectly symmetric head is difficult to build and a little asymmetry can cause large drift. Additionally, because the coarse Z- approach is a free rotation down a ramp, which has a variable starting point, bring the STM to a microscopically repeatable location on the crystal is impossible. Sometimes it is desirable to image the surface, retract, laser irradiate or employ another technique, re-approach and image the difference. Our beetle STM has little to no chance of finding the same (μm^2) area on the crystal to examine differences in this manner.

A second generation STM that has been built in the Harrison lab is an isothermal single tube design based on Mugele's⁴¹ design. This system allows a very high resonance frequency of the STM and mount, and low thermal drift due to its symmetric construction and quick thermal equilibrium. The isothermal system also has built in tip exchange and the ability to use larger samples than for the beetle design. The isothermal system should excel at scanning tunneling spectroscopy, because the tip should be radiatively cooled and therefore very stable. However, there are disadvantages to Mugele's isothermal

system, such as: limited scan range due to low temperature piezos, no macroscopic motion across the crystal, and a much more difficult approach mechanism.

The last design that will be mentioned here is one that was developed by Pan at Berkeley.⁴² This is an increasingly popular design that allows for good thermal stability, high resonance frequency, and the ability to retract from the sample a distance of 15 mm and then re-approach to the sample within 200 Å of the previous position.

The explanations of advantages and disadvantages described here are somewhat biased based on my extensive experience with the beetle STM, limited experience with the isothermal STM, and only reading about the Pan design. Therefore, before a true conclusion is drawn about any STM design it is advisable to read the literature available and contact people directly operating the various systems.

- ¹ Webster's Dictionary
- ² E. Chevreul, Ann Chim 94, (1815) 80-107
- ³ US Patent No. 2,451,804
- ⁴ "Enriching the Earth", Vaclav Smil 2001 MIT Press, Cambridge
- ⁵ "Chemical Kinetics and Dynamics" J. Steinfeld, J Francisco, W. Hase, 2ed 1999, New York
- ⁶ DFT calculations done in house with the Newrock lab computers.
- ⁷ "Introduction to Surface Chemistry and Catalysis" G. Somorjai, 1994 New York
- ⁸ H. Leidheiser, Jr. and A.T. Gwathmey, J. Am. Chem. Soc. 70, (1948) 1206
- ⁹ R. Hoffman, American Scientist 86(4) (1998) 326
- ¹⁰ R. G. Musket, W. McLean, C.A. Colmenares, D. M. Makoweicki, W. J. Siekhaus, Appl. Surf. Sci. 10 (1982) 143.
- ¹¹ "Low Energy Electrons and Surface Chemistry" G. Ertl, J. Kuppers, 1985 Weinheim
- ¹² "Concepts in Surface Physics" 2nd ed. M. C. Desjonquieres, D. Spanjaard, 1998 New York
- ¹³ G. Binning, H. Roher, C. Gerber, Weibel, Appl. Phys. Lett. 40 (1982) 178.
- ¹⁴ G. Binning, H. Roher, C. Gerber, Weibel, Phys. Rev. Lett. 50 (1983) 120.
- ¹⁵ T. Hanaguri, C. Lupien, Y. Kohsaka, D-H. Lee, M. Azuma, M. Takano, H. Takagi and J. C. Davis, 430 Nature 1001-1005
- ¹⁶ T. Mitsui, M. K. Rose, E. Fomin, D.F. Ogletree, M, Salmeron, 422 Nature (2003) 705
- ¹⁷ J. A. Stroscio, and R. J. Celotta, 306 Science (2004) 242-247
- ¹⁸ M. Hendriksen, H. Zeiflemaker, H. G. Ficke, J. W. M. Frenken, Rev. Sci. Instrum. 69 (1998) 3879
- ¹⁹ H. Okamoto, D. M. Chen, T. Yamada, Phys. Rev. Lett. 89 (2002) 256101
- ²⁰ R. Young, J. Ward, F. Scire, Rev. Sci. Instrum. 43, (1972) 999
- ²¹ K. Besocke, Surf. Sci. 181 (1987) 145
- ²² J. Bardeen, Phys. Rev. Lett. 6 (1960) 57-59.
- ²³ J. Tersoff, D. R. Hamann, Phys. Rev. B 31 (1985) 805
- ²⁴ N. D. Lang, Phys. Rev. Lett. 56 (1986) 1164.
- ²⁵ C. Nagl, O. Haller, E. Platzgummer, M. Schmid, P. Varga, Surf. Sci. 321 (1994) 237-248
- ²⁶ L. Gracia, M. Calatayud, J. Andres, C. Minot, M. Salmeron, Phys. Rev. B 71 (2005) 033407
- ²⁷ J. A. Kubby, J.J. Boland, Surf. Sci. Rep. 26 (1996) 61-204
- ²⁸ C. E. Sosolik, J. A. Stroscio, M. D. Stiles, E. W. Hudson, S. R. Blankenship, A. P. Fein, R. J. Celotta, Phys. Rev. B 68(14) (2003) 140503
- ²⁹ R. Garcia, J.J. Saenz, N. Garcia, Phys. Rev. B 33 (1986) 4439
- ³⁰ C. Sachs, M Hildebrand, S. Volkening, J. Wintterlin, G. Ertl, J. Chem. Phys. 116 (2002) 5759-5773
- ³¹ M. Robler, P. Geng, J. Winnertterlin, Rev. Sci. Instrum. 76 (2005) 023705
- ³² K. Itaya, Nanotechnology 3 (1992) 185-187
- ³³ L. Masson, D. Albertini, F. Thibaudau F. Salvau, Surf. Rev. and Lett. 5(1) (1998) 55-61
- ³⁴ D. M. Eigler, E. K. Schweizer, Nature 344 (1990), 524-526
- ³⁵ B.C. Stipe, M. A. Rezaei, W. Ho, Science 280 (1998) 1732-1735
- ³⁶ P. Sutter, P. Zahl, E. Sutter, J. E. Bernard, Phys. Rev. Lett. 90, (2003) 166101
- ³⁷ Y. Hasegawa, J. F. Jia, K Inoue, A Sakai, T. Sakurai, Surf. Sci. 386, (1997), 328-334
- ³⁸ D. Hoffmann, J. Seifritz, B. Weyers, R. Moeller, J. Elec. Spect and Rel. Phen. 109 (2000) 117
- ³⁹ Park and Barret Methods of Experimental Physics Vol 27 (Scanning Tunneling Microscopy), Editor J. A. Stroscio, 1993, San Diego
- ⁴⁰ M. Okona, K. Kajimura, S.Wakiyama, F. Sakai, W. Mizutani, M. Ono, J. Vac. Sci. Technol. A 5 (1987) 3313
- ⁴¹ F. Mugele, Ch. Kloos, P. Leiderer, Rev. Sci Instrum. 67 (1996) 2557
- ⁴² S. H. Pan, E. W. Hudson, J. C. Davis, Rev. Sci. Instrum. 70 (1999) 1459

CHAPTER 2

INSTRUMENTS AND TECHNIQUES

2.1 OVERVIEW:

The STM UHV chamber has been created to investigate thermal, electron, and photon driven chemistry of small molecules.¹ While all of the molecules reported in this dissertation have been studied in the Harrison lab before,^{2,3,4,5} probing of the local chemistry by STM is a new addition to the repertoire of analysis techniques used and is starting to drive the lab in new and unexpected directions. Previous analysis of the induced chemistry of molecules on the surface has always averaged over all molecules. The STM can complement macroscopically averaged techniques very well by examining the molecules that are left on the surface after heating or laser irradiation to answer such questions as: is there a particular arrangement of molecules or fragments left on the surface after a photoreaction, or what was the initial arrangement of molecules on the surface prior to the photoreaction, or more importantly is there evidence of site-specific chemistry where molecules have reacted differently, say along the step edges vs. the terrace. The latter question has yet to be answered, but with the STM and chamber working well, these questions are possible to study in earnest. To accomplish these STM experiments there are a number of items that need to be understood and used, such as the STM, UHV chamber, laser, and other surface analysis techniques.

The primary instrument that is used in the chamber for probing the chemistry of small molecules is the STM. The current generation of STM is a Besoke style where the head is made of copper and the base has sapphire balls. This latest generation of STM has been designed to be as symmetric in construction as possible to eliminate the effects of thermal drift. Because the temperature of the crystal can be varied, STM images can be taken at any temperature in the range of 18 K to \approx 373 K (limited by epoxy and silver solder), but sample temperature instabilities can result in large image drift due to non-uniform expansion/contraction of materials. Details on construction, operation, and analysis of the beetle STM can be found in Chapter 3 and similar details about a single tube isothermal STM can be found in Appendix F.

To explore adsorbate photochemistry, an ArF laser is coupled to the chamber to induce photoinduced dissociative electron attachment (DEA) or adsorbate photochemical reactions. Photochemical deposition from adsorbed methane allowed these radical species to be studied by STM. Photofragmentation of adsorbed methyl bromide was used to generate bromine atoms and methyl radicals in the past using a Lambda Physik ArF excimer laser.² The latest sets of experiments utilizing a laser were performed with the new GAM Laser Inc. excimer laser. The GAM laser is easy to use and by varying the excimer gas, can lase at different wavelengths. The laser can be run as a F₂ excimer producing 157 nm light, ArF – 193 nm, KrF - 248, XeCl - 308, or XeF - 351 laser light. To reduce the time of irradiation, the GAM laser can be run at rates up to 125 Hz compared to the 20 Hz repetition rate of the Lambda Physik laser. The increase in repetition rate allows for shorter irradiation times and longer STM imaging sessions. To

to avoid damage to the crystal from laser heating and ablation the laser intensity was limited

to $< 5 \text{ mJ/cm}^2/\text{pulse}$.

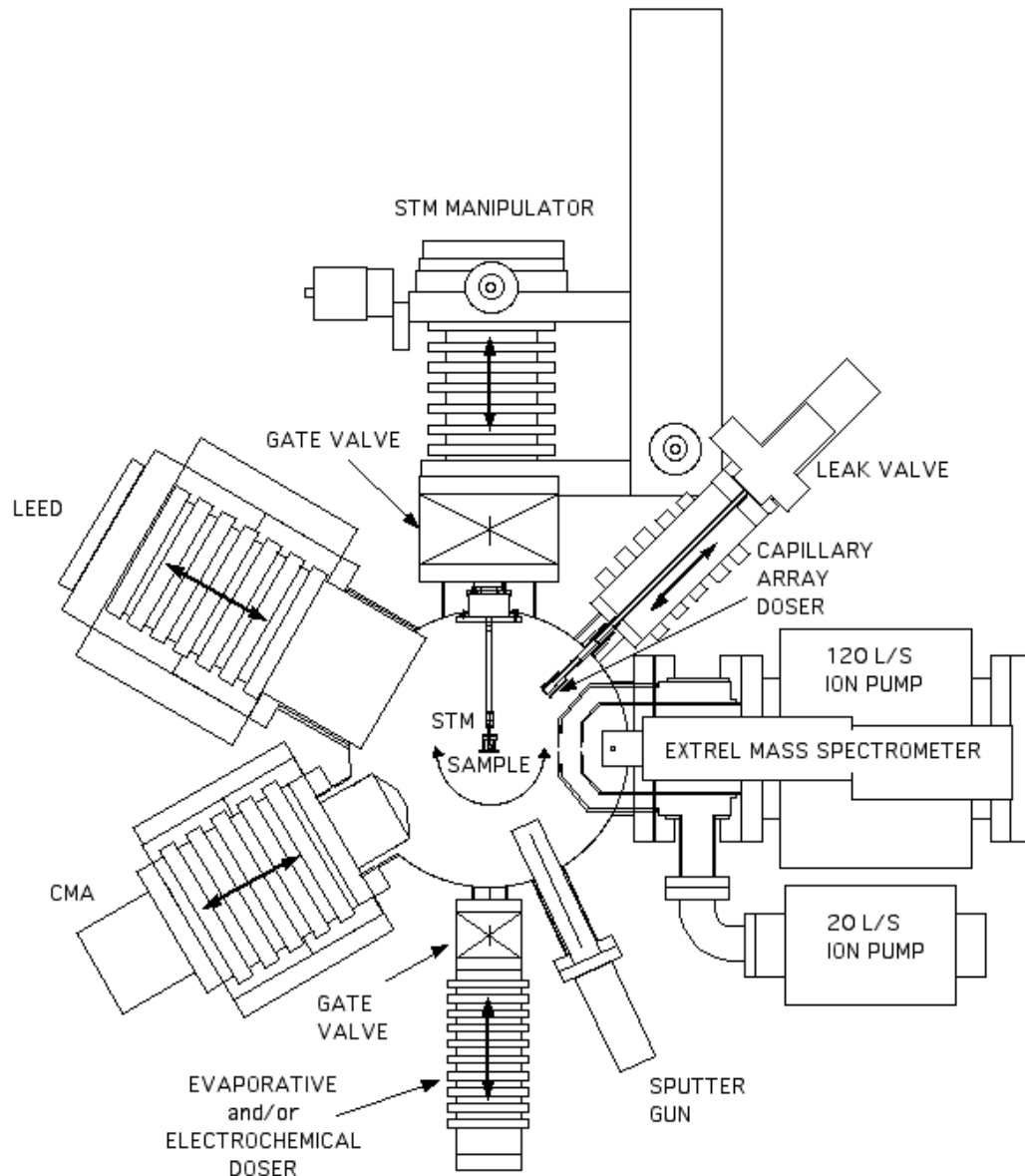


Figure 1 Diagram of the instrumentation available in the STM UHV chamber that are all aligned in one plane so the crystal can be rotated to any position.

The ultra high vacuum chamber housing the STM and various other surface analysis techniques was designed by Ray Yuro⁶ and Dr. Hongwei Xu. The chamber was

designed to be a unique and versatile chamber that allows complete temperature control over the crystal throughout an experiment, proceeding from crystal cleaning, gas dosing or other surface preparation, STM imaging and experimenting, then finally post analysis of adsorbed molecules by thermal programmed desorption. To accomplish this, the crystal was mounted in a manipulator that has 3 degrees of freedom (X,Y and ϕ) allowing 360° rotation of the crystal around a plane in which all the surface analysis instruments are oriented (Figure 1). Minor adjustments of the X and Y crystal position within the instrument plane can be done by micrometers attached to the manipulator. The chamber typically includes instruments to perform: scanning tunneling microscopy, Auger electron spectroscopy, and a differentially pumped mass spectrometer to perform thermal programmed desorption and residual gas analysis. Other instruments that are available but not currently attached to the chamber are: low energy electron diffraction, reflection adsorption infrared spectroscopy, and work function measurements with a Kelvin probe. Molecules can be dosed from a point source gas doser, or an additional load lock port in the instrument plane that can be used to insert a molecular bromine doser or an atomic Cs source. Before any surface analysis or adsorbate dosing is done, the crystal is cleaned with repeated cycles of Ar^+ ion sputtering and O_2 TPD's or high temperature oxidation.

2.2 UHV CONDITIONS AND CHAMBER:

To ensure that the platinum sample crystal is kept as clean as possible all experiments are preformed in an ultra high vacuum chamber. The typical operating pressures in the chamber are 6×10^{-11} torr when the crystal is at room temperature and 4×10^{-11} torr when the crystal is cooled. The rationale behind using ultrahigh vacuum

conditions is if the available number of molecules within the vacuum system is small enough, the surface will not adsorb a significant number of molecules over the time period of an experiment. (A single STM imaging session typically runs for three to six hours). The sticking coefficient is defined through the expression for adsorbate coverage Θ ,

$$\frac{d\theta}{dt} = Sf - k_d\theta$$

where k_d is the thermal desorption rate and,

$$f = \frac{\rho}{4} \langle v \rangle = \frac{P}{\sqrt{2\pi m k_b T_g}}$$

is the flux from an ambient gas at temperature T_g . The sticking coefficient can vary from 0 to 1, where the limit of 1 means all impinging molecules adsorb.⁷ At low temperatures, $k_d \rightarrow 0$ for most species and the total coverage of unwanted species (contaminates) on the surface will depend on their sticking coefficient, mass, pressure and time. A worst case scenario is that a surface will have a contamination of 1 ML after a gas exposure of 1 Langmuir ($1 \text{ L} \equiv 10^{-6} \text{ Torr}\cdot\text{s}$). Every decrease by a factor of 10 in pressure will increase the amount of time by a factor of 10 it takes for the surface to become contaminated by a monolayer of material. (Hence the drive for UHV conditions).

The pressure in the UHV chamber is maintained by a system of pumps. Initially the chamber is pumped down by the manifold Balzer TPU-062 turbomolecular pump which is backed by a Fisher Scientific D8A mechanical pump. Once the turbomolecular pump has achieved a pressure of less than 1×10^{-6} torr, the Physical Electronics D-I ion pumps in the chamber are turned on and the chamber is valved off to isolate the manifold

turbomolecular pump. There are 3 ion pumps located in the UHV chamber. Two of the ion pumps are used to differentially pump the mass spectrometer. The mass spectrometer runs through the center of the 120 l/s ion pump and the 25 l/s ion pump is used for the first differential pumping stage. The third ion pump has a speed of 640 l/s and pumps the main chamber. In addition to the ion pumps there is a Physical Electronics titanium sublimation pump (TSP) that is particularly effective for H₂ and helps bring the chamber pressure down into the 10⁻¹¹ Torr range. There is also some cryopumping by the cold crystal and ultrastat surfaces which is unintentional and occasionally unwanted. Previously, a 220 l/s ion pump was used with a Non-Evaporable Getter pump (NEG). However, it was discovered after pumping problems increased the chamber pressure to 3 x 10⁻¹⁰ Torr, that the NEG is made of an alloy material that is poisoned by halides, and that the product of the alloy and halide forms an outgassy compound.⁸ Pumping experiments were preformed to determine the effective pumping speed of the NEG after contamination, and it was determined that the originally 770 l/s pumping speed of the NEG was reduced to 1 - 2 l/s. The NEG and 220 l/s ion pump were replaced with a 640 l/s ion pump and TSP combination that yields 10-11 Torr range pressures.

With the addition of the large volume 640 l/s ion pump and a VAT pump isolation valve, there have been some venting problems with the chamber. Normally when venting the chamber for maintenance all of the ion pumps, ion gauges and hot filaments are turned off and the chamber opened to the manifold turbomolecular pump which then is then turned off and slowly spins down. Once the turbomolecular pump has spun down to 50 – 60% of its normal speed of 60,000 RPM, a solenoid valve is opened that lets zero grade nitrogen into the middle of the stack of turbo pump blades which: a) slows the

turbo pump and b) fills the UHV chamber with clean nitrogen so there is no possible contamination of oil or hydrocarbons into the chamber from the pumps or atmosphere. While moving the UHV chamber from the photochemistry lab to the current STM lab, the chamber was completely vented (normally the VAT gate valve that isolates the 640 l/s ion pump is closed so the entire chamber is not vented during chamber maintenance). Somehow by venting the entire chamber there was some backstreaming of mechanical pump oil which caused many months of cleaning and high temperature baking to get the chamber back to proper UHV conditions. (Cleaning the hydrocarbons from the chamber was done by flowing nitric oxide into the chamber with a pressure above the turbomolecular pump of 1×10^{-3} Torr and baking for half a day at 400 K. After which continued baking at 400 K with no gas flowing for one week cleaned everything back to UHV). To eliminate the possibility of mechanical pump oil backstreaming into the chamber, a UHV compatible valve was attached to the back side of the mass spectrometer which should be connected to a zero grade nitrogen source to vent the chamber, should ever the need arise to vent the entire chamber.

To insure that the chamber will reach the desired UHV pressures it should be leak checked and baked. Leak checking of the chamber was done with the mass chamber spectrometer set to look for helium. Helium gas was sprayed around those conflat flanges that were recently changed or were suspected to leak. Leak checking of the gas manifold and other high vacuum components can be done with the Balzer He leak detection instrument. If any leaks are detected in the chamber or manifold tighten or replace the connections to make them leak tight. Once the UHV chamber has been pumped down and is leak tight, it is necessary to bake the system out to obtain UHV. Baking a UHV

chamber is done to quickly remove the outgassy molecules adsorbed on the surfaces of the chamber. The main contaminant that is removed in baking is water adsorbed on the walls of the chamber. The removal of these outgassy adsorbates is exponential in temperature and linear in time. So, if one wanted to wait years for the chamber pressure to reduce from 1×10^{-8} Torr to 1×10^{-10} Torr, it's possible, however baking the chamber at a temperature of 400 K will achieve the same results within a few days. More details on baking the system using a bakeout box can be found in the bakeout document of Appendix E.

2.3 COOLING AND TEMPERATURE CONTROL:

To keep precise temperature control over the crystal conditions, the sample crystal is cooled from an Oxford Ultrastat and the back of the crystal is heated by e^- bombardment from a tungsten filament. The Ultrastat is used in conjunction with a transfer arm that flows either liquid nitrogen or liquid helium. The liquid boils at the end of the ultrastat tip where a copper braid is attached between the crystal and ultrastat. The cryo-liquid absorbs heat from the copper braid relayed from the sample crystal which allows us to cool the platinum crystal to a low temperature of 18 K. The crystal can be heated to a temperature of 1250 K by e^- bombardment.

The temperature of the crystal is monitored by a Eurotherm 900 EPC temperature controller by measuring the voltage across the 0.005" dia. K type thermocouple wires spot-welded to the side of the Pt(111) crystal. To calibrate the temperature of the crystal, the heat of sublimation of molecular multilayers desorbed from the surface are measured as described by Menzel⁹ (step by step instructions for low temperature Eurotherm 900

EPC calibration can be found in Dr. Zehr's dissertation.)¹⁰ Additional temperature monitoring of the Ultrastat is incorporated into the Oxford Ultrastat ITC4 controller. The Ultrastat contains a Rh-Ir resistance thermocouple that measures the temperature of the ultrastat cold finger down to 4.2K.

There are three methods that can heat the crystal. The first and main method of temperature control is using the Eurotherm to control a Kepco ATE 15-6M DC power supply to vary the voltages and currents applied to the heating filament behind the crystal. Radiative and/or e- bombardment heating can be employed depending on how the biasing power supplies are configured. To help the Kepco heat the crystal, two 915-0.5N Bertan 100 W DC power supplies are used. One Bertan supply floats the Kepco and filament at -500 V to push the electrons away from the filament, and a second supply is typically run at + 300 V (limited by the Eurotherm's maximum D.C. bias voltage) and sinks a maximum of 0.200 Amps of current pulled to the crystal and mount from the filament. When the two biasing supplies are used, the crystal is heated via an e-bombardment process. However, if the biasing supplies are turned off, the crystal and mount are heated almost exclusively by a radiative heating process. The crystal/mount can only just keep up with a 10 K/s ramp rate in the TPD spectra when both biasing supplies are used. If radiative heating is used exclusively to heat the crystal, there is no chance of the crystal reaching 1000 K (typical end point for TPD spectra). The other two methods used to heat the crystal are to use the Oxford Ultrastat controller to apply power to a nichrome wire wrapped around the coldfinger, or secondly, to adjust the flow of cryo liquid being supplied to the Ultrastat. These last two methods can release a large amount of adsorbed gas from the Ultrastat which can increase the chamber pressure by an order

of magnitude or more for a short duration. They are used only for heating the crystal during STM experiments where a temperature range of 18 K – 373 K (limited by STM materials) is attainable using the Ultrastat temperature control.

2.4 SAMPLE HOLDER AND MANIPULATOR:

The main focus of the UHV STM chamber is the transition metal single crystal sample where surface adsorbates and reactions are studied. An elaborate scheme for holding, rotating, and isolating the crystal both electrically and thermally from the

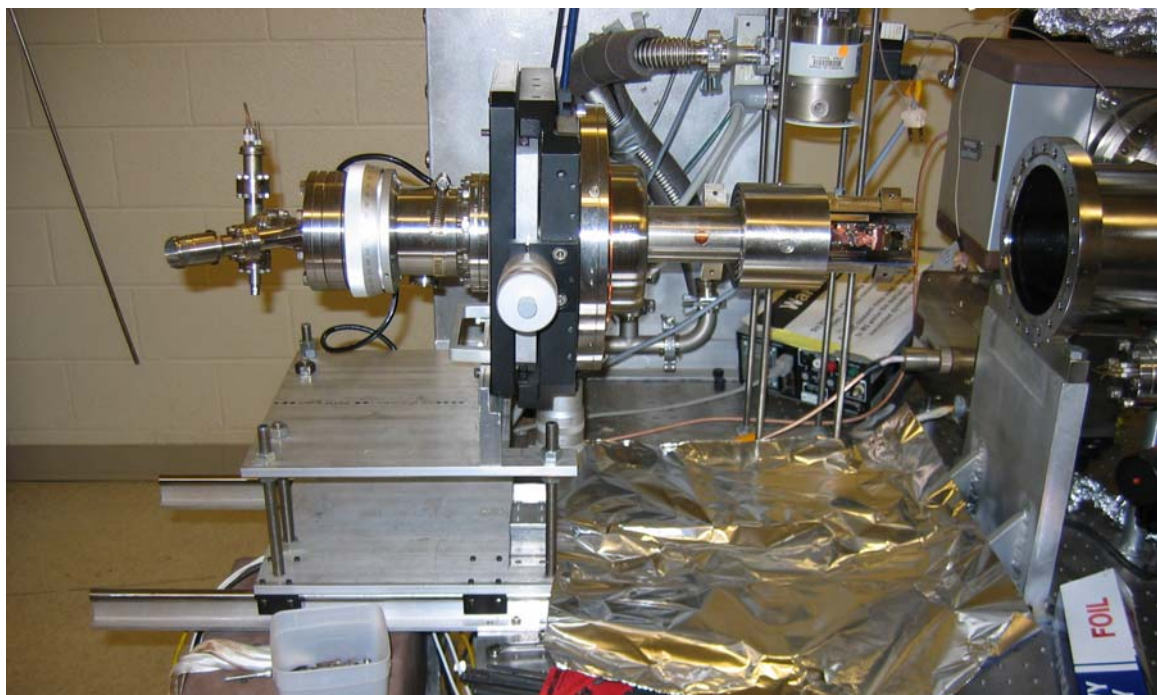


Figure 2 A picture of the crystal manipulator removed from the UHV chamber for maintenance. On the right of the manipulator are the concentric tubes for vibration dampening, middle (black anodized aluminum) is the adjustable bellows with rotary cuff attached on the left side, and on the far left is the feedthroughs for the ultrastat and electronics.

chamber has been devised. The major component in this system is the crystal manipulator, around which everything else is built.

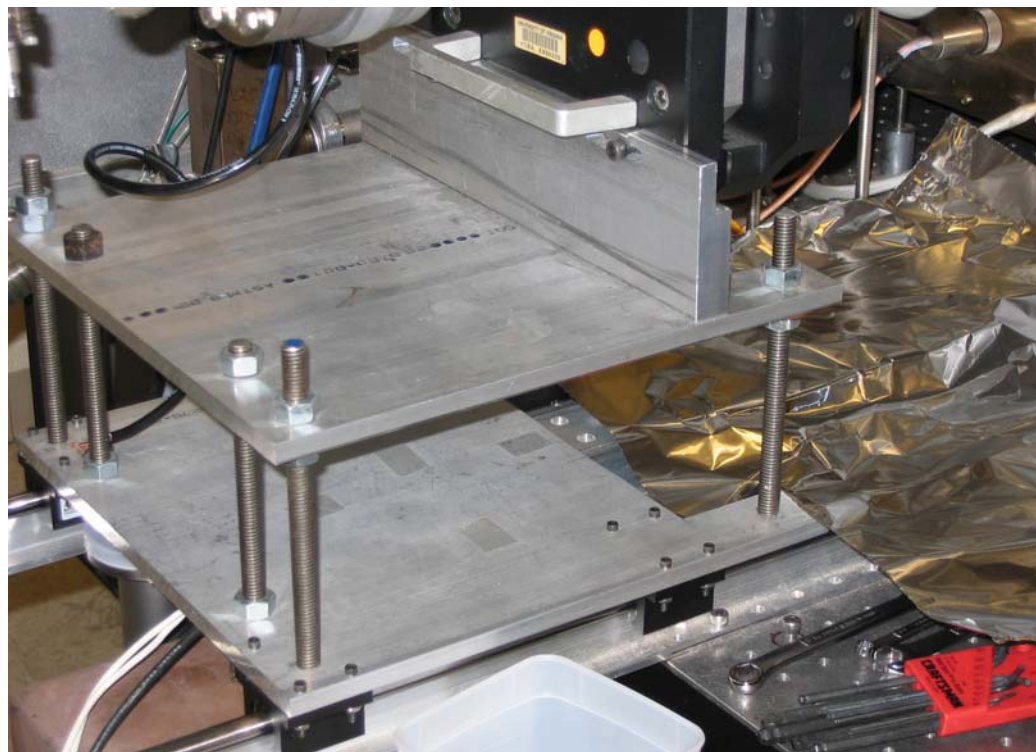
The manipulator consists of a differentially pumped rotary cuff that was made by Vacuum Generators, an Ultrastat cryo-cooler from Oxford used in conjunction with their transfer arm, a liquid He / N₂ tank, and a number of concentric tubes separated by Viton to achieve vibration isolation. The translation stage / rotary cuff assembly has an 8" conflat flange on one side that bolts to the UHV chamber, and on the other side has a 4.5" conflat flange where the ultrastat is attached. The rotary cuff is pumped down initially by the gas manifold turbomolecular pump, then isolated from the manifold and pumped exclusively by a 220 L/s PHI ion pump (due to the relatively high pressure of a 10⁻⁶ Torr and high argon content of the air gas load, this pump may need to be rebuilt periodically. Instructions for rebuilding are found in Appendix D). The rotary/roughing cuff is used so that when the crystal is rotated from one instrument position to another, there is little or no increase in the pressure of the main chamber from gas leaks. Next, a support tube that is welded to a 4.5" double sided conflat flange is attached to provide solid support for the concentric vibration isolation tubing. After the support tube the Oxford Ultastat is inserted. A picture of the assembled manipulator can be seen in Figure 2. The manipulator translation stage from Vacuum Generators allows up to +/- 12.5 mm of movement of the crystal in both the X and Y directions by micrometer dials and a flexible bellows (in the plane of the 8" conflat flange face). The adjustment of crystal position is important because not all of the instruments are aligned to within a millimeter of the center of the chamber. Adjustment of the crystal position allows only a limited ability to take measurements along the crystal length.

One degree of freedom that is lacking in the manipulator is the ability to move the crystal in and out of the chamber (perpendicular to the plane of the 8" conflat flange). This makes alignment of the crystal position in the "Z" direction extremely important. The decision to omit the Z degree of freedom was to increase the vibrational stability for STM. Problems in the Z alignment arise due to the small sample acceptance size of the mass spectrometer and AES. Our mass spectrometer is a differentially pumped system with 1/8" apertures which is designed to sample only the atom/molecules coming off the 5 mm dia. Pt(111) surface during TPD and not the mount and Ultrastat. Because this alignment is important, and the turn around time of the chamber for crystal adjustment when testing by TPD is over a week, there are a few ways that have been developed to insure that the crystal is aligned properly. The first step is to use a micrometer to measure the crystal position with respect to a fixed point such as the end of the support tube before any adjustment is made to the crystal or vibration isolation stages. By measuring the position initially, the crystal can be moved back to a position that is close to the correct alignment after crystal maintenance. Once the crystal is close to the correct alignment, one of two methods can be used. One method utilizes a jig that is attached to a 2 $\frac{3}{4}$ " conflat that is attached to a 6" to 2 $\frac{3}{4}$ " conflat reducer, which then is attached to the 6" chamber flange where the STM normally is bolted too. The jig is a straight aluminum rod that has been milled to a point on one end. This jig is then lowered into position over the platinum crystal. The end point of the jig should be located at the exact center of the UHV chamber. The crystal position can then be moved in or out to get the point of the jig to be located over the center of the platinum crystal. (NOTE: when using this method always lower the platinum crystal when inserting or removing from the chamber. This

should limit the potential for scratching or damaging the polished platinum crystal.) The second method that is more often used is, to align a HeNe laser to pass the laser beam through a series of apertures within the mass spectrometer and chamber. The laser will enter the mass spectrometer through a window on the back near the electrical feedthroughs, and then pass through the ionizer and the two 1/8" apertures that make up the differential pumping stage. If the laser passes through all of these apertures without being blocked or reflected then the beam should pass through the center of the chamber, where the crystal position can be adjusted until it intercepts the laser and reflects the beam.

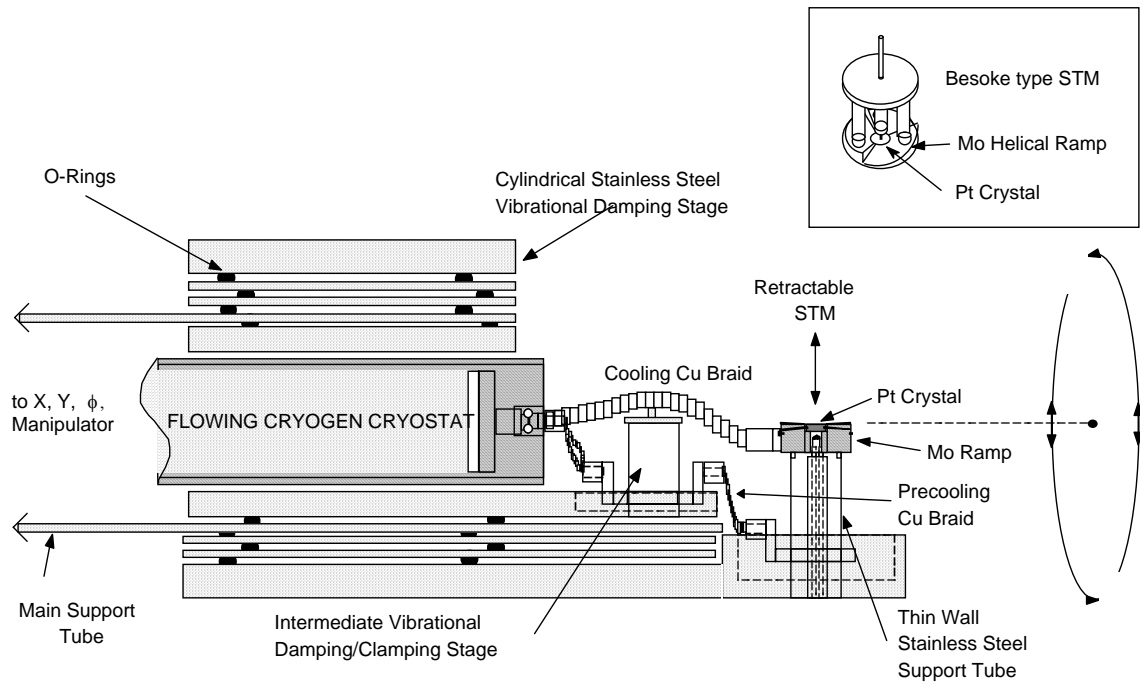
An additional note about the manipulator is that removing and reinserting the manipulator for crystal alignment or basic maintenance has been made much much easier

Figure 3 Picture of the linear translation stage used to insert and remove the manipulator from the UHV chamber. Showing how the manipulator is held in position by the translation stage.



by the implementation of a linear translation stage to hold the manipulator. This stage moves on four linear bearing, and can be adjusted to any height or tilt for manipulator manipulation. To use the translation stage the roughing cuff flexible hose needs to be removed and the manipulator rotated and raised to allow the holder to be slid up to the base of the manipulator where holes in the translation stage align to the holes along the bottom of the manipulator as seen in Figure 3. Fine adjustment of how the manipulator fits into and is removed from the chamber can be done by the micrometers attached to the manipulator.

Figure 4 Cross sectional view of the vibration dampening stage of the STM with crystal mount attached.



The Ultrastat has an opening on the end for the cryo transfer arm, and two mini-conflat connections. These mini-conflat connections are where the electrical connections for crystal bias, thermocouple, and electron bombardment heating filament are made. All

of these electrical wires are isolated by fiberglass braid and are run down the length of the ultrastat inside the support tube.

The crystal is held in place by a crystal mount that is attached to the vibration isolation stages of concentric stainless steel tubes by a thin walled (0.005" thickness) 304 stainless steel tube with many holes in a hexagonal arrangement all around it. This effectively acts as a thermal break between the crystal mount and the huge mass of the vibration dampening stage. An assembly diagram of the crystal mount and vibration dampening stages can be seen in the Figure 4.

2.5 CRYSTAL MOUNTS:

There are two different style of crystal mounts that can be used in the STM UHV chamber. The original style (Figure 5), is a large block of Mo that has been machined to accommodate a 4.9 mm dia Pt(111) crystal with 1 mm dia holes on the side of the crystal spaced every 120 degrees. The crystal is then held down in place by tungsten posts attached to Mo holders that bolt into the Mo mount. Then a copper braid is bolted into the Mo mount to cool the crystal. The final feature of the Mo mount is, the three ramps cut into the block at a 3° angle to allow coarse approach of the beetle STM. The molybdenum material is used due to its refractivity and hardness. This style of crystal mount has been used for

Figure 5 Original Pt(111) crystal mount made of solid molybdenum. The circular ramp is used for coarse STM approach.



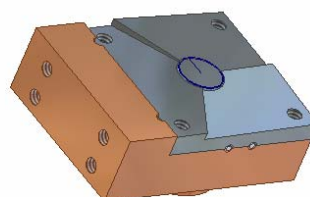
many years in this lab with good success. However there are problems associated with it such as: being very difficult and expensive to machine, and it doesn't allow electrical isolation of the crystal from the huge mass of the concentric tubes of the vibrational dampening stage which is detrimental for scanning tunneling spectroscopy. However, the problem that I dislike the least is; to heat and cool the crystal for a TPD run, typically takes 30 minutes or more, because the Mo mount heats up the same as the crystal, and has to cool back down before the crystal can cool. An associated problem with the mount heating up along with the crystal is that the mount and copper braid start to create secondary peaks in the TPD spectra due to molecules reabsorbing on the crystal and desorbing towards the mass spectrometer.

The second style of crystal mount (Figure 6), improves on the shortcomings of the original design, and allows for easy accommodation of differing crystals and STMs. However, it is not without its problems, currently it has one fatal flaw of vibrational stability, which should be easily fixed with a new tophat shaped crystal.

The new mount is made out of two materials, and is bolted together to sandwich the crystal into place. The bottom part is made of OFHC copper, and the top is made of either 304 stainless steel or nickel.

Because the mount is modular it is possible to attach a stainless steel mount that has a 3° ramp cut into it for the beetle STM course approach, or a separate magnetic nickel mount that can be used for the isothermal single tube STM. The first crystal tried with the new mount was a spare 5 mm dia Pt(111) crystal that was

Figure 6 Image of the isolated crystal mount with the beetle STM ramp installed.



previously used with the original Mo mount. To use this crystal, two $\frac{1}{2}$ mm dia Pt wires were spot welded to the back of the Pt crystal and the platinum wires were then sandwiched between two alumina sleeves that were held in place between the copper base and the stainless steel ramp. By isolating the crystal in this manner, the crystal can be biased for STM without biasing the rest of the manipulator, and the heating and cooling of the crystal is greatly improved. The ultimate temperature that the crystal was able to reach with He cooling was 23 K, which is very close to the low temperature achieved with the original amount. However, the cooling rate from > 1000 K with the new mount runs between 5 and 8 minutes compared to the 25 to 35 min for the Mo mount. Also the heating ramp rate for the isolated crystal is much greater than the non isolated crystal. Typical heating of the non-isolated crystal to keep up with an 8 K/s heating ramp rate for TPD requires the Kepco ATE 15-6M to be run at a minimum of 4 amps output with a -500 V filament bias, and +300 V crystal bias. On the isolated mount, a 15 K/s heating ramp rate could be achieved while reducing the Kepco output to 3.8 Amps with a filament biasing of -500 V and a grounded crystal. In addition to the greatly improved heating and cooling the secondary peaks seen in the TPD spectra from heating of the mount and copper cooling braid were eliminated. Even with all the improvements the new isolated crystal mount has over the original Mo mount, it is not being used in the STM UHV chamber because of a few very detrimental noise resonance frequencies seen in the STM. The noise spectrum of the STM tunneling current showed an increase in 1.5 kHz and 4 kHz noise, and a decrease in the 60 Hz noise. The most likely cause of the enhanced noise is the lack of a strong contact between the platinum crystal and the 0.5 mm dia. spot welded platinum wire which supports the crystal. A proposed solution to

this problem is to use a tophat style crystal which has a rim that can be sandwiched between two sapphire washers. The tophat sapphire sandwich would provide a strong and rigid contact between the crystal and mount/STM.

2.6 VIBRATION ISOLATION OF THE STM:

Vibration isolation is key to generating high quality STM images that can be used for understanding the atomic scale chemistry of small molecules adsorbed on the Pt(111) surface. Therefore, an elaborate series of springs and masses are used to reduce or eliminate as much building, mechanical, and audio vibrations as is humanly possible. The desired result is to maintain a variation between the STM tip and crystal of less than 0.01Å. To achieve this high level of stability two basic ideas are used: keep the resonant frequency of the system as low as possible and keep the resonant frequency of the STM head as high as possible. To start with, the STM chamber which is quite heavy sits on a Newport RS4000 optics table of very significant mass and the entire system is floated by compressed air filled bladders in the Newport I-2000 isolators. This provides the first stage of vibration dampening of the system. The large mass of the chamber and table softly coupled to the building floor provide a very low frequency resonance of the system, because the resonance frequency is a function of the mass and spring constant by Eq (2.1), where k is the spring constant, and μ is the reduced mass of the system,

$$\omega = \sqrt{\frac{k}{\mu}} \quad (2.1)$$

The second part of the system vibration dampening is different than what was originally in the chamber. The second system is a series of concentric stainless steel tubes separated by a Viton (fluoroelastomer) cord based on a design by Comsa.¹¹ Each stage of the concentric ring dampening has a different mass and therefore different resonance frequency; therefore, even if noise is driving the resonant frequency of one vibration stage, it should be eliminated by the next. The original chamber used only two concentric tubes for vibration dampening, one for the bracing of the copper cooling braid, and a second to hold the crystal. In the current generation of dampening there are four stages of concentric tubes separated by Viton to eliminate vibrations (Figure 4). The concentric tubes have grooves machined along the insides of the tubes in which 1/8th inch diameter pieces of Viton cord are placed. The Viton cords are pieces of #2-227 O-rings that can be purchased from Parker in a vacuum baked condition to reduce outgassing.

To get the best performance from the fluoroelastomer as a damped spring element, the cord is compressed to 90 % of the original diameter. This requires the concentric tubes with the Viton be press fitted together. The durometer of the Viton cord should be the standard Shore A-70 durometer hardness. If softer Fluoroelastomer cord is used such as A-40 or A-50, the cord has a more difficult time supporting the large mass of the concentric tubes, which results in a sagging movement in the crystal position by as much as 2 mm or more due to gravity. The sag in crystal position can short the crystal to the heating filament. While it is desirable to decrease the spring constant of the fluoroelastomer given equation(2.1), it does not work in our case past A-70 durometer hardness.

To keep the resonant frequency of the STM high a Besocke style of head is used.

The Besocke (beetle) style typically has resonance frequencies above 4 kHz due to its rigid compact design.¹² Some groups have reported mid-range resonance frequencies of 500 to 1500 Hz in their STM heads,¹³ which is usually attributed to the tip exchange mechanism in their particular beetle. Details of the Besocke (beetle) design can be seen in the wiring and STM construction portion of the dissertation (Chapter 3).

The STM system described here has very good vibrational stability and, when using a good tip, can relatively easily resolve the 0.02 Å atomic corrugation of the Pt(111) lattice (Figure 7). However, when the crystal is cooled additional vibrational noise makes imaging the Pt(111) lattice nearly impossible. Some of the problems associated with imaging low corrugation surfaces during cooling is: noise from boiling liquid N₂ or He, and more building, mechanical, and audio noise picked up from the attached coolant transfer arm.

To reduce noise from boiling cryo-coolant, if possible, use liquid helium. The helium apparently doesn't boil as vigorously as liquid nitrogen, producing less noise. It is still possible to produce atomic resolution images of high corrugation surfaces while cooling with liquid nitrogen, but atomic resolution of the Pt(111) lattice has not been achieved. With both liquid helium and nitrogen there are certain games that can be played to help reduce noise from boiling, such as adjusting the flow rate so the spatial position where the coolant boils in the Ultrastat is altered. By reducing the flow, it is possible to make the coolant boil in the transfer arm before it reaches the cold finger that attaches to the copper braid and crystal. While this does help to a small extent, the price in increased crystal temperature is rarely worth it. Alternatively, if the flow of coolant is increased, the

amount of boiling at the end of the cold finger can also be reduced, resulting in less noise from boiling, but crystal temperature rises (not much) and there is increased noise from freezing of the Tygon tubing that connects the transfer arm to the pump which pulls the coolant out of the Dewar. Experimenting with coolant flows can be useful for adjusting noise levels in the STM.

Minimal adjustments for noise reduction associated with the transfer arm have been made, and here lies a reasonable opportunity to reduce noise to improve image

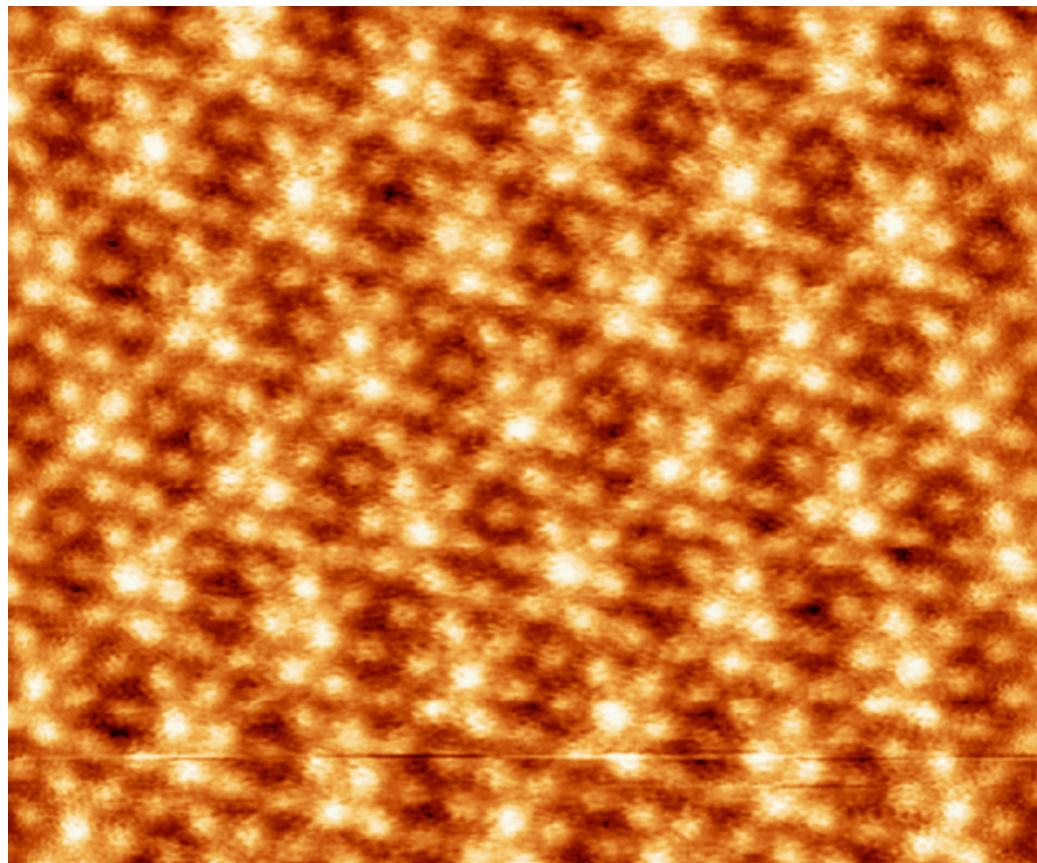


Figure 7 Image of the Pt(111) lattice taken at room temperature with a Besocke style STM. Imaging conditions were 1.92 nA and +40 mV biasing, image is approximately 60 Å by 60Å.

resolution. Current conditions allow for atomic resolution images of surfaces and so eliminating transfer arm noise has not been fully explored. The liquid coolant Dewar is

raised off the floor of the building by a $\frac{1}{2}$ inch thick plate of aluminum that is supported by pads of Sorbothane. The transfer arm itself has thick foam rubber tubing wrapped around it to reduce vibrations from movement due to audio noise and bumping by people walking by. While this may not be the ideal setup, it is one has worked for us.

The last item to mention about vibration reduction in the STM, is that all the vacuum pumps in the UHV chamber are vibrationless. None of the ion pumps or TSP pumps have moving parts. In addition, the manifold turbomolecular pump and mechanical backing pump are turned off during STM operation.

2.7 CLEANING OF THE Pt(1 1 1) CRYSTAL:

Cleaning of the crystal surface can be accomplished in one of two ways. There is a physical cleaning¹⁴ and there is a chemical cleaning.¹⁵ The physical cleaning of the crystal is done by Ar⁺ ion sputtering. Sputtering of the surface is done using a PHI 04-161 sputter gun controlled by a PHI 20-045 sputter gun control. In ion sputtering, electrons boiled off a filament wire are accelerated to strike gas molecules typically argon, and create ions. The argon ions are accelerated out of the ion gun at high potentials, typically 0.5,1,1.5 or 2 keV. The high energy ions have more than enough energy to break any chemical bonds of atoms or molecules on the surface. The ions hitting the surface fragment adsorbed molecules and eject or sputter away atoms. Typical conditions of Ar⁺ sputtering are: emission current of 30 mA, beam voltage of 500 V for periodic crystal cleaning, and 1000 V for initial cleaning of the surface after venting, and always in an argon environment of 5.5×10^{-5} Torr Argon for 10 minutes at a time.

Important note for sputtering is always turn off the ion pumps in the chamber before backfilling with argon and evacuate with a turbomolecular pump.

Chemical cleaning of the crystal can be done by either high temperature oxidation or oxygen TPDs. By dosing molecular oxygen on the Pt(111) surface, it falls apart to form an atomic oxygen species that will react with atoms or molecules left on the surface after sputtering. In cleaning by oxidation, one raises the crystal temperature in an O₂ atmosphere up to a point where the oxidation products will be desorbed from the surface as soon as they are formed and pumped away. The crystal temperature is typically 700 K for oxygen burning. Because the sticking coefficient of oxygen onto the platinum surface is very low at 700 K a continuous flow of oxygen is passed across the crystal at a chamber pressure of 2×10^{-9} Torr (when the crystal is in front of the directed doser; a local pressure of 10 – 100 times greater) to adsorb enough oxygen to react with all surface contaminates. Typically, oxygen burning is done for 5 to 10 minute intervals followed by oxygen TPD.

An oxygen TPD is used to determine if the crystal is chemically clean or not. Dosing oxygen at low temperature allows the atomic oxygen to react with contaminates in an order with temperature that reflects the amount of energy required for reaction. If multiple oxygen TPDs are run on a surface that was partially clean the order of peaks observed would be CO formed on the first TPD. On the second TPD CO₂ is observed desorbing from the surface and finally water is seen desorbing from the surface typically on the third oxygen TPD. Then on the fourth oxygen TPD, a recombination peak of molecular oxygen (T at 750 K) is seen indicating that the oxygen atoms have nothing left

on the surface to react with except each other, which indicates a clean surface, and also that the mount is not excessively outgassy.

2.8 INSTRUMENTS:

2.8.1 MASS SPECTROSCOPY:

The mass spectrometer plays a vital role in surface science analysis, from analyzing the gases in the chamber (Residual Gas Analysis, RGA), to chemical identification of molecules coming from the crystal surface in Thermal Programmed Desorption (TPD), or during a laser induced photochemical reaction studied by Time of Flight (TOF) spectroscopy to name just a few. The mass spectrometer in the UHV STM chamber is a quadrupole mass analyzer made by Extrel, and controlled with a 020-2 Extrel Ionizer control and a 011-1 quadrupole power supply. The mass spectrometer components internal to the UHV chamber are a 041-11 ionizer, $\frac{3}{4}$ " diameter quadrupole rods for mass filtering, and an electron multiplier with conversion dynode.

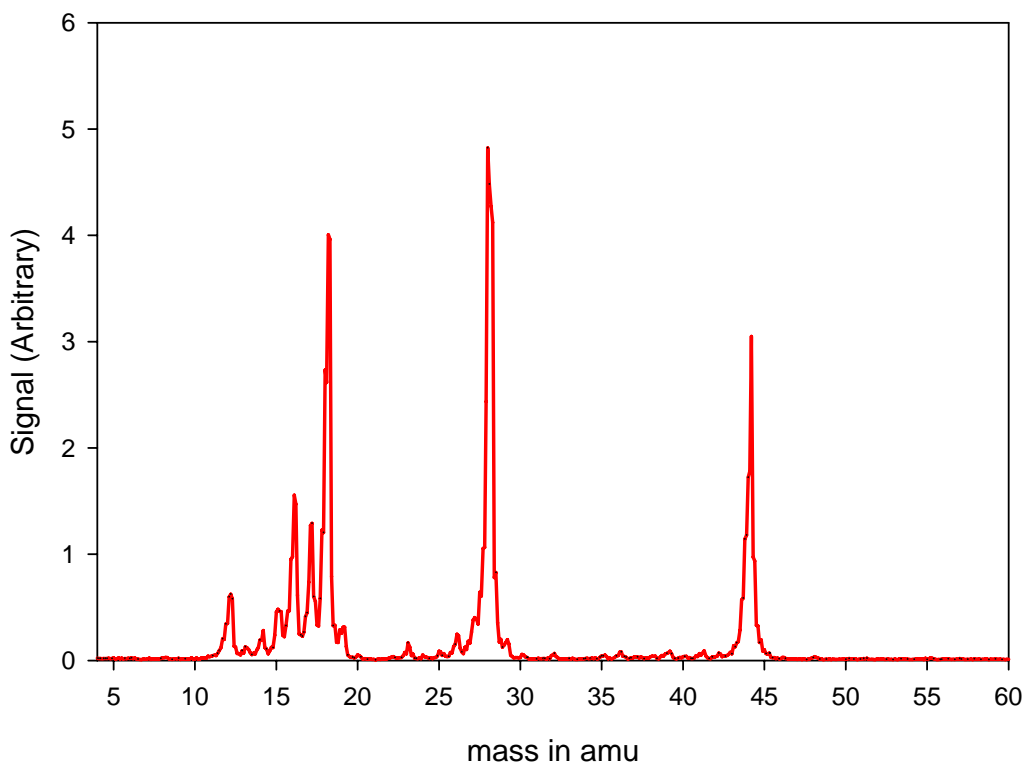
The quadrupole mass spectrometer is one of many possible designs, but perhaps is the most common for surface science. It operates by detecting ionized molecules that are filtered by their mass-to-charge ratio (m/e). The separation of masses is done by a rapidly changing (radio frequency, RF) electric field potential applied to two opposing rods, and an inverse electric field is applied to the other two opposing rods. The applied oscillating potential follows equation (2.2).

$$f(t) = U + V \cos(\omega t) \quad (2.2)$$

Where U is a DC voltage potential, V is the amplitude of the oscillating potential and ω is the frequency of oscillation. A combination of the constant U potential and oscillating V potential is found that allows an ion with a specific m/e , to travel the length of the quadrupole filter without being sent off course. However, if the ion is not of the correct m/e , the potentials applied to the quadrupole rods will induce the ion to oscillate with increasing amplitude such that it collides with the quadrupole rods or surrounding metal canister. This action results in a m/e of a selected beam of ions allowed into the detection system.

By examination of equation (2.2) it is seen that the potential applied to the quadrupole rods effect the mass selection as described in the previous paragraph.

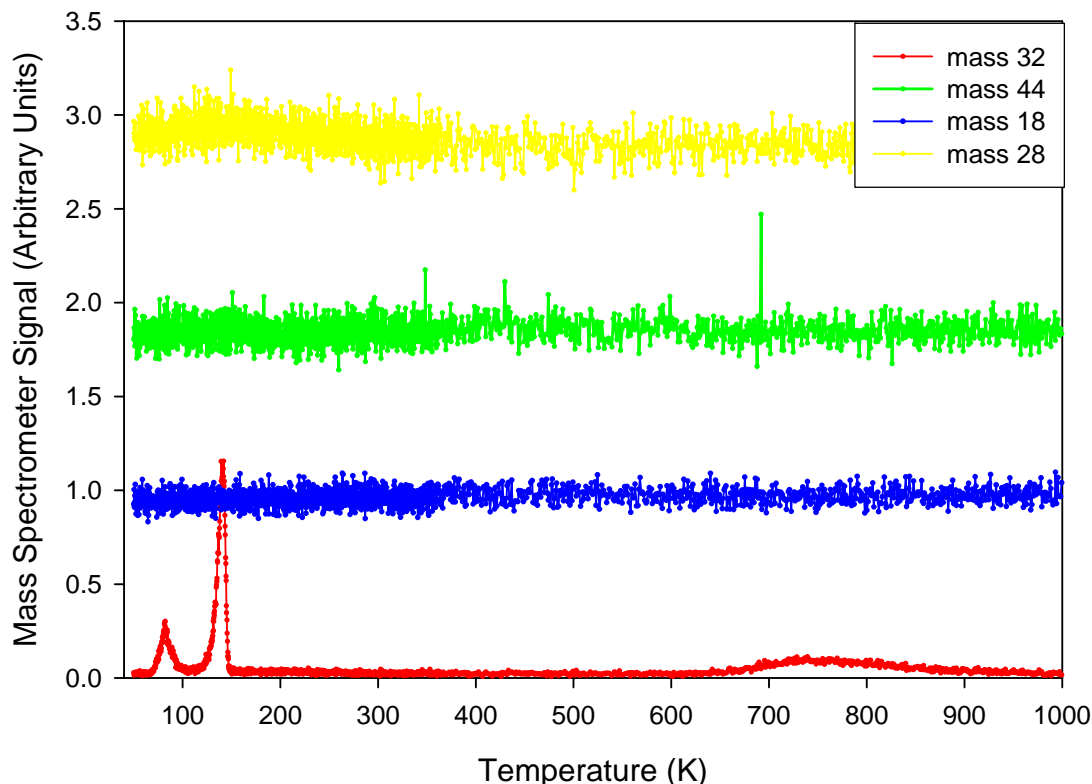
Figure 8 RGA of the UHV Chamber at a pressure of 8×10^{-11} Torr.



However, it should also be noted that the rf frequency plays a role as well. To exploit this fact three different quadrupole Q-heads can be used with the radio frequency power source to change the range of masses that can be scanned and analyzed by the mass spectrometer. The three Q-head available to us are a # 10, 13, and 15 head. The 10 Q-head can detect a mass range of 0 to approximately 18 amu, the 13 Q-head has a range of about 1-130 amu, and the 15 Q-head which is normally used with the UHV STM has a range of about 4 to 400 amu.

Detection of m/e selected ions is done by an electron multiplier and conversion dynode. The potential applied to the multiplier is 1550 - 1650 V, depending on the

Figure 9 Thermal Programmed Desorption Spectrum showing, CO, CO₂, water, and molecular oxygen desorbing from the Pt(111) surface. The molecular oxygen trace shows the characteristic physisorption chemisorption and recombination peaks respectively increasing in temperature of a chemically clean Pt(111) surface.



strength of the TPD signal and the background pressure in the mass spectrometer chamber, and the conversion dynode is held at -4100 V. As the mass selected ion current is amplified by the electron multiplier, a Stanford Research Systems SR570 low current pre-amplifier is used to convert the small current to a voltage that is detected by a National Instruments card in the data acquisition computer. There are many possible settings on the SRS pre-amp but the ones that work best are: an “Inverted” signal with high bandwidth +12 db filtering, and a detection level sensitivity of either 1 nA/volt or 500 pA/volt. The sensitivity level and filtering can be adjusted to suit the speed requirements for the data to be taken. (n.b. at high sensitivity the time constant increases and may exceed the nominal front panel settings – see SRS manual for details.)

Operation of the mass spectrometer for the various analysis techniques is simple. First, the mass spectrometer is tuned so the detected mass is maximized and the DC balance of the system is set to zero as described in the Extrel Quadrupole Control manual.¹⁶ Second, the detected mass is calibrated, and then the ionizer control is adjusted to maximize the signal level. Once the mass spectrometer is set, a Residual Gas Analysis (RGA) showing all the chamber gasses can be seen (Figure 8). An RGA will show the relative amount of the different gases in the UHV chambers and is very useful for diagnosing leaks or hydrocarbon contamination of the vacuum system. An RGA shows that the predominant constituent gases of the chamber are carbon monoxide, carbon dioxide, water, methane and their fragments.

By using the Labview program TDSM1.vi a thermal programmed desorption spectrum can be taken. The TPD program records the intensity level of one or more selected masses to be studied as a function of a linear rise in the crystal temperature. The

program also records the time taken since the start of the TPD spectrum in case post-analysis of the heating rate is necessary such as during temperature calibration. A TPD spectrum has many purposes. A TPD spectrum can be used for determining: the correct temperature of a crystal, a surface coverage of a given molecule, and the average binding energy of an adsorbate to the crystal surface. Also by careful analysis of the leading edge and peak desorption temperature, information on the kinetics by which the molecule desorbs from the surface can be gained. A typical oxygen TPD spectrum can be seen in Figure 9.

To generate a TPD spectrum a symphony of instrumentation must work in conjunction to produce a controlled sample temperature ramp, mass detection at multiple m/e ratios and recording of all necessary information. To produce a linear temperature ramp, a Eurotherm is used that contains preset PID values and a predetermined program that is run. The Eurotherm program controls the heating of the crystal by applying voltages to a Kepco power supply. Currently, the Eurotherm program number 3 is used for TPD spectrums. The program produces a linear increase in crystal temperature from its base temperature of ~ 20 K to 300 K at 2 K/s. After the program reaches 300 K an increase of ramp rate to 8 K/s is used until a terminal temperature of 1100K is reached at which point the program terminates, heating stops, and the crystal temperature returns to its base value of 20 K. When the Eurotherm program is run the Kepco power supply and the Bertan biasing supplies are turned on, as well as the TDSM1 program.

While it is possible to perform time of flight (TOF) analysis of molecular species or fragments desorbing from the crystal surface in the STM UHV chamber, it is difficult given the low signal levels seen in TOF due in part, to the small acceptance area of the

differentially pumped mass spectrometer and the relatively small sample size. Therefore, all of the TOF analysis of small molecules studied by the STM has been left to the photochemical chamber, which is much better suited for TOF studies. Aspects of TOF analysis will therefore be very briefly explained here. Typically, the TOF is recorded on a SRS multichannel scalar that records the time in microseconds after the molecule has been desorbed from the sample surface by a pulse of laser light. Because each pulse releases a very small flux of molecules from the surface (e.g. 0.001 ML/pulse) many pulses of the laser are required to build up an integrated detected signal as a function of time after the laser pulse. Once the molecules have been desorbed off the crystal surface they drift to the ionizer approximately 10 cm away. The ionized molecules are quickly accelerated into the drift region of the quadrupole mass filter whereupon they make impact with the electron multiplier. The time for ions to traverse the mass spectrometer varies accordingly to equation(2.2).

(2.2)

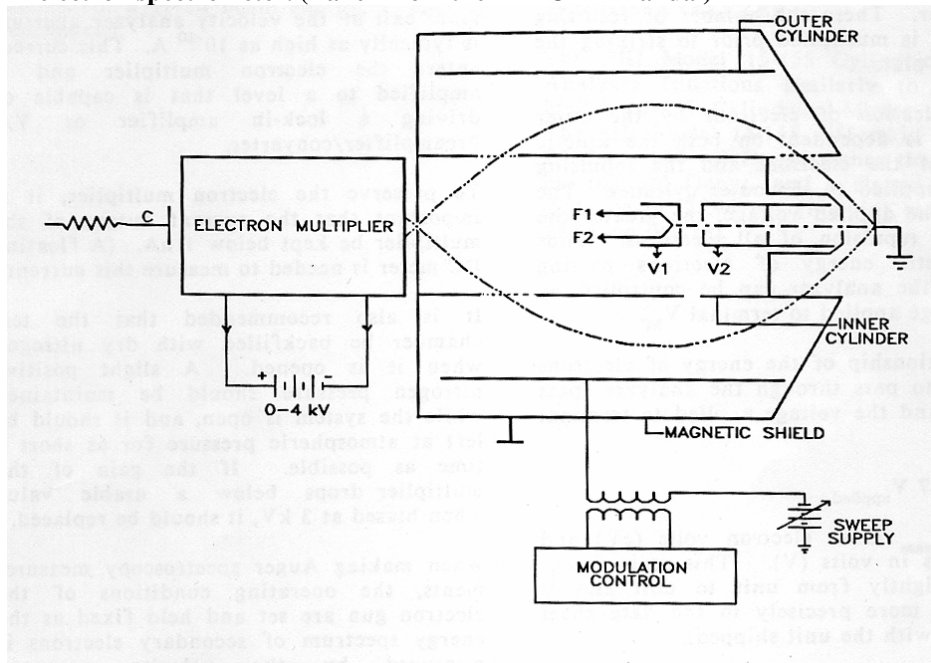
$$t = \frac{L}{\sqrt{\frac{2qU}{m}}}$$

where the time it takes the molecule to traverse the drift region is t, L is the length of the drift region, m is the mass of the molecule, q is the ion charge, and U is the ion energy with respect to the grounded mass filter. The ion flight time must be subtracted from the recorded time of arrival spectrum to yield the TOF spectrum from surface to mass spectrometer ionizer.

2.8.2 AUGER ELECTRON SPECTROSCOPY (AES)

Auger electron spectroscopy is an important and, perhaps, the most widely used technique in surface science. AES is used to determine the elemental composition of the sample crystal or

Figure 10 Diagram of the single pass cylindrical mirror analyzer Auger electron spectrometer. (Taken from the PHI CMA manual)



the amount of impurities present. It is a secondary electron process that was first observed by the French physicist Pierre

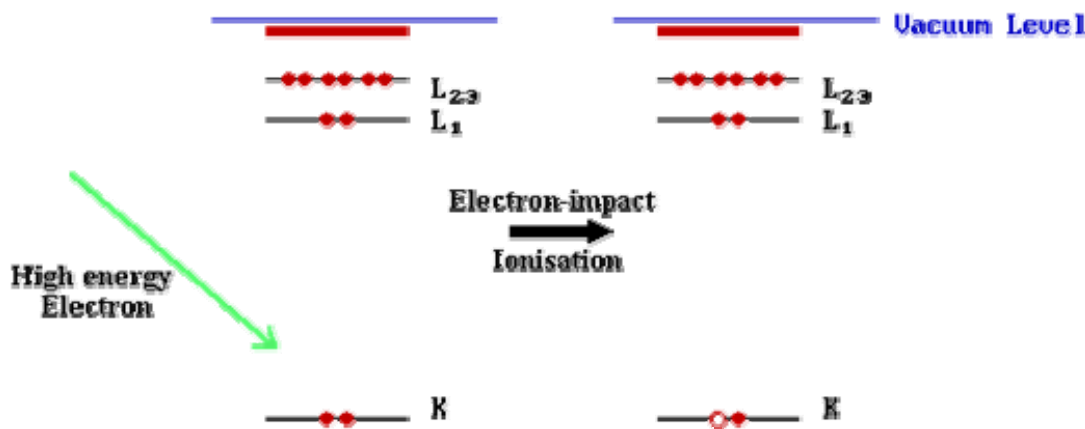
Auger (hence the name). Auger spectroscopy works by a few steps. First, injection of a high energy electron into atoms on the sample surface causes an ionization event by removal of a core level electron. Second, is the emission of a low energy secondary electron from the ionized atom (Auger process) that is collected for the third step. In the third step, the collected Auger electron is energy analyzed to determine the elemental composition of the atoms.

An electron gun is used to irradiate the crystal surface with high energy electrons. The UHV STM uses the 10-155A single pass cylindrical mirror analyzer (CMA) from

Physical Electronics (Figure 10)¹⁷ to energy analyze the electrons and it holds a centrally mounted electron gun. The electrons are created in the center of the instrument by a filament that is heated to boil off electrons. The electrons are then accelerated by a set of electron optics. The energy of the electrons leaving the CMA are regulated by a Physical Electronics 11-010 5 kV electron gun supply. This supply typically runs at 2 mA emission current at 3 kV beam energy during operation.

By using 3 kV electrons, core energy electrons are easily knocked out of the

Figure 11 Ionization event of the core level electrons in an atom by the 3kV electron beam from the electron gun supply.

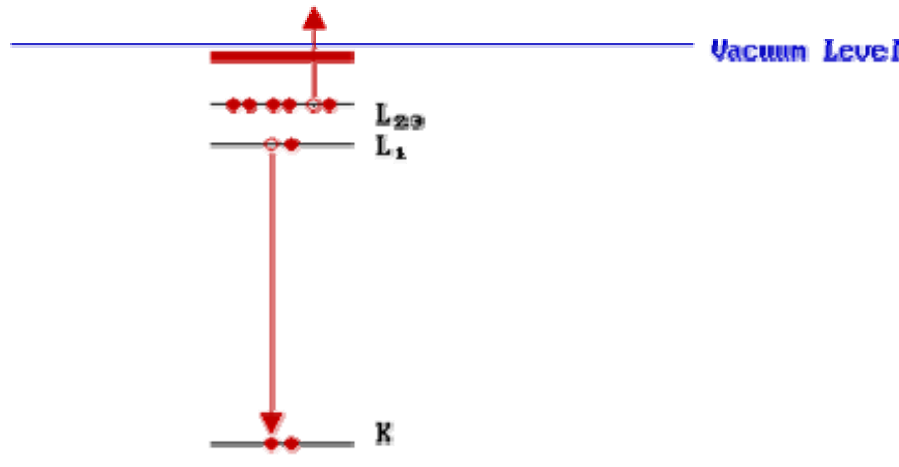


atoms, causing an unstable state within the atom. The atom relaxes by filling in the core level with an electron from a higher energy valence level (Figure 11). When the valence level electron falls down into the core to fill the void, it must release the energy difference between the electronic energy levels. There are two ways that the high energy electron can release this energy to fill in the core level: 1) radiative emission of a high energy photon of light, or 2) donation of the excess energy to a neighboring electron which then has enough energy to escape the atom. The second method results in the

emission of an Auger electron (Figure 12). The electron kinetic energy used to determine the identity of the element. The kinetic energy measured follows the equation(2.4).

$$KE = (E_K - E_{L_1}) - E_{L_{23}} \quad (2.4)$$

Figure 12 Ejection of an Auger electron from the atom with a certain kinetic energy.



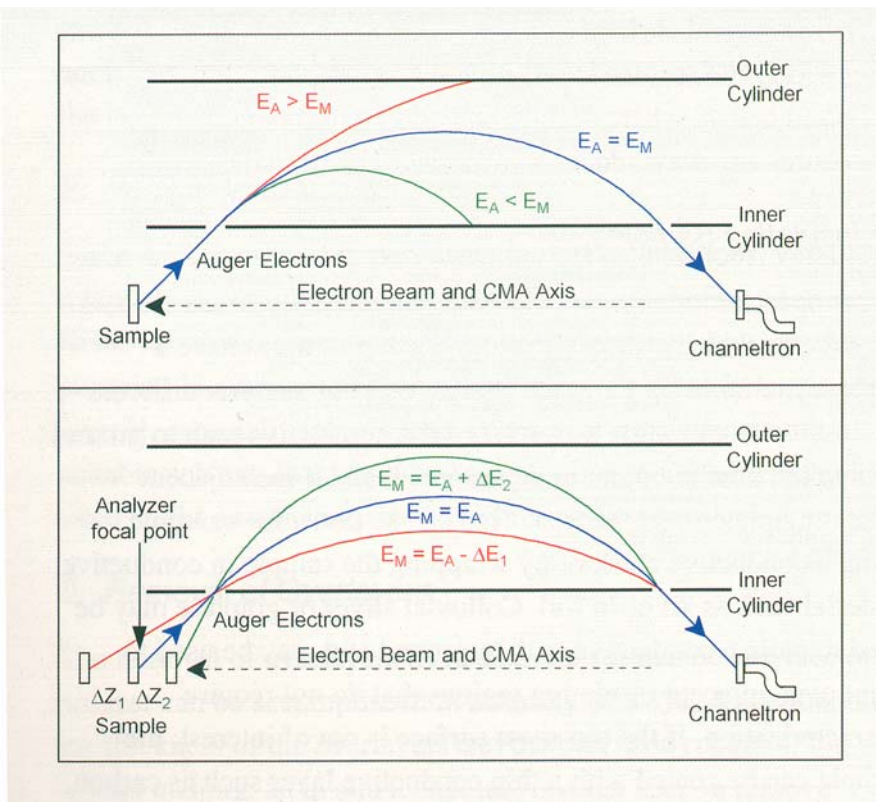
where E_K is the binding energy of the electron in the K level, E_{L_1} energy of the L1 level, and $E_{L_{23}}$ energy of the L23

level. This equation shows that the Auger transition is characterized by the initial hole location, and the location of the final two holes.

To measure the kinetic energy of the Auger electrons, the CMA uses two concentric cylinders that are charged to different voltages and the varying voltage potential between the two cylinders allow for energy selection of the incoming electrons by letting only certain kinetic energy electrons follow a path within the analyzer that ends at the electron multiplier (Figure 13).¹⁸ The inner cylinder is keep at ground, and the outer cylinder potential is varied by the 32-150 Digital AES controller. By adjusting the potential on the outer cylinder a pass energy range from 0 to 3200V is possible from the AES controller.

The energy filtered Auger electrons are collected by a Channeltron electron

Figure 13 Schematic showing the energy selection of Auger electron emitted from the crystal surface (taken from the PHI Auger Spectrum Handbook) (a) Energy filtering (b) Variation of pass energy with sample position.



multiplier. A PHI 32-100 electron multiplier supply provides power to the Channeltron and the PHI 96B V/f preamplifier, with the multiplier typically run at 1000 V. The detected signal on the Channeltron is then converted from a voltage to a

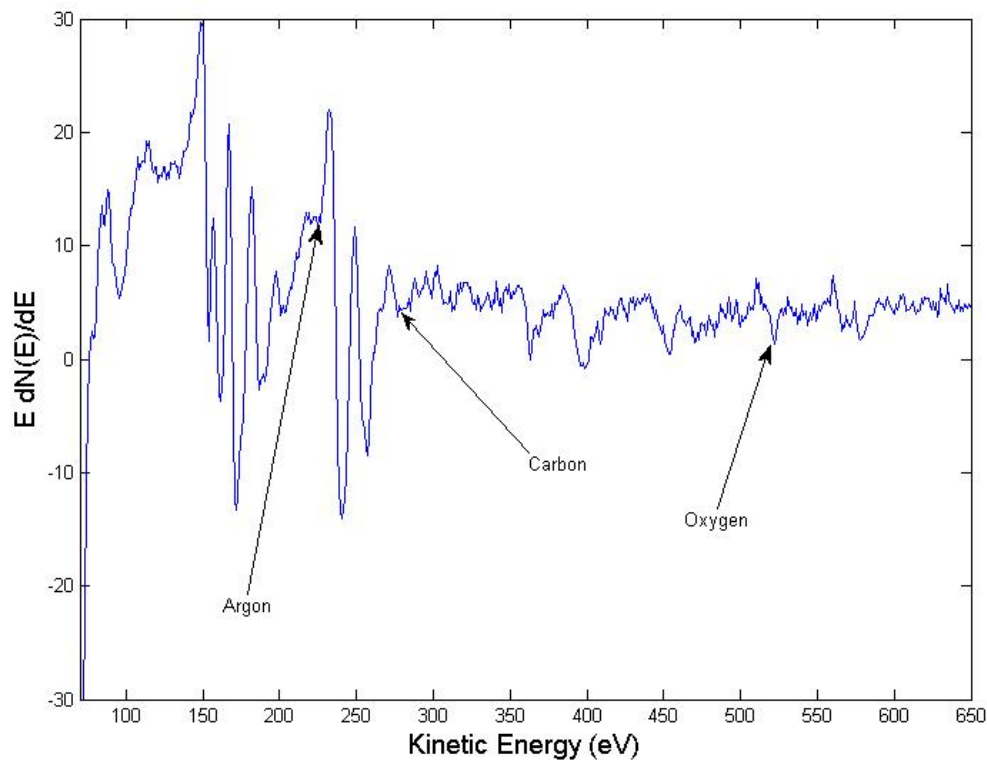
train of TTL logic pulses whose frequency is linearly related to the signal voltage.

The TTL pulses are read by the computer program via a PHI 137 PC card. This produces a characteristic spectrum of peaks displayed on the screen as a function of the voltage on the outer CMA cylinder. The energetic peak positions in these Auger spectra are then compared to a list of peak positions for all elements found in a Auger handbook from PHI. The handbook contains spectra of all elements (except H and He) that are taken as standards, because each element has a characteristic fingerprint of Auger peaks

at various kinetic energies. A typical Auger spectrum for our Pt(111) crystal is shown in

Figure 14.

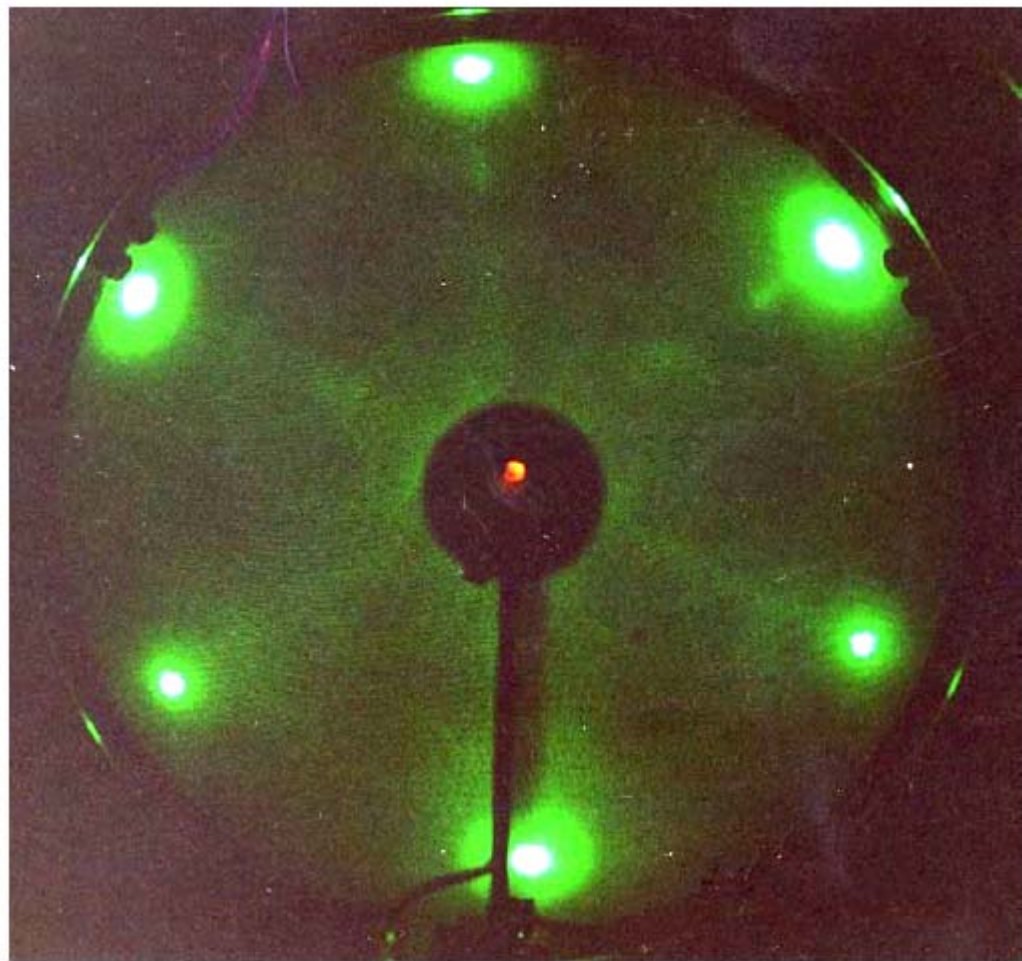
Figure 14 A differentiated Auger electron spectrum taken of a relatively clean Pt(111) surface after argon ion sputtering and oxygen burning. There are three labeled peaks for argon, carbon and oxygen, and the rest of the peaks are characteristic of platinum. The Auger spectrum was taken with the single pass CMA of the STM UHV chamber.



2.8.3 LOW ENERGY ELECTRON DIFFRACTION (LEED):

Low Energy Electron Diffraction is a structural technique used to examine ordering of the surface, or adsorbates on the surface. The images seen in LEED are a reciprocal lattice view of the surface such as seen in the LEED image of the Pt(111) surface in Figure 15 . The images seen are formed when a collimated beam of monoenergetic electron in the energy range of 20 to 500 eV are diffracted off the crystal

Figure 15 An image of a clean Pt(111) surface as seen in the reverse view LEED instrument. The six spots forming a hexagonal pattern are part of the reciprocal lattice of the hexagonally close packed platinum surface.



surface. The diffracted electrons impact a phosphorescent screen that lights up where hit with electrons.

The LEED instrument used in the STM UHV chamber is a reverse view Princeton Research Instruments RVL 8-120. It is used in conjunction with the Physical Electronics 11-020 LEED electron gun source.

2.9 EX100F GAM EXCIMER LASER SET-UP AND OPERATION:

Our GAM EX100F (Serial Number EX100F/125-132) is a state-of-the-art in 2005 excimer laser. This laser produces 10 nanosecond pulses of varying power depending on the excimer gas and repetition rate used. The most likely gas that will be used in the laser is an ArF mix which produces 193 nm light. It is also possible to run the laser with F₂ – 157 nm, ArF – 193 nm, KrF – 248 nm, XeCl – 308 nm, XeF – 351 nm with little to no change in the laser except the gas. The repetition rate of the laser can be varied by the computer from 16 Hz to 125 Hz. (If a repetition rate lower than 16 Hz is necessary, use of an external trigger is necessary.) Other important specification of our laser are: beam size – 7 mm x 2 mm, HV range of 12.5 – 16 kV, Average energy per pulse at the laser with 13 kV @ 20 Hz is 8 mJ/pulse @ 193 nm, and at 16.5 kV @ 10 Hz the laser produces 11.5 mJ/pulse at 157 nm. The laser is air cooled, and plugs directly into a standard 110 V AC electrical outlet.

Gases used for this laser can be ordered directly from Spectra Gases. GAM has its own mixture specifications for the gases that are a standard product from Spectra Gases. For an ArF tank the part number is EX0GAMFAHN-3. (Other part numbers for the different gases can be found in the user's manual.) The one thing to note about this

mixture of gas is that there is very little fluorine used (0.17% F₂). Therefore, it is possible to use standard copper or stainless steel tubing that connects directly from the cylinder regulator to the gas input connections on the laser without using a cross purge system like those used on the other excimer lasers in the lab. The cross purge system is internal to the laser assembly and is controlled by a personal computer. As long as the pressures are set correctly on the gas cylinder regulators the PC takes care of everything else. (The correct pressures for the ArF mix should be in the range of 40-43 psi, and the He balance tank should be 5-10 psi without exceeding 10 psi.)

The laser is controlled by an external PC connected to the laser by a PCI – 1711 card, and run by a proprietary program from GAM Laser. This makes the laser very simple to operate. However, there are enough instructions in the manual to use an external trigger and external programming to operate the laser without the use of the GAM Laser program.

Initially, the PCI card needs to be set up and then the GAM Laser software loaded on to the PC. After the initial setup, or any time a new laser gas is used, the laser setup in the GAM software must be run and the correct gas and laser chosen from a list. This is done to set the fill pressure of the laser tube, each gas has a different pressure needed and for F₂ the pressures are substantially different than for other fills. After the setup has been completed connection to the laser and operation is possible.

To operate the laser two switches must be turned on. First is a key interlock, and second is the breaker switch next to the key, which completes the power circuit for operation. There are two interlock keys sent with the laser, and each laser has a unique

key so do not loose the keys. Otherwise, if the keys are lost, the unit will need to be sent back to the factory for a new key interlock to be installed.

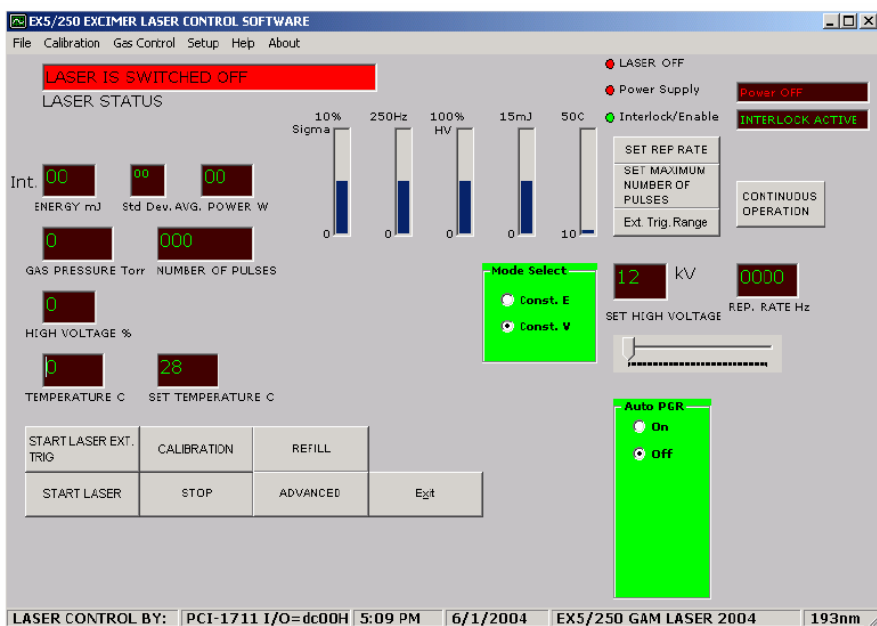
For troubleshooting the laser power up, make sure that both the key and the breaker switch are turned on. If the laser still will not power up, check the emergency kill switch at the front of the laser. Our laser was shipped with the emergency kill switch engaged which had to be pulled out, the force required to pull out the kill switch was surprisingly large, so a light tug on the switch will not suffice to disengage the kill switch. Conversely, just brushing up against the switch will not turn off the laser, the switch needs to be deliberately pressed.

Step by step instructions for attaching a new gas cylinder to the laser can be found on page 23 of the laser manual. The basic steps are; attach both the mix gas and balance gas to the laser and make sure they are leak tight. Proceed to the ADVANCED screen in the software and find the “PUMP PREMIX LINE” button. Then with the gas cylinder main value shut, the premix line can be pumped out all the way up to the cylinder by the mechanical pump internal to the laser assembly. The line is then pumped down for 10 min after which the regulator value is closed to the pump, and the gas cylinder valve opened and closed again to pressurize the regulator which is then opened to the pump to flush out anything in the line. Repeating this flush sequence two more times ensures the line is free of contamination. Then, once the line is flushed, all valves in the laser are shut, and the gas line is adjusted to a pressure of 40-43 psi. To replace a Helium balance cylinder the procedure is the same as described above where the line is flushed multiple times and then pressurized to 5-10 psi.

Once the gas cylinders are connected and the lines flushed, replacing the gas inside the laser tube is very easy. In the GAM Laser software there are three methods to choose from, an “AUTOFILL”, “PARTIAL GAS REPLACEMENT”, and a manual “PUMP OUT and REFILL”. All of these options are available in the REFILL window. Both the “AUTOFILL” and the “PUMP OUT and REFILL” remove all of the gas from the laser tube down to 100 Torr and then refills the laser to the appropriate pressure. The preferred method of gas replacement for the laser is the “PARTIAL GAS REPLACEMENT”, where by the laser tube is pumped down to approximately 1600 torr and then repressurized to 2600 Torr for ArF. This method is fast and reduces possible contamination from leaks by never allowing the system to go below atmospheric pressure. Four partial refills are equivalent to one full refill of the laser tube.

After the laser is on and filled with gas, running the laser is simple, and mostly controlled from the front screen of the GAM Laser software (Figure 16).

Figure 16 Screen capture of the GAM Laser main operation window.

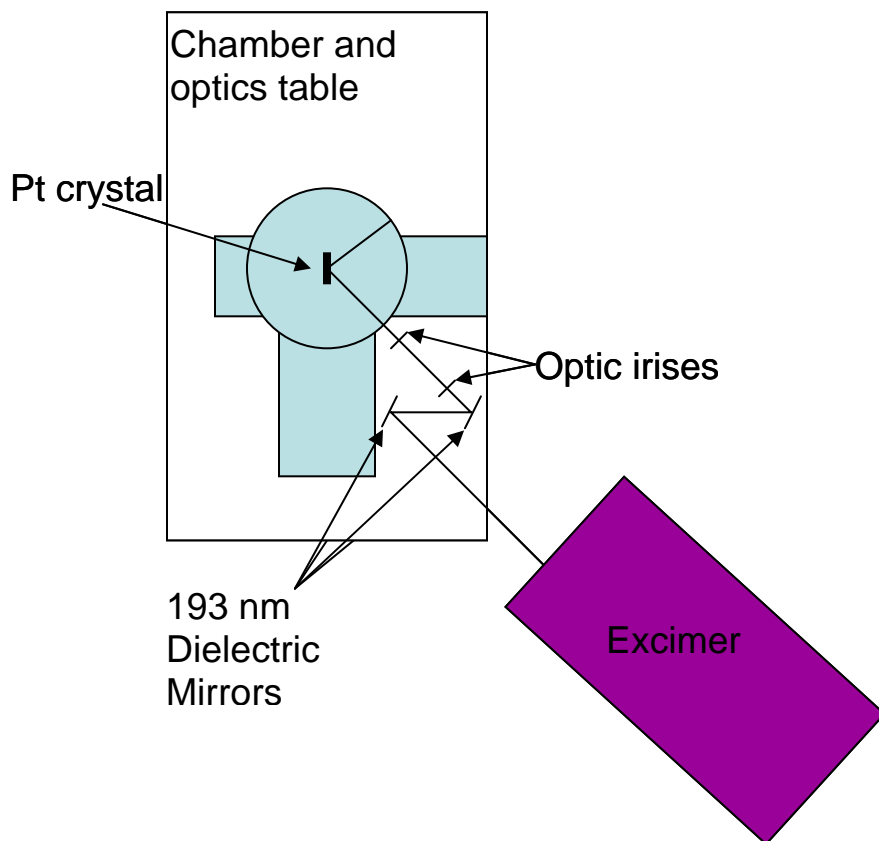


By adjusting the slider on the right side of the screen, the high voltage applied across the laser tube can be varied from 12 to 16 kV. The repetition rate can be set by clicking the “set rep rate” button which brings up a small box that a rep. rate can be entered into. Another button on the right is “set maximum number of pulses”, by clicking this any number of pulses can be entered from 10 to 10 million. (There is also a continuous operation button that can be used for continuous operation and will only cease firing once the “stop” button on the left has been pressed.) Because our laser is air cooled it should not be allowed to run continuously for extended periods of time. The laser chamber and thyratron temperature will increase during use and can become damaged if allowed to get to a temperature above 50° C. Therefore the chamber temperature is displayed on the front screen. It is recommended that for an air cooled laser that the laser be run in an 80% duty cycle where it may be run for 10 min. and then allowed to cool for 2 min. (@ 125 Hz that is 75,000 pulses for every ten minutes of operation. When compared to the 20 Hz operation of the other excimer lasers in the lab, it would take over an hour to generate as many pulses.)

To get the laser light into the STM chamber is something of a trick. The laser can not be attached to the STM chamber optics table due to size and vibrational constraints. Therefore, the laser sits on a separate table that is close to the optics table but not touching. The height of the laser assembly has been adjusted so that the output of the laser light is roughly the same height off the floor as the Pt crystal in the chamber is above the floor. The laser port on the chamber enters on a 45 degree angle from the crystal normal, so to minimize beam steering the laser has been set up on this 45 degree angle as well. (A diagram of the laser assembly and chamber can be seen in Figure 17.)

Because the 193 nm light is difficult to reflect, dielectric mirrors are used instead of ordinary mirrors to do fine steering of the beam into the chamber. The problems associated with the laser and chamber being decoupled is that every time the optics table is floated for STM use, the laser alignment needs readjustment. To try and minimize the amount of adjustment that introduces laser light into the chamber, two optics irises have been placed inline from the 2nd mirror to the crystal. Therefore, after the chamber has changed positions relative to the laser, the two dielectric mirrors can be used to adjust the beam until the laser light passes through the two irises in line with the crystal indicating that the laser alignment is correct once again. The iris are also there to serve in a secondary capacity to cut the laser beam size down so only the crystal is irradiated and not everything around the crystal.

Figure 17 A diagram of the laser alignment input in to the STM UHV chamber.



2.10 ALKALI AND HALOGEN DOSERS:

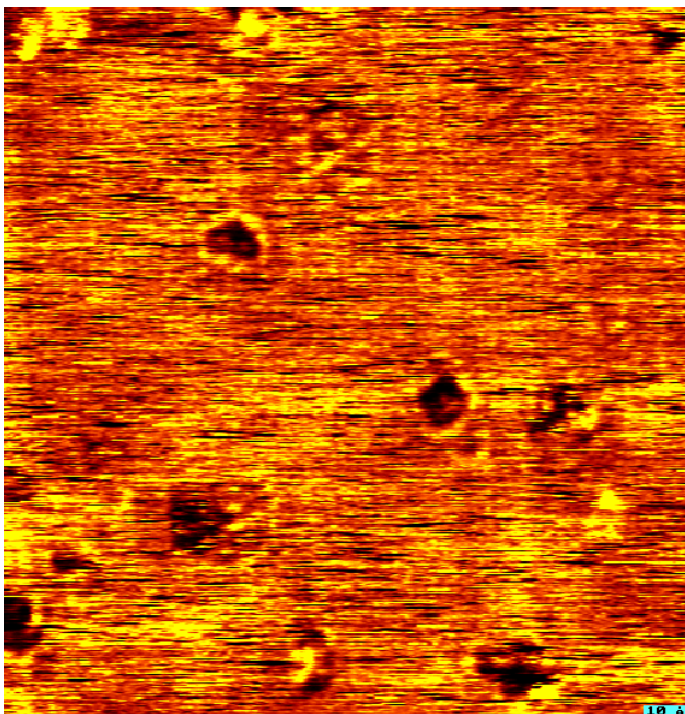
Both the molecular bromine and atomic cesium dosers will be discussed together in this document. The dosers have been designed to work from an interchangeable platform that can accommodate either one. However, due to the small size of the aperture that the doser must pass through, there is only space for one doser or another, which is why it was designed to be easily interchangeable but not to accommodate simultaneous dosing.

The molecular bromine doser has been used for previous experiments,¹⁹ examining the diffusion of Br atoms across a Pt(111) crystal from a dissociatively adsorbed molecular precursor state. Because this experiment was done by a post-doctoral

associate, Dr. Hongwei Xu,

working on the UHV STM

Figure 18 An initial image of the bromine covered surface showing very faint 3 x 3 ordering under the noise. (125 x 125Å image taken at 1 nA and .5 V bias.)



chamber before I joined the STM chamber project, no written documentation of the doser design or its operation has previously been made. Therefore, the design, operation and some of the problems associated with previous bromine dosing will be included in this dissertation. A few images of bromine atoms were taken

during my initial introduction to the operation of STM seen in Figure 18. Also some LEED images were taken, showing some interesting and unexpected results: A proposed observation of an electron stimulated rearrangement occurs. The LEED results are briefly reviewed in the “Future Experiments” (Chapter 8).

Design of the bromine doser was taken from a paper by N. D. Spencer et al.²⁰ in JVST A where an UHV compatible solid state electrochemical cell is described to produce halogen gases such as bromine, chlorine, iodine and, perhaps, fluorine. The doser consists of a base, top/culminating emitter, Pyrex tube holder, Nichrome heating wire, and a solid chemical pellet. The pellet should be made from spectroscopy grade AgBr which comes from Aldrich in a powder form. The lore passed around the lab for forming the pellet is different than that described in Spencer’s paper. The paper describes heating the AgBr to melt it and pouring it into a mold to form the pellet. However, the lab experience is to use a press to form the pellet by compressing the AgBr in a stainless steel piston mold that get compressed by the 10 ton hydraulic press in the student machine shop located in physics. The latter method seems to work well and has been used in our UHV STM chamber. Once the pellet has been formed, a Ag foil needs to be attached to one end of the cylindrical pellet and a Pt mesh attached to the other end. The Ag cathode and Pt anode need to be heated and pressed into the AgBr pellet to attach them. A Bunsen burner can be used to heat the materials for attachment.

To operate the molecular bromine doser, an electrical potential is applied across the pellet from the Pt mesh to the Ag foil. By applying an electric current, the AgBr goes through an electrochemical process which separates the Ag^+ and Br^- of some molecules, and the electrical potential drives the bromine ions towards the Pt mesh. The biggest

advantage of this doser is, because it is driven by an electric current, it is easy to turn the dose on or off, or even pulse the doser and deliver an exact amount of molecules to the surface in a chopped molecular beam.

The migration of ions in the solid pellet is through defects in the AgBr lattice. This migration is a slow process at room temperature. Therefore, to increase the production of bromine delivered to the surface, the pellet is heated to approximately 550 K which greatly increases the mobility of the ions within the pellet. However, heating something to 550 K in a UHV chamber can raise the background pressure of the chamber which is undesirable. To avoid this, Spencer introduced a small amount of CdBr, to create more defects in the AgBr lattice. This would reduce the operating temperature of the doser for production of useful Br₂ flux. The problem is that the Cd will be ionized just as the Ag atoms are, and the Cd outgassing seems to cause major problems with the Pt crystal. There has apparently been Cd that vaporized into the chamber from the pellet, or possible the doser may have been run in reverse at some point which inadvertently caused dosing of Cd. Either way, a considerable problem is that Cd forms an alloy with Pt.²¹ To remove the Cd-Pt alloy numerous cycles of very high temperature Ar⁺ sputtering has to occur. This was my first job when I took over the STM chamber; I spent about two weeks sputtering the crystal at 1250 K to remove the Pt-Cd alloy. Therefore, while using a Pt crystal in the UHV chamber do not add the CdBr into the doser pellet for bromine dosing it is not necessary for satisfactory Br₂ dosing.

The standard conditions that the bromine doser should be run at are: the manipulator that holds the doser should be extended as far into the chamber as possible,

the doser heated to 550 K, and a potential of 12 V with a current of 1 mA should be applied by the Keithley 224 programmable current source.

As stated earlier the doser is assembled on an interchangeable platform that can be used with either the molecular bromine doser, or the atomic cesium doser. The platform consists of a tube that is welded to a 2 ¾ in conflat flange on one end and has a flat face on the other where a base mount is attached. All the electrical wires are run along the tube and attached to a mounting point just below the base mount. From there either the bromine doser or Cs doser can simply be attached to the base mount by 4 screws, and connecting the corresponding wires. The base tube is very long and is used to get the doser close enough to the crystal so preferential dosing of the crystal is done and not the entire manipulator. Additionally, because the doser / manipulator is attached underneath the chamber it runs up through a 6 inch hole in the optics table. The size of the doser precludes it from being wrapped with heating tape for bakeout, so built into the center of the base tube is a halogen heating lamp that is used to bake the doser out. This heater operates just like the halogen heating lamp inside the UHV main chamber.

The connections on the 2 ¾ inch flange are: 2 sets of thermocouple feedthroughs and 3 high voltage feedthroughs. Two of the thermocouple feedthroughs are actually used for a thermocouple to measure the temperature of either the bromine pellet or the Cs doser depending on which is attached. The other thermocouple feed through is used in the bromine doser to deliver the current across the solid pellet. The high voltage feedthroughs are more complicated. Due to the limited number of feedthroughs, the center pin is pulling double duty, and is used for a ground connection for the Nichrome heating wire, and as the second connection line for the bakeout lamp. A normal variac can be used to

run the bake out lamp in the doser by connecting one line to the lamp pin and the other line to the “ground/center” pin on the flange. The Nichrome can be heated by a DC current from the ATE 20-25M Kepco supply and is connected across the pin that connects to the Nichrome wire and the “ground/center” pin on the flange.

The Cs doser is much simpler than the Bromine doser in construction, and the Cs doser is designed to make exchange of the Cs source very simple. The Cs doser consists of two semi-circular pieces each with a post attached to them, and a Cs containing boat.

The Cs boat is mounted from one post to the other simply by folding the ends of the metal boat down so it can be held in place against the post by screwing down a second half of each of the posts sticking up from the semi-circle pieces. Each half of the Cs doser has an electrical connection to one of the high voltage pins on the UHV flange, So that by connecting the metal Cs boat across the two posts (Figure 19), a DC current can

Figure 19 Cs doser source, seen are two separate segments with the Cs boat connecting the two halves.



be applied to the Cs boat, which resistively heated the boat releasing Cs atoms into the chamber.

The problem with the Cs doser is that the amount of Cs released is exponential in temperature and can not be simply turned on and off for pulsed dosing like the bromine doser. The resistive heating takes time to bring the boat up and down in temperature. Therefore to operate the Cs doser a thermocouple is attached to the middle of the Cs boat.

This helps to get regular repeatable doses by rotating the crystal into dosing position once the Cs boat has been brought up to temperature, and then the crystal can be rotated away to halt dosing. The temperature of the Cs boat may vary depending on the amount of Cs desired, but the typical temperature range for dosing is around 700 K. (The Cs coverage can be measured by Auger electron spectroscopy).

The Cs boats that are used can be purchased from SAES getters. These boats contain a Cs compound that undergoes a chemical reaction when heated to release Cs gas. The boat is approximately 32 mm long, 3 mm wide with a small slit along the length of the boat that the Cs is emitted from. The product number for ordering from SEAS getters is Cs/NF/2.2/12/ FT 10+10.

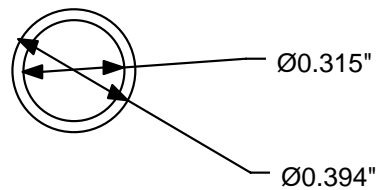
Included below are the design schematics for the bromine doser, cesium doser, and the base mount system.

Bromine Doser Tube

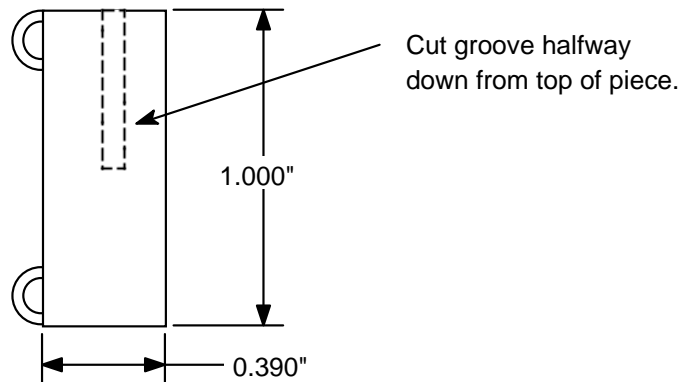
Material: Quartz

2 copies

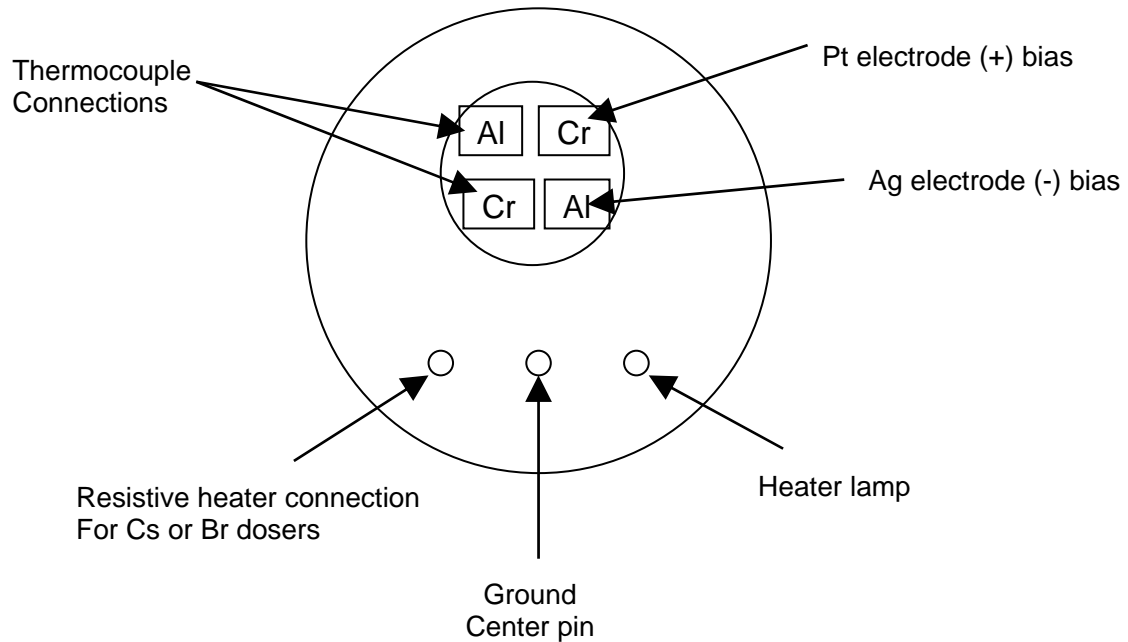
Top View

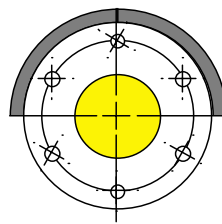


Side View

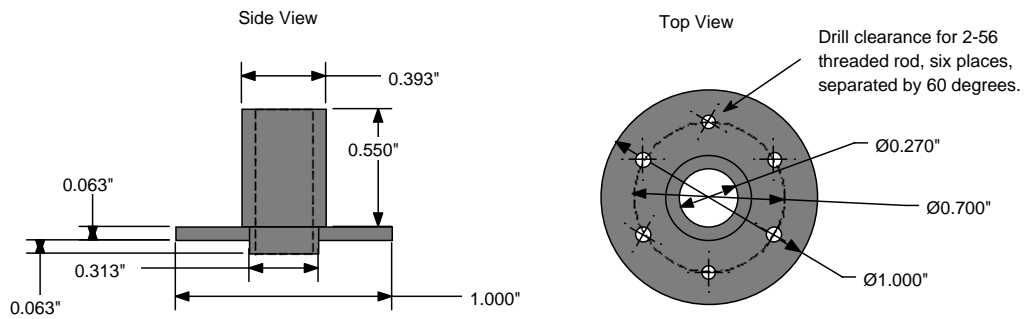


Cs/Br Doser feedthrough connections

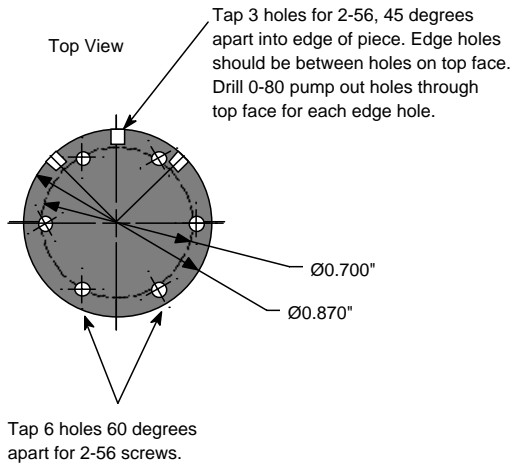




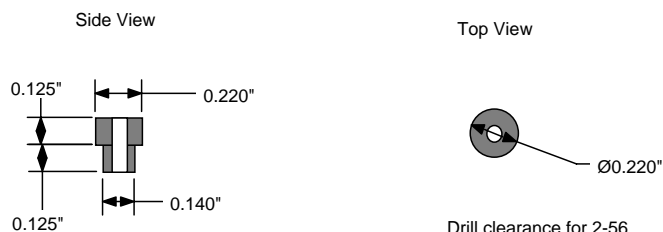
Face Plate - Bromine doser
Material: 304 SS
1 copy



Mount for doser assembly
 Material: 0.125" thick 304 SS
 1 copy

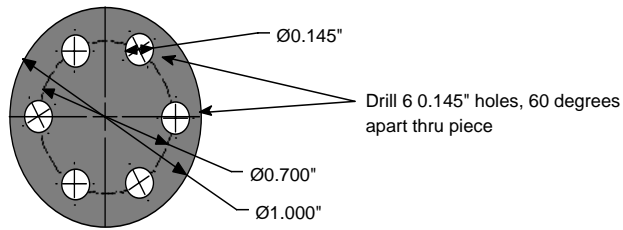


Electrical Isolation Pieces
 Material: Macor
 4 copies

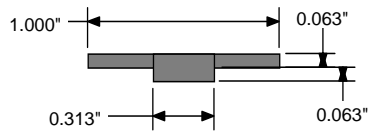


Bottom Plate
Material: 0.125" thick 304 SS
1 copy

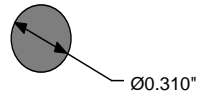
Top View



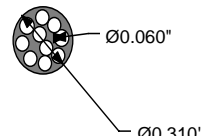
Side View



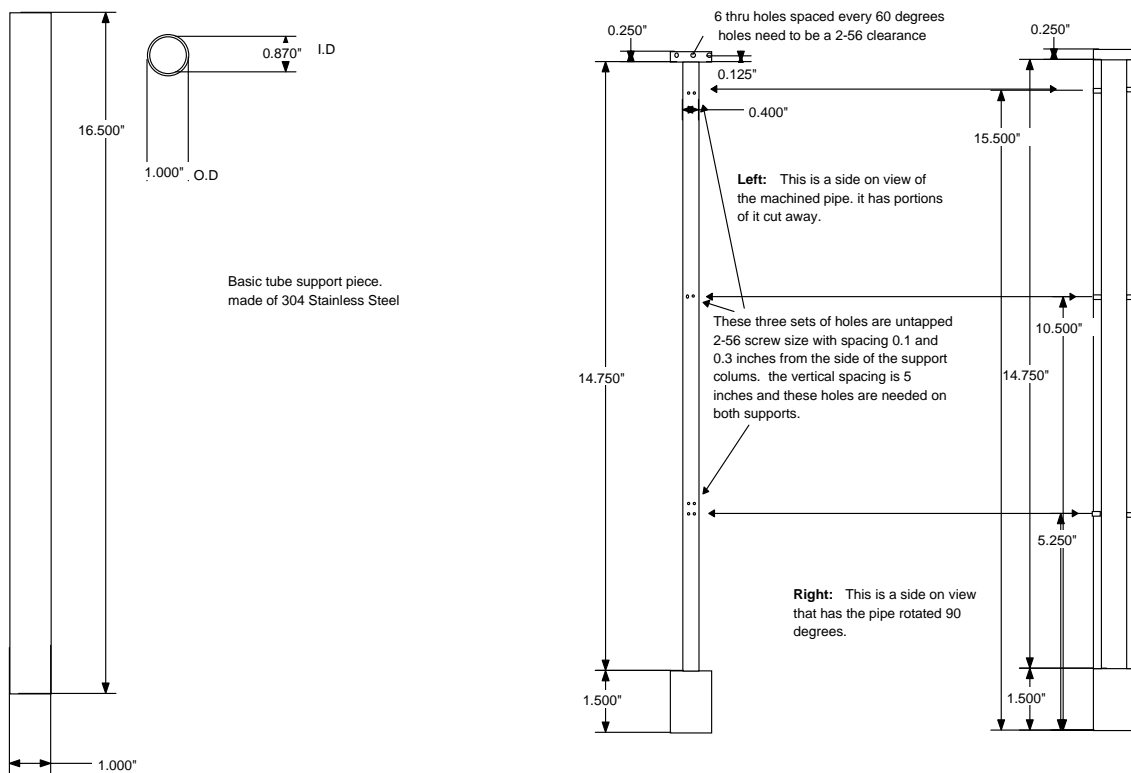
Upper pressure plate
Material: 0.063" thick 304 SS
1 copy

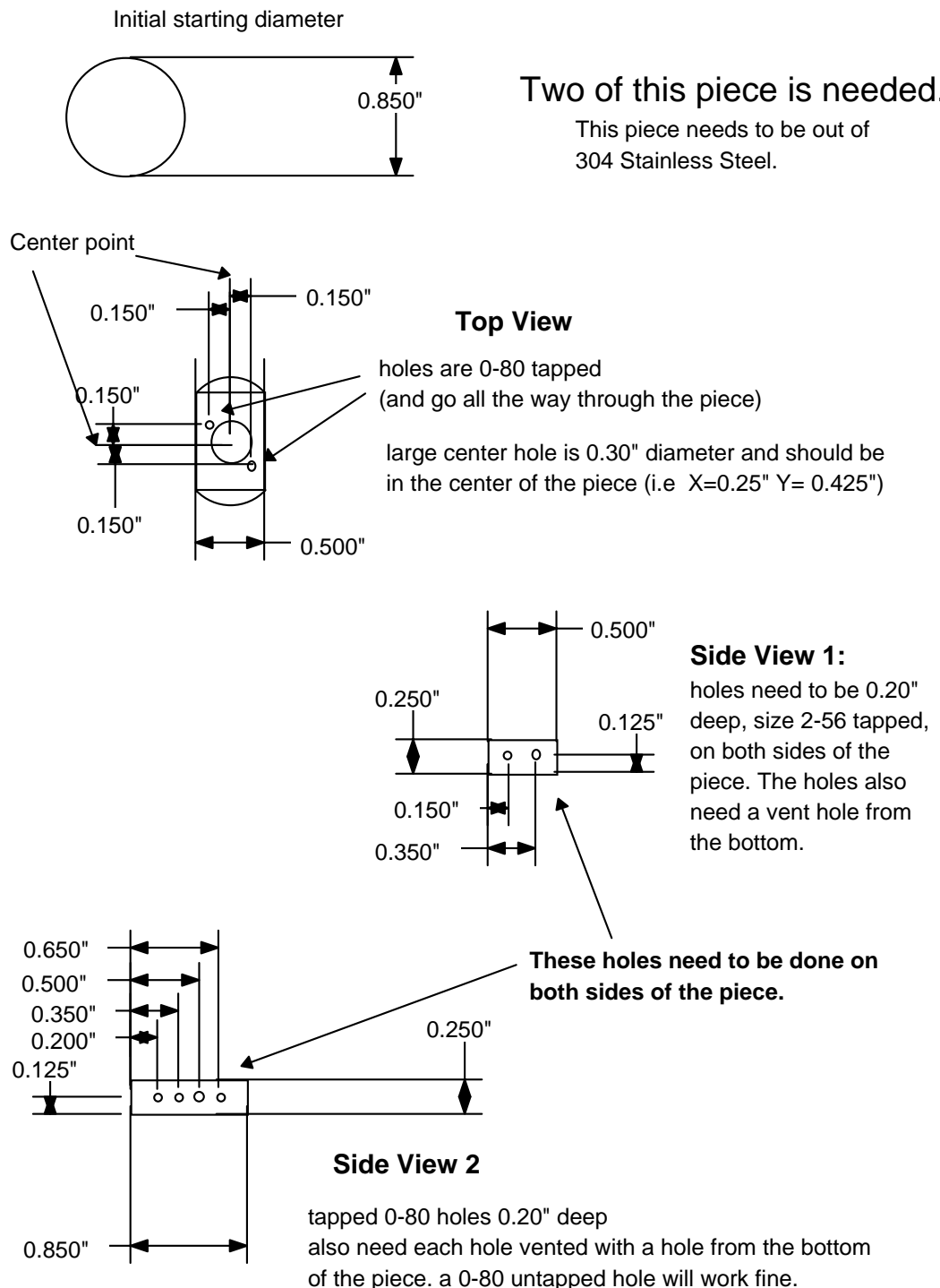


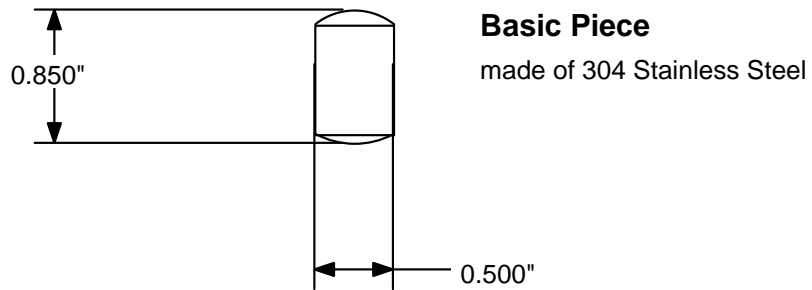
Lower pressure plate
Material: 0.063" thick 304 SS
1 copy



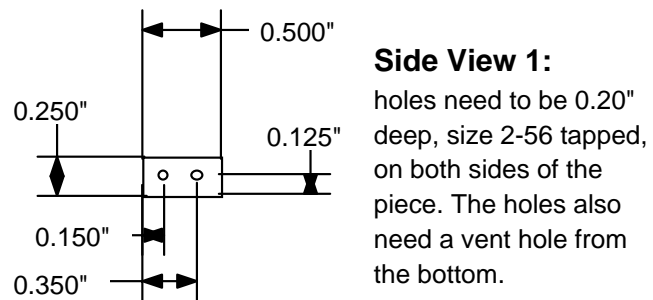
On lower plate, drill as many .060" holes as possible while keeping structural rigidity.



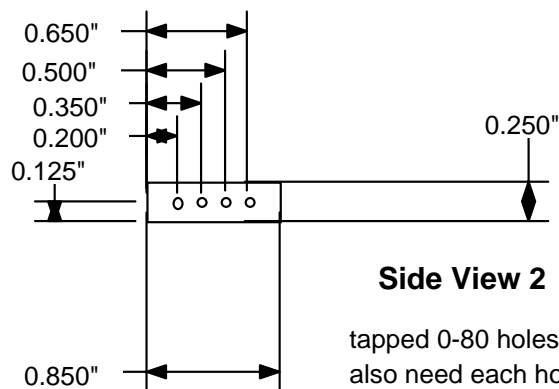


**Basic Piece**

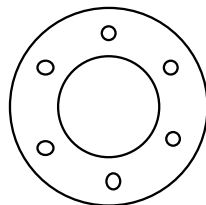
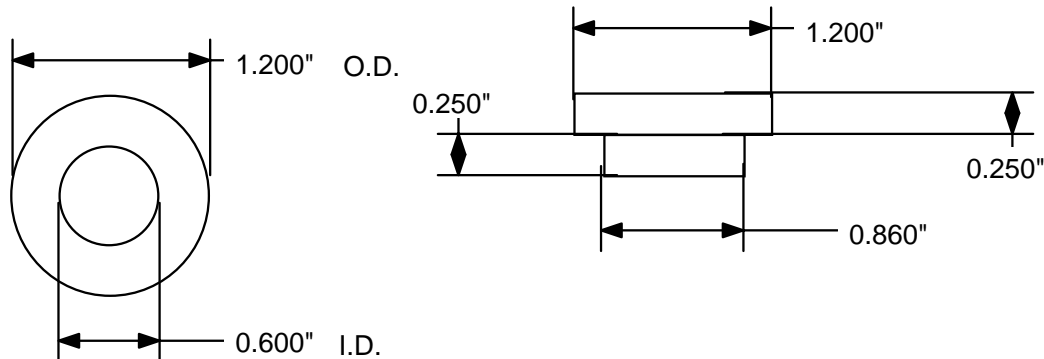
made of 304 Stainless Steel

**Side View 1:**

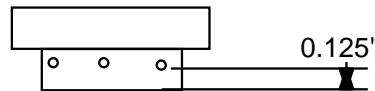
holes need to be 0.20" deep, size 2-56 tapped, on both sides of the piece. The holes also need a vent hole from the bottom.

**Side View 2**

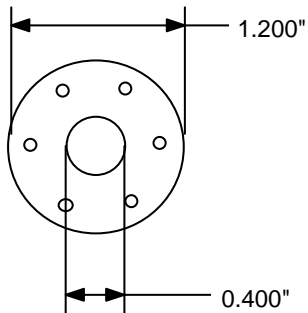
tapped 0-80 holes 0.20" deep
also need each hole vented with a hole from the bottom of the piece. a 0-80 untapped hole will work fine.



Holes are 2-56 tapped holes
spaces every 60 degrees on a
0.9" diameter circle

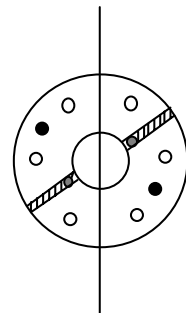
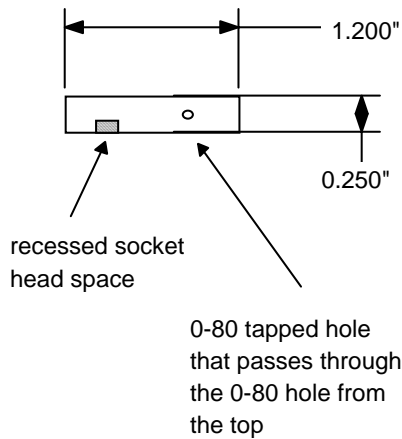


there needs to be 6 holes around
the piece centered 60 degrees
apart from each other.
2-56 tapped screw holes.



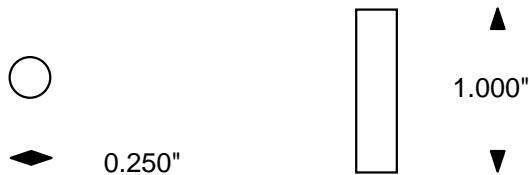
The two smaller holes are 0-80 holes untapped and go all the way through the piece. They should be on a 30 degree separation from the other holes and 180 degrees apart from each other. they need to be on a 0.5" diameter circle there also needs to be a 0-80 tapped hole running perpendicular through this hole (shaded area)

The holes above are 2-56 untapped sized holes, spaced every 60 degrees on a 0.9 " diameter circle

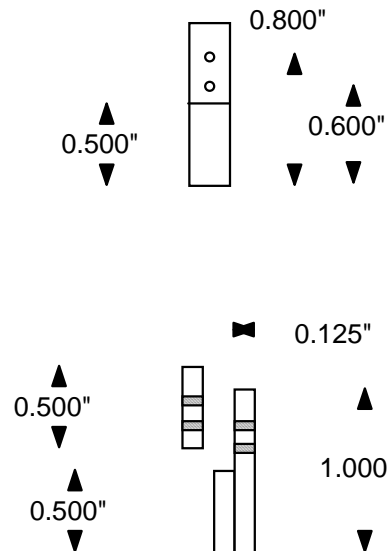


The black holes are 2-56 untapped holes that need to have a recessed area of 0.1 " for the socket screw head to fit into. The two holes need to be placed on a 30 degree separation from the other holes and 180 degrees apart from each other.

Then the part needs to be cut into two pieces along the above line so that the two can be electrically isolated from each other.

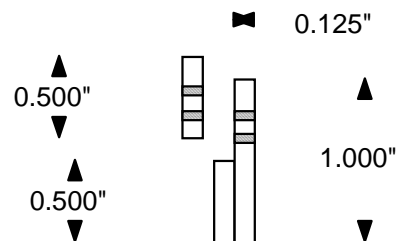


The basic starting piece for the Cs holder is a .250" by 1" 304 Stainless Steel rod



Side view 1:

There needs to be two holes of 2-56 tapped holes all the way through the piece. The where the 0.5 " line is the piece needs to be cut half way through.



Side view 2:

This shows how the piece needs to be cut in half lenght wise to the middle of the piece so that a section comes away. (This is later used to hold a flat piece of metal later)



Bottom view:

This shows a 2-56 tapped hole that is 3/8 inches deep.

- ¹ DOE Grant # DE-FG0595ER14563
- ² H. Xu, R. Yuro, I. Harrison, Surface Science 411 (1998) 303-315
- ³ R. Zehr, I. Harrison, work to be submitted
- ⁴ R. Zehr, C. French, B.C. Haynie, A. Solodukin, I. Harrison, Surface Science 451 (2000) 76-81
- ⁵ H.L Abbott, I. Harrison, J. Phys. Chem. B 209 (2005) 10371
- ⁶ "STM studies of Br on Pt(111), Thesis by Ray Yuro 1997
- ⁷ J. L. Beeby, Bal K. Agrawal, Surf. Sci. 122 (3) (1982) 447-458
- ⁸ Private communications with SAES getters
- ⁹ H. Schlichiting, D. Menzel, Rev. Sci. Instrum. 64(7) (1993) 2013-2022
- ¹⁰ "Photoinduced Electron Transfer Chemistry at Surfaces: Photochemical Activation of N₂ CO₂, and CH₄ on Pt(111)" Dissertation Robert Zehr 2005, University of Virginia
- ¹¹ S. Horch, P. Zeppenfeld, R. David, G. Comsa, Rev. Sci. Instrum. 65(10), (1994) 3204
- ¹² K. Besocke, Surf. Sci. 181 (1987) 145
- ¹³ S. Behler, M. K. Rose, D. F. Ogletree, M. Salmeron, Rev. Sci. Instrum. 68 (1997) 124
- ¹⁴ T. Farrell, J. Phys E: Sci. Instrum. 6 (1973) 977-979
- ¹⁵ John T. Yates "Experimental Innovations in Surface Science", (1998) Springer-Verlag New York
- ¹⁶ Extrel Mass Spec manual
- ¹⁷ "Instruction manual PHI 10-155/15-155 Cylindrical Mirror Analyzer"
- ¹⁸ "Handbook of Auger Electron Spectroscopy", 3rd ed. Ed. C.L. Hedberg, 1995 Eden Prairie
- ¹⁹ H. Xu, I. Harrison, J. Phys. Chem B, 103(51), (1999) 11233
- ²⁰ N.D. Spencer, P. J. Goddard, P. W. Davies, M. Kitson, and R. M. Lambert, J. Vac. Sci. Technol. A, 1(3), (1983) 1554
- ²¹ L. Arnberg, Acta Cryst. B36 (1980) 527-532

CHAPTER 3

STM OPERATION, DESIGN, CONSTRUCTION AND TIPS

3.1 SPM-32 PROGRAM DESCRIPTION AND OPERATION:

The SPM-32 program was written by Frank Ogletree at Lawrence Berkeley Laboratories, and is distributed by RHK Inc. to be used in conjunction with RHK's SPM-100 or SPM-1000 electronics controllers (described separately under STM electronics). The program was originally written in the early nineties under the dark reign of DOS. Many improvements have been made over the years, however, until the 2005 release of RHK's new XPM Pro software, the Scanning Probe Microscopy software was limited to use on Windows 98 or older systems, which needless to say causes some problems, mostly in memory management. The new XPM Pro software is written for windows XP and seems to be a bad facsimile of the latest/last version of SPM-32 written by Dr. Ogletree, which truly is a well formed program.

The SPM-32 program started life exclusively for STM but has continued to grow and evolve into a versatile and complex SPM program that encompasses STM, AFM, NSOM, or virtually any scanning probe microscopic technique that can be imagined. The complexity is controlled by a slew of settings that are kept in a parameter file which the SPM-32 accesses during start up. The parameter file "SPM32.prm" (30 print pages of

settings) contains all the information associated with approach, calibration, imaging and spectroscopy, plus many settings for all other SPM techniques that don't apply to our STM.

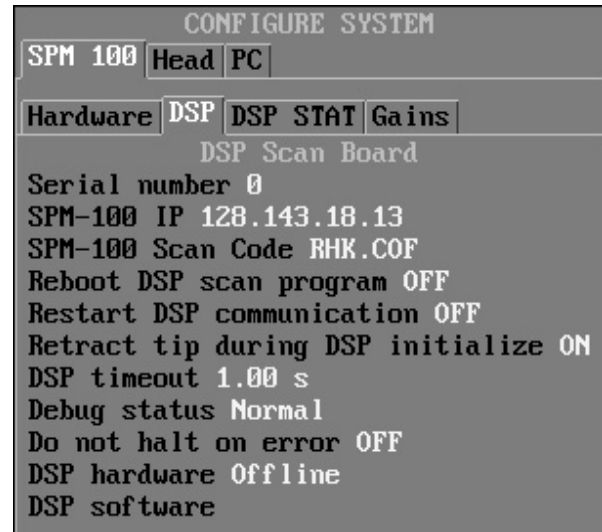
One of the problems of using a Windows based system is occasionally the communication between the SPM-32 program and the parameter file gets disrupted, which has the possibility of modifying the parameter file in unwanted ways. Therefore, once a working parameter file has been created it is imperative that a backup copy be made and updated with each successful configuration change to the parameters in the SPM-32 program.

After startup of the SPM-32 program, many windows appear. In my current



configuration there is an image window, a line scan window, and at a minimum the Parameter windows “Image Control” seen upon SPM-32 startup. Often times, I may have the “Scan Area Window” and a “Spectroscopy” window for I/Z curves open as well as the windows “Approach Control”, “System Settings”, and “Point Spectroscopy”. Additional parameter windows that I don’t keep open are: “Configure System”, “Image Spectroscopy”, “Analysis & Processing”, and “Display”. While a detailed description of everything in the SPM-32 software can be found in the SPM 32 user manual (nicely written), a broad overview of the settings and a brief explanation why I have the values set the way I do for our current STM setup is contained within this document.

The initial set up for the SPM-32 software requires establishing communication with the control electronics, via a 12 bit PCI DAC board and an Ethernet connected DSP board. Most of the communication settings can be found in the “Configure System” window. Other parameters for environmental setup can be found mostly in the “System Settings” window. To start with, the initial setup under the “SPM 100” tab then the “Hardware” sub-tab within the “Configure System” window the Electronics type needs to be set to RHK SPM-100 version 8 DSP scan control. This sets the type of controller used; there is a list to choose from which includes all older RHK controllers. Versions of the controller earlier than rev. 8 contain no DSP electronics, therefore some options may be



unavailable if a version older than 8 is chosen. Then under the tab “DSP” within “Configure System/SPM 100” The IP address of the SPM 100 is set. Currently the IP address of our SPM 100 is 128.143.18.13 and the computer IP address is set to 128.143.18.59. Both the computer and SPM 100 need static IP addresses due to the very rudimentary networking of the SPM 100. The RHK manual describes three ways to connect the SPM 100 to the computer with an Ethernet connection; 1) a stand alone isolated network with a direct connection between the computer and SPM 100 using a cross over cable. 2) a networked LAN connection where both the computer and SPM 100 are connected to a LAN through a router/switch or hub. 3) a combination of 1 & 2 where the computer and SPM 100 are connected together through a cross over cable, and a second Ethernet card is installed in the computer for a network connection. In the chemistry building at UVA the only possible connection scheme is 1 or 3. By connecting the SPM 100 to the internet as in scheme 2 there was too much network traffic for the low level networking capabilities of the SPM 100 to filter out. After this was discovered, a switching hub which should act as a first stage filter for network traffic was installed, with the SPM 100 and computer connected to it directly and the LAN connected to the input, giving a somewhat isolated local LAN between the computer and SPM 100, which still allows an internet connection for the computer. The network switch still allowed too much network traffic through, which interfered with communication from the computer. Therefore, it was decided to isolate the computer and SPM 100 from the net and just use the crossover cable. A second Ethernet card was not installed in the computer as a precaution to minimize IRQ interference within the computer.

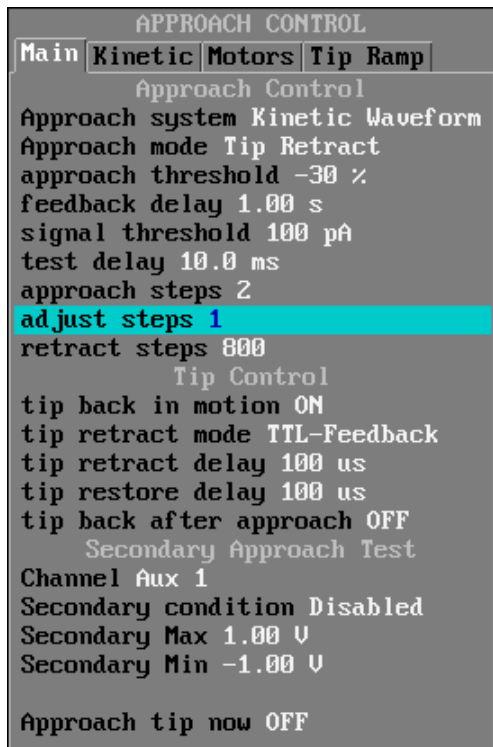
Other initial settings within the “Configure System” SPM 100/DSP; “SPM-100 Scan Code = RHK2K_01.COF” this is a program that allows communication between the SPM 32 program and the control electronics, upon start up this code is downloaded to the scan board and is resident there until power down. Another setting that needs to be correct is the A/D card type in the computer used for communication. This setting is found in “Configure System/PC”. The card that we use is a 12 bit 2821 DAC with a 150kHz clock, therefore the setting is “DT-2821-F 150 kHz”.

Environmental setting within the “System Settings” window controls how you interact with the SPM 32 program and how items are displayed. Within the “Pref” tab Use Angstroms is ON (just makes imaging and other parameter settings easier to deal with but it’s not mandatory.) The Interactive windows set to “Mouse select” which makes the window that was clicked the active one. There are other settings within this tab that are easy to experiment with and may be useful or not. Occasionally when the SPM 32 program is acting up turning the Debug messages to ON can be of great value, but otherwise these just waste desktop space.

The “file” tab in “System Settings”, contains many parameters that need to be set, some parameters need to be edited every time the SPM 32 program is run. To start with the Default disk is set to D:\. The STM computer has partitions set up on the hard drive to isolate all STM work, which gives 10 GB of working disk space. Once the partition is full, most of the images are transferred to the E: or F: partitions for accessible storage and to burn to DVD or CDs for archival storage. The “Default comment” parameter is a space that is filled in every time a change is made in the surface being imaged. It stores 512 k of text message that describes the surface parameters such as: “Pt(111) surface with 0.50

ML MeBr dosed at 20 K and annealed to 104 K, cooled and imaged at 20 K.” Other information such as the bias voltage and tunneling current are automatically included in the page information with the default comment for each image. The next important settings that need to be configured each time a surface is imaged is the “Save Auto name” needs to be ON and the “root” set to something meaningful to the image or operator, but can only use 8 characters (DOS names), and the index should be set to something that can be easily incremented and understandable. Therefore most of the images collected in the past have been something of day/month/index.sm2 “25apr001.sm2”. With this configuration the “autoincrement index” needs to be ON as well. All of these settings are not necessary but as stated earlier there are problems associated with using a DOS based program, most notably the memory management within the DOS operating system. Through the years there have been numerous times when the SPM 32 program just crashes, and if the images haven’t been saved to disk they are lost forever. Needless to say this is very aggravating if the imaging session has not been completed and some very good images are lost before being sorted and saved. After a few experiences with the program crashing and loosing good images, a solution was created by setting the “Page save mode” in the “Image Control (window) / Scan (tab) / Options (sub-tab) / Save/Display Options (heading)” to “index and disk”. With the page save mode set to “index and disk”, every completed image acquired is saved to disk, and therefore is not lost in the event of a computer crash. The problem with this solution is that it generates an excessive amount of data. Therefore analyzing the images after the session is finished and distinguishing which files can be deleted or kept for further analysis is necessary. This solution is possible because the autoincrement index option is turned ON.

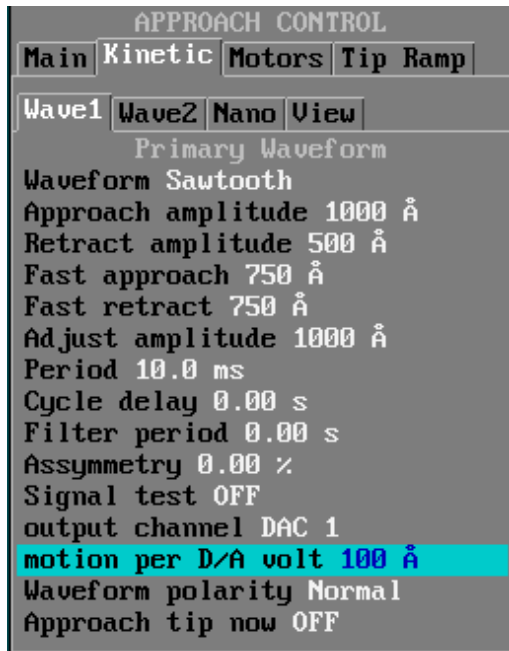
The last page of environmental variables to be set is located in the “System Settings” “Screen” tab. It is recommended that the screen resolution be set as high as possible for convenience, Some of the other settings are just to give a little bit more control over the GUI form of the SPM 32 program. Being it is a program written in DOS that creates its own windows environment there is more control over the interaction with those windows from settings in the Screen tab.



Once the initial SPM 32 program communications and environment is set, parameters that control the STM and how it operates can now be dealt with. The first to be addressed here is the STM Approach. All of the settings to control the coarse approach of the STM are set in the “Approach Control” window. This window has four tabs that contain additional sub-tabs with settings. The tabs “Main” and “Kinetic” contain all the setting necessary for STM coarse approach. Within the “Main” tab, the

Approach system needs to be set to “Kinetic Waveform”, by using the kinetic waveform approach many factors about the voltage output of the control electronics can be manipulated by settings under the “Kinetic” tab. Perhaps the most important setting of how the STM approaches the surface is the “Approach mode” used, it is important this parameter is set to “Tip Retract”. In the tip retract mode an approach cycle consists of ramping the scan piezo towards the surface to see if a tunneling current is detected, if not

the STM take a coarse step towards the surface and then again extends the scan piezo to test if a tunneling current is detected. Once a tunneling current is established that falls within the defined parameters set in the approach control window, the coarse approach process is halted. There are other approach modes that are much faster but have a higher risk of crashing the tip into the surface. Other parameters in the “Main” tab are “approach steps”, which I have set to two in order to decrease the approach time. It is possible to set this value higher but not recommended. By setting the approach steps to two, the tip retract mode tests for tunneling current and then take two steps towards the surface before testing for a tunneling current again. It is safe for us to do this because the change in Z by one coarse approach step is about a third of the Z scan range. The other two parameters that are of consequence in the “Main” tab are “approach threshold” and “retract steps”. The retract steps sets the number of steps to take in retracting the STM typically this is left set to 1000. However, if the approach only took 100 steps, then for that retract the number of steps need to be reduced so that the STM doesn’t retract off the back of the ramp. The “Approach threshold” is typically set in the range -50 to -20 %, which means that the tip is going to be set to $-Z\%$ of the Z scan range away from the surface. (Important to note: the scale starts at +100 % as fully extended toward the surface and -100 % as fully retracted from the surface. When this % is 0, meaningful images can be acquired. At values other than zero the D/A gain has to be set too low to keep the DAC from saturating, so surface detail is lost. A value of $-Z\%$ on approach allows for a large initial drift towards the surface that should hopefully settle down around 0%. Otherwise the Z offset knob on the controller is used to bring the Z scan into range.)



Within the “Kinetic” tab under Approach control, the “Wave1” tab is where our approach waveform is adjusted (which Wave, 1 or 2 is used for approach is set jointly in the “Approach / Kinetic / Wave1” by setting the output channel to DAC 1 and waveform approach to DAC 1 within the System settings-DAC window. If Wave 2 is needed, either set its output channel to DAC 1, or set it to DAC 2

with the waveform approach then set to DAC 2). A sawtooth waveform is used for both the approach and retract, with amplitudes of 1000 Å each (distance measurements here are meaningless because the approach distance cannot be calibrated). Other settings include the “Adjust amplitude” which dictates how big a step the STM takes when fine adjusting the Z position, this is typically set to a fractional amount of the approach amplitude (200 Å). Enable bipolar waveform is another parameter that needs to be set to OFF for a safer approach, while turning this parameter to ON creates a faster approach time by doubling the voltage swing applied to the piezos, it can make the approach step larger than the range of the Z scan which could then cause a tip crash.

The other sub tabs under the Kinetic tab is, Wave 2 which has all the same settings as in Wave 1, but allows a second approach waveform to be set. This typically is not used by us, but may be usefully in the future for defining a second STM. There is also

a Nano tab that contains settings for a different approach form. The most interesting tab is View, this tab allows the user to view the approach waveform that is set for approach.

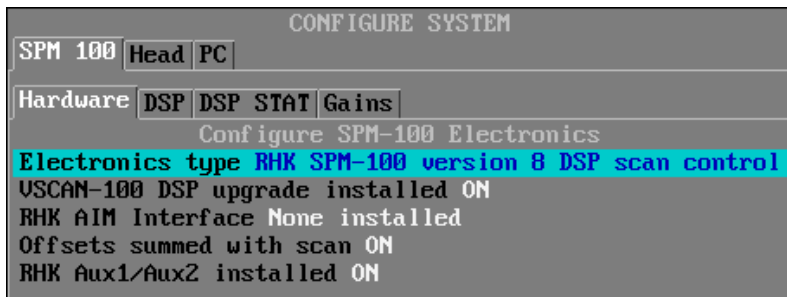
As mentioned above the output of the approach waveform should be assigned to DAC1. Part of this was set in the Approach Control menu and part set in the System Settings menu under the DAC tab. Other important DAC settings in the System Settings DAC tab are: IV spectroscopy, Z Spectroscopy out, and Lithography. Which DAC is assigned to each of the previous parameters is important in proper operation of the current STM. The other settings are important for the more advanced users when deeply interested in STM spectroscopies. Other parameters that have been used on this STM system have been, IV, Variable gap mode, Multivolt output, and CITS output. Although it is possible to do these secondary spectroscopies with our STM, the STM drift and stability render almost all of the information gathered from these techniques useless. Therefore, I will not cover an explanation of these modes and the appropriate settings here. If an understanding of these secondary spectroscopies is desired, information can best be found by first reading and fully understanding the SPM32 manual and secondly from STM spectroscopy books such as Wisendanger's "Scanning Tunneling Microscopy III".

The number of DAC outputs available on the SPM 100 controller is two. Therefore many of the DAC assignments in the SPM-32 program may have multiple parameters simultaneously assigned to one DAC. In the latest revision of the control electronics there is a DSP output that helps to alleviate some of the problems but, even so, occasionally when multiple spectroscopic techniques are needed on the same image a

rewiring of the back of the SPM 100 has to be done between spectroscopic runs. To keep things as simple as possible my DAC assignment is keyed to what I use the most. Therefore, Approach waveform is set to DAC 1 (always), I/V spectroscopy is set to DAC 2, I/Z spectroscopy is set to DSP DAC, and Lithography output is set to DAC 2 (always wired unless I/V spectroscopy is wanted).

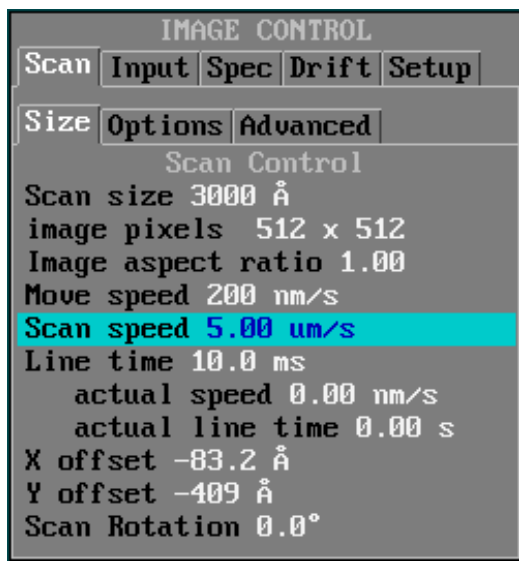
The Configure menu contains many important settings for a properly functioning STM. The first level of tabs within this menu is SPM 100, Head, and PC. The SPM 100 tab has been mostly covered

in the initial set up section of the SPM 32 operation, it does contain a sub tab “Gains” that all should be



left set to 13 (gain of Op Amps) for all XY& Z settings, the bias should remain set to 1 V and the current monitor needs to be updated with each change of the pre-amp or jumper setting in the secondary pre-amp stage. If the STM current monitor is not set properly the recorded current will not be accurate, but will not interfere with proper STM operation. Another tab, “PC” was also covered in the initial setup. This leaves the “Head” tab with many settings to be explained. Within the Head tab there is all of the calibration settings for the piezos. The current settings for the beetle STM is X motion per piezo volt 195 Å, Y motion per piezo volt 235 Å, Z linear motion per piezo volt 21.2 Å. Each of these parameters is determined by imaging a known surface and using the known distances to generate a Å/V setting. (Details on how calibration is done can be found in the STM

calibration section (3.3.) The other settings in this tab are Offsets summed with scan, and XY&Z offset per piezo volt. In our current generation of beetle STM (STM H in the RHK manual) the X and Y offsets are summed into the scan piezo. So, the offsets summed with scan is set to ON, and the X & Y offset per piezo volt is identical to the scan X and Y motion. The Z offset is left uncalibrated and is not summed into the scan head.



The menu window that will be used the most in day to day operation is the Image Control window. This window contains the tabs DSP, Input, Options, Spec, and Setup. Within the DSP tab are all the settings for acquiring an image. Most parameters in the DSP tab are self explanatory such as Scan size. By clicking on this parameter another input window pops up to accept any squared area setting with length units of Å. A setting of 500 would then be a 500 Å x 500 Å scan area. The other parameters of scan rotation and X & Y offset are similar in operation to the parameter scan size; any value can be input within the range of the STM. The Image aspect ratio should be left at 1.0. The Scan speed and Line time parameters can be extremely important in acquiring good images, by changing the Scan speed, the tip rastering speed across the surface is changed. A typical scan speed for a single line will be 100 ms, but this value can vary greatly depending upon the vibrational noise present. Beneath the line time parameter the number of pixels

each image contains can be set, there is a list to choose from that corresponds to binary sizes (i.e., 2^n) up to a scan size of 1024 x 1024 pixels. Next there is the Scan type, this is a new feature accessible due to the DSP board. Traditionally, only a triangle type waveform was used in image acquisition. Now there is a choice of linear (triangle) or sinusoidal (a half sine wave). Using a sinusoidal scan waveform noise in the image is easier to identify, and the act of scanning should induce less noise in the image. (The sinusoidal waveform is a single frequency compared to the triangle waveform which is comprised of many different frequencies; this reduces the chance of exciting resonant frequencies in the STM head that contribute to poor images.) Other settings in this tab are; Move speed set no higher than 500 nm/sec, and Standby action set to image start.

Under the Input tab in the Image control window there are a few important settings. Depending on what is being imaged it is necessary to turn on different inputs. Most all of the images that are acquired in this lab are done in constant current mode, Therefore, the Topography parameter is turned ON. The Current parameter should be turned ON if acquisition of images in a constant height mode is desired. Other parameters can be turned ON to acquire secondary information, along with the topographical image, such as Aux, Aux 1, and Aux 2. These Auxiliary inputs can take the output from a lock-in or other spectroscopic source and save those images synchronously with the topographical image.

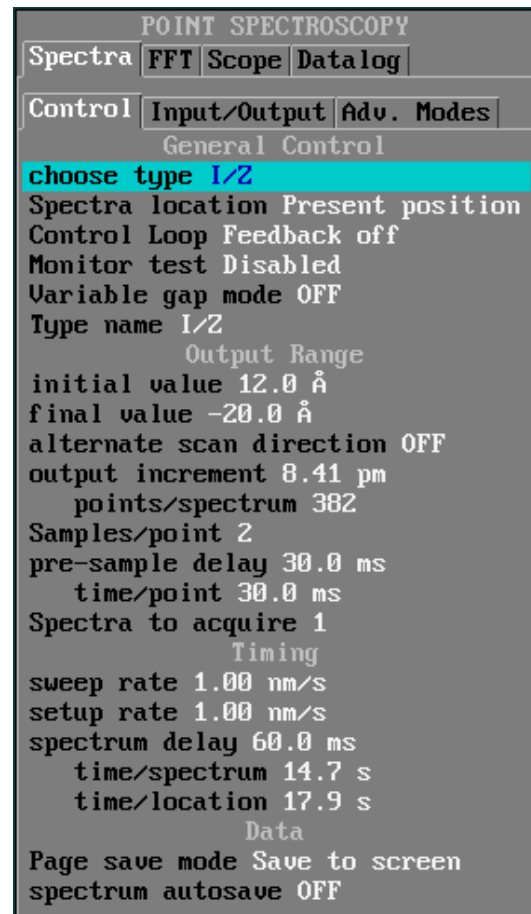
The Options tab within the Image Control window contains two important parameters. The first is the Line display, with the line display turned ON a scope window opens up and displays each line acquired during image acquisition. By examination of the

line scan it can be quickly determined if the image is a good one or if some settings need to be changed. The second parameter has been discussed previously, the Page save mode, this should remain set to Index and disk.

If scanning tunneling spectroscopy is required, parameters within the Spec and Setup tab should be examined and set appropriately. However, if are not being acquired these tabs can be ignored. Some spectroscopies do not require anything to be set in the tabs such as I/V, and I/Z. However, if CITS, multivolt, dI/dZ, or AFM modes are desired there are parameters that must be set.

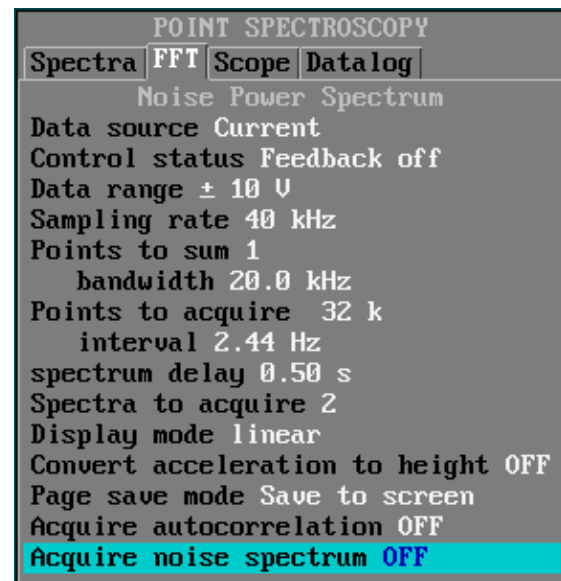
The Point Spectroscopy menu window

contains parameters for setting I/V, and I/Z curves, FFT, scope, datalog and some lithography. Both the I/V and I/Z tab contain two sub tabs of Control and Input/Output. In the Control tab of I/V the Control Loop is set to Feedback OFF, Variable gap mode OFF, and Threshold OFF. The Initial and final voltages can be set to whatever value is desired within a 10 volt range. After the range is set the size voltage increments can be set. The smaller the voltage increment, the better the resolution of the scan. However,



increasing the number of steps increases the time required for each scan, and the tip has to be stable (no drift) over the time required for an accurate I/V curve. The reason the acquisition time increases with increasing resolution is that there is a stabilization interval currently set to 50 ms after each voltage increase. With all the parameters in the Control tab set, the Input/Output tab parameters must be set. For an I/V curve the channels to acquire is 1 with Channel 1 set to Current and a range of +/- 10 V. The output channel is set to DAC 2. The STM bias mode is turned ON and the output volts per D/A volt are 1 V.

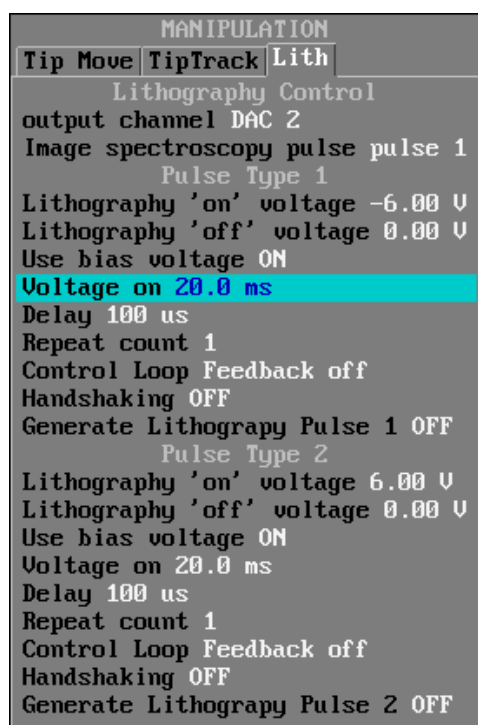
The I/Z spectroscopy tab has many of the same settings as the I/V tab. The Control loop has the “Feedback off” set, and an initial and final tip height is set, and the height increment sets the resolution of the scan. When performing a light tip crash, a range of + 8 to 15 Å is set for the initial height, with a final tip height greater than -10 Å. A typical height increment used is 0.05 Å. While tip crashing, the stabilization can be turned OFF. However, if meaningful I/Z curves are needed an initial height setting that does not place the tip in the surface should be set (e.g., -2 Å), and a stabilization time in the range of 50 ms after each height increment should be used. The Input/Output tab in the I/Z tab requires that the Channels to be acquired is 1, with Channel 1 set to Current, and the output channel for I/Z



spectroscopy set to DSP DAC. Also the tip motion per D/A volt should be set to the same value as the Z scan motion (i.e., 21.2 Å).

The FFT tab is very useful for diagnosing noise within the STM. Typically the Data source used for FFT is Topography (Current can also be used to examine more electrical issues), The control status is typically set to Feedback on to see how the tip is moving as a function of the noise (it is also possible to run this with the Feedback off if the tip position is very stable). The rest of the parameters can all be experimented with to generate a spectrum that is suitable for your needs.

Another important window is the Manipulation window. There are many tabs included in the window such as Acquire, Tip Move, Lith, and Tracking. The only tab that is useful to this STM setup is the Lith. Within the Lith tab two voltage pulse types can be



created. This is extremely useful while scanning to help keep the tip clean and sharp. The Output channel should be set to DAC 2. Underneath the output control there are two sub menus; Pulse type 1 and Pulse type 2. Both of the pulse types have the same parameters; an ON voltage and an Off voltage, also included are some delays and repeats. Typically an ON voltage pulse would be set to 3 or 4 volts and the OFF set to 0. The current configuration has Pulse 1 set to -6.0V,

and Pulse 2 set to +6.0V (However + and - 3.5 V is typical). Both pulses should have the Use bias voltage ON. The delay in each pulse is referenced to a trigger.

A very useful feature designed into the SPM32 program is the defining and using of Hot Keys. The use of Hot Keys allows quick and easy access to functions that may be buried within tabs of windows. The best and most frequently used form of Hot Keys is voltage pulses. The voltage pulses that were defined in the previous paragraph have been assigned to the keys “shift P” (Pulse type 1), and “shift Q” (Pulse type 2). With these keys defined, if the tip suddenly changes while scanning, hitting shift Q or P during the scan can sometimes bring the resolution back by removing the obstruction or picking up another molecule to tunnel from. Another useful Hot Key is “Shift N”, by typing this a FFT noise spectrum can be acquired.

The predefined Hot Keys are also very useful for STM operation. Most of the function keys on the keyboard have been assigned a particular STM function as well. The functions that are used most are F6 = image start acquisition, F5=Auto zero Image contrast, F7= switch scan directions, and F2=stop image scan.

If a numerical key pad is included on the keyboard, additional functions that translate the STM tip can be used as well. 8=shift up, 4=shift left, 6=shift right, 2=shift down. Moving the STM around the surface in this manner is preferred over adjusting the voltage knobs on the front of the SPM-100 controller because, with the DSP, the computer can keep track of precisely where the tip is. The program doesn’t know the absolute position on the surface if manual adjustments are made on the controller. This

being said it really doesn't matter if manual adjustments are made or not because the thermal drift with our STM is large enough that any position that you would direct the computer to return to would be very far off the desired location.

For a full listing of the defined Hot Keys go to the Help menu / Help Resources / User Hot Keys.

SPM32 DEFINED HOT KEYS	
F1	Main Menu
F2	Stop Acquisition
F3	Finish Image
F4	Save Image
F5	Autoscale Image
F6	Start Image Scan
F7	Swap X/Y Scan
F8	Close Image Scan
F9	Change Scan Focus
SHIFT-F9	Autoscale Focus
>	Focus shift up
<	Focus shift down
.	Focus expand
,	Focus contract
F10	Scan Area
F12	Data Index
+	Tip Step Out
-	Tip Step In
CTRL-H	Set Hot Key
CTRL-W	Redraw screen
CTRL-U	Set low res
CTRL-T	Clear text

SPM32 DEFINED HOT KEYS 2	
4	Image Shift Left
6	Image Shift Right
8	Image Shift Up
2	Image Shift Down
3	Image Expand
1	Image Contract
7	Image Rotate +
9	Image Rotate -

USER DEFINED HOT KEYS	
SHIFT-P	Lithography 1
SHIFT-N	Noise Power
SHIFT-Q	Lithography 2

Once a properly setup parameter set is created, the use of the SPM32 program for STM image acquisition is quite easy and straight forward. The approach is accomplished by left clicking on the screen and drag down to Approach which then brings up an Approach menu where Tip Approach is clicked and the approach is started. Once in

tunneling range, set the desired image size, scan speed, and other desired parameters and start the image scan by pressing F6. To stop the scan press F2 and occasionally take a I/V or I/Z curve to see how the tip is surviving. As needed trigger the voltage pulses to help clean up the tip or do the occasional tip crash if the tip needs to be reconstructed.

3.2 RHK SPM-100 AND ASSOCIATED ELECTRONICS:

There are three main electronic components from RHK that are used; the SPM-100 (contains HV drivers, scanning, long term integrator card, and feedback components), the PPC-100 (external box used for beetle STM approach), and the RHK family of pre-amps (IVP-200 & IVP-300 used in conjunction with a secondary amp IVP-PGA (14-1104090)).

First, let us explain the preamps. Currently, the Harrison lab has two different preamps for use. There is the IVP-200 which has a gain of 10^8 V/A (100 mV/nA), and the IVP-300 with a gain of 10^9 V/A (1 V/nA). Both the 200 and 300 preamps are designed for extremely low noise with a flat gain response over their entire frequency range. The frequency range for the IVP-200 is 50kHz, and 5kHz for the IVP-300. (Note: when changing preamps the displayed tunneling current in the SPM 32 program does not change unless the tunneling current gain setting is adjusted in the SPM-32 software. The displayed tunneling current on the SPM-100 will not change either, because, the SPM-100 electronics are calibrated only for a preamplifier combination that generates a gain of 100 mV/nA (10^8 V/A)).

Figure 1 Pictured below is the IVP family of RHK Pre-amps. The smaller boxes are the first stage amplification of the tunneling current and are connected to the isolated BNC feedthrough on the STM chamber. The larger box on the right is the second stage amplifier and can be used to adjust the overall gain of the pre-amp system and introduce noise filtering by an adjustable bandwidth response.



There are two stages of the tunneling current amplifiers (Figure 1). Both stages are located external to the STM chamber with the IVP-200 or IVP-300 connected to the STM chamber (tunneling current wire) through an isolated BNC feedthrough connector. It is important that this feedthrough be an isolation connector to reduce possible ground loops which would lead to unnecessary noise added to the tunneling current. The second stage is connected in-line between the pre-amp (IVP-200 or IVP-300) and the SPM-100 electronics. This second stage is identified as IVP-PGA. Unlike the pre-amps, the IVP-PGA has internal settings that controls how it operates. Firstly, there is a jumper setting

that sets the polarity of the gain stage. Both pre-amps are non-inverting, so the IVP-PGA should be set to non-inverting. The second set of jumpers in the IVP-PGA is for gain. The IVP-PGA is a variable gain amplifier and can have gains of 1X, 10X, or 100X. Typically this is left set to a unity gain, but is easily adjusted to accommodate smaller tunneling currents when desired. There is a third set of jumpers in the IVP-PGA to set the bandwidth of the amplifier. Seven filter settings are possible that range from none, to 150 kHz, to 500 Hz. The setting chosen depends on the imaging application. For very high speed imaging, a high bandwidth is necessary. For very low noise measurements a small bandwidth filter is appropriate. For general imaging I typically keep the bandwidth set to 5 kHz, which is also the bandwidth of the IVP-300 pre-amp. Additionally there are gain and offset adjustments that can be made to the IVP-PGA to correct for any non-zero voltages produced when no signal is applied.

The RHK SPM-100 control electronics is the heart of our STM imaging operation (Figure 2)¹. The internals of the electronics box consists of a power supply unit, waveform generation circuits, data acquisition circuits, and high voltage drive circuit boards. Most of the electronics are treated as a black box instrument where you accept what you get, and if there are problems RHK needs to fix them. However there are still a number of items in the electronics that can be set by the user for various purposes. As stated earlier the SPM-100 and SPM 32 combination has grown into a versatile platform for doing all kinds of scanning probe microscopies. The high voltage drive boards are designed for flexibility. By setting the correct jumpers on each board the electronics are able to accommodate many different scanner configurations. A listing of the major scanner designs are listed in the SPM-100 user manual along with the

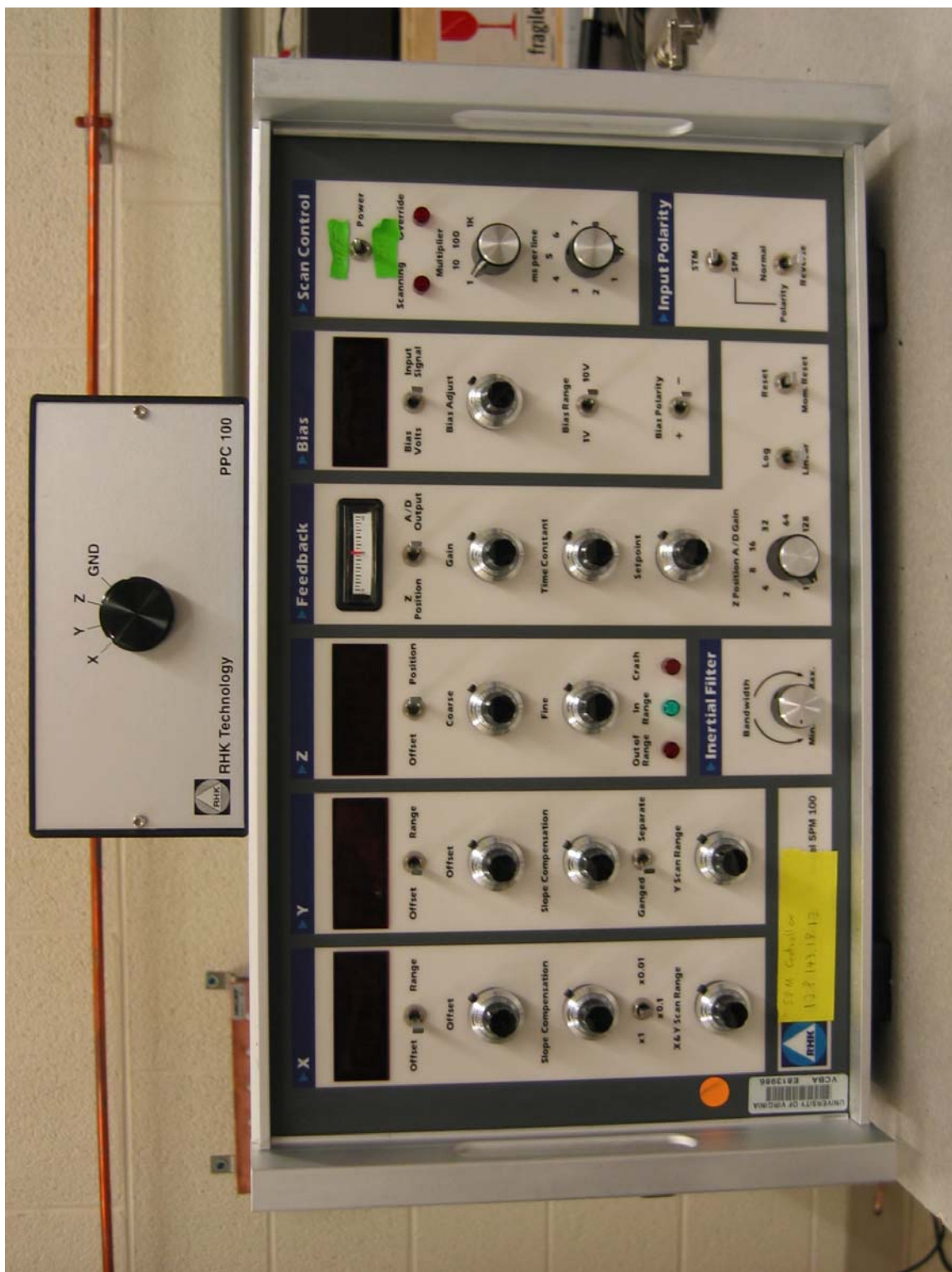


Figure 2 The RHK SPM-100 electronics

corresponding jumper settings used. The design of the Harrison lab STM would fall into the category of type H, (the X,Y,& Z scan are applied to the center piezo along with the X & Y offsets, and the Z offset is applied to the inner electrode of the outer piezo legs. Additionally the outer piezo legs are used for the inertial (coarse) approach. The jumper settings for type H STM are described in the wiring a STM section. Although most of the various STM configurations are listed in the user manual, not all are listed and at this point it is helpful to consult the electronics schematics that were included with the user's manual to determine which jumpers should be set to what connectors. An example of this would be, when the inner electrode of the scan piezo becomes corrupted by connection to another ground or spurious voltage source, but you don't want to break vacuum just yet and fix the STM. In this case, it is possible to rewire the jumpers so that the scan voltage is applied to the outer legs of the STM along with the Z offset. Obviously this is not an ideal situation but it can and has been done and atomic resolution was still achieved (of course, the time constants and gains have to be monitored very closely when trying to set this up.)

Perhaps the absolute best thing that RHK implemented in the design of their SPM-100 electronics was to include a current limiting resistor that would fry before the expensive precision operational amplifiers would. If there are ever any problems in the wiring of the STM, this resistor acts as a fuse which saves the op-amps. When wiring an STM for the first time, or any other time, it is all but impossible not to have some error in which none of the 21 0.005" dia. wires touch and shorts to another or to another part of the chamber. Even with numerous resistance tests done, it is possible to make a mistake. When that occurs and one of the Op-Amps tries to bring ground up to 130V, a 4.99

kOhm resistor is blown, which breaks the connection from the Op-Amp output to a piezo. When one off these resistors blows it is easy to identify first by the smell and then by looking at the card. By examining which resistor blew on which card, it is easy to narrow down which of the wires is the offender.

When a resistor does

Figure 3 High voltage card for the RHK electronics. There are four PA-83 OP-Amps on the card with heat sinks and each OP-Amp has associated with it a resistor that can be replaced. At the base of the card there are three jumpers that adjust how the card operates.



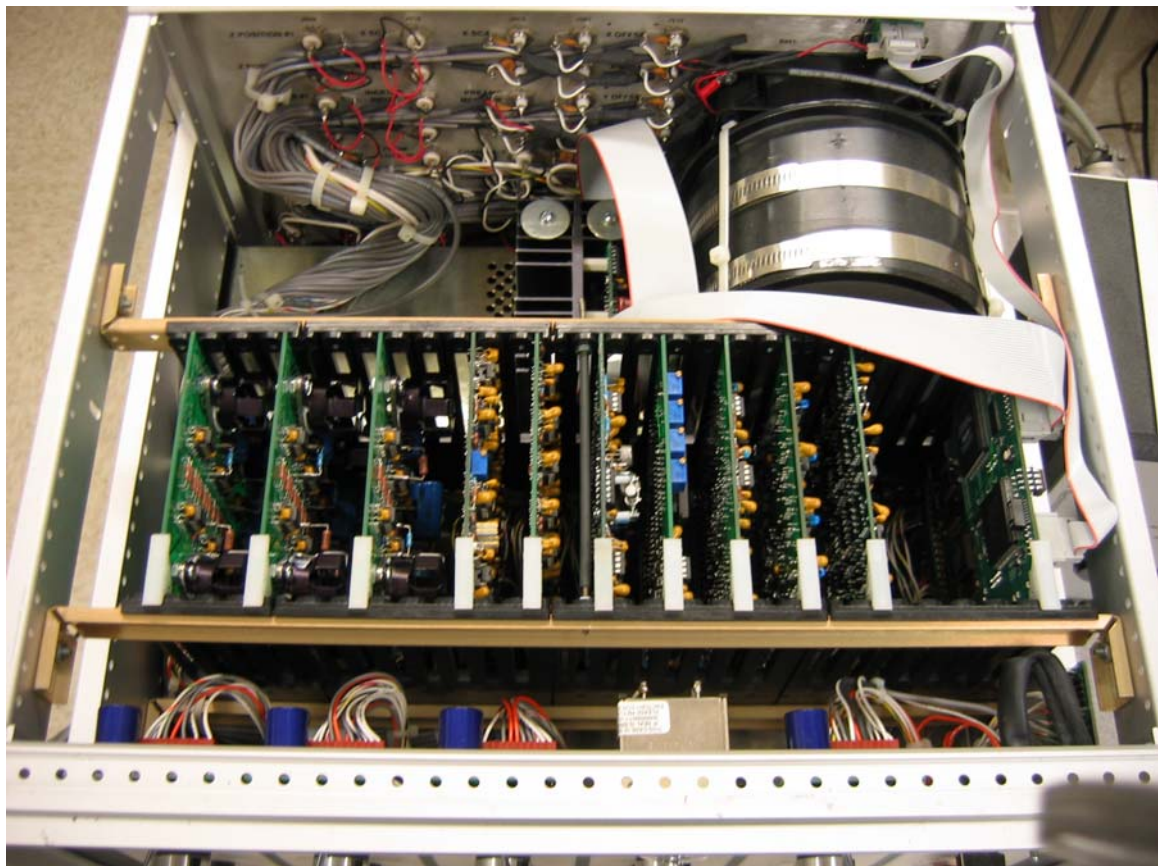
blow, simply remove the HV card (Figure 3) from the electronics and unsolder the bad resistor then reattach a new 4.99 kOhm resistor in its place. The card is reinserted into the electronics for use after the offending wiring problem is fixed.

The internals of the SPM-100 house an optional card that we chose to have installed, the long term integrator (LTI) card. The purpose of this card is to help eliminate the need for continual manual corrections made to the Z offset in order to keep the tip close to the surface when the scan DAC is not saturated but operating at very high A/D gains. This can be a very useful card to have when there is a small slow drift in the Z direction. The card works by monitoring the direction of the voltage applied to the scan

piezo to keep the tip at a precise current, and then calculates an offset voltage that can then be applied either to the scan piezo itself or to the Z offset. In our case it is applied to the Z offset to minimize the chance of Z scan piezo voltage saturation. To wire the LTI card for operation, a BNC coaxial cable should be connected between the LTI card output on the back panel, to the Z position modulation inputs located on the back panel. According to RHK the LTI card can be connected and used at all times. However, in practice the LTI card should be connected after initial tip approach and a substantial time has passed for the STM drift to settle down to the point that the LTI card can keep up with the drift. In my experience using a T BNC connector connected to the LTI output and a coaxial cable connected to a multimeter to monitor the output of the LTI is the best way to monitor what is going to be applied to the Z offset before connecting the LTI card. While RHK says that it's alright to connect the LTI card anytime during STM operation, I have found this not to be the case. An example: when connecting the LTI card during operation if the tip distance is such that the Z scan voltage is stable at a negative value (meaning the tip is not at the center of the Z scan range, farther away from the surface than it should be) the LTI card sees this and wants to apply a voltage to move the Z scan voltage back to zero. To do this the card generates a positive voltage anywhere from 0 to 10 V which when connected to the Z modulation gets multiplied 13 times. Depending on how much voltage is ultimately applied this can be very detrimental to the STM tip. Imagine a STM that was an angstrom too far away from the surface for perfect tunneling conditions and instantaneously a 130 V was applied to the Z offset resulting in a distance change of 1000 angstroms towards the surface. Unless the gain was extremely high and the time constant very low the STM will not react fast enough to account for the sudden

change in distance. Because of our STM tunneling conditions the gain is kept very low (in the range of 0 - 0.7 out of 10) and the time constant relatively high (2.3 out of 10) which doesn't respond instantaneously. So for our typical tunneling conditions, simply connecting the LTI card can easily result in a catastrophic tip crash. This is why the multimeter is used, the tip can be adjusted so that the voltage output from the LTI card monitored by the multimeter, can be set as close to zero as possible. When the LTI card produces a voltage within a few tens of mV's of zero the card can safely be connected to the Z position modulation connector.

Figure 4 An internal look at the electronics of the SPM-100. The HV cards are the 3 on the left hand side.



There are other cards located inside the SPM-100 such as the DSP board, a log amplifier board, and an offset board. On some of these boards there are jumpers that can be set. However, there should be no reason to make adjustments to these boards unless instructed to do so by RHK.

Figure 5 Image of the front panel of the SPM-100



The front panel of the SPM-100 (Figure 5) is where a lot of adjustments are made. To describe the front panel and its operation, it is

useful to notice that the panel is divided up into sections for easy identification. The first section to be discussed is the “Scan Control”. Within this section the SPM-100 can be powered on / off and have its scanning speed set by the “multiplier” and “ms per line” knobs. Previous versions of the SPM-100 without the DSP circuitry required the scan speed to be set and adjusted by these knobs, and that functionality is still present in the revision 8 electronics, however it is best to leave the scan speed controlled by the DSP board. To set the electronics to obtain the scan speed from the DSP board, the “ms per line” knob needs to be set to zero (the zero is not labeled it’s just assumed to be located between the 1 and 9).

The section “Input Polarity” is located just below the Scan Control and contains two switches. The only switch that affects the operation of our STM is the STM / SPM switch. For correct operation of the STM the switch needs to be flipped to STM. While the switch is set to STM an extra gain inverter is applied to the feedback line to insure correct motion of the tip with a change in tunneling current. With the STM selected the Normal / Reverse switch is ignored -a switch only relevant to other SPM techniques.

The “Bias” section contains a digital LED numerical display, a knob and 3 switches. The display shows either the bias voltage or the tunneling current depending on the setting of the top switch. The only knob in this section is used to adjust the bias voltage. This knob has a range from 0 to 10 and is multiplied by 0.1 X or 1 X depending on the bias range switch, which can be toggled between a 1 V and 10 V range. The third switch in this section selects the polarity of the bias voltage.

Within the “Feedback” section there are many adjustments that can be made during STM operation. This section contains an analog panel meter at the top that displays either the Z position of the STM tip or the A/D output depending on which way the toggle switch below the meter is set. There are two other toggle switches in this section that are rarely or never used. The Log / Linear switch changes the behavior of the feedback loop in the SPM-100, One might assume that it would be better to use the log setting for STM operation, however, the correct setting is linear, (log theoretically can be used but in discussions with RHK they were unable to get it to work and are at a loss to explain why.) The last switch is the Reset / Mon. Reset, and it is a three way toggle. This switch is normally in “neutral” and is only used when doing field emission. The correct way to use the switch is explained in the field emission document. Along with the toggle

switches there are three knobs and a binary selector switch. The binary selector switch is labeled “Z Position A/D Gain”, and there are settings of 1,2,4,8,16,32,64,128. While the STM is approaching, the correct A/D Gain setting is 1. A setting of 1 has the lowest Z position resolution with the highest useable Z range. After approach it is necessary to increase this A/D Gain so atomic resolution can be achieved. Generally to get a good image of the surface, the A/D Gain is set at 64 or 128 depending on how much drift is present.

The A/D gain resolution is explained by looking at the number of bits present in the ADC card and the range that it has to cover. The card that comes with the STM electronics has a 12 bit ADC which renders 11 useable bits due to the parity bit. This gives 2048 bits to divide the range up. If the A/D gain is set to 1, the bits divide up equally the 130 V offset that can be applied. This gives a 0.0634 V/bit resolution. Taking the bit resolution multiplied by the Å/V of the Z piezo (22.1 Å/V) generates a height resolution of 1.40 Å/bit, not nearly good enough to achieve atomic resolution. However if the voltage that the ADC has to encompass is reduced, then the distance resolution will increase. Therefore, at a A/D gain of 128 (130 V/ 128) the voltage range that the ADC has to cover is 1.01 V. Which gives a bit resolution of 0.000496 V/bit (1.01/2048), multiplying this bit resolution with the Å/V of the Z-scan piezo gives a height resolution of 0.011Å which is possible to image low corrugation surfaces.

$$\frac{V}{\# \text{ of Bits}} \times \frac{\text{Piezo } \text{\AA}}{V} = \frac{\text{\AA}}{\text{Bit}}$$

The three knobs located within the Feedback section all have ranges from 0 to 10 and control from top down; Gain, Time Constant, and Setpoint. The Setpoint is the tunneling current value and is calibrated such that with a gain of 10^8 (1 nA/V) a setting of 1 corresponds to a tunneling current of 1 nA. The Gain and Time Constant knobs effect how the tunneling current feedback system operates. These two knobs can be thought of as the Proportional, and Integrative bands of a PID setting respectively. The Gain should be operated at as high a level as possible without putting the feedback into oscillations, and the Time Constant should typically be run in a range of 2.2 – 2.4.

The “Z” section on the front panel of the SPM-100 contains only two knobs, a switch, an LED display, and some indicator lights. The LED display will show the offset voltage applied to the outer piezo legs or the voltage that is being applied to the Z scan piezo depending on which way the toggle switch is flipped (Offset or Position respectively). The two knobs are again 0 to 10 knobs which control the voltage applied to the Z offset used to keep the Z scan piezo at the optimal applied voltage setting of zero. The Coarse knob is used for large movements and the Fine knob is used for a more detailed control over the Z position. An important note about the initial setting of both knobs are; a knob setting of 5 corresponds to an output voltage of 0 V, therefore with values greater than 5, a positive voltage is applied; with values less than 5 a negative voltage is applied. During approach the setting of both coarse and fine knobs should be set to 5 which produce a range of adjustments used to compensate for the tip drift towards/away from the sample surface. The indicator lights that are just below the fine adjust knob gives a quick visual check of the condition of the tunneling current. When tunneling, the “In Range” light should remain illuminated. The other indicator lights are

fairly self explanatory as “Out of Range” and “Crash”, but can be somewhat confusing when doing tip manipulation procedures. It is important to note that the indicator lights are not actual displays of the tunneling current but indicators of the voltage being applied to the scan piezos. Therefore, when a voltage of +130 V (maximum of SPM-100) is applied to the piezo to try and move the tip closer to the surface and the set tunneling current is still not reached the out-of-range light will turn on. Alternatively, when the SPM-100 applies a -130 V potential to the scan piezo to retract the tip fully and still measures a tunneling current higher than the set tunneling current (setpoint i.e., 1 nA), the crash light is illuminated. The indication of crash or out of range is not dependent on the tunneling current, just the voltage applied to the piezo, so when the “tip withdraw” is activated in the SPM-32 software the crash light is activated.

Located just below the Z section of the SPM-100 on the front panel is the inertial filter. The inertial filter is used in the STM tip approach. When using a sawtooth approach/retract waveform, a high frequency noise can result from sharp changes (e.g. take a Fourier transform of a triangle signal). To minimize this effect an in-line inertial filter is inserted which is a variable low pass filter that smoothes out the transitions in the sawtooth waveform. The typical setting for us is approximately 9 o’clock on the knob. This filter can be adjusted from no filtering (all the way counter clockwise), to very large amount of filtering (fully clockwise). Running the approach with an inertial setting higher than typical will result in a slow and poor approach because the slip stick motion of the beetle needs a relatively sharp voltage transition for the quick snap to break the static friction holding the balls to the mount. The setting of the inertial filter must be adjusted

for each STM used. It was found that a setting of approximately 12 o'clock was needed for a heavy STM with tungsten carbide balls.

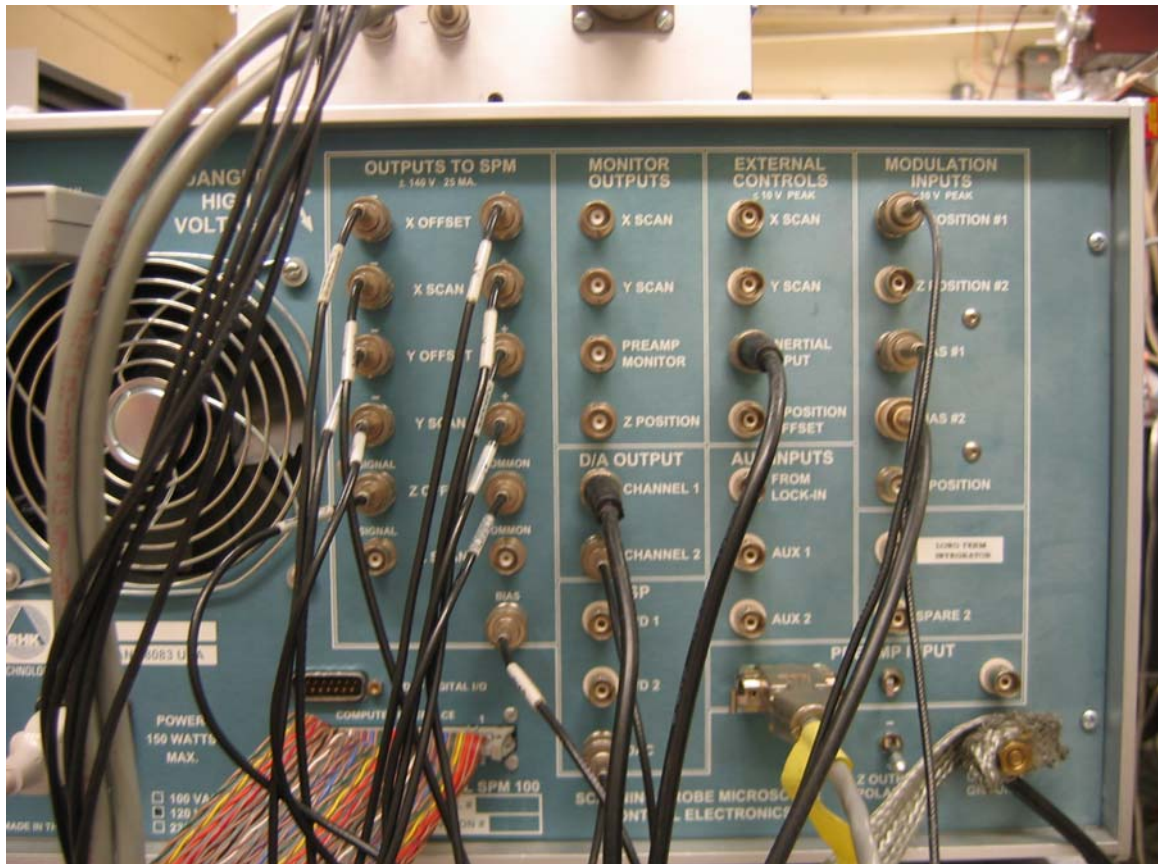
The last two sections on the front panel of the SPM-100 can be discussed together because they have many of the same functions. These sections are controls for the "X" and "Y" offset/scans. Both sections have the LED display that shows a voltage applied to the offset or a voltage that controls the scan range of the STM depending on the position of the toggle switch below the LED display. The toggle switch is mostly left in the offset position. Below the LED display and toggle switch is an offset dial with a range from 0 to 10. Here again, the offset dial needs to be set to 5 initially to apply zero voltage to the piezos. After approach the offset knobs can be used to move the tip in either direction +X/Y or -X/Y. Below the offset knobs is a very important knob that adjusts the scan slope. The slope compensation knob is used when the STM tip is not tracking across the sample surface perfectly parallel to the surface normal. In this case, the Z position A/D gain may have to be lowered to 64, or worse yet 32, in order to keep the scan within the range of the ADC card, and the lowered A/D gain will begin to limit the Z resolution in the Z direction (at A/D gain of 128 the Z resolution is 0.01 Å/bit, at a A/D gain of 32 the Z resolution is 0.044 Å/bit). Therefore, it is important to adjust the slope compensation knob until the Z-line scan shows a horizontal terrace. (zero voltage output for these knobs is for a setting of 5). Finally, let us address the scan range adjustments. There are two toggle switches and two 0 to 10 knobs. The first toggle switch within the X section adjusts the scan range by factors of 10. Typically this is set to X 0.1, and occasionally when very small scans are required the X 0.01 setting is used. The second toggle switch dictates how the range knobs operate. In previous versions of the RHK SPM-100 the scan

range for X and Y could be set separately. This functionality was very rarely used because it resulted in some odd images where in the X direction there might be a resolution of $0.1\text{\AA}/\text{pixel}$ and in the Y direction a resolution of $10\text{\AA}/\text{pixel}$ depending on how the range knobs were set. We now gang the two range settings of the SPM-100 together and they are controlled by just one knob located in the X section. The toggle switch below the Y slope compensation knob can be set to separately control the X and Y scan ranges individually if necessary.

The back panel of the SPM-100 is where all electrical connections are made. This back panel (Figure 6) is divided into sections much like the front panel, with some connections being self explanatory and others requiring a bit of insight. Briefly, the sections and their connections will be described. Afterwards, the more specialized connections for spectroscopy and tip manipulations will be described.

The initial SPM-100 connections include the 120 V 60 Hz power connection and a 50 pin ribbon cable connection to the Data Translations DAC card in the computer. An Ethernet connection to the computer accesses the DSP card in the SPM-100. However, the SPM-100 does not have a 10/100Base-T connector that is typical for a PC. A 10Base-T to AUI converter is required to connect to the AUI connection of the SPM-100.

Figure 6 Back panel of the SPM-100 where all electrical connections are made to operate the STM.



Outside the defined sections on the SPM-100 back panel, there are two other important considerations. The first is a toggle switch to adjust the Z output polarity that should be left set to + for normal STM operation. The second item is the chassis ground connection post which provides a central termination point important for eliminating ground loops.

The first section of connectors on the back panel is the output to the piezos. All of these connections utilize BNC connectors for easy connect/disconnect. There are outputs for + and – X offset, + and – Y offset, + and – X scan, and + and – Y scan. There is also a connection for the bias voltage and connections for the Z scan and Z offset. Both of the Z scan and offset connections have a BNC connector labeled “Signal” and one labeled “Common”. Most of the connections in this section are self evident and a more detailed description of where each connector leads to can be found in the STM wiring document. A quick recap of these connections are: the four X and Y scan outputs go directly to the scan piezo on the STM, and the four X and Y offset connections get plugged into the PPC-100 (discussed after the back panel description) which are divided up and redirected to the 12 electrodes on the legs of the STM. The Z scan connection has one wire that is connected to the “Common” connection (doesn’t matter if the Z scan or offset common is used). The one wire that is connected to the common runs directly to the scan piezo to ground out the interior wall of the scan piezo which limits noise on the tunneling current wire. The Z offset has a single connection to the “Signal” BNC connector which runs to the interior portion of the three legs of the STM. Because the tunneling current is collected at the tip in our home built STM the bias BNC connects to the crystal sample.

Next, there is a section of monitor outputs. These outputs can be plugged into an oscilloscope to monitor how the signals are changing. The typical outputs that are monitored are the pre-amp tunneling current and the Z position. It is important to monitor both of these outputs to examine the noise in the system. By looking at the pre-amp output, the gain knob on the front panel can be adjusted to give the optimal amount of gain without exciting oscillations of the tip from noise. Additionally, by connecting the

pre-amp and Z position monitor outputs to a digital FFT scope or spectrum analyzer a “real time” view of the noise can be seen, which is extremely useful when looking for sources of noise.

Below the monitor outputs section there is a D/A output section. This section contains a Channel 1 and Channel 2 output BNC’s. These outputs are used to help control the operation of the STM, where the functions that either DAC 1 or DAC 2 are assigned to can be found within the SPM-32 software, and is discussed above in the software section. The typical DAC 1 is assigned to the STM approach, and has a BNC cable connecting it to the “Inertial Input” BNC within the External Controls section. The DAC 2 output is usually used for a spectroscopy or tip manipulation purpose. It can be connected via a BNC cable to any of the connectors in the External control section or Modulation Inputs section.

Below the D/A output section is the DSP, which could be lumped in together with the D/A output section, because it is typically used as another D/A output that can be controlled easily by the computer. The DSP DAC BNC connector can be used as another spectroscopy or tip manipulation output that can be connected to any of the connections in the External Controls or Modulation Inputs sections.

Another section of connections on the back panel of the SPM-100 is the “External Controls”. These connections are used to create movement of the STM tip in some fashion. The connections can accept up to a 10 V input signal. There are connections to control the X or Y scanning of the tip. There is also a connection for the inertial input used for tip approach, and a Z position offset that is used in conjunction with the long term integrator card. The connection for the inertial input has been discussed above and

typically takes an input from the DAC 1 output. The Z position offset applies a voltage to the interior of the piezo legs of the beetle STM.

The sixth section on the back panel is Aux inputs. These are 0 – 10 V inputs and are used mostly for spectroscopy. The difference between the external control, modulation inputs, and the Aux inputs are that the Aux inputs are used for monitoring/recording signals such as a signal from a lock in amplifier to do a dI/dV or dI/dZ spectroscopies. Once the signals have been connected to the SPM-100 via the Aux inputs, the corresponding input in the SPM-32 software program can be activated to monitor the signal.

One of the last sections on the back panel is the Modulation Inputs. These inputs are like the External Controls in that they accept inputs of 0 - 10 V. However, the modulation inputs section contain inputs to modulate the Z position (2 inputs), and the Bias voltage (2 inputs), and one X position input. The Z position connections is used for spectroscopies such as I/Z or dI/dZ, and the bias modulation connections can be used for I/V and dI/dV spectroscopies. There is even a possibility for improved spatial resolution in the X direction if a lock-in is used to apply a small dither to the X position and the dI/dX signal is recorded (Ideally this would eliminate some lateral noise in the STM and lock on to how the current changes when scanned across the surface).

Below the modulation inputs section are two connectors that are labeled Spare 1 and Spare 2. There connectors are open on the interior of the SPM-100 and are therefore free to be used for extra cards or functions that the SPM-100 can accommodate. Presently, we have one of the Spare connections attached to the long term integrator card

(LTI), which then connects to the Z position offset input amongst the back panel external controls using a BNC coaxial cable.

The last section on the back panel of the SPM-100 is the Preamp input. There are two possible connections that are used to connect a preamp to the SPM-100. There is a 9 pin connector that is used with the RHK IVP-series amplifiers, which contain connections for the signal, ground, a +/- 5 volt power connections and a +/- 15 V connections for supplying power to the op-amps. Alternatively, a home made preamp system can be used that uses only a shielded tunneling current voltage that connects via a BNC connector. It is important to make sure that the selector switch is set to the preamp system being used.

Now the connections for the different spectroscopies and tip modification methods are discussed: First, we'll consider the connections used for I/V spectroscopy. Monitoring how the current changes as a function of voltage can help give insight into surface states of the sample and reveal some of the characteristics of the tunneling tip. The connection for I/V spectroscopy is to use a BNC cable to connect the DAC 2 output to the Bias 1 input. Alternatively, I/Z spectroscopy can be used to examine how the tunneling current is dependent upon the distance away from the surface. The information in I/Z spectra can be used to estimate the local work function of the surface. I/Z spectroscopy requires a BNC cable to join the DSP DAC and the Z position 1 input. As it turns out, the I/Z spectroscopy mode is very important in tip modifications, where an I/Z spectrum is run for which the initial tip height setting makes the tip touch the sample surface and then it is retracted to form an atomically sharp tip. Other spectroscopies include dI/dV and dI/dZ modes where a small dither is applied to the bias or tip height

respectively and a lock-in is used to extract the appropriate signal which is input in to either the lock-in or aux inputs within the Aux inputs section. To achieve some of the tip modification necessary for our STM's operation a voltage pulsing technique is used requiring a connection from the DAC 2 output to either of the bias inputs within the Modulation inputs section. The last connection that needs to be made is the long term integrator card that has an output in the Spare section (on our SPM-100 it is labeled long term integrator (LTI) card). Connect the LTI output to the Z position offset within the External controls section.

The last item that needs to be discussed is the role of the PPC-100 (Figure 7) in the overall STM electronics scheme. The PPC-100 is an external box purchased from RHK that functions as a variable splitter and voltage divider to connect 12 different electrodes on 3 piezos from just 4 inputs coming from the SPM-100 (only 2 are use). With the PPC-100 in-line connection the SPM-100 is able to drive the beetle STM. The PPC-100 is simple in

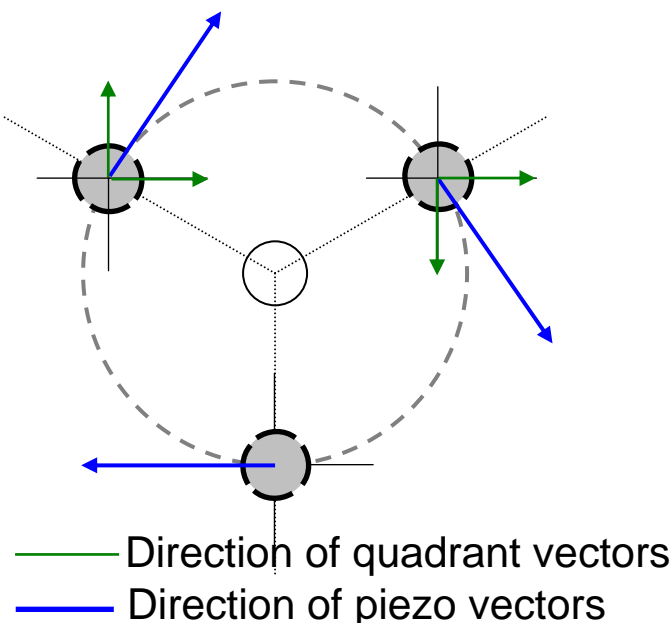
operation and has a large front panel selector switch with four settings: ground, Z, X, Y. When the STM needs to be approached or retracted from the surface, the switch must

Figure 7 The PPC-100 is used for the beetle STM approach and retract. Depending on the PPC-100 setting the STM can approach/retract from the crystal, or move macroscopically in either the X or Y direction.



be set to Z. Alternatively, to increase the scan range of the beetle STM the selector switch can be set to either X or Y and an approach/retract voltage pulse applied to the legs in order for the STM to move macroscopically in the X or Y directions. (Note: this is possible because our beetle STM is set with an internal coordinate system where all of the piezos are oriented such that there is an X and Y axis system for the STM as a whole. See wiring the beetle STM for a detailed piezo alignment description.) The last position the switch can take is ground. The ground setting is used to ground out all of the external electrodes on the leg piezos to minimize electrical noise from capacitive coupling from the leg wires to the scan wires and also to eliminate the risk of introducing shaking of the STM by having an oscillating voltage on any of the outer electrode on the legs that would cause an expansion or contraction of the piezo when compared with the Z offset voltage applied to the inner wall of the leg piezos.

Figure 8 Diagram showing the X –Y global coordinate system for the STM.



As stated previously the PPC-100 is set for a specific type of beetle STM that have the piezos organized in a global coordinate system (Figure 8). However, it is possible to adjust how the PPC-100 operates with an understanding of its internal electronics. The internals take the input from the + and - X offset

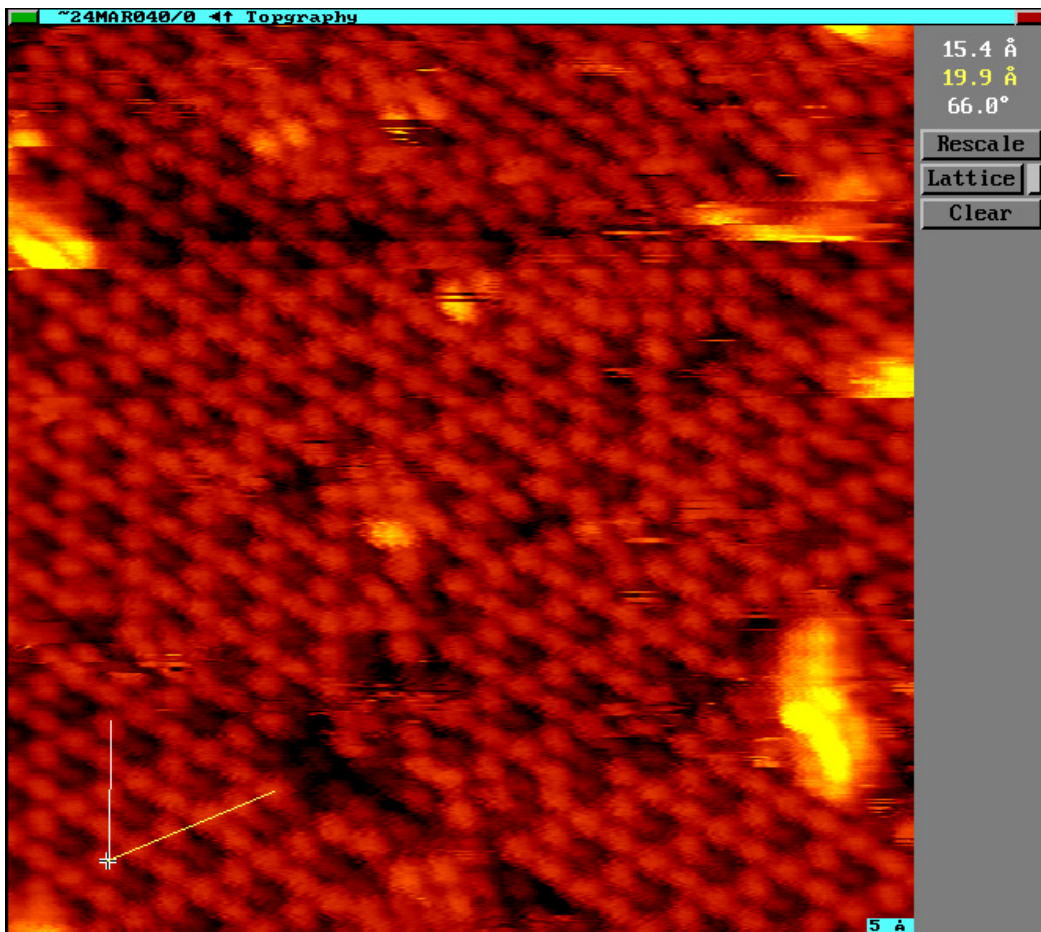
from the back of the SPM-100 and use only these two inputs for Z approach. When the selector switch is in the Z position, the two X input are diverted into a bank of 12 variable resistors. The outputs of these resistors are directed to the quadrant electrodes on the three piezo legs. Because not all electrodes are oriented along the rotation axis of the STM, varying voltages are needed to compensate so that the summed motion vectors applied to each piezo leg results in a movement that is tangential to the rotation of the STM. If a different arrangement of piezo electrode is used, adjustment can be made to the variable resistors to get the summing of voltage generated movement vectors to generate the desired movement. Additionally, if the motion of our current beetle piezo electrode arrangement is producing odd movement, changing the resistances within the PPC-100 to get the correct motion may be necessary.

3.3 CALIBRATION OF THE PIEZOELECTRICS:

3.3.1 X & Y PIEZO CALIBRATION:

The lateral calibration of the STM is simple when done with the SPM32 program. First a rough range of the piezo need to be set which can easily be determined by the formulas for piezo movement.^{2,3} After the rough calibration has been set an atomically resolved image of a known surface should be acquired. This image may look distorted, but represents the first stage in calibration. Typically, I use an oxygen (2x2) lattice on the Pt(111) surface imaged at 20 K as my calibration standard. It is important to note that the calibration of the STM should be done at the temperature at which the majority of the images of interest will be imaged since the piezo voltage response is temperature dependent. The piezo distance/voltage sensitivity at 4 K is half the sensitivity at 300 K. If a room temperature calibration is desired the Pt(111) surface is the ideal calibration

standard. Once repeatable images can be acquired under various scanning conditions to ensure there are no tip peculiarities, calibration can be done. Click on the upper left hand corner of the image to access the cursor control mode in image analysis. Next select image lattice. This produces a side window where some parameters can be input, and on the image a V is generated with points on it labeled A, B and C. The point labeled C is the origin of a lattice. Place that on top of an atom of oxygen, and move the ends of the V with points labeled A and B to other atoms on the surface (it is best to maximize the distance of the lines A and B to increase the averaged accuracy.) On the right hand side of the image, length values for the A line, B line and the angle between A line and B line are displayed. Click on the Lattice button, this brings up another window that asks for the correct distance of line A. Then, it asks what is the correct distance for line B and finally the correct angle between A and B. The correct distance value of A and B can be determined by counting the number of atoms of oxygen along line A and multiplying by [2 * Pt(111) atom spacing (2.78Å)], the same is done to determine the correct distance for B, and the correct angle should be some multiple of 60 degrees. Once all this information has been entered into the lattice inputs the program spits out a correction factor for X and Y. This correction factor is then multiplied to the initial X and Y scan sensitivity parameters, and the resulting values are henceforth used as the calibrated piezo distance per volt sensitivities.



3.3.2 VERTICAL CALIBRATION OF THE SCAN PIEZO:

The vertical calibration of the scan piezo is very simple. Like the lateral calibration an image of a surface is necessary. It is best to image the clean/bare Pt(111) surface and find an area that contains 3 to 8 terrace steps. The lattice constant of the crystal is used to determine the height of the monatomic steps, which is then compared to the height value measured in the image, a formula of (3.1).

$$\text{Calibration}_{\text{Corrected}} (\text{\AA}/V) = \frac{\text{Calibration}_{\text{current}} (\text{\AA}/V)}{\left\{ \frac{\text{Height}_{\text{measured}} (\text{\AA})}{\text{Height}_{\text{Actual}} (\text{\AA})} \right\}} \quad (3.1)$$

can be used to determine the correct calibration of the Z scan that is then entered into the Z motion per piezo volt within the Config window. Items to be aware of while calibrating the Z scan are: it is best to average over multiple step to reduce measurement error which is why finding an area with multiple steps is used. Secondly it is also important to be aware of what is being imaged, not all steps in the terrace are one atomic layer high. Make sure that the measured terraces are a known number of atomic steps high when used as a known standard. Typically if multiple terraces are imaged the smallest step height would correspond to a single atomic step. Note that a single step on a Pt(111) lattice is 2.27 Å high, different from the in plane atomic spacing of 2.769 Å⁴.

Additional reading to help in the calibration of piezoelectrics for scanning probe microscopy use, can be found in many journal articles.^{5,6,7}

3.4 STM NOISE:

There are many possible sources of noise while doing STM experiments. If atomic resolution images are desired it is important to understand three basic issues: What noise is problematic, how that noise is entering and affecting the tunneling current, and how to look for noise sources. Most noise can be broken up into two main categories: electrical noise and mechanical noise.

3.4.1 MECHANICAL NOISE:

Mechanical, also referred to as vibrational, noise can affect the measured tunneling current in two ways. First, there is a change in separation between the tip and sample that is exponentially amplified by STM. Secondly, motion of the tunneling current wire can capacitively couple to ground or other line voltages around the tunneling current wire causing current spikes that are amplified by the pre-amp. There can be many mechanical noise sources that affect the STM system such as cryo-coolant boiling (either He or N₂), building/ground vibrations from a truck driving by, or construction, or acoustic noise from mechanical pumps or even people talking (an STM can be used a very expensive microphone.) One additional problematic source of noise for a variable temperature STM is varying temperatures causing thermal expansion/contraction generating undesired motions and thermal drifts.

3.4.2 ELECTRICAL NOISE:

After eliminating as much vibrational noise as possible, the task is to eliminate electrical noise. Electrical noise may have many possible causes. The laws of physics prevent removal of all electrical noise. However, a thorough understanding of the causes mixed with careful design can minimize the electrical noise to a level adequate for STM to achieve atomic resolution on virtually any conductive sample.

One persistent form of electrical noise that can not be fully eliminated is Johnson noise, sometimes referred to as thermal noise. Johnson noise^{8,9,10} is a function of random collisions of charge carriers (electrons) caused by thermal fluctuations within a material.

Typically, Johnson noise is discussed for resistors, such as those found in STM pre-amps.

The governing equation to calculate the lowest possible noise voltage within a resistor is:

$$V_n = \sqrt{4k_b T R \Delta f} \quad (3.2)$$

where k_b is Boltzmann's constant, R is the resistance, T the temperature in Kelvin and Δf is the measurement bandwidth. To convert the tunneling current into a measurable voltage for the STM electronics it is passed across a large resistor in the pre-amp (taking advantage of Ohms law, $V=IR$). The high resistance resistor gives the pre-amp its gain. The IVP-200 uses a $100 \text{ M}\Omega$ resistor. According to equation (3.2) at room temperature (RT) the variation in voltage produced by the $10^8 \Omega$ resistor over a 5 kHz bandwidth is 90 μV which correlates to a variation of 0.9 pA of current, which is a very small amount compared to a typical tunneling current of 1 nA. The use of the IVP-300 that uses a $10^9 \Omega$ resistor can generate 0.28 mV of voltage noise at RT over a 5 kHz bandwidth. This 0.28 mV corresponds to a tunneling current variation of 0.28 pA which is still small compared to the 100 pA tunneling current typically used with the IVP-300. However, if much lower tunneling currents are used the Johnson noise may need to be reduced by cooling the preamp resistor to temperatures below RT.

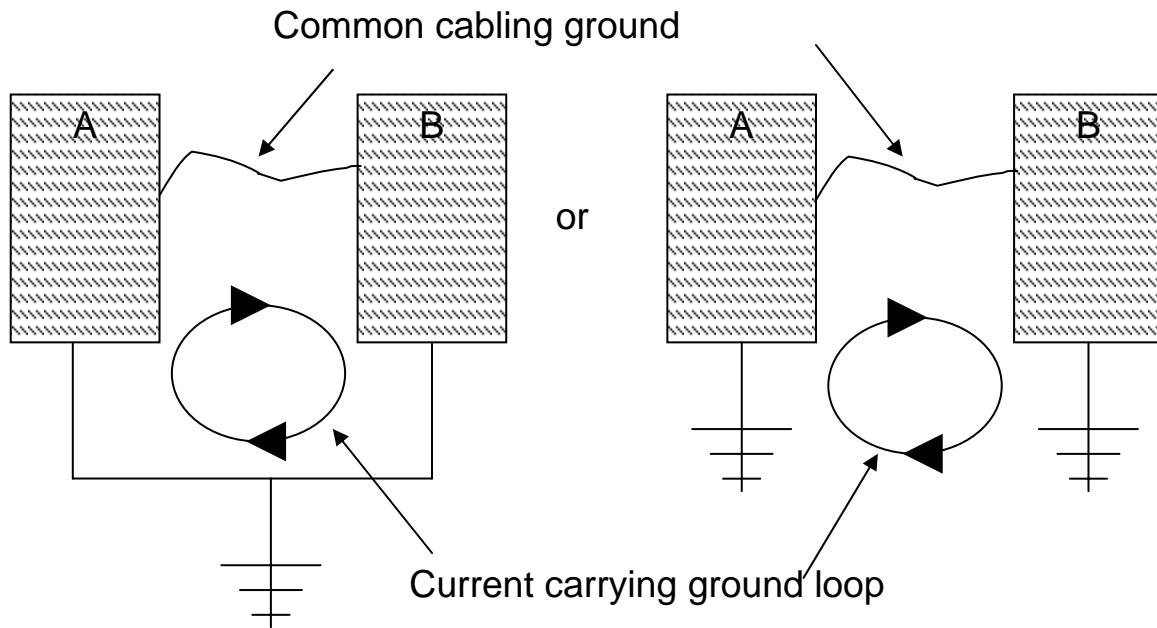
Another form of electrical noise that can cause problems for the STM is capacitive coupling. In our STM system the tip is held at a virtual ground and the bias voltage is applied to the platinum crystal. Because the tunneling current wire conducts extremely small signals it is very sensitive to fluctuations in the surrounding electric field. Therefore, this wire needs to be shielded as much as possible. To do this we run the tunneling current wire through a grounded stainless steel tube that goes from the STM to

where the wire exits the UHV chamber. Additionally, we shield the tunneling current wire from the tip to the stainless steel tube by grounding the interior of the scan piezo and running the tunneling current wire through the center of the piezo up and out of the STM. By shielding the tunneling current wire in this manner we greatly reduce the pickup that high and rapid voltage changes from the scanning and offset wires could impart onto the tunneling current wire (i.e., cross talk).

A third type of electrical noise that can impact the measured tunneling current is called flicker noise. This noise is caused by poor electrical connections, and it generates 1/f noise or “pink” noise. The amount of noise incurred from this source of noise should be minimal.

The fourth source of noise is shot noise. This is caused by the random emission of electrons or conduction of electrons across potential barriers. However, this particular type of noise is small and has little effect on the measured tunneling currents.

The last and largest source of electrical noise is improper grounding or creation of ground loops. A proper ground is required for precision voltage measurements when the signal voltage needs to be compared against a reference ground or predefined voltage as in our STM. To avoid ground loops make sure there is only one ground connection for all items, or there are exactly equal resistances from voltage sources to ground. In reality adjusting the resistance paths from two different pieces of equipment to ground is near impossible.

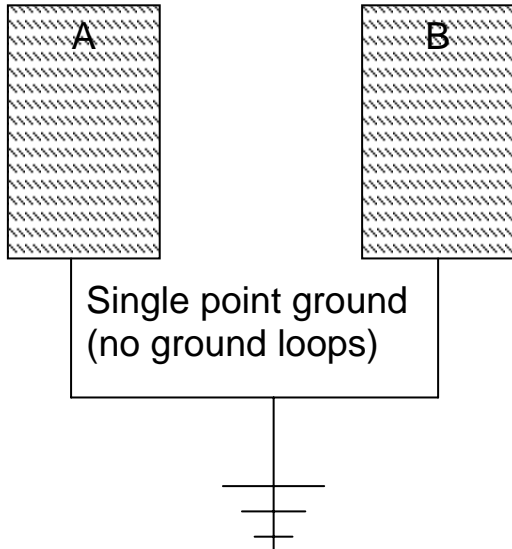
Figure 9 Ground loop scenarios caused by a common cable shielding

Ground loops occur when faulty wiring or improper wiring practices allow stray currents to flow to ground. There may be two or more possible pathways to the earth or a common ground point in the building.^{11,12} Diagrammatically a ground loop can be seen in Figure 9. This shows that two pieces of equipment have a common connection between them with each having a connection to earth ground. A stray current on one of the two pieces of equipment will generate a ground loop condition. A proper grounding situation would look more like Figure 10. In this figure there are multiple pieces of equipment that are all grounded to one point which eliminates the possibility of a stray current finding a secondary path to ground which would cause the ground loop.

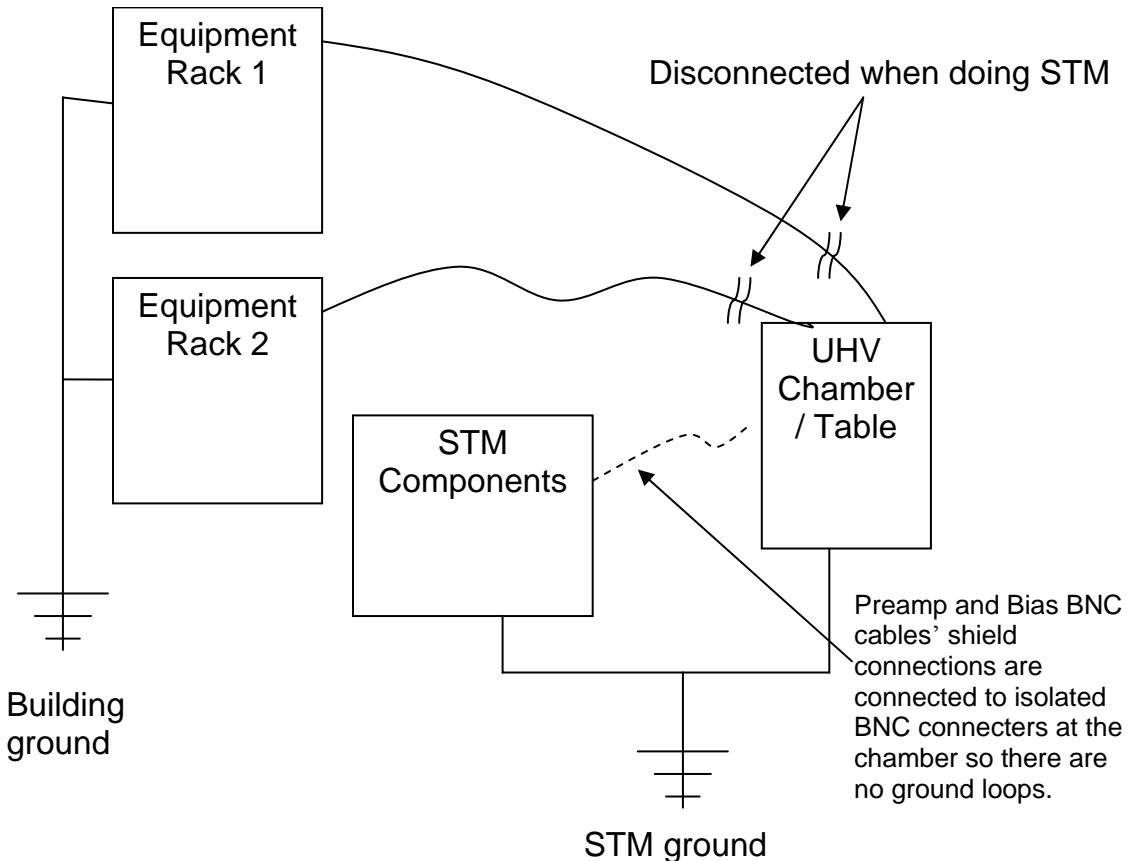
The STM chamber has multiple connections to ground and to many different pieces of equipment which in turn may have more connections to ground. This tangle of connections makes looking for ground loops in the system difficult and potentially dangerous if care is not taken to make sure a proper ground for all equipment is maintained. To avoid ground loops, the STM maintains two electrical break points from the chamber which is grounded to the STM-100. The first STM electrical break point is where the tunneling current wire exits the chamber and enters the pre-amp, through a

ceramic spaced feedthrough. The second electrical break is at the chamber manipulator.

This is where the bias voltage for the STM enters the chamber; the ground plane for the manipulator is separated from the main chamber by a Teflon ring system that the manipulator rotates on. Both the tunneling current wire and bias wire have isolated shielding around them that terminates at the back panel of the SPM-100 electronics. The SPM-100 electronics are



grounded from a common ground post on the back of the SPM-100 to a grounding bar and an 8' grounding rod driven through the lab floor into the earth

Figure 11 Grounding schematic of the UHV STM chamber

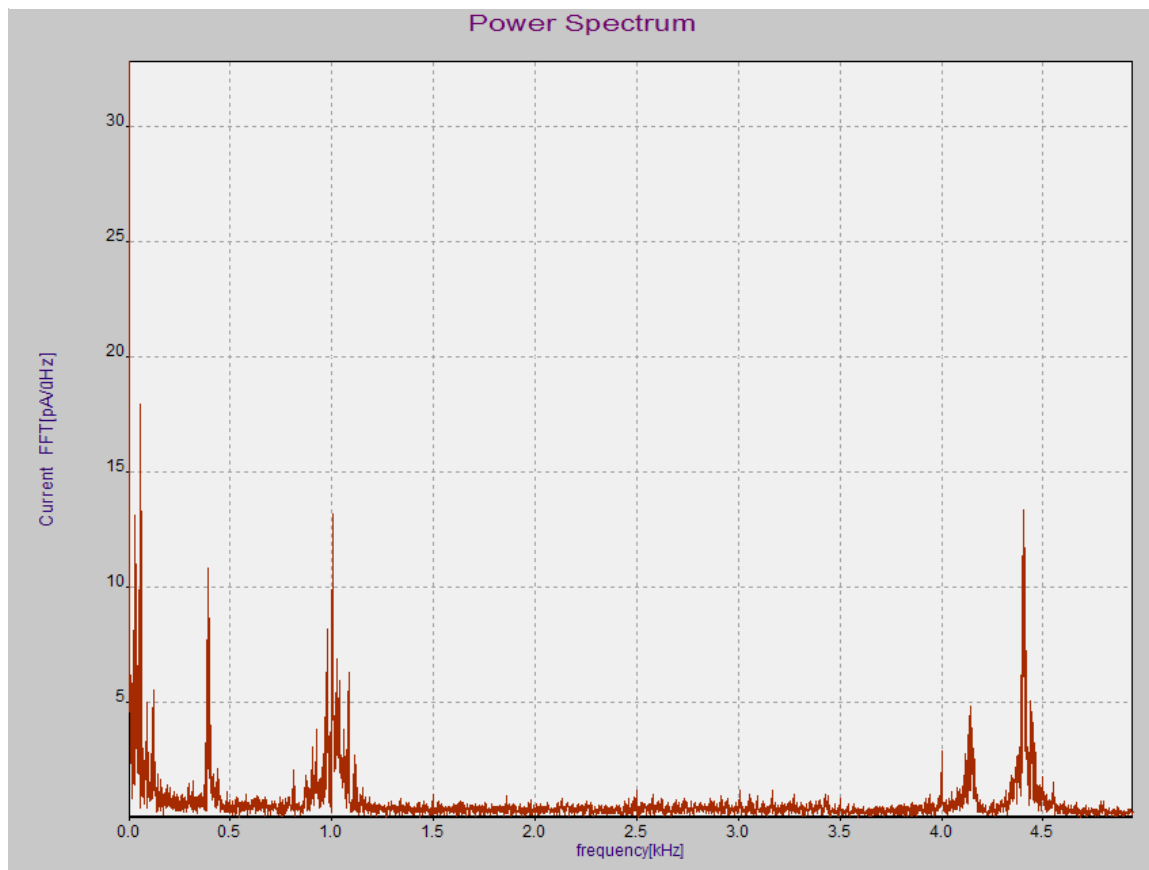
that is dedicated to the STM. To simplify everything, all STM components are isolated from building ground and grounded to the ground rod system for the STM. When doing STM all connections to equipment such as the mass spec. and AES are removed so there is not a shared ground from the chamber to the building ground. An illustration of the STM grounding can be seen in Figure 11. The reason that such lengths were taken for grounding the STM is that: 1) discussions with RHK discovered that a clean ground is one of the very best things one can do to help reduce noise and is the first thing that they recommend. 2) testing of the building ground from one circuit to another and a copper pipe all showed low resistances to each other but the voltage potential between them

varied as much as 7 V with a 60 Hz oscillation on it (there is some poor wiring of instruments somewhere in the building!)

3.4.3 HOW TO LOOK FOR NOISE:

To look for detrimental noise frequencies, many techniques are used. The most basic way is to use the “Noise Power” FFT built into the SPM-32 software. This is a

Figure 12 A typical noise power spectrum that shows frequency components of 440, 1050, 4250 & 4400 Hz with some low frequency noise in the 60 Hz range.



useful and relatively easy way to look for noise on the tunneling current. The program runs a portion of the tunneling current into a circuit that performs a FFT and outputs a

display on the screen that is representative of the noise in the system. (The current revision 8 electronics utilizes the DSP chip for the FFT which allows for more freedom in adjustment of the signal sampling conditions.) A typical noise spectrum looks like Figure 12. When there is very regular and continuous problematic noise this method works very well. However, the biggest problem with the SPM-32 FFT method is that the outputs are “snap-shots” in time of the tunneling current conditions and are not a continuous look. Examination of the noise on the tunneling signal while imaging is impossible. So, while using the noise power spectrum in the software is very useful it is not necessarily the best way to eliminate noise problems.

A better way to look at the noise in the tunneling current when eliminating noise sources is to use a spectrum analyzer. We are lucky enough to be able to borrow a good HP 6354A analyzer from the Deaver lab just about anytime we need it. Another analyzer that we can occasionally use is the Harrison digital oscilloscope from the ultrafast lab. The digital scope has a FFT function in it that works as a good spectrum analyzer, but has some problems at high frequencies because of the sampling and quick switching of a signal that is not exactly repetitive. Neither analyzer introduces noise into the STM images and both are helpful for a real time look at the noise frequencies on the tunneling current. They can be used to quickly observe how turning off and on equipment or suspected sources of noise affect the tunneling current.

Another very simple and low tech way to look for noise sources is to directly listen to the tunneling current and/or drive frequencies to find frequencies that add noise. To listen for noise, take the output “preamp monitor” from the monitor outputs section on the back of the SPM-100, and plug it into a stereo or speaker system (I used an old

portable JVC “boom box” that was able to produce a very good range of frequencies particularly at low frequencies with its “hyper bass” output on.) Once the connections have been made, turn on the stereo and listen to the signal, being careful not to turn the volume up too much so as to drive increasingly positive feedback of noise into the STM. While listening to the signal walk around and listen to equipment / fans / anything that might be producing the frequency of noise you’re interested in removing. Ideally, once the noise source has been identified it can be turned off to see if there really is a change in the observed noise signal. If there are too many noise frequencies in the tunneling current it may be necessary to draw some of them out. This can be done by using a signal generator to drive a particular frequency into the stereo that is then amplified and listened to. This allows you to focus more intently on a single frequency while you are looking for noise and can potentially be used to see if that frequency is driving the noise seen in the tunneling current. Some frequencies may be filtered out by the STM dampening system when coming from outside the chamber. Sometimes higher frequency components may enter the system and ultimately be converted to drive a lower frequency resonance. These methods of listening to the signal and its pure frequencies are very useful to identify external noise sources that one may or may not be able to turn off and on to look for changes in the noise spectrum.

A final method for identifying noise sources is simply to systematically go through and start turning everything off. This can be a lengthy and difficult process due to the fact not all equipment can be turned off, or requires an act of God (or possibly facilities management to turn off and on the exhaust fans, AC ducts, etc.)

An accelerometer can be used to test for vibrations and whether a room is suitable for STM experiments. An accelerometer is simply a piezoelectric that is attached to a mass that vibrates causing the piezo to produce a voltage at the frequency of the oscillating mass. The use of an accelerometer is a crude method because of its small mass and poor low frequency response, a better method that was not available to us, is to use a geophone. A geophone works on the same principle of the accelerometer but uses a magnetic mass around a spring suspended coiled wire to create a signal.

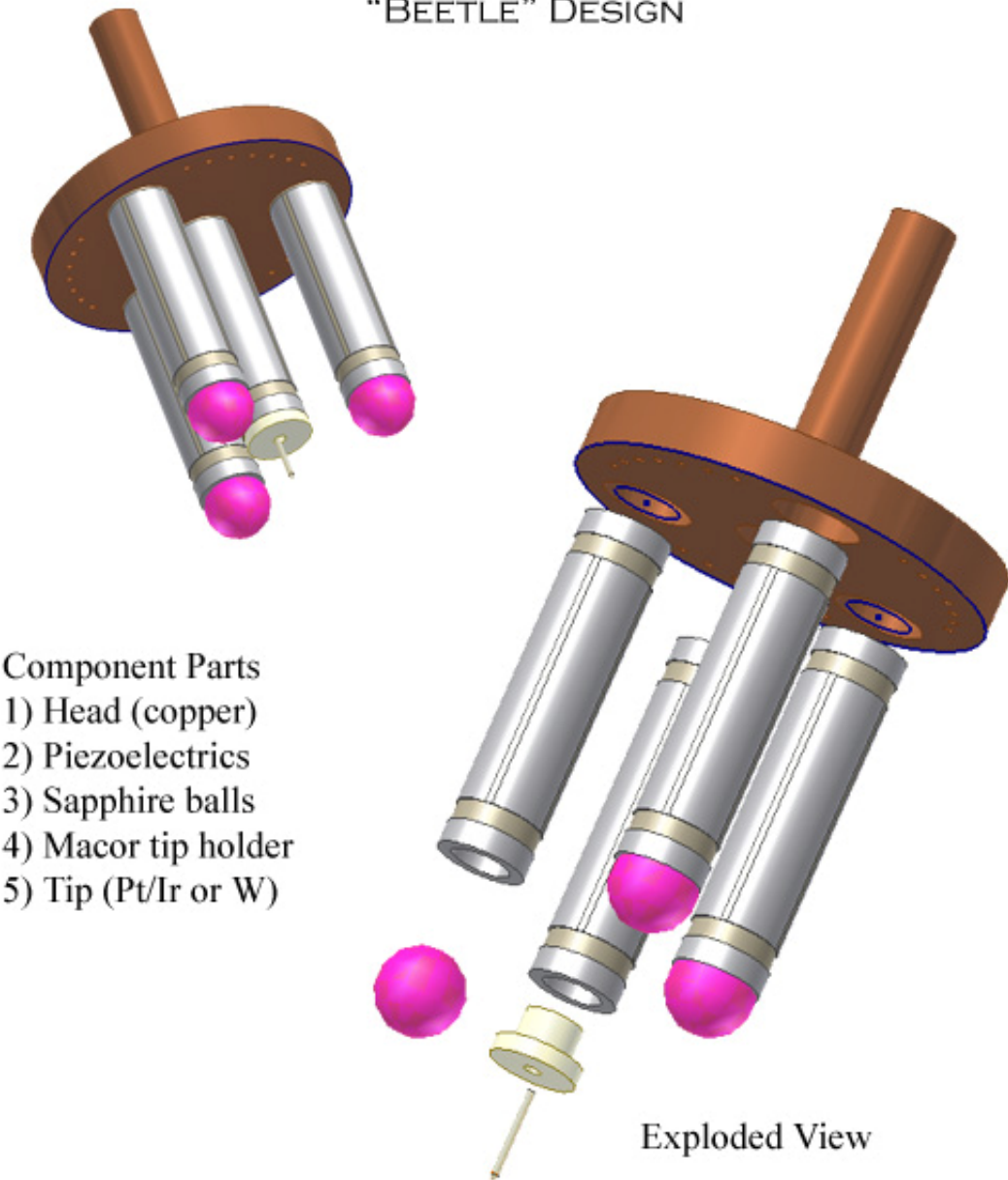
The major noise sources that instigated the transition from the Harrison photochemistry lab (Chem Rm 162) to the new STM lab (Rm 104) were fundamental frequencies generated by the ArF excimer laser and pumps on the photochemistry chamber. The problematic frequency assigned to the excimer laser was 381 Hz. This seems an odd frequency but repeated testing identified it to be the problem and it seemed to come only from the laser power supply and not the laser operation itself. Frequencies of 770 Hz, 120 Hz, and 20 Hz were assigned to the turbomolecular pump, the mechanical pump, and the cryo-cooler from the photochemistry chamber, respectively. The assignment of frequencies to the photochemistry chamber was difficult due to the inability to repeatedly turn off and on the equipment to be certain that the frequency in question would disappear and reappear. Therefore, most of the assignments were made by listening to the noises produced and comparing them to frequencies, from a signal generator.

The current STM room (Chem # 104) is a big improvement over Rm 162 because the detrimental frequencies from the photochemistry chamber were removed. However, Rm 104 is still far from ideal. Problematic noise frequencies are 440 Hz and 1.1 kHz,

presumably from the air handling/climate control system. The biggest problem in the room is an unidentified intermittent noise with a broad range of frequencies that totally disrupts imaging, but luckily does not damage the tip. The noise is a short duration resonating noise that is most likely a liquid N₂ tank venting its pressure. The location has yet to be identified because it is over by the time I can run to the door to listen for its location. However the most likely locations are the adjacent NMR, ultrafast laser lab, or the Harman lab. My best guess at this point is the Harman lab's dry boxes are being refilled from a liquid N₂ tank. Because the ultrafast laser lab is located directly above the STM lab if anything gets dropped on the floor it is heard in the STM room and noise is seen in the STM image. Presumably, the best way to eliminate most of the noise from the ultrafast lab would be to install a drop ceiling using acoustic ceiling tiles. This would likely also reduce miscellaneous noise clutter within the STM room itself.

A final note about electrical issues is: switching power supplies can be very bad for an STM's noise performance. There are some high quality high frequency supplies that have frequency components beyond the 5 kHz bandwidth of the STM but most should be avoided and definitely not connected to the same electrical circuit as the SPM-100 or STM computer. An example of this was a 1 GB Iomega Jazz drive that was used for data backup until the power supply was found to be producing a horrible 60 Hz (and harmonics) noise on the measured STM tunneling current.

VARIABLE TEMPERATURE SCANNING TUNNELING MICROSCOPE
“BEETLE” DESIGN



3.5 BEETLE STM CONSTRUCTION:

Before construction of the Beetle STM is undertaken, a few key items need to be addressed, such as: what solder to use and remove, how to use and remove the flux, and what epoxies too use and how.

The only solder that can be used in the UHV chamber is silver solder which is free of high vapor pressure metals like lead and tin. Furthermore, the use of one soldering iron exclusively for silver solder is necessary to eliminate the possibility of non-silver solder contamination. In our case the silver solder iron is the free standing model that does not connect to a base.

The flux used with the silver solder is a highly corrosive compound that is water soluble. When using this flux, place a drop on the part to be soldered, make the soldering connection and immediately wash the connection with water to remove the flux.

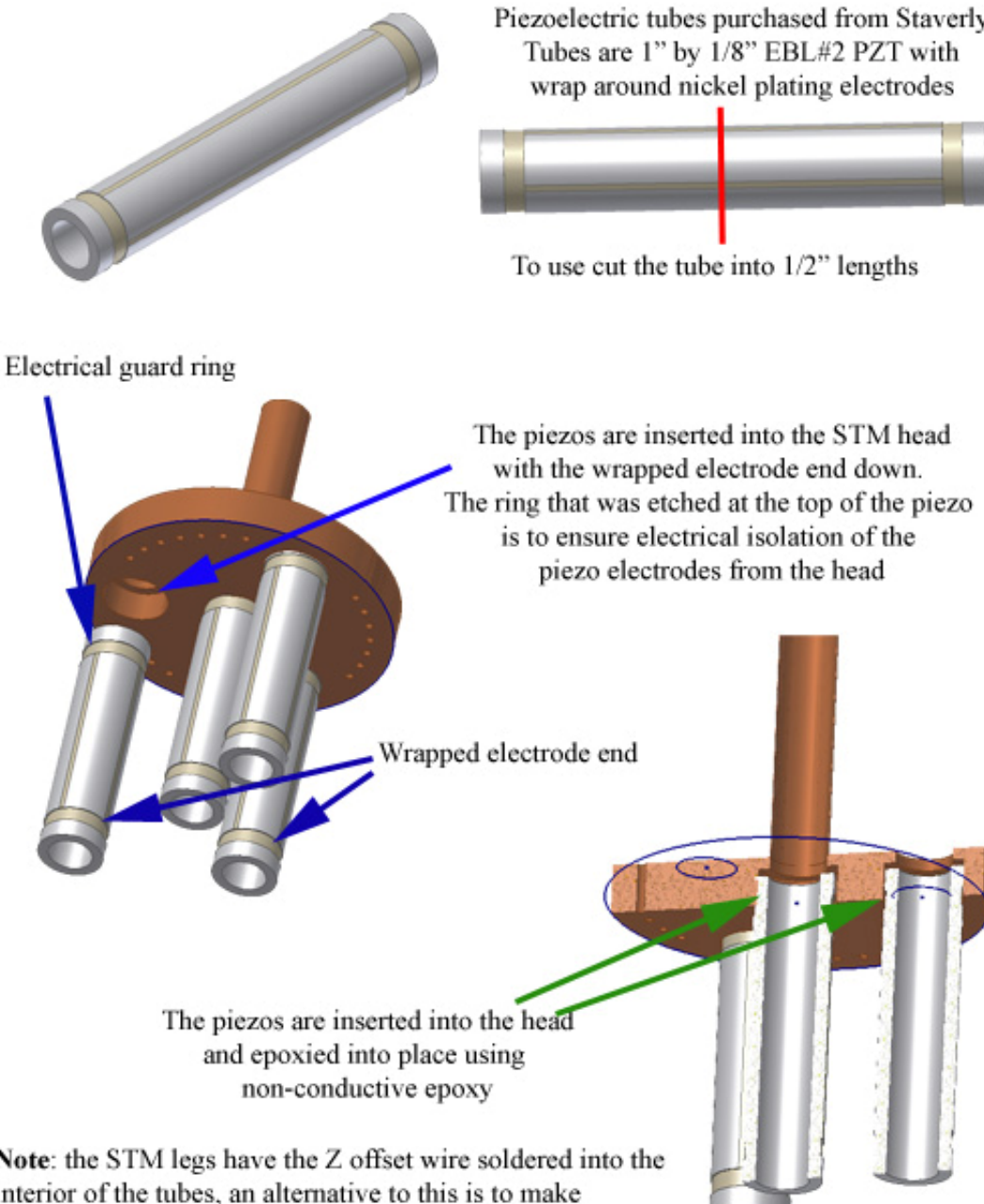
There are two different epoxies that are used when constructing the STM, a H61 non-conductive epoxy, and a H35-175MP conductive epoxy from Epoxy Technology. Both are single component epoxies and have short shelf lives. The epoxies are heat cured to a temperature of 180 degrees Celsius for approximately 2 hours to harden.

A listing of all material used in the STM construction can be found below.

Materials that are needed to construct an STM head.

- 1.) Piezoelectric ceramics
 - a. From - Staverly Sensors Inc. E. Hartford Ct.
 - b. Type - EBL # 2 (nickel plated)
 - c. Dimensions – 1” length x 1/8” diameter x 0.020 wall thickness.
- 2.) Macor nonporous machineable glass/ceramic
 - a. From - McMaster-Carr (purchased new before machining)
 - i. Dimensions – 1/8” thick rod
- 3.) Stainless Steel Hypodermic tube stock
 - a. From – McMaster-Carr
 - i. 22 Gauge tube for holding the STM head
 - ii. 24 Gauge tube for the tunneling current tip holder.
 - iii. 23 Gauge tube (it's possible use for either purpose, to hold the head or the tips. It's just nice to have around.)
- 4.) Copper wire
 - a. From – California Fine Wire
 - i. Kapton coated (polyamine)
 1. 0.010” dia. About 30 ft. needed

- 2. 0.002" dia About 20 ft. needed
- ii. Razor blade, glass microscope slide, and cigarette lighter. (to remove the kapton coating on the wire.)
- 5.) Thermocouple wires
 - a. From – California Fine Wire
 - i. 0.005" dia. bare wire, both Alumel and Chromel
- 6.) Sapphire/Ruby balls
 - a. From – Swiss Jewel Co.
 - i. 1/8" dia.
 - b. (1/8" Tungsten Carbide ball came from McMaster-Carr)
- 7.) Silver Solder & Flux
 - a. Eutecrod 157 with flux
 - i. From - Eutectic Corp.
 - 1. Free of Cd, Pb, Zc, and Sb
 - 2. Melting point 220 C
 - 3. Used for Surgical Instruments
 - b. Silver solder & flux from National Welding Supply in Richmod, Va.
 - i. Repackaged by National Welding Supply – it is a J.W. Harris equivalent of the Eutecrod 157.
 - ii. Free of Cd, Pb, Zc, and Sb
 - iii. Contain approximately 96 % Sn and 4 % Ag
 - iv. (packaged with it's own flux)
- 8.) Epoxy
 - a. From – Epoxy Technology, Billerica, MA
 - b. Conductive epoxy
 - i. Product name – H35-175MP
 - c. Non-conductive epoxy
 - i. Product name – H61
- 9.) STM Head material
 - a. Potential materials
 - i. Aluminum - Easy to machine and clean, but large difference in the thermal expansion coefficient between Al and the piezoelectric ceramic.
 - ii. Macor - Harder to do fine detail machining, very fragile when completed, However it has approximately the same coefficient of thermal expansion as the piezoelectric ceramic.
 - iii. Super Invar - Very difficult to machine But has a zero coefficient of Thermal expansion, and its derivative at room temperature.
- 10.) Microshield/ Microshield remover
 - a. From – SPI-Chem, West Chester, PA (www.2spi.com)



Note: the STM legs have the Z offset wire soldered into the interior of the tubes, an alternative to this is to make the wire connections to the wrap around electrode on the exterior of the legs.

2nd Note: if the STM uses electrically conductive balls at the base the wrap around electrode should be etched away to avoid possible shorting to the crystal mount.

3.5.1 ETCHING THE PIEZO TUBES:

Etching nickel-plated piezoelectric tubes is not a difficult task, it just requires following a few simple rules. These rules are simple and are at the heart of good UHV construction techniques. Rule number one is: keep things clean! Rule number two is: KEEP THINGS CLEAN! (If in doubt, refer to rule number one). The third rule would be: don't try to take short cuts. Be aware that the processes will take time and plan accordingly. Rushing through a job just means you're going to spend more time in the future fixing things that you didn't do correctly the first time. Rule number four is understand what you are doing, and to use that knowledge to make useful tests after each step.

The piezoelectrics that we use in the construction of our STM head are EBL Type # 2, purchased from Staveley Sensors Inc. located in East Hartford, Connecticut. These piezos are not stock items and have a long lead time for arrival. Currently, it takes approximately four to five weeks between ordering and delivery, so plan accordingly! The dimensions of the nickel-plated piezoelectrics used by our beetle STM, are 1/2 inch in length, by 1/8 inch outer diameter, with a 0.020 inch wall thickness (It is cheaper to purchase longer tubes, so we buy one inch long tubes and cut them to length, in-house). The EBL type # 2 piezos have a Curie temp of 350° C. If they are heated beyond their Curie temperature they will lose the ability to flex/bend (a brief introduction on how piezoelectrics work can be found in the STM wiring section). Other pertinent information for the EBL # 2 piezos are: thermal coefficient of expansion is (not reported however, most piezoelectric materials have an expansion in the range of 3.0 to 7.0 ppm/°C), density

of the material is 7.5 g/cm^3 , a thermal conductivity of $1.5 \text{ W/(m }^\circ\text{C)}$, and their industry type designation is PZT-5A.

Before etching the PZT's get Willie in the glass shop to cut the piezos into two equal $1/2''$ length pieces, down from their ordered length of one inch. Once the PZT's are cut to length they will fit on the Aluminum mandrels for scoring and etching. (see Figure 13 for all needed pieces)

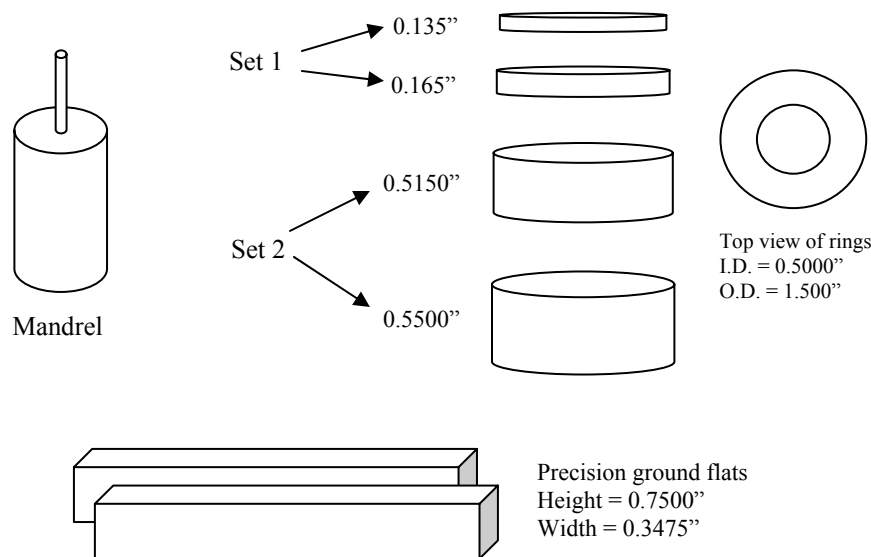


Figure 13 The mandrel used for etching the piezos is shown on the left, and the four rings that are placed around the piezo on the mandrel that are used to cut the rings into the piezos are shown on the right. At the bottom are shown two precision ground flats used to cut the quadrants on the piezos.

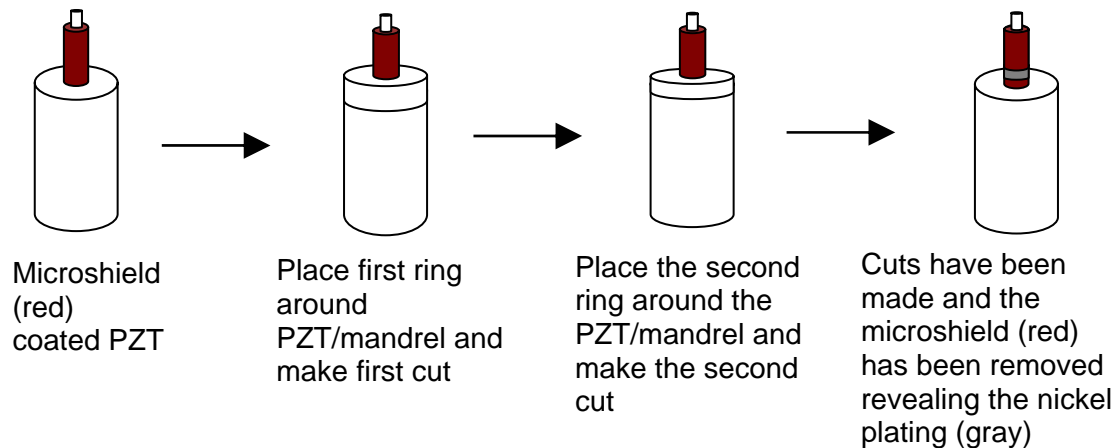
Next, the PZT's need to be affixed to the mandrel. The lore that was handed down to me on how to affix the PZT to the mandrel was to heat up the mandrel on a hot plate. The hot plate needed to be approximately 60° C , which is about the melting point of paraffin wax. Once the mandrel is heated place a small piece of paraffin on the tip, then after the paraffin starts to melt, place the PZT on the mandrel and remove from the heat. The reasoning for this was; the wax would solidify and hold the PZT in place and also

make a seal around the inside of the tube which would protect the nickel plating while etching. This is a good idea only in theory. In fact, the wax tends to melt down and around the outside of the PZT which causes considerable problems while etching, not to mention that removing the wax from the PZT tubes can be difficult. Therefore, the method that I recommend is to paint a light coating of microshield onto the mandrel post that the PZT tubes fit over. Then immediately put the PZT tube onto the mandrel. Once the PZT tube is on the mandrel wait about five minutes to let the microshield start to dry, sticking the PZT to the mandrel. After five minutes are up, it is possible to put a light coating of microshield onto the exterior of the PZT tube. The thickness of the microshield coating doesn't really matter, what matters is that every bit is covered. There are advantages and disadvantages to both thick and thin coats. The advantage of a thin coat is that the small slices that you cut and remove come away from the PZT cleanly and tend not to get caught up on the sides of the microshield, however, the thinner coatings tend not to come away from the PZT in one piece, meaning that it's easier to pull and break a few tens of microns layer of microshield than a thicker one. I prefer to put a coating on that is thin enough to see the PZT through it, but still thick enough to remove the cut sections with one pull, (i.e. a thickness on the order of a couple hundred microns.) The other key to applying microshield is to make the coating as smooth as possible without any bubbles. If bubbles appear, try to fix them or strip the microshield away and start over. The last step in applying the microshield to the PZT tube is to put a good thick coating or "glob" around the top and bottom of the tube to make a good seal and make sure that no etching solution can ever get down into the interior of the PZT.

After the microshield has been applied to the PZT/mandrel assemble, let it dry for at least 4 hours. Applying the microshield and letting it dry overnight would be advisable. The time it takes the microshield to dry is one of the slow steps in the STM construction but it needs to be done correctly or the microshield will pull away from the PZT tube while in the etching solution and potentially ruin the PZT. With this in mind, if a cut in the microshield is off and needs to be repaired, you will have to repaint the PZT and wait the required time for the microshield to dry. Therefore, to etch one PZT tube could take days if there are multiple errors or problems with the microshield sticking. The main problem with the microshield not sticking to the PZT tube after scoring, deals with the cleanliness of the PZT. The microshield will not stick to wax or oils on the surface of the PZT that might come from the paraffin, fingerprints, dirty gloves, etc... (If in doubt see rule number one.)

Figure 14 Diagram of the cutting the rings around the piezoelectric (to be done with the wrap-around electrode at the top).

Ring cut for both leg and scan PZT's

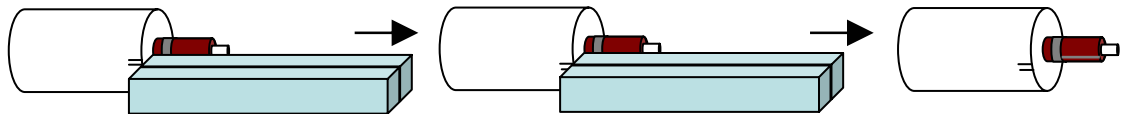


Once the microshield is applied, two sets of cuts are required to remove sections of the microshield and make the legs of our “beetle” type STM, where as three sets of cuts are required for making the center or “scan” piezo. The first set of cuts are made for both the legs and scan PZT’s (Figure 14), it is a circular cut around the base of the piezo used to electrically isolate the tube from the STM head. To make the cut place one of the smaller rings down around the PZT tube so that it sits on the mandrel. Then take a razor blade that is pressed flush against the ring, cut down into the microshield on the PZT, continue the cut moving the razor blade all the way around the PZT tube DO NOT LIFT THE RAZOR BLADE UP AND START AGAIN AFTER ROTATING, MAKE ONE FLUID CUT. For the second cut of the first set, remove the first ring and place the second of the smaller rings down on the mandrel, cut into the microshield just as in the first cut making ONE fluid motion all the way around the PZT. After the first set of cuts is done, you should be left with a 0.030” inch band around the PZT that can be removed by tearing and pulling the microshield away from the surface. This should leave a very well defined area of the PZT exposed for etching, beginning 0.135 inches above the bottom of the PZT tube.

A few other notes about scoring the microshield for removal: apply pressure to the knife while cutting, but not excessive pressure, the idea is to cut the microshield but not to cut the PZT tube (cutting deeper into the tube will weaken it, leading to a potential cracking point if pressure is applied to the tube). Also it is advisable to make only one cut or one pass of the knife for each scoring line. If a scoring line is cut over and over again the microshield along that cut is going to get rougher and rougher, resulting in an ill defined edge to the quadrant when etched.

The second set of cuts, are to make the $\pm X$ and $\pm Y$ quadrants (Figure 15). This second set of cuts can be done for both the STM scan piezo and the legs. (However, I recommend ordering one piezo with quadrants already etched to make the scan piezo.) To make the cuts for the quadrants place the mandrel on its side and align the precision ground flats to the marks on the mandrel, while lightly pressing the flats against the PZT

**Figure 15 Cutting the microshield for etching the quadrants on the piezoelectric
Making cuts for the X and Y quadrants**



Place mandrel with PZT on its side and line up the ground flats with the mark on the edge of the mandrel. Then make a cut with the razor blade.

Line up ground flats with the next mark on the mandrel and make the second cut

Remove the flats and the very small strip of microshield.

This procedure is repeated three more times to make all four cuts which separate the quadrants of the PZT. There are marks on the mandrel spaced 90 degrees apart that are used for aligning the cuts on the PZT tube.

tube. This gives you a straight line that you can score the microshield with. Once the first cut has been made rotate the mandrel to the next mark and score the microshield in the same manner as the first cut. After both cuts have been made for a particular quadrant take the Exacto knife and very carefully pick up an end of the microshield strip that you just created and remove the strip from the PZT leaving an exposed line that is about 100 - 200 microns wide. It is sometimes best to do the strip removal under a microscope. These cuts need to be done three more times spaced 90 degrees apart from each other, (just follow the marks on the mandrel). This is the most probable place for error, which would

mean that you must go back and repaint the PZT and start over. HOWEVER, DO NOT remove the PZT from the mandrel or move its relative position on the mandrel!!! The reason for this is the cuts that you just made for the quadrants may leave disruptions on the PZT that could potentially electrically isolate part of a quadrant if the relative position on the mandrel is moved and then etched.

The third set of cuts, are for the scan piezo only. They are just like the first set of circular cuts in figure 2 except that the 0.035 inch microshield band to be removed is cut at the top of the PZT tube and is used to connect the interior of the PZT to a grounding wire. The method used is to place one of the larger set of rings down on the mandrel and run the razor blade around the PZT tube to cut a circle around it. Once the first cut is made remove the ring from the mandrel place the second large ring on the mandrel and make the second cut. After the second cut, remove the ring and remove the 0.035 inch band of microshield from the PZT. It is important to pre-determine what is the top or bottom of the PZT. The wrap-around electrode needs to be used for making the electrical connection from the outside ring that is isolated from the rest of the outer electrodes by the third set of cuts described above to the interior electrode.

Once all the cuts are done and the appropriate microshield has been locally removed, the time has come for etching. The etching solution is a mixture of 1/3 nitric acid, 1/3 sulfuric acid, and 1/3 distilled water by volume. Be sure that when working with acid and water that appropriate gloves and safety goggles are worn at all times. Also it is advisable to work using one of the fume hoods. The decision on how much etching solution to make is up to you. However, a 300 ml amount is very convenient to make and is more than enough to etch all the PZTs for a single STM. Therefore, to make 300 ml of

solution, measure out 100 ml of distilled water, conc. nitric acid, and conc. sulfuric acid in graduated cylinders. Make sure that all liquids measured are at the same temperature to insure accuracy. When mixing, use a large beaker and add the H₂O first. Then add one of the acids and allow to cool. Next add the other acid, cool to room temperature, and transfer to a storage flask. When adding the acids to the water, it may be advisable to do this in a water bath or at least a larger secondary container to contain the solution should the beaker crack and break from the heat of mixing.

Once the etching mixture is ready and cooled, place about 60 ml into a clean 100 ml beaker. Then place the mandrel with the sectioned microshield piezo tube on it into the solution. Completely immerse the piezo tube in the etching solution for five minutes. After the five minutes are up remove the mandrel/piezo from the solution and wash thoroughly with distilled water. Examine the etched areas under a microscope. If it looks like the removed microshield sections still have some nickel on them place the mandrel/piezo back into the etching solution to etch for a few more minutes. The time required to etch the piezos will depend on the age and number of times the solution has been used. Older solutions may require up to fifteen minutes for complete etching. A brand new solution should process the nickel plating on the PZTs in five minutes. After the piezos have been etched and look good under the microscope remove all the microshield from the piezos and test to see if the quadrants and bands are isolated from one another. If they are not isolated as you want you have one of two options: Option 1 is to let the piezo sit overnight and make sure that it's dry and then test to see if it is isolated in the ways that you want. Option 1 can work if the initially measured resistances across the quadrants are on the order of 10's of MegaOhm's. Ultimately the completely

dry quadrant resistances must be more than $40\text{ M}\Omega$. Option 2 is to repaint the piezo with microshield, cut, and re-etch. Option 2 can only work if you haven't removed the piezo from the mandrel already.

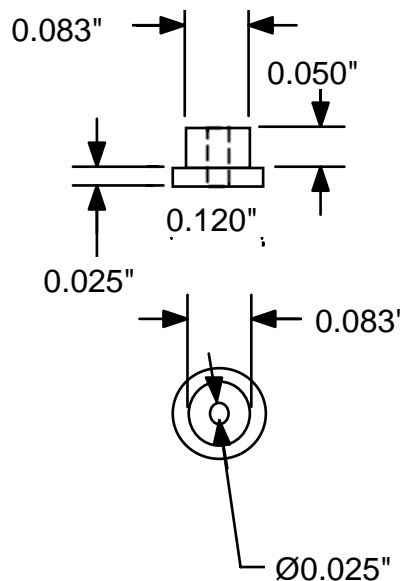
After the piezos have been etched and you are confident that they will work correctly, you may soak the mandrel/piezo in acetone to remove the piezo from the mandrel. Once the piezo is free of the mandrel, clean it thoroughly in acetone.

3.5.2 “BEETLE” TYPE STM ASSEMBLY:

The assembly of our beetle STM is accomplished in six different subassembly phases: Preparation (ordering and getting all the pieces machined), formation of the scan piezo, affixing all the piezoelectric parts to the STM head, construction of the STM legs, soldering, and final assembly/testing. A few of these divisions of labor overlap, but it's easier to think of them in discrete chunks that can be completed in a methodical fashion. This is how they will be presented.

The first item on the agenda is to organize all the components that compile a STM. That means getting the piezos ordered, cut, and etched (the details of etching can be found in the etching manual), machining the macor tip holder and the STM head, ordering or confirming that other components are here such as: ball bearings for the base of the STM

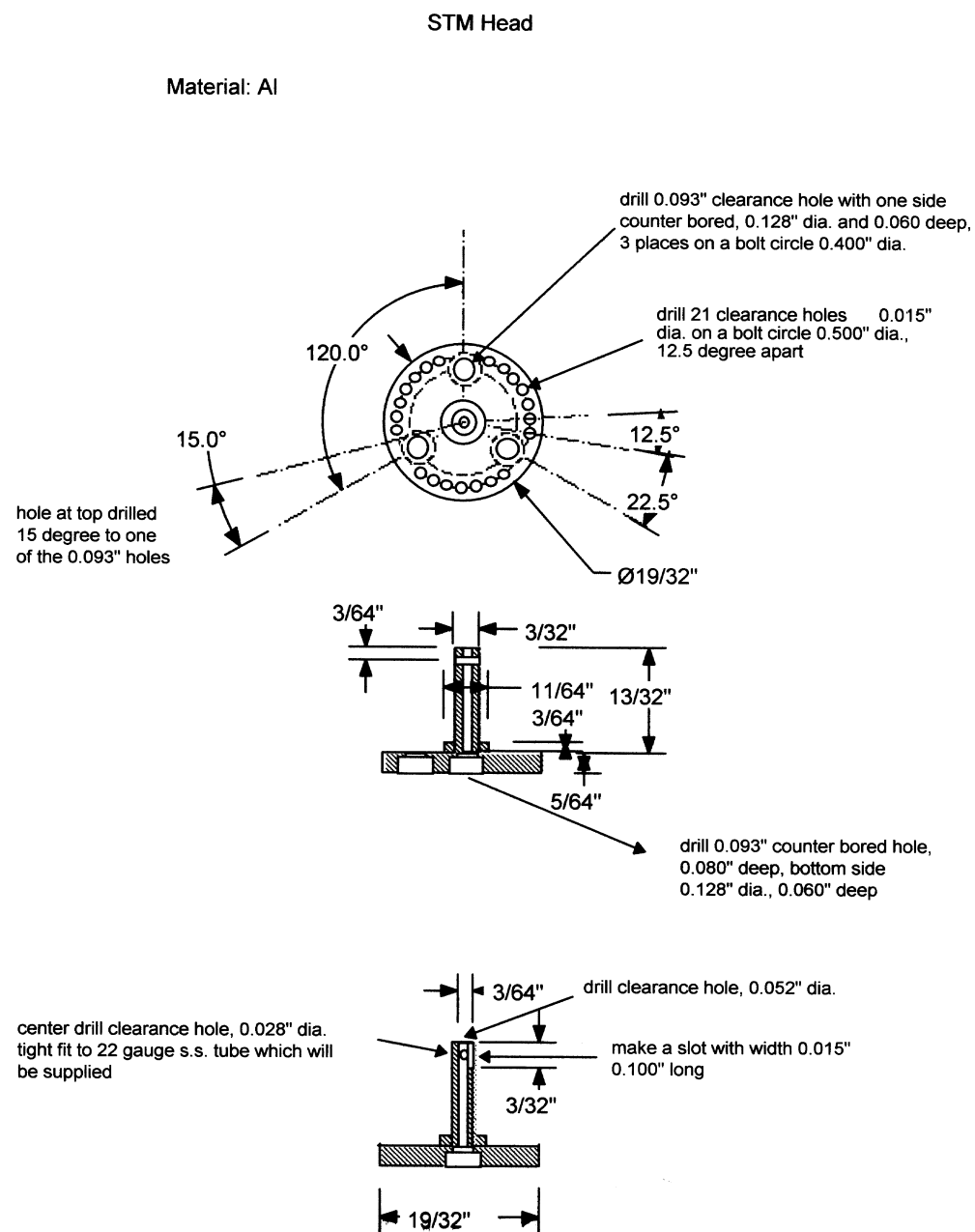
Figure 16 Macor tip tube holder



and both 0.002" and 0.010" diameters OFHC copper kapton coated wire for soldering.

The preparation of the piezos should be done according to the etching manual. Further more, it is assumed from here on that the piezos are done so the rest of the assembly is ready to proceed. However, a good use of time would be to work on and finish the following preparation steps simultaneously while cutting and etching the piezos.

The two pieces that need to be made in the machine shop are the STM tip holder and the STM head. The tip holder is made out of a non-conducting, nonporous machineable glass/ceramic known as Macor (see Figure 16), and is easy to make (no explicit machining instructions are required). However, the construction of the STM head (Figure 17) requires decisions to be made and also testing while machining. The first decision that you will have to make is; what material should you make the head out of? Materials tried to date have been: Super Invar, aluminum, copper, and macor. Each of these materials has their strengths and weaknesses. The Super Invar has a zero thermal expansion coefficient and first derivative with respect to temperature at RT.¹³ However, at lower temperatures these are not zero and this leads to very very long thermal drift times on the order of 1 to 2 hours before it stabilizes at the surface temperature. The aluminum head is a very large improvement over the Super Invar in terms of the thermal drift time! The aluminum head may take only 20 to 45 minutes (depending on the material of the balls at the base of the STM) to come to a stable Z height. The down side of aluminum is, its expansion coefficient is roughly five time that of the piezoelectric ceramics. Aluminum's good thermal conductivity mixed with its large expansion coefficient leads to a very fast vertical thermal drift that may require the STM to be

Figure 1 The “Beetle” STM head, (can be made from invar, copper, aluminum, or macor)

stepped back away from the crystal or stepped closer to it depending on the STM's change of temperature. At the time of this writing the Macor STM head has not been tried. However, its expansion coefficient should be very similar to that of the piezoelectric it's attached to which leads us to think that it may be a very good material to make the head out of. Another advantage of the Macor head is that it is electrically non-conducting, which means less problems of shorting from the tunneling current wire to the STM ground. To insure good electrical shielding the Macor head is coated with gold on its exterior by Willie in the departmental glass shop. During machining the STM head it is highly recommended that you take a piezoelectric tube over to the machine shop and let them try to fit the tube into the four counter-sunk holes that the tubes will be epoxied into on the head. This is necessary because, the dimensions of the tubes coming from Staveley are not as precise as they would have you believe. Therefore it is quicker and easier for the machinist to check the sizing on the fly, while machining. The object is to get the piezoelectric tubes in the holes with very little play so they will be aligned as straight as possible. Nevertheless, there has to be enough play in the fit to allow some epoxy to get between the tubes and the head.

The next step in preparation is to decide on what type of material the balls at the base of the STM are going to be made of. The two materials that have been used so far are: ruby/sapphire and tungsten carbide. Just like the different materials for the head, there are advantages and disadvantages to both. The ruby/sapphire balls conduct heat very well at very low temperatures (< 100 K) therefore if the sample and mount are at very low temperatures; the limiting thermal conduction contributing to thermal drift is the

piezoelectric and head material. At higher temperatures the limiting thermal conduction of sapphire may be inhibitive to a stable tip height if materials are being slowly cooled and therefore have some long time constant to reach a thermal equilibrium. The WC balls advantage is that they do not seem to be the limiting step in the thermal conduction process of the STM, at any temperature. WC balls however have a big drawback when compared with the sapphire/ruby balls, which is they are electrically conductive. This becomes a problem if particulate matter falls down into the center of the outer piezos and causes a short circuit from the WC ball to the inner wall of the piezo. The best solution that I have found as a work around for this is to mix a slurry of nonconductive epoxy (H61) and acetone. The epoxy/acetone mixture should have the consistency and look of skim milk. Once your mixture is created dip half of the WC ball into the mixture and then place the ball on a hot plate to set. This procedure will put a very thin coating of epoxy on the surface of the balls which will not interfere with them being mounted on the legs of the piezos. The alternative to this is putting large globs of epoxy on the balls and have the STM leaning in weird directions from unequal amounts of epoxy on the three balls.

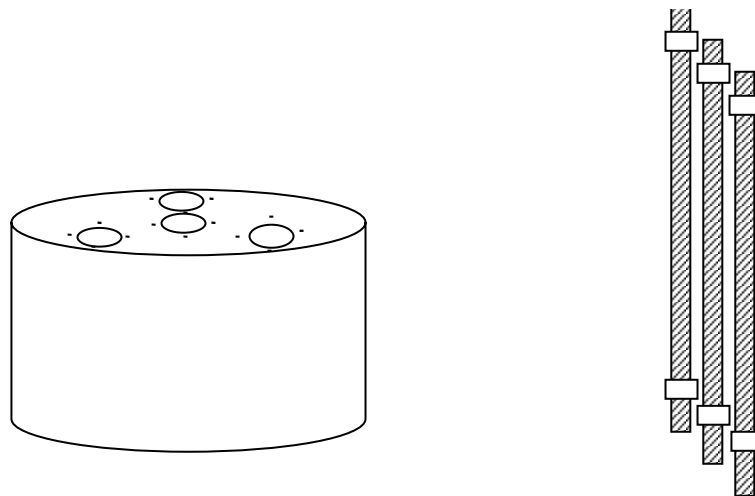
The kapton coated copper wire can be ordered from California Fine Wire Co. with little trouble, it may however take a couple weeks for them to ship the order. This really should not be a problem since previous orders of the kapton coated 0.002" and 0.010" wires were ordered on a 1000' spool, So there should be enough for a couple STM's. The amounts you will need to build an STM are: approximately 25 seven inch strands of the 0.002" wire, one three foot 0.002" wire, and four one inch long pieces of the 0.010" wire. Once the wires are cut they will have to have the kapton removed off the ends so that the solder will stick to the copper. Stripping the kapton off of wires can be done several

different ways; the best way that I have found is simply to scrape the end of the wire with a razor blade/knife, working all around the end of the wire to expose the copper. The second method is to use a lighter or small propane torch to burn the kapton off of the copper. However, keep two things in mind, that copper is a very good thermal conductor and if you heat the copper too long you may burn yourself. Secondly, this method does not work on 0.002" wire because the copper will burn just as fast as the kapton coating.

The first stage in the STM assembly is to work on the scan piezo. The scan piezo consists of 4 parts; the piezoelectric, the macor tip holder, the hypodermic tube, and a copper wire. Step one is to place the $\frac{1}{2}$ inch 28 gauge hypodermic tube through the hole in the macor piece. Set the macor holder/tube complex face down on the table so the tube is sticking straight up in the air. Now, apply a small bit of nonconductive epoxy to the top of the macor holder around the S.S. tube. Then carefully pull the S.S. tube half way out of the macor holder and push it back in. This is to get some epoxy on the shaft of the hypodermic tube so it may more securely hold onto the macor holder (be careful not to fill the end of the hypodermic tube with epoxy!). Next place the holder complex on a hot plate and cure the epoxy. Next, solder one of the 0.010" copper wires into the hypodermic tube on the opposite end from the macor piece. Once the wire has been soldered into place **do not bend it**, keep the wire as straight as possible, the best idea for this is to take a short piece of Teflon tubing that snugly fits over the wire and hypodermic tube and keep it on throughout the rest of the STM assembly. The last step in the scan piezo assembly stage is to epoxy the piezo to the macor/tube/copper wire complex. To do this you will use the conductive epoxy product H35-175MP from Epoxy Technology. Place a small amount evenly around the lip of the macor piece, being sure not to apply

too much epoxy, which might lead to a connection from the hypodermic tube to the inner wall of the piezo. Once the conductive epoxy is on the macor piece carefully slide the piezo down over the hypodermic tube then press the piezo down onto the macor piece. To hold the macor and piezo together I suggest setting the macor holder, face down on the hot plate and set the STM head into place on the piezo. The weight of the head can press down on the piezo and macor holder, which should balance there as long as it isn't bumped. The curing time for the epoxy can be anywhere from 1 hour to 5 hours depending on the age of the epoxy and the curing temperature. The recommended temperature to heat the epoxy to is 180° C for 2 hours. If, however, the epoxy doesn't seem to set, bake for a longer period of time. It is highly recommended that you bake longer than you think that you need to. If you have any doubt as to whether the epoxy is cured or not you may sonicate the part in acetone. If it falls apart it wasn't done! Once the epoxy is fully cured there is no way (short of chipping it off) to remove it. So, be sure to eliminate any electrical shorts or faulty connections before the epoxy is cured.

Figure 18 Assembly jig for the beetle STM



The next subassembly process to be done is to attach all of the piezos to the STM head. The equipment required consist of an aluminum holder and three 0-80 threaded rods with nuts (Figure 18). The three leg piezo tubes should be placed in the aluminum holder and their cuts, to define the quadrants on the piezo, should line up with the dots on the edge of the holes, and the band of isolated nickel electrode on the tubes should be exposed i.e. not in the aluminum holder holes. Then place the scan piezo with the macor/hypodermic tube/wire complex into the center hole with the macor complex going into the hole in the aluminum holder. Next, place a dab of epoxy around the top edge of all the piezos, being careful not to fill in the tube! It is best to have almost no epoxy on the interior of the tube! Once the epoxy is on the tubes, slowly and gently place the STM head on top of the piezos, so that the piezos all fit into the counter sunk holes in the STM head. Now that the head is on, recheck the alignment of the quadrants on the piezos to the dots on the aluminum holder. Make sure that the three outer (leg) piezos are oriented correctly. The scan piezo positioning is not critical, being that its X-Y orientation is set by the scan tube itself and is unaffected by the relative orientation of the coordinated system of the STM head. However, for soldering purposes it is recommended that you align the scan piezo with the markings on the aluminum holder. Now that the STM head is lightly attached you need to take the three threaded rods and fit them down through the STM head, through the interior of the leg piezos and out the bottom end of the aluminum holder. Then tighten the nuts from the threaded rod down onto the STM head and the bottom of the aluminum holder. (CAUTION, over tightening of the threaded rods can crack the piezos) So, gently tighten the nuts down to make all the different pieces one

tight unit. Then just before baking to cure the epoxy, make sure again that all the piezos are oriented correctly. Bake at 180° C for two hours to cure the epoxy.

At this stage the complex is starting to resemble an actual STM, just without wires and a base to stand on. Therefore, this subsection of the assembly contains information on how to attach the inner wires and balls to the legs of the STM complex. The first thing to do is to remove the STM complex from the aluminum holder. Now that the STM complex is free of the holder, hold it securely on its side (I recommend, holding it with the electrician's alligator clip stand.) Next take one of the 0.010" copper wires and stick it down from the top of the STM head through the interior of one of the leg piezos. Make sure before trying to silver solder (**always make sure that silver solder is used for UHV work!**), that the kapton has been removed from the end of the wire. Once the wire is in place, take the soldering iron for the STM and get just a little blob of solder on its tip (**the soldering iron that is used for the silver solder must only be used for silver solder and not regular solder to eliminate non UHV compatible contamination of STM materials and ultimately the UHV Chamber**). Then hold the copper wire by the end that is sticking out the top of the STM head and hold the wire down so that the tip of the wire is making contact with the interior of the piezo leg, about three millimeters above the opening at the bottom of the piezo leg. Next, attempt to solder the wire into place on the interior of the piezo leg by lightly pressing the tip of the soldering iron into the bottom opening of the piezo leg. When the wire is soldered to the interior of the piezo, test it to make sure there is an electrical contact. Then do the same thing to the other two legs of the STM.

Now that the wires have been securely attached to the interior of the piezo legs it is time to epoxy the balls that form the base of the STM into place. The balls that can be used (as previously discussed) are ruby/sapphire or tungsten carbide (if the tungsten carbide is used it must be pre-processed as discussed earlier in the STM assembly document.) This portion of the assembly is easy, simply invert the aluminum holder that was used to assemble the piezos to the head, and set the balls of your choosing into the three small holes that the threaded rod went through. The small holes are enough to keep the balls from rolling around on you while attaching them to the STM complex. Once the balls are set on the aluminum holder; set the STM complex down on top of the balls. When the complex is on top of the balls apply small dabs of non-conductive epoxy around the joints between the balls and piezo legs. Make sure that there is a solid connection between the piezo and the balls without applying too much epoxy, only enough epoxy to hold the balls in place is required. Secondly, with the epoxy make sure there are no air bubbles trapped in the epoxy (future outgassing risk). So, be careful how you apply it. Once the epoxy is applied cure the epoxy in the usual manner.

The next sub-assembly task is to make all the electrical connections to the piezos. This requires using the soldering iron, 0.002" dia. copper wire, and a very steady hand. The biggest recommendation that I have about this step is not to do strenuous exercise just before attempting this and to lay off caffeine for a week prior to soldering. With this step I can only tell you what worked best for me, you may find your own method that works best for you. I used the electrician's alligator clip stand to hold on to the STM so that it would be suspended in air giving me 360 degree access to the piezos. It seemed to be easiest to work from the center out, so I started soldering the wires for the scan piezo

first. Perhaps the best way to solder the copper wire onto the piezo was to first tin the end of a 0.002" wire (no flux is required but it can be used if desired). Next, take a thicker wire to dip into the flux, and then place a drop of flux from the thick wire onto the spot that you want to solder the 0.002" wire onto the piezo. Then obtain a small drop of solder on the tip of the soldering iron. Now use the tweezers to hold the wire against the piezo and touch the soldering iron to the piezo and 0.002" wire. Ideally, only a touch of the soldering iron to the piezo and wire should be necessary to make the connection. However things can go wrong, the wire may not stick to the piezo, or the wire doesn't seem to wet and therefore will not go into the molten solder leaving a glob of solder on the piezo. These are the most common failures, however, the wire can break meaning it has to be done again, there are many other reasons that the act of soldering may need to be repeated for a single wire. The problem with this is that it can leave the drop of solder all gray and discolored. Ideally this solder drop needs to be a shiny silver to minimize the surface area and emissivity. Once you have the scan piezo wires soldered into place and the connections look good and are actually connected continue on soldering the outer legs of the beetle STM.

The final soldering and assembly of the STM can be done partly in the STM holder (Figure 18) or in position on the STM stalk/flange. The STM needs to start out in the STM holder, so that all the wires can be soldered to push pin connecters that are arranged on a circle around the STM holder. Once the wires from all the piezos are connected to push pin connecters (refer to wiring diagram for proper order of connections around the circle). The next three connections that should be soldered are the Z offset connections to the interior of the outer legs of the STM. Each of the outer legs should

already have a 0.010" wire sticking out the top of the STM head. The way to connect these wires is to place just a very small drop of flux on the tip of the Z offset wire and solder to the 0.002" wire just as you would the piezos, with a minimal amount of solder and as cleanly as possible. Once the 0.002" wire is attached solder the other ends of the 0.002" wires to its corresponding push pin connector. Next place the STM holder with the STM in it under the stalk/flange to be connected to. Coming out the end of the stalk should be a 0.002" in wire. This 0.002" wire needs to be soldered to the 0.01" wire coming out of the center of the STM head (the tunneling current wire). The tunneling current wire can be soldered to the STM in the same manner as the 0.002" wire connecting to the Z offset wires, however be EXTREMELY careful not to get any flux down the sides of the 0.010" tunneling current wire. If flux does drip down into center of the STM head wash it out immediately, if not sooner, with water, and allow adequate time to dry before continuing. One other thing to be wary of is solder dripping down into the STM head, don't let this happen as it could create shorts in the tunneling current.

Once the tunneling current wire is connected, lower the stalk/flange so that the Vespel piece on the tip of the stalk now just covers the protrusion in the center of the STM. Once the Vespel piece is in place take the 22 gauge stainless steel hypodermic tubing and run it through the opening on the one side of the Vespel then through the holes in the top of the protrusion on the STM head and finally out the other side of the Vespel piece. Once this is done the stalk/flange is connected to the STM and the STM can be picked up by the stalk/flange assembly. However, before the STM is moved, the push pin connectors should be connected to the wires in the Teflon piece. Once all the connections have been made test the resistance from every wire to every other wire to

make sure everything is isolated. If all the connections are not isolated, resistors will be blown in the STM control electronics (the measured resistances should be infinite on the multimeter, i.e., $R > 40 \text{ M}\Omega\text{s}$).

3.5.3 WIRING A BEETLE STM:

There are many types of Scanning Tunneling Microscopes (STM) currently in use around the world today. Among the different types are: disc; one, two and three bar designs; and the tube designs such as single tube, double tube, and perhaps the most widely used STM of all, the multi-tube or “beetle” design as it is sometimes called.

Historically, we have chosen to use the beetle design in our lab because it has many favorable traits. The beetle type STM is prized for its extended range of motion in the X and Y directions, its ease of approach to the crystal and its small rigid size that gives resonant frequencies typically $\geq 7 \text{ kHz}$.

The symmetric construction of the beetle design tends to minimize thermal drift, making it well suited for variable temperature experiments. The STM tip is located at the X-Y axis origin and therefore when the STM head expands or contracts, it theoretically does so in reference to the X-Y center of the STM. So, the tip will remain in the same position in regards to the X-Y axis. During the thermal expansion/contraction of the piezos, the position of the STM tip should stay in the same Z position as well with the beetle design. The construction of our beetle STM uses 4 equal length PZT tubes, that have three outer legs to stand on, and a inner PZT to do scanning. So, when there is thermal expansion of the legs there should be a corresponding thermal expansion in the scan tube leaving the tip at its original Z position, (if the assumption is made that all the

PZT are in thermal equilibrium). Thermal problems with this design are; there are uncompensated expansions and contractions of other materials, such as the head and balls of the STM and the crystal and mount.

At low temperatures (≤ 100 K) the hysteresis and drift of PZT can become significant, worsening under larger applied voltages. Which are often required in single tube STMs. The attractiveness of the beetle STM is that once the approach of the tip to the surface is done, the STM may not need any voltage applied to any of the piezos to keep it in its operational position (the ideal case). So once scanning is started it may take only a few volts applied to the piezos to scan the area of interest which can help limit the hysteresis and drift. The latter problems are most noticeable when the piezos are driven to significantly different positions with larger applied voltages.

The beetle STM consists of four piezoelectric tubes each with one end tightly bonded to a head plate and the other end free to create movement of the STM. There are three outer piezos referred to as “legs”, (because these piezos are what the STM stands on). The obvious advantage of using three legs for this is that three points uniquely define a plane. Two legs won’t suffice and if more than three legs were used, there could

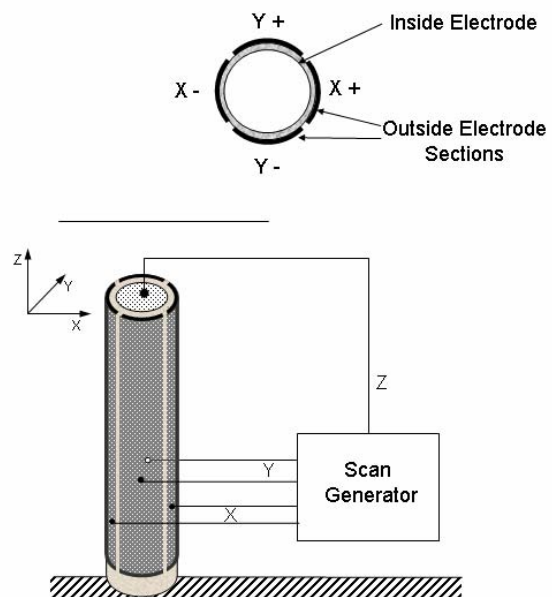


Figure 19 Tube piezo electrode configuration

be legs floating free in space adding detrimental resonance frequencies to the STM. In order to give the STM a solid base, the free ends of the three leg piezos are bonded to balls on which the STM makes point contacts with the sample holder and slides on during coarse approach.

The fourth piezo used in the beetle STM is referred to as the “scan” or inner piezo. It is set in the center of the STM head between the leg piezos. The scan piezo is where all of the tip scanning and data collection takes place. It is divided up into four quadrant electrodes and a ring electrode that connects to the interior of the piezo used for grounding. The scan piezo contains a tip in a macor/hypodermic tube holder that is bonded to the free end of the scan piezo with an epoxy.

Movement of the piezo is achieved by applying electrical potentials across the various electrodes on the PZT’s in one or more axis. All four of the piezos have a similar electrode structure to them (See Figure 19). The four quadrant electrodes are grouped in to two sets, the X coordinate movement and the Y coordinate movement. Displacement is typically accomplished by applying a positive potential to the one of the outer electrodes and a negative potential to the opposing outer electrode. The inner electrode is grounded or has a small potential that is somewhere in between the potentials applied to the outer electrodes to create a Z displacement offset (which will be explained later).

Movement of the piezo crystals is governed by a few simple equations. These equations take into account the length (l), the thickness (t), inner diameter (ID) and outer diameter (OD) of the tube, and the voltage (V) that is being applied to the electrodes. Also important is the piezo strain coefficient and the applied electric field direction.

The strain coefficient indices are 1, 2, & 3 which can loosely be thought of as X, Y, & Z coordinates, respectively. Typically, the strain coefficient representation looks like: d_{ab} where a and b are any of the 1, 2, or 3 indices. The a index indicates the direction of the applied electric field and the b index indicates the corresponding piezo displacement direction. The coordinate axes are defined by the direction of the piezo polarization. The poling direction is considered to be the Z axis which is the only unique directional axes. The X & Y axes can be arbitrarily assigned with respect to azimuthal angle.

Typical strain coefficients are d_{31} or d_{33} . Both of these strain coefficients have the applied electric field parallel to the poling direction of the piezo (their first index number is 3). For the first strain coefficient, the direction of movement (i.e. expansion/contraction) is perpendicular to the direction of the applied electric field, and for the second the expansion/contraction is along the Z direction, parallel to the applied electric field.

A positive strain coefficient leads to piezo expansion upon application of a positive applied electrical field along the strain coefficient directional axes.

The strain coefficients for the PZT-5A type piezoelectric are:¹⁴

$$d_{31} = -1.73 \text{ \AA/V} @ 293 \text{ K} \quad d_{31} = -0.31 \text{ \AA/V} @ 4.2 \text{ K}$$

$$d_{33} = 3.80 \text{ \AA/V} @ 293 \text{ K} \quad d_{33} = 0.69 \text{ \AA/V} @ 4.2 \text{ K}$$

The basic equation for a bar or strip piezo is equation(3.3):

$$(3.2) \quad \Delta l = \left(\frac{l}{t} \right) d_{31} V$$

Essentially the same equation is used for the Δl of the tube piezos given by equation(3.4):

$$(3.4) \quad \Delta l = d_{31} \frac{V \times l}{OD - ID}$$

Equation (3.5) is the radial equation for tube motion. The radial equation of motion for a tube is dependent upon the strain coefficient and the voltage applied.

$$(3.5) \quad \frac{\Delta r}{r} = d_{33} V$$

Perhaps the most useful equation that is needed when discussing the movement of the STM tip is the one that describes just how far the tip can move in the X and Y direction. More simply put what is the working range of the tube piezo? The equation for X and Y motion is equation(3.6), where d_m is an average diameter of the tube.

$$(3.6) \quad \Delta X = \Delta Y = \frac{0.9d_{31}VL^2}{d_m}$$

$$d_m = \frac{(OD + ID)}{2}$$

The simplest case is when the inner electrode is grounded and each quarter of the piezo can be thought of separately. Under these conditions the tube can be thought of as a bar or strip piezo. Applying a potential difference across the wall of the tube extends or contracts the quadrant of the piezo depending on the direction of the electric field. When anti-symmetric outer voltages are applied to opposing quadrants of a piezoelectric tube, one quadrant of the tube will contract while the opposite quadrant expands. Since both quadrants are firmly attached to one another the combined expansion and contraction produces a bending or curling of the piezoelectric.

By applying the correct voltages in the proper time sequence it is possible to make the STM “walk” as seen in Figure 20 In step 1, everything is at equilibrium and the STM is at rest, no potentials are applied. In step 2, the voltage potentials are slowly ramping up on the electrodes. One of the outer electrodes will ramp up to +130 V and the opposite quadrant electrode ramps to -130 V, with the inner electrode grounded at all times in this simple discussion (later it will be explained how a voltage on the inner electrode can be used to cause a Z motion offset, and why). Step 2 results in a bending of the piezo as described earlier. So, now with the leg of the STM attached to the crystal mount, the bending of the piezo will result in the STM head moving in the direction of the bend. Once the bending is at a maximum (and the voltage is at a maximum), step 3 occurs. In the third step the voltage applied is suddenly dropped to zero, so that the piezo snaps back to a straight position directly under the STM head. This abrupt motion is much like a tablecloth being pulled out from under a dish on a table. The trick is to make the head heavy enough so that the inertia of the head is larger than the frictional force of the STM balls sliding on the crystal mount. If the head is sufficiently heavy then the STM head will essentially remain where it was when the piezos were bent. The legs moving underneath the head allows the STM to walk in the direction of the original leg bend. If the head is too light or too heavy, the STM may not move anywhere at all (folk lore suggests an STM head weight of 1 to 2 grams is OK for our configuration).

To move the entire STM up or down in the Z plane without walking up or down a ramp is accomplished by the Z-offset. The Z-offset is a small variable voltage that is applied to the interior of each leg of the STM. The way that it works is by simply extending or contracting each quadrant of the piezos by the same relative amount.

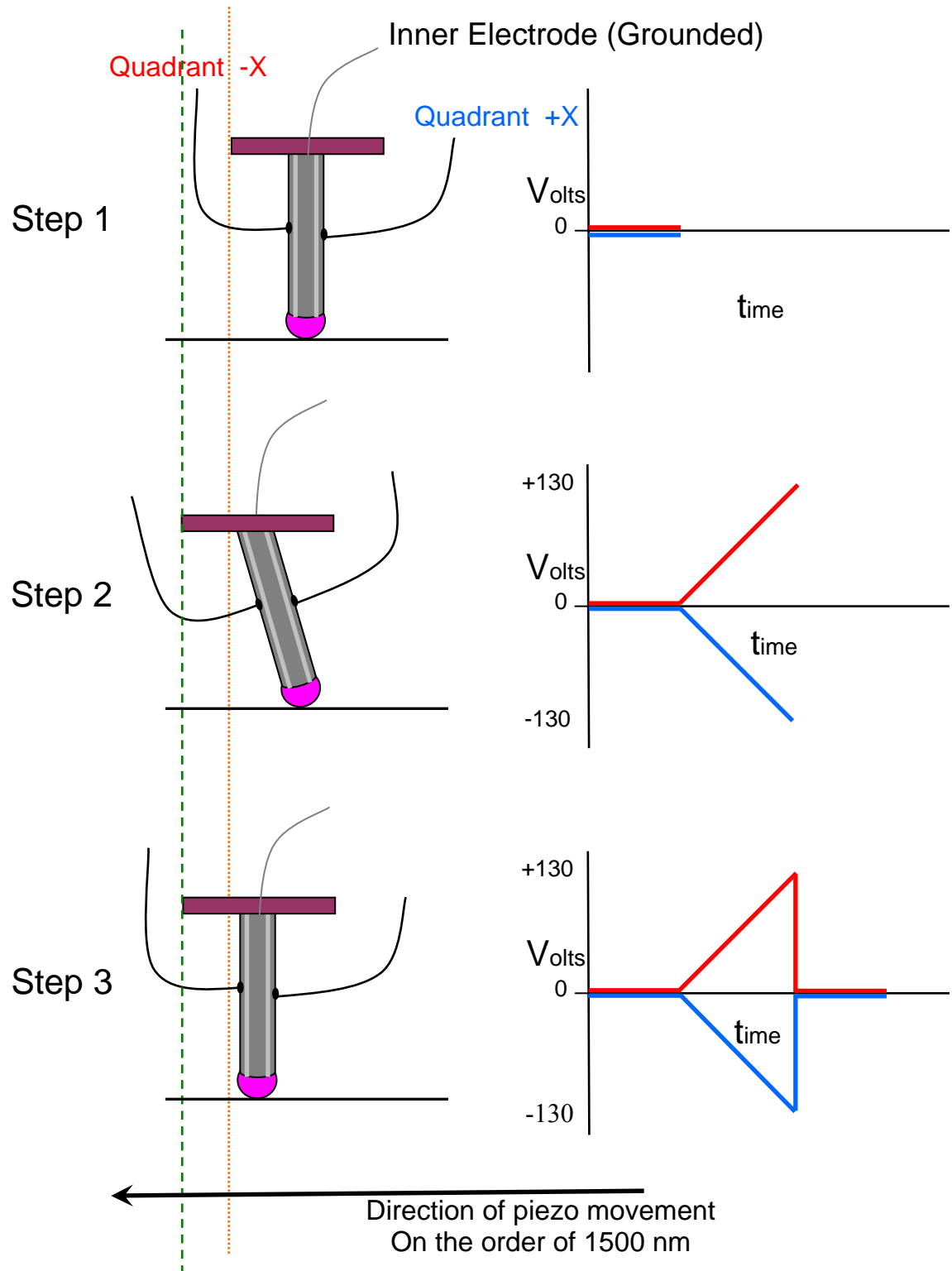
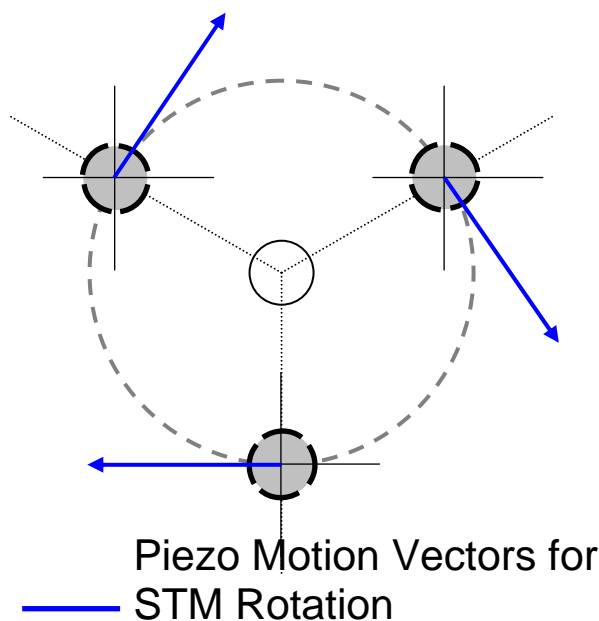
Figure 20 Piezo movement with voltage sequence

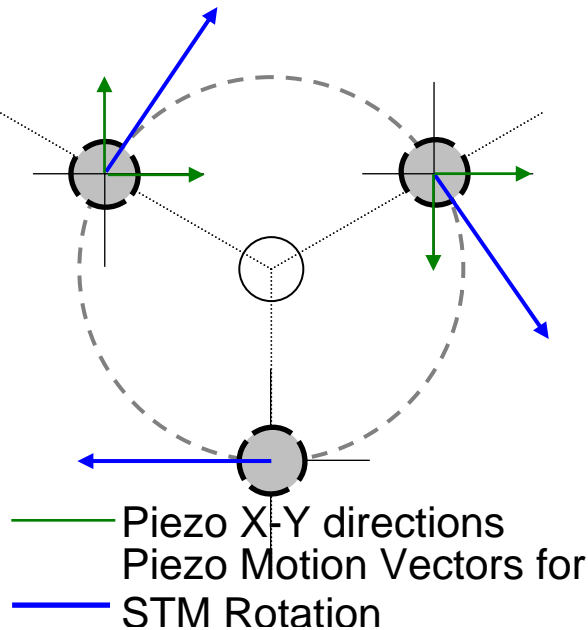
Figure 22 One configuration of the piezo leg orientation and the resulting vectors of the piezo movement vectors needed for rotation motion (i.e. STM coarse approach in Z)



quadrants of the piezo are therefore each arranged perpendicular to the tangent on the edge of the STM head. In this configuration there are only two of the four quadrants on the piezo that are ever used. This layout can simplify wiring; however, it reduces the adaptability of the beetle STM. This lack of adaptability is reflected in the

Now that the general motion of the piezos is well understood it is possible to discuss the arrangement of the piezos and their electrodes. There are two possible arrangements of electrodes shown here for a radial motion beetle STM. The first possibility is seen in Figure 21. This configuration shows two quadrants of each piezo to be arranged in a direction parallel to the tangent of the STM head edge. The other two

Figure 21 Our piezo electrode configuration that has the same X and Y axes on all piezos.



overall reduced scan range. This orientation of the piezos allows only for rotation around a single point and so if the crystal is rough or distorted at that location the only way to move to a different location macroscopically is to retract the STM tip, lift the whole STM off of the mount, and translate the STM to a different location on the mount.

If the electrode configuration for the piezos shown in Figure 22 is used, the extended scan range limitation that was described for Figure 21 no longer applies. Figure 22 shows a positioning of the electrodes into an X – Y coordinate system for the STM head. Meaning one of the three legs has an orientation that is the same as the legs in the previous example (Figure 21), and the other two piezos have the division between the quadrants lining up either perpendicular or parallel to the tangent to the edge of the STM. This electrode configuration allows the STM to walk in the X and Y directions. It is possible to apply voltages to only the \pm X electrodes and move the STM in the X direction, or apply voltages to the \pm Y electrodes and move in the Y direction. This increases the X-Y scan range of the STM almost indefinitely. However, the draw back to this configuration is that it is more difficult to wire and requires extra electronics to mix the voltages from the back of the STM controller to the correct X and Y electrodes on the STM to get the proper rotational motion for the coarse Z tip approach (solved by the RHK PPC-100).

The basics of rotation for any beetle STM is to make the sums of the displacement vectors for each electrode on each piezo to add up to a vector that yields motion tangent to the STM head. Application of three of these displacement vectors spaced 120 degrees apart leads to a torque about the center point of the STM head giving a rotation. In the case of Figure 21, the vectors are built-in, because the electrodes are oriented tangentially

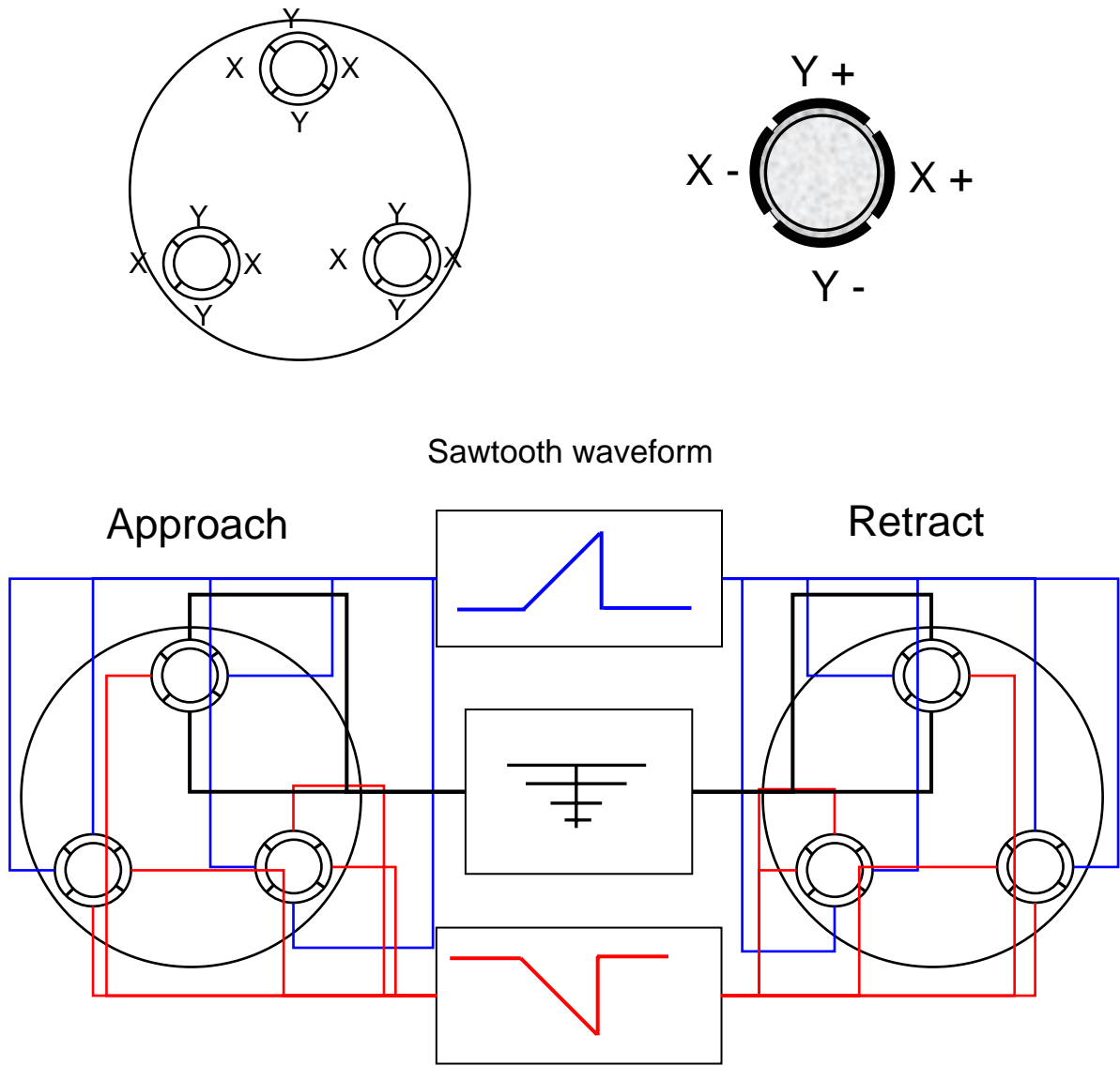
to the STM head. Therefore, rotation naturally results by applying voltages to the opposing quadrants of these electrodes. In Figure 22, it is not so simple. Two of the piezos have their electrodes pointing off-axis from the STM head tangent. Therefore, there needs to be a mixing of the movements of all four quadrants on these two electrodes. The simple way of looking at is would be to think that the two piezos are only cut into halves instead of fourths. Each half would act in the same way as in Figure 21, now that half of the piezo is in the direction of the head tangent.

There are other piezo-electrode configurations that can lead to vectors that sum to give a rotation which has not been shown or discussed here. The examples given above are the two basic orientations, and the second one (Figure 22) is the design used for our STM.

Each different configuration requires that the voltages be mixed and applied to the correct electrodes on the piezos. One can not simply connect the + X line out of the back of the STM control electronics to all of the +X sides of the piezos and expect it to walk. The voltage that the control electronics produces on the +X may need to be connected to all the leading movement sides of the piezos which could be the +X, -X or even $\pm Y$ electrodes. This has the potential to make wiring a complete nightmare. However, it is easily taken care of by use of a secondary electronics box that mixes the voltages automatically for you to get the correct voltages to the correct electrodes on the STM to make it rotate. The box is made by RHK and has the designation PPC-100. This box will be discussed later under the in the electronics section. (The voltages that are produced from the PPC-100 can be seen in Figure 23, and where they are applied for Approach and Retract.)

When wiring the STM it is useful to prepare and clean all the wires and accessories that you need before starting to solder. The wire used is 0.002" dia. kapton coated copper cut to lengths of about 17 cm, (22 to 30 of these wires should be prepared). To cut the wire, place it on a glass slide and cut with a razor blade. Next the Kapton coating needs to be removed off both ends of the wire. The best way of removing the Kapton is by scraping with a razor blade. *If the flame removal method is attempted, the copper wire will burn just as fast as the Kapton coating.* The wire is very fragile and can be cut or broken very easily while removing the Kapton. I like to place the wire on a glass slide again and scrape the wire with the back side of the razor blade so that I'm not actually cutting into the wire more like rubbing with a sharp instrument. It is necessary to try and scrape the Kapton off of all sides of the wire. So, once the Kapton has been removed on one side rotate the wire and scrap again. It should be fairly obvious as to whether the Kapton coating is removed or not, because, fresh copper is bright and shiny and the Kapton coating is a dull orange. Only a fraction of an inch of the wire is needed to have the Kapton remove, somewhere around $\frac{1}{4}$ " to $\frac{1}{2}$ " is needed. The rest of the wire needs to retain its Kapton coating so that there are no electrical shorts later on after wiring. Both ends of the wire need to be clean of Kapton and tinned with silver solder.

Figure 23 Approach and Retract waveforms that are applied to each piezo electrode.



On Approach, the positive sawtooth waveform is applied to:

$$\begin{aligned} &+X_1, -X_2, -X_3 \\ &+Y_2, -Y_3 \end{aligned}$$

the negative sawtooth waveform is applied to:

$$\begin{aligned} &-X_1, +X_2, +X_3 \\ &-Y_2, +Y_3 \end{aligned}$$

On Retract, the waveforms are switched, so the electrodes that had the positive sawtooth, now have the negative and the electrodes that had the negative sawtooth waveform now have the positive.

Tinning of the wires is done best by melting a drop of silver solder on the soldering iron tip and then dipping the end of the wire into the flux. Then immediately dip the wire into the melted solder on the soldering iron tip. Once the wire has been removed from the molten drop of solder on the iron it will be tinned with silver solder. It is then imperative that the tinned wire be washed off with distilled water. (*In truth, as soon as any wire, piezo, or etc. that has had flux on it and is done being soldered it needs to be washed with water to remove the flux. The flux is a very corrosive aqueous solution of HCl, NaCl, and NH₂Cl that will eat up surfaces if it's left on for too long. Also, because it's a water soluble solution, it needs to be washed off with water. Acetone, methanol or other organic solvents will not work.*)

Once all the wires have their ends tinned. Turn the STM upside down and use a jeweler's clamp to hold it in that position. Next, look at the configuration of the wires in Figure 24, it shows the position of each electrode and the wire that runs to it. The tinned wires need to be threaded through the corresponding hole on the STM head and then soldered to the corresponding electrode on the corresponding piezo. It is important to note that the configuration shown in Figure 24 is not the only one that can be used. It is simply the one that I use, and seems to be the easiest to solder the connections too. Also, it minimizes the wires crossing around the STM. However, any arrangement that you would like to use can be used, it just needs to be **written down as the connections are made!!!!**

The easiest way to solder the wires onto the STM head is to start from the center and work outward. Therefore, start making all the connection on the scan piezo and then the electrodes facing the scan piezo. Finally solder the electrodes that you can easily get

to from the outside. It is highly recommended that you use a thicker wire that has been dipped into the flux to transfer a drop of flux onto the piezo electrode surface and then hold the end of the 0.002" dia wire with tweezers, and have a drop of solder on the soldering iron ready to go so that the wire and the soldering iron touch the piezo electrode at the same time. Then remove the soldering iron to allow the solder to cool. It is best to use a very small amount of solder and to have the solder spot on the piezo electrode be a bright shiny spot, and not a dull gray one. A shiny drop of solder indicates a good clean surface where a dull gray one can be a dirty and porous one that has a large surface area, which can be more difficult to pump out in vacuum later.

Once all the wires are soldered onto the STM, it is best to place the STM into its aluminum/Plexiglas holder. This now allows you to CAREFULLY separate out the wires and make the soldering connections to the push pins that are used to connect the STM to the control electronics. The way to make the connections to the push pins is to first attach the push pins onto the posts around the Plexiglas holder. Then place a drop of flux on the side of the pin that you are going to solder the wire too, and solder just as you have soldered the other end of the wires to the piezos. It is not recommended that you try to solder the wire into the interior of the hole of the push pin, because the opening is supposed to take a 0.032" dia and not a 0.002" dia wire. Therefore, soldering the wire into the hole of the push pin just uses up a lot of solder and makes a weaker connection that is more difficult to ensure is electrically connected to the piezo.

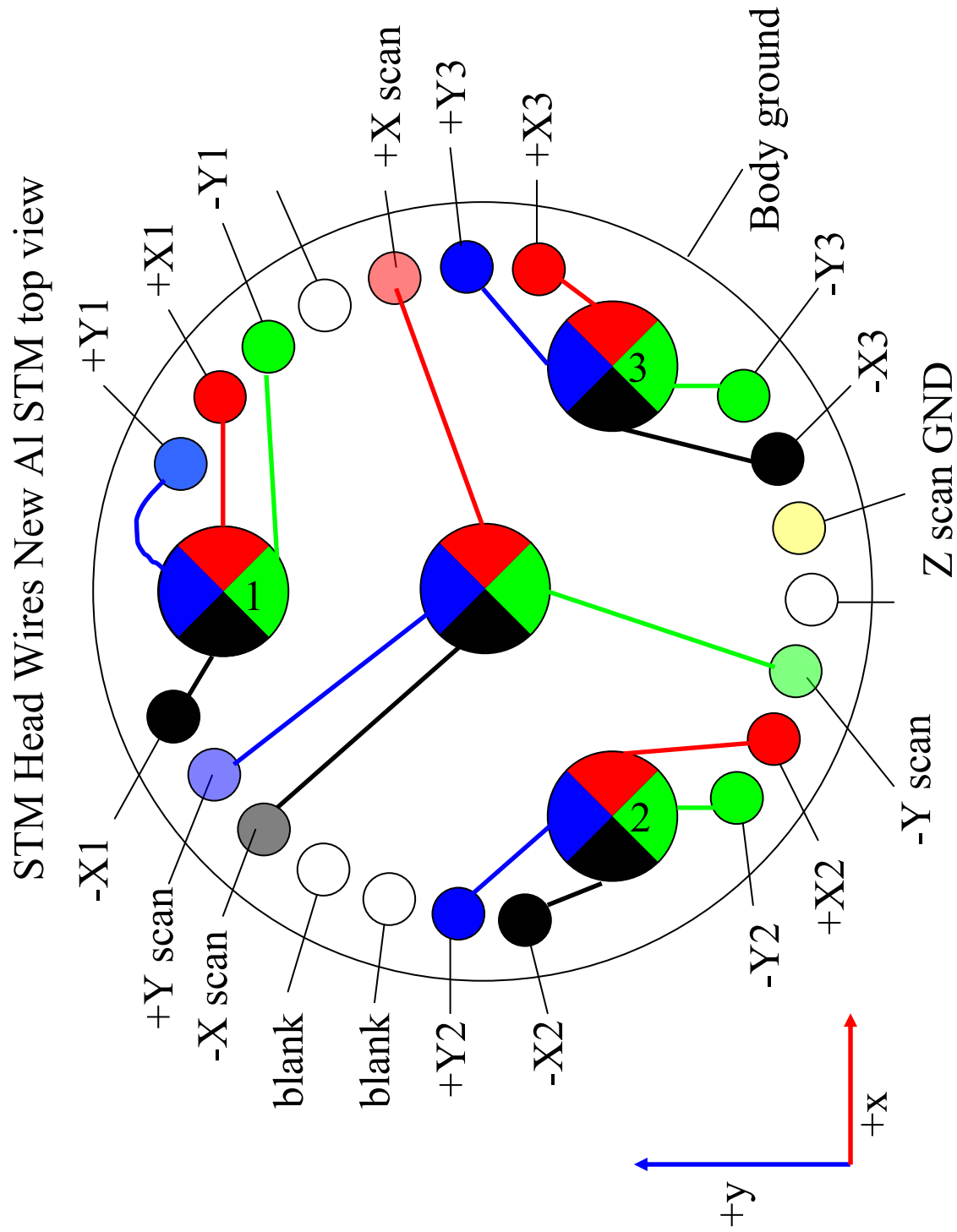
The last three connections that need to be soldered are the wires for the Z-offset. These wires can be difficult and require a light touch. The use of flux and solder should be minimized here. Only enough of each to make a secure connection should be used.

Finally once all the soldering is done it is now time to connect the STM. To do this leave the STM in its Plexiglas holder and place the whole assembly under the STM stalk. Next, lower the STM stalk down close to the tunneling current wire sticking out the top of the STM. Then **VERY VERY CAREFULLY** solder the 0.002" dia wire that is sticking out of the end of the stalk to the 0.010" dia wire coming out of the top of the STM. To make this connection use **VERY** little flux and a small amount of solder, only enough to make the connection secure.

Once the tunneling current connection is made and it is secure, lower the STM stalk down farther so the holding pin can be inserted. The Vespel (brown plastic) piece needs to go around the stalk on the STM head. Once the Vespel piece has been lowered into position, slide the 22 gauge stainless steel tube through the opening in the side of the Vespel and then into the hole on the STM head stalk. The hole in the STM is drilled to be a 22 gauge hole so the tube will be a very tight fit. It may be necessary to use a 23 gauge tube and distort it slightly to make sure the tube will not easily slide back out of position. So, once the tube is in the STM head, it may be necessary to bend the tunneling current wire out of the way to allow the tube to slide though to the other side of the stalk on the STM head and out the other side of the Vespel piece. The stainless steel tube needs to be about 1 inch in length to allow for side to side movement of the STM in the Vespel holder and still be held by it.

After the stainless steel tube is in place, it is now time to connect the head grounding wire. The head is grounded to the mounting stalk by the 0.002" dia wire that was epoxied onto the side of the STM head. This wire needs to be soldered onto the 0.010" wire that is attached to the mounting stalk by a screw.

Figure 24 A view looking down on the beetle STM head and a suggested arrangement of wires that go through which hole and attach to which piezo electrode.



Now that the STM is physically connected to the mounting stalk, raise the STM up and out of the aluminum/Plexiglas holder that it was in. Only raise it high enough to have the STM clear the aluminum holder. So, if the Plexiglas piece moves it doesn't try to take the STM with it and potentially break it. However, the STM can not be raised too high because the wires are not connected yet. This is the time that you need to look at the arrangement of the wires on the Plexiglas holder and compare them with the arrangement of wires on the Teflon ring that is connected to the mounting stalk. (The current arrangement can be seen in Figure 25.

There are a few things to note about the Teflon ring. First is, there are three places held for thermocouple wires. Two of the places are for the individual thermocouple wires to come down and connect too, and the third place is where the two thermocouple wires make a connection and take a temperature. The second thing to note about the Teflon ring is that its configuration is not set in stone! If it works better with a different arrangement of electrodes, then arrange them the way that would be better. The third item to notice would be that there are three different wires that say Z-offset. These three wires are all connected by jumper wires on the top side of the Teflon piece. So, there is no difference in one Z-offset versus another. The reason that all the Z-offset wires are connected together on the Teflon ring as apposed to on the STM head, is because it makes for much simpler diagnosis of electrical problems associated with individual Z-offset electrodes and it is easier to wire.

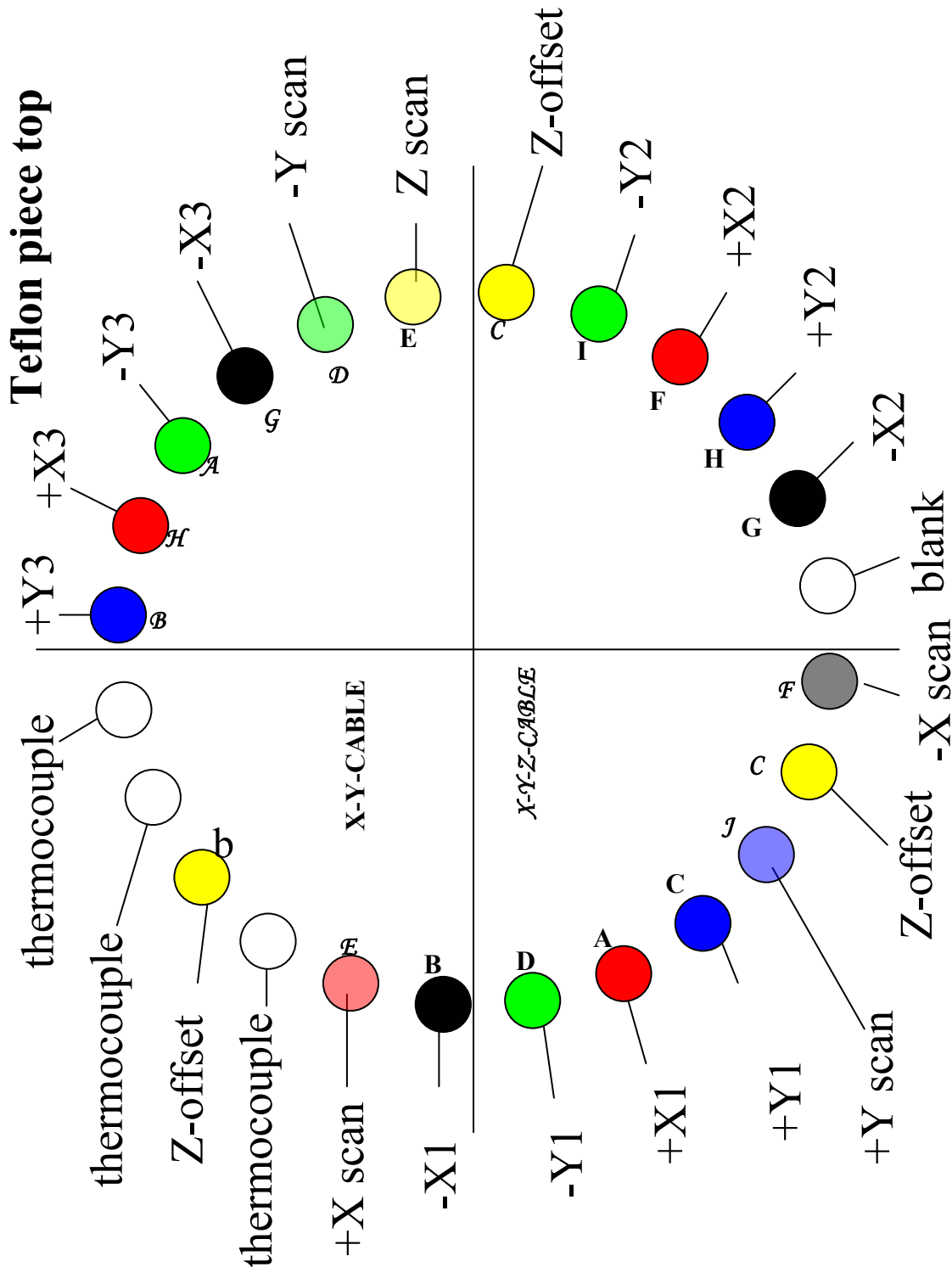


Figure 25 A wiring diagram for the Teflon ring around the STM support stalk which provides an intermediate anchoring point for the electrical connections. View looking from above towards the STM

In truth, there are only two things that you need to know when wiring the STM, you're A-B-C's and to be able to count to 3. The whole task from this point on reduces to a matching game of connecting the wires on the Plexiglas holder to the corresponding wires on the Teflon ring. Table 1 shows the connections from the PPC-100 to the feedthrough on the UHV flange. From this table it is a simple job of following the wire from its feedthrough, to the Teflon ring, then to the STM head and finally to the individual electrodes on the different piezos. Figure 26 is a graphical representation of Table 1, so as stated before it's simply a case of following the line from the individual piezo, to the feedthrough connector.

Table 1 has two parts to it because there are eighteen connections that need to be made, and each feedthrough connector has 10 pins. Therefore, two different feedthrough connectors have to be used. The first called the X-Y cable connector contains a thick single gray cable that includes most of the wires for piezos 1 and 2. The second part of Table 1 illustrates the cable connector named X-Y-Z. The X-Y-Z cable connector includes a single gray cable and five black coaxial cables. This X-Y-Z cable connector contains the wires for scanning, and also the wires for piezo 3, as well as the Z-offset wire.

Table 1a
X-Y Cable

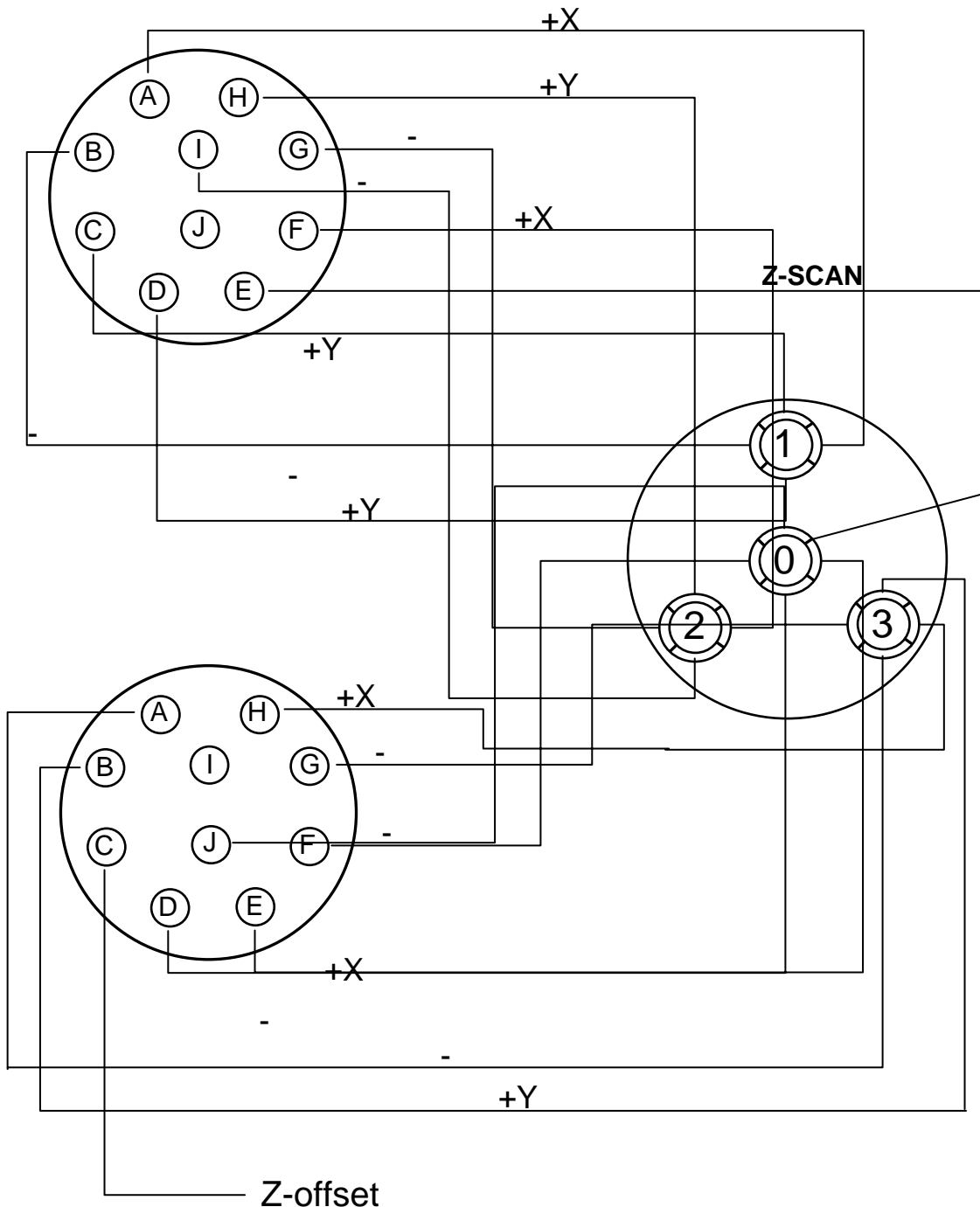
<i>UHV 300 Amphenol Conn</i>	<i>Wire Color</i>	<i>Function</i>	<i>PPC-100 (26 pin Conn.)</i>
A	WHT/BLK	+X1	A
B	ORG/BLK	-X1	B
C	GRN/BLK	+Y1	C
D	RED/BLK	-Y1	D
E	BLUE	Z-Scan GND	E
F	WHT	+X2	F
G	ORG	-X2	G
H	GRN	+Y2	H
I	RED	-Y2	J
J	BLK	COM 2	K

Table 1b
X-Y-Z Cable

<i>UHV 300 Amphenol Conn</i>	<i>Wire Color</i>	<i>Functi on</i>	<i>PPC-100 (26-Pin Conn.)</i>
A	RED	-Y3	P
B	GRN	+Y3	N
C	COAXIAL	Z1,Z2, &Z3	STM 100 > Z- OFFSET
D	COAXIAL	-Y0	STM 100 > -Y SCAN
E	COAXIAL	+X0	STM 100 > +X SCAN
F	COAXIAL	-X0	STM 100 > -X SCAN
G	ORG	-X3	M
H	WHT	+X3	L
I	BLK	COM 3	R
J	COAXIAL	+Y0	STM 100 > +Y SCAN

Figure 26 View of the connections made from the Amphenol 10 pin connector to the piezo electrodes.

X-Y Cable

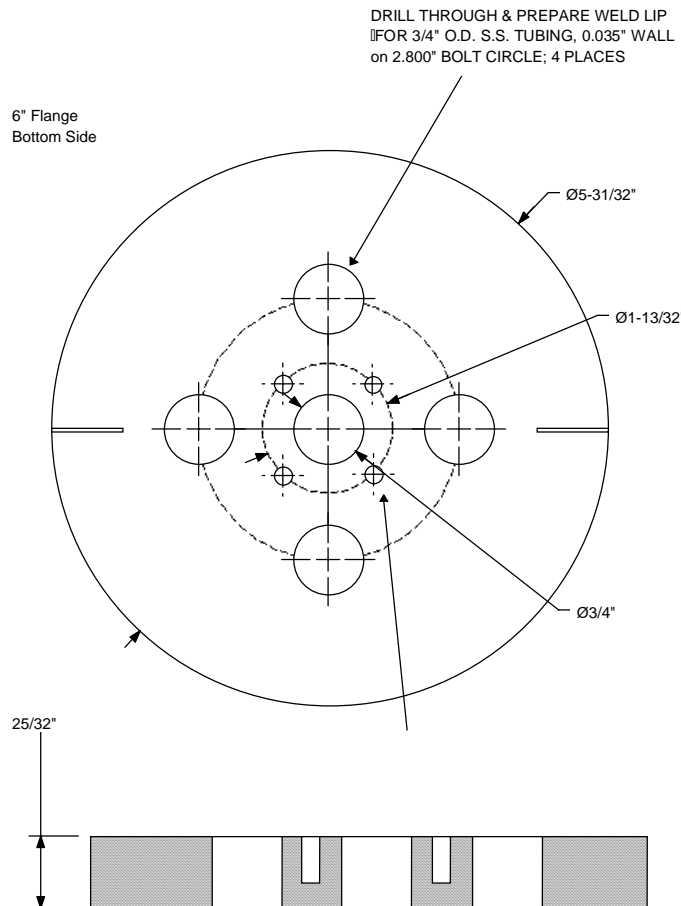


The last piece of information that one needs to know about wiring the STM is configuring the STM mounting stalk. The mounting stalk is simple in design: it consists of the main 6" stainless steel UHV flange four or five (depends on which main flange is used) mini conflat half nipples that have been welded onto the top side (air side) of the main flange and the STM mounting stalk that is bolted into position on the bottom side (vacuum side) of the UHV flange.

The four or five mini conflat nipples are arranged in a square pattern with the fifth mini conflat in the center of the square (see Figure 27). Two of the conflats are used to

connect the amphenol

Figure 27 Blueprints for the 6" flange used to attach the STM and support stalk.



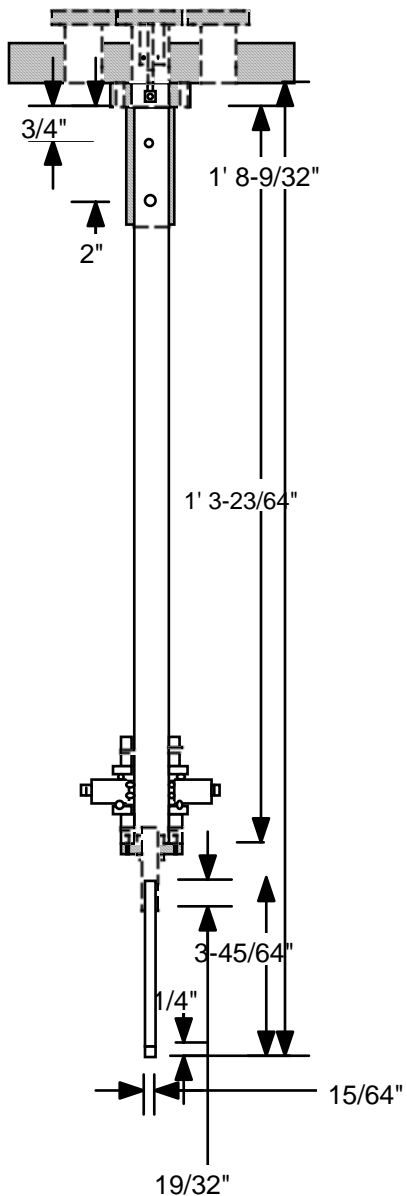
feedthrough that allow the STM wires to enter the UHV chamber. A third conflat is used to connect a thermocouple feedthrough. The fourth conflat in the square can be used as either the tunneling current wire feedthrough or can be left blank and used some other way later on. If there is no fifth conflat connector then the fourth conflat will have

to be used as the tunneling current feed through. However, if there is a fifth conflat feed through in the center of the main flange it is highly recommended that you use this one for the tunneling current wire.

The reason that it is advisable to use the center mini-conflat for the tunneling current wire connection, is because there is less wire that will not be electrically shielded by the STM mounting stalk. Also, using the center conflat for the tunneling current wire connection makes it easier to wire, because it's just straight up and down though the mounting stalk. Where as if the off center conflat is used you have to make a 0.002" wire loop out of the mounting stalk, down around more shielding and finally up to the tunneling current feed through.

With either design it is essential that the mounting stalk and the main flange be electrically isolated from one another. This is done to insure a stable and reliable reference ground for the STM to compare the tunneling current too. It does this by using an isolated wire/ground feed through around the tunneling

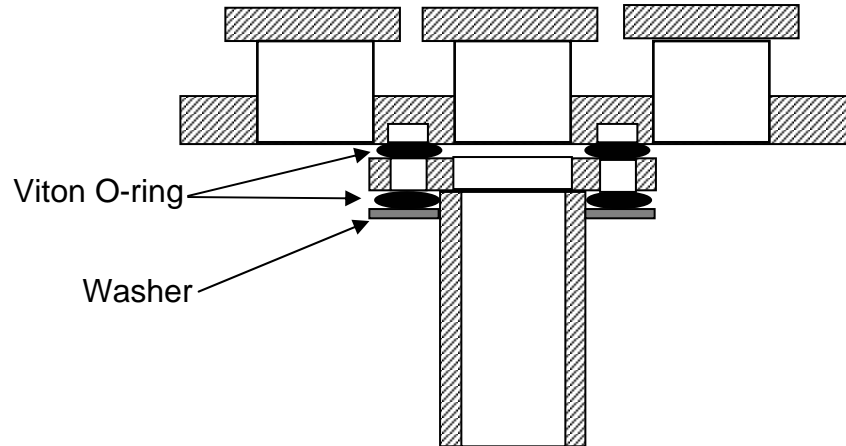
Figure 28 Blueprint for the STM support Stalk.



current wire. This means that the mini conflat connector that is used for the tunneling current wire has a ceramic spacer which breaks up the ground connection from the grounding shield that the BNC connects too and the metal piece of the feed through that gets bolted onto the flange. The isolated ground that the BNC connects too, is connected to a wire in the vacuum side that get attached to the STM mounting stalk (Figure 28) so that there is a continual shielding or faraday cage from the STM tip all the way to the preamps/controller that is protecting the tunneling current wire from stray electronic noise that interferes with the very low currents that are being measured in the experiments.

The isolated feed through is only the first step in electrically isolating the mounting stalk from the main UHV flange. The rest of the isolation is accomplished by Viton and alumina tubing. If the mounting stalk was bolted directly onto the 6" UHV flange it would result in a ground loop. So, to get around this, the bolt holes in the mounting stalk are drilled larger than what the bolts need, and an alumina tube that has an inner diameter clearance equal to that of the outer diameter of the bolts are placed around the bolts and into the bolt holes in the mounting stalk. The use of the alumina tubing will not by itself isolate the mounting stalk from the UHV flange. The final stage in the isolation is to use Viton washers. The Viton ring is placed on both sides of the mounting stalk so that the bottom of the bolt head is not touching the mounting stalk and the top face of the mounting stalk is not pressing flush against the bottom of the UHV flange, it will be sitting away from the bottom of the UHV flange by the thickness of the Viton (a representation of this can be seen in Figure 29).

Figure 29 Diagram showing how the STM support stalk is connected to the 6" flange that electrically isolates the stalk from the UHV chamber.



3.6 STM TIP CREATION

Contents:

- Intro/Background
- Terminology
- Generic electrosharpening
 - Coarse*
 - Fine*
- W (tungsten) tips specifics
- Pt/Ir 10 or 20 tips specifics
- Judging sharpness
- Storage of fabricated tips.

3.6.1 INTRODUCTION / BACKGROUND:

Perhaps the most important aspect to high level STM image acquisition is a sharp tip. In recognition of this fact, multiple groups have dreamt up many schemes, spent much time, and written numerous papers^{15,16,17,18,19,20,21,22} all in the quest for a reliable

and repeatable tip. The best tip that one can hope for would terminate in a single atom and would have a known chemical composition.

The instinctive reasoning for a sharp tip is that, the sharper the tip, the better the *absolute* resolution (disregarding bias voltage effects).

Real world experience might tell us it's all but impossible to distinguish objects that are separated by a distance of only a few Angstroms with a 20 or 30 Angstrom sized object. However, in STM the particle that is actually doing the measuring is the electron and not the atoms at the tip. Therefore, in theory there is no reason why fraction of an angstrom resolution is not achievable. So why do we bother trying to get a very sharp tip? The reason lies in the mathematics of quantum mechanics and the tunneling mechanism of electrons. The electron has to have points of origin and destination. The probability (P) of tunneling and therefore the current measured depends exponentially on the distance (z) between these origins and destination points, as dictated by the tunneling equation(3.7).

$$I \propto Ae^{-2\kappa z} \quad (3.7)$$

The symbol κ contains other factors that will affect the tunneling probability such as the work function (ϕ) of the surface, and the bias voltage potential (E) between tip and sample equation(3.8) that are not discussed here.

$$\kappa = \sqrt{\frac{2m(\phi - E)}{\hbar^2}} \quad (3.8)$$

Still the main focus in Eq (3.7) is the exponential dependence of the tunneling probability vs. distance. Therefore, if the surface is flat and smooth, like Pt(111), the shape of the tip and where the electrons tunnel from in the tip are of great importance for a good image (see Figure 30). If the apex of a tip terminates in a single atom, due to the exponential

nature of tunneling, nearly all of the electrons are collected/transmitted from the one terminal atom. However if the tip is blunt, meaning a radius of curvature greater than 20 nm at the tip apex, the electrons that constitute the tunneling current can come from various places on the surface and tip, leading to a low resolution or blurred image.

If the STM tip has a radius of curvature that is less than 20 nm, then things begin to look good. There may not be a stand alone single atom at the very apex but if there is one that is more prominent than the others around it, most of the tunneling current will be localized on the one atom. However this also limits your ultimate resolution in the z axis. For if there are two atoms at the tip apex and the second atom is only 0.1 Å farther away from the surface than the first atom, it will be difficult to distinguish a corrugation of the surface that is greater than 0.1 Å. On a surface with a very small corrugation one of the atoms dominates the tunneling current contribution, but with a larger corrugation, if the atom that is doing all the tunneling moves closer to the surface while directly above the depression in the surface electron density, the second closest atom that is offset from the first atom may start to take over the tunneling on a different part of the surface leading to a slightly distorted or blurred image with poor contrast (Figure 31). For corrugations that are very small, the primary problem is mechanical or electrical noise that is larger than the z axis movement of the STM tip being rastered across the sample.

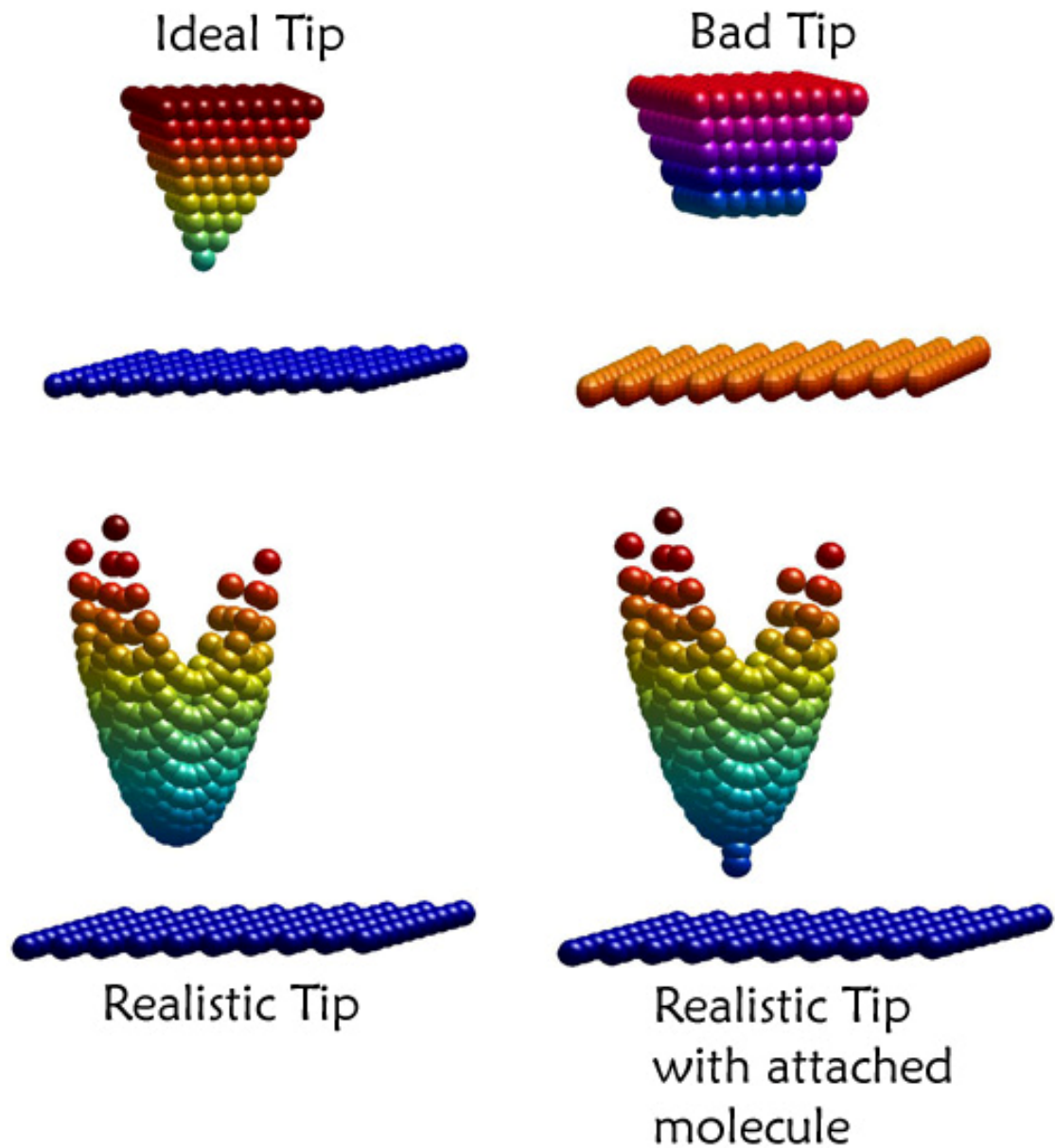


Figure 30 Theoretical images of various STM tips ranging from an ideal single crystal tip to a bad tip, a more curved realistic tip and an ideal realistic tip with an attached molecule through which tunneling can occur. (images generated with MatLab)

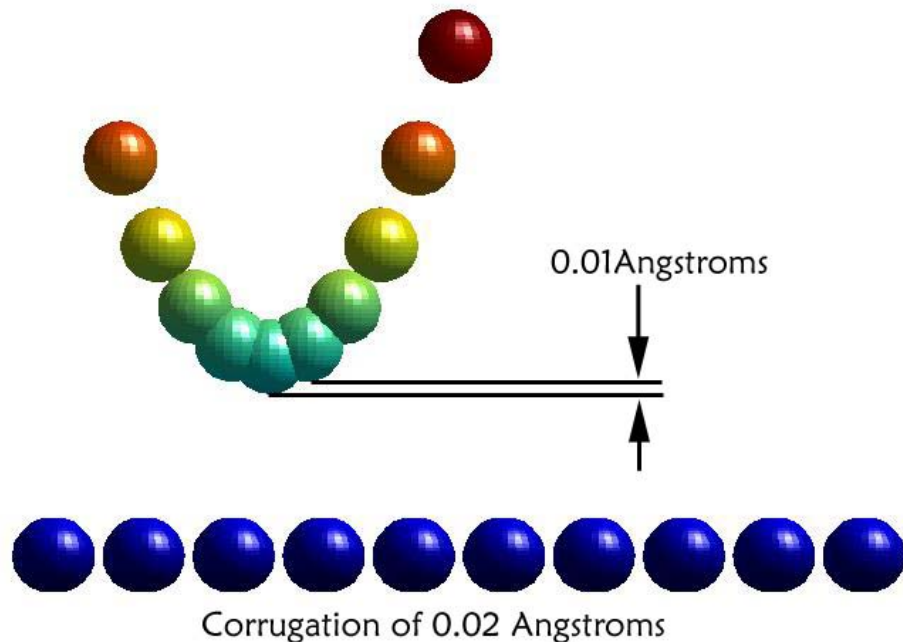


Figure 31 Theoretical section of a STM tip where the height distance of the secondary atoms of the tip is not sufficiently far away from the surface so that the tip structures limits the observable corrugation of the surface by artificially decreasing the tip movement due to increased tunneling of electrons from/into the surface via the secondary tip atoms during tip rastering.

The history of trying to make very sharp tips did not start with the advent of the STM. The need and process started many years earlier with the Field Ion Microscopy (FIM) community. Many of the techniques that they pioneered can easily transfer to the creation of STM tips. This fact is exemplified in that our current AC polishing system was designed and built by an old time FIM guru, Dr. Allen Melmed (<http://www.customprobes.com/>). Field ion microscopy can be done on most any single crystal metal surface that can be sharpened to a point. However, in the STM community,

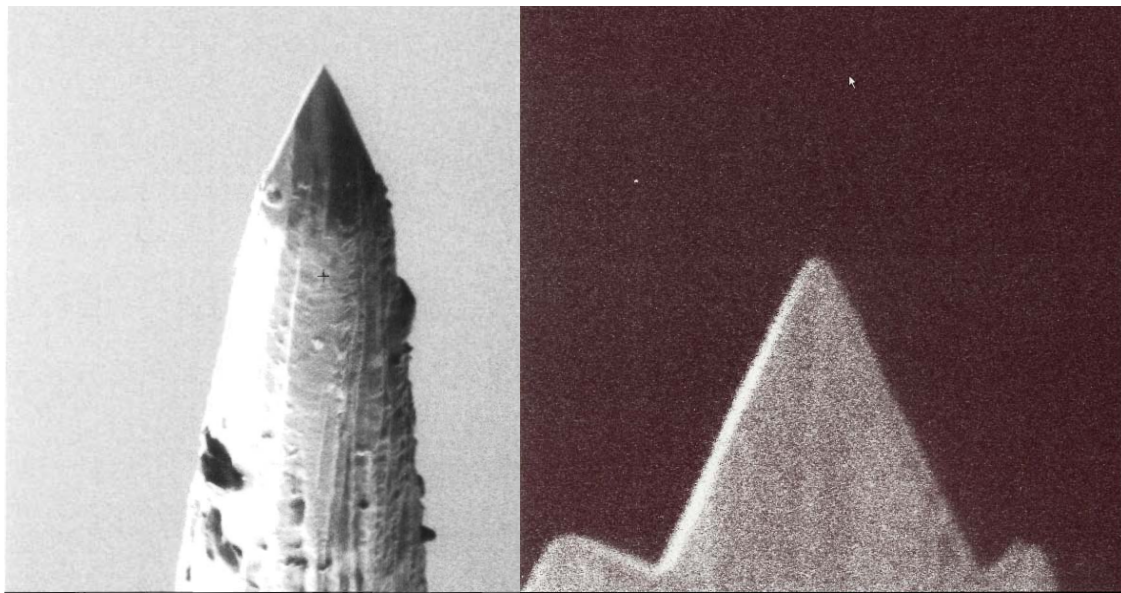
tungsten and varying alloys of platinum-iridium are used almost exclusively, with the exception of a few experiments that also probe the characteristics of the tip material (such as silicon tips for energy filtering.²³ Fe or Ni tips for magnetic measurements, electron spin polarization experiments,²⁴ and superconducting tips for examination of superconducting surfaces).²⁵ But W and Pt is probably what 95% of the STM community use. With a slightly larger percentage using W tips over a Pt-alloy. The affinity for W tips is mainly because of its ease of etching, strength, and good d_z^2 orbital character (meaning the apex atom may have an orbital pointing towards the surface). The advantages of Pt-alloys are that they generally don't form thick nonconductive oxides, and these are softer metals that can be quickly cut mechanically to an atomically sharp terminus.^{26,27}

There are three main methods that have been described in journals or handed down by word of mouth that can be used to make STM tips. However, not all methods are created equal and not all are easily available to every STM group. The first method is the cut and pull²⁶ noted above. Second, is electrochemical etching/polishing which is probably the method in most widespread use.²⁸ The third method requires a Focused Ion Beam (FIB) machine to mill the tips.^{20,19} There are other options to create or modify tips on the microscopic level but these are the main methods that can be done outside the STM whereupon the tip can be introduced into the instrument, possibly under UHV conditions.

The cut and pull method is perhaps the simplest but also the most unreliable. Some people will say that only 1 in 10 tips are good. In my experience this average is closer to 5 or 6 in 10 that are useable (not necessarily atomic resolution good, but useable). The procedure for this method is simply to take a pair of very sharp wire cutters

(superstition will say that Snap-on tools cutters are the best, but you must find what works for you.) and cut at an angle along the wire, then once the cut is half way through the wire, pull the cutters through the rest of the cut so that what is left on the tip of the wire is a tear and not a cut. This method is much more of an art than a science, so what works for one may not work for another practitioner. The technique has yielded good results for me and is described here as: first clamp one end of the wire (typically 0.010 dia. 90%Pt 10%Ir) into a vise then hold the other end with a pair of needle nose pliers and pull taut, next make a nick in the wire at about a 45 degree angle to the perpendicular of the wire. Making certain that the cut does not cut all the way though. Once the nick in the wire is made, use the needle nose pliers to pull and break the wire at the place where the nick was made. Obviously there are limitations as to what metals may be prepared with this method. Tungsten is too brittle and hard to use, so most commonly Pt/Ir wire is used. The important points in this procedure are that the cut can not go completely across the wire and that the cutters or pliers must never touch the very end of the freshly torn wire.

Figure 32 SEM scans of tips in the FIB instrument. The right image is 9 μ m across, and the image left is 2500 nm across.



The second etching method is the most commonly used by STM groups in one form or another. It's simple in concept but becomes more difficult in detail. The basic idea behind this approach is that it is possible to place a wire electrode to be etched into a solution along with a counter electrode that will not be etched or not significantly etched, apply a voltage between the two electrodes and wait until etching is complete. The solutions and voltages used vary from metal to metal so there's no one-catch all procedure. The details of what procedures are used for what metal will be discussed later in the paper. Most journal articles found will use W wire, and only a few will use Pt-alloy wire.

The third method requires the use of a Focused Ion Beam machine and is therefore not accessible to many STM groups. The FIB uses a focused beam of high energy Ga ions to microscopically mill away parts of the wire to leave a very sharp tip. Within this method there are two main procedures to attain viable STM tips. Both

procedures require the use of an already coarsely etched/cut wire ending in a tip of a few 10's of microns radius at the most. The coarsely formed tip is inserted into the FIB to be processed in one of two ways. The first procedure is a macroscopic common sense approach where the beam of ions is run at an angle to the tip and the wire is cut on an edge on one side of the tip, much like using a knife to whittle a point on a stick of wood (Figure 32). Then rotate the tip so that the other side is now at the same angle to the ion beam and mill away a wedge. So, now where the two planes that were milled away meet, there is a very sharp transition. The problem is that this milling leaves a very sharp edge and not a point. To create a point the tip needs to be rotated ± 90 degrees and milled another time. So, the tip at this stage is a sharp edge but a shorter one than in the previous stage. The trickiest part is the 4th cut which is 180 degrees from the 3rd cut. This final cut has to intersect the exact place where the 3rd cut comes to its side of the point. Ultimately this will generate a tip that has a small pyramid structure at the end. Making all of the cuts line up just right is very difficult and usually leaves you with a tip that is sharp but not terminating in a single atom.

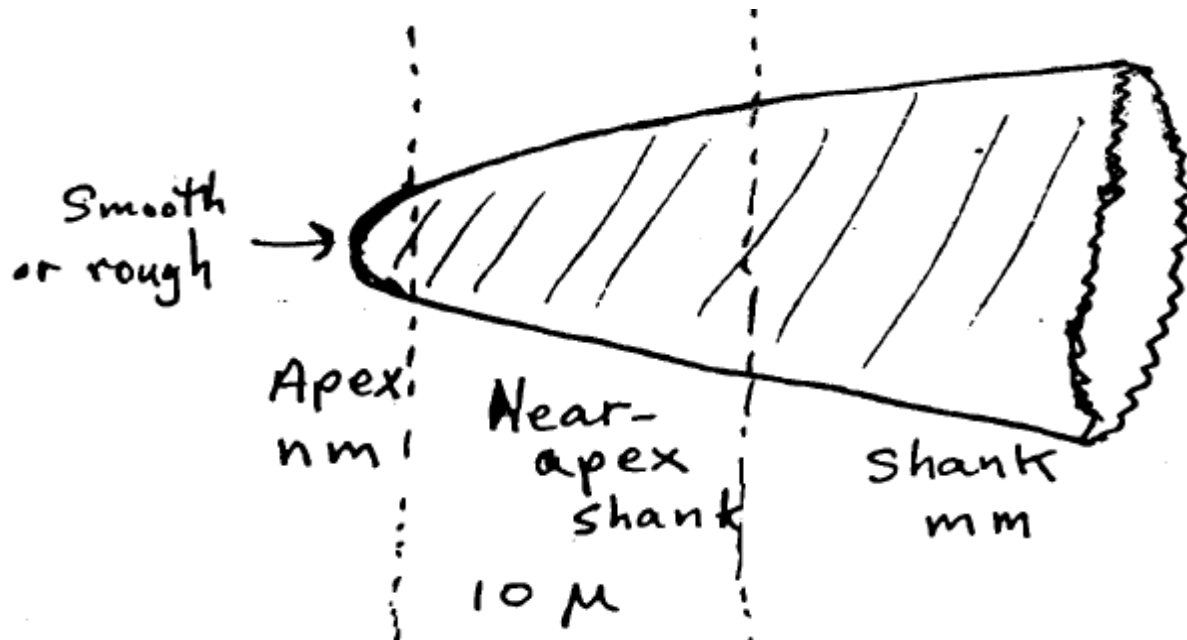
The second procedure used to mill tips requires a little faith and short milling times. In this procedure, the previously coarsely etched tip has a relatively sharp apex terminating in about 100 to 200 nanometers (not sharp enough for STM imaging.) This sharp tip is placed directly in the line of the ion beam path, so that the tip is being hit with ions head on. This will mill away the apex of the tip, but not as fast as the rest of the shaft of the tip. The theory states that the apex of the tip will be hit, but being it represents a much smaller cross sectional area than the shaft of the tip, it will be milled at a lower rate than the rest of the tip. This translates into a procedure that will neck down

the near apex region of the tip and give a nice sharp tip.²⁰ (Note: the Ga beam may chemically modify the tip surfaces!)

There are other methods of in situ tip sharpening such as: field emission, ion sputtering (unfocused ion beam), heating of tip (both resistive and electron bombardment), and light crashing of the tip into a surface. These methods of tip preparation work only on already sharp tips and can be used to shape a tip generating not so good images to a tip that generates great images. These methods are discussed after the etching procedure.

3.6.2 TIP AND TIP PREPARATION TERMINOLOGY:

Figure 33 Pictorial description of the regions on a STM tip.



The STM tip can be broken down into three areas (seen in Figure 33): The apex, the near apex shank, and the shank. The apex of the tip is considered to be only the first few nanometers, and can terminate in a rough or a smooth surface. The near apex shank is approximately the next 10 micrometers of the tip. Then the shank is considered to be everything else which in our STM is on the order of 8 to 12 mm. In all references to the "STM tip" we are considering the apex of the tip unless otherwise stated.

Other terms that will be mentioned here will be polishing, and etching. These two terms may seem to be synonymous with one another, but they are not. Etching refers to a large scale removal of materials, whereas polishing is a removal of very small amounts. These two terms, in reference to tip fabrication, spawn the idea of a two step approach. First the coarse etch, and secondly a fine polish. The reason the distinction between the

two is important is because coarse etching generates the basic shape of the tip, and fine polishing narrows the apex down and structures it into a usable STM tip.

Other terms that will be used are front polishing and back polishing. These two terms are used in conjunction with the fine polish apparatus called the “micro manipulator”. The difference between front and back polishing is very much as it would seem. Front polishing is referring to removal of material from the apex region of the tip, and back polishing is the removal of material from the near apex region and leaves the apex of the tip untouched.

Generic Electrosharpening:

3.6.3 COARSE ETCHING:

Regardless of the metal being used to create a tip, there are certain guidelines, rules, techniques, and hidden issues to be aware of.

- Initial cleaning of the wire
- Electrolyte (chemical composition, Concentration, pH)
- Wire immersion (depth, alignment)
- Counter-electrode (materials, size, shape, position)
- Container (material, size, shape)
- Temperature
- Voltage (kind, magnitude)
- Liquid-wire surface tension
- Process stopping (when, how)
- Post-polish wash (chemicals, duration, method)
- Chemical and electrochemical interactions (container, electrode)
- Solution impurities / changes in time

Just as in good UHV practice's cleaning is a very important task, and will be visited frequently in the many steps of STM tip creation. Initial cleaning can be as simple as making sure there is no dirt and debris on the wire, or doing a quick wash with acetone to remove any hydrocarbon build up. The initial cleanup of certain metals can also be done by electrical methods, for example the W wire is held at a potential of about 35 V-AC and is quickly dipped into the KOH etching solution. This dipping removes the oxide layer on the W wire and the wire should now look shiny compared to the dull gray color it was before.

The cleaning done after etching and polishing is completed in pure distilled water. The tip is dipped into the water and held steady. It is not recommended to swirl the tip around in the water. The swirling action effectively increases the cross sectional area of the tip in the water, and if there is any microscopic particulate matter in the water the chances of the tip picking it up is greater if the tip is moving than if the tip is dipped and held motionless. The tip should be held in the water for a period of approximately 20 seconds.

Next to consider is the electrolyte. Not all metals will etch in the same electrolyte. An example: W wire is etched in a 3M KOH solution, and Pt-alloy wire uses a (sat.) CaCl_2 solution. Other electrolytes can be used as well. W will etch in NaOH and Pt-alloy wire can be etched in a solution of NaCN ,^{29,30} or molten salts³¹ (not highly recommended).

These two example metals etch using different methods, the W wire reaction is fairly well understood and proceeds through oxidation of the W surface, which can be removed to reveal a fresh surface to etch. The Pt-alloy reaction is not very well

understood and is still a matter of debate among chemists/metallurgists. However, for etching to occur the solution has to be basic. There seems to be more of a problem with keeping the CaCl_2 solution from becoming neutralized by contamination or by cleaning of the solution than the KOH. Therefore the CaCl_2 solution needs to be replaced approximately every 10 tips. The CaCl_2 solution when etching will become black with particulate matter. It is necessary to remove this “gunk” by a physical or chemical means. The gunk can be removed from the CaCl_2 solution by introducing HCl into the electrolyte. The HCl will resolubilize the black particulate matter but at the expense of neutralizing the pH of the solution.

Figure 34 Picture of a basic tip etching set up where there is a power supply some etching electronics and a beaker that the tip metal is placed in vertically to etch.



The depths to which all wires to be coarse etched are dipped is the same. The depth is set to 1/8th of an inch for our apparatus. This depth is determined by the thickness of a piece of Plexiglas that is placed under the beaker containing the electrolyte solution. The procedure used to set this depth is as follows: first adjust the wire so it is held with the clamp on the etching stand, making sure that the wire is perpendicular to the surface normal, then use the z motion stage to adjust the height of the wire over the solution so that the wire just touches the surface of the electrolyte, next lift the beaker up slightly and slide the Plexiglas spacer underneath the beaker. Now all tips should be etched virtually the same way. By keeping the depth that the wire penetrates into the solution consistent, other parameters such as contact area should be constant as well. Therefore, for a given time, voltage and electrolyte concentration all tips should emerge almost identically in shape and quality from run to run. The basic etching set up can be seen in Figure 34.

The counter-electrode that is generally used is a carbon rod. These rods are used because they are cheap, easy to use, and generally don't chemically disrupt the electrolytes used, thus making it our universal counter-electrode. Because of the AC voltages that are used by our system the shape and position of the counter electrode are of little consequence. However, if a DC voltage is used to do the etching, the position and shape of the counter electrode may have an impact, because there can be more direct channels of ion flow to and from the wire electrode to the counter electrode. This established flow of ions may make etching on one side preferential to the other thus creating an asymmetric tip. This shortcoming with DC etching can be overcome if a beaker like that seen in Figure 35 is used. As for the size of the electrode, it is rather

inconsequential as long as it is thick enough to last an entire etching without having to be replaced if some of the counter-electrode is removed.



Figure 35 Picture showing the etching beaker with a side arm for the counter electrode, used to prevent disturbances in the solution near the tip metal from bubbling at the counter electrode.

The container used for etching W or Pt-alloy wire is a Pyrex glass beaker of 250 ml in size. Other materials can be used such as a polyethylene, Teflon or even an unreactive metal depending on what element/alloy is being etched. The material that the container is made from is really only important if the electrolytes attack the container walls, or if the container leaches out contaminates (example: do not use a Pyrex/glass beaker to etch Si tips, the Si in the beaker walls will interfere with the

etching process.) The volume of the beaker, matters only in terms of making sure that there is enough electrolyte to do an etching without much contamination of the electrolyte (with a 250 ml beaker filled, the electrolyte should last several coarse etchings.)

One of the most important factors in coarse etching is deciding at what voltage to etch. Here again there is no set standard for all metals, in fact there is no one set voltage to use for a given metal, trial and error will guide you to the setting that will work best for your application. The first decision to make when choosing a voltage is whether to use AC or DC potentials. A DC voltage etching technique has been discussed in papers for many years and seems to be prevalent throughout the STM community. The choice of using DC voltages dictates what material wire is used, and that the operator terminates the etch or has a trigger switch that terminates the etch at a certain spike in current (or some specified event). For W, the DC etch proceeds only through oxidation of the W wire, so it is possible to build up a thick non-conductive layer on the tip that would need to be removed by some other means *in situ*. The AC etch proceeds something like the DC etch, without a quick termination or the

continual build up of oxide. The AC process uses no quick shutdown electronics so etching continues until it halts on its own. It also uses the

Figure 36 Picture of the microscope and micro positioning device that holds a metal loop of wire with a drop of solution that is passed back and forth over the tip apex.



AC cycle to its' advantage, where half of the voltage cycle oxidizes the W wire and the other half drives the newly oxidized W off the wire exposing fresh W to be etched. This

leaves, at the most, a few monolayer thick non-conductive oxide on the wire surface, which can be tunneled through.

As stated earlier different metals require different etching procedures. If a Pt-alloy wire is chosen to be etched then an AC voltage potential is required. The etch seems to eat away the Pt almost like a spark eroding process rather than by chemical means. Consequently there is that there is significant heat that is built up at the apex of the tip which will generally wear away to a point. At which time the heat generated seems to remelt the apex of the tip and cause it to form a microscopic dot on the end of the near apex region. The dot is removed in the fine polishing stage.

3.6.4 FINE POLISHING:

Most of the parameters discussed for coarse etching apply to the fine polishing procedures. Concerns such as container material and initial cleaning are not applicable, but the electrolyte, counter electrode, voltage, liquid surface tension, and especially wire immersion depth and knowing when to stop are all important.

The fine polishing apparatus looks like Figure 36, it consists of four main components, a microscope, a micromanipulator, a loop of wire containing a drop of electrolyte, and a tip to be polished.

The microscope is a generic variable stage microscope that has 3 different objective lenses (a 4X, 10X, and a special far focal length 50X) and one 10X ocular lens. Unfortunately due to the special focal length of the 50X lens the three lenses are not parfocal. What this means is that it's not possible to use the lower magnification lenses to center the tip in the field of view and then switch to the highest magnification lens,

everything will be out of focus and you will have to search for the tip in the Z axis again, and most likely in the X and Y plains as well. So it's advisable to just start out with the high magnification lens and search for the tip only once. To find the tip with the high magnification it is easiest to move the tip and holder past the focal point of the microscope. Then slowly move the stage out and wait until there is a visible contrast that will indicate the edge of the tip holder. Once the edge has been located, move along that edge and find the shaft of the tip. Refocus on the shaft of the tip and move the tip farther out following the edge of the tip. Once the shaft of the tip starts to taper off to the apex region of the tip, it will be necessary to readjust the position of the microscope stage and refocus on the tip.

Once the tip is centered and focused, retract the tip from the field of view by adjusting the lateral position knob on the microscope translation stage. With the tip out of the way, position the wire loop with the drop of electrolyte into position under the microscope field of view. Adjust this wire loop and droplet so that when the loop is moved in and out by the micromanipulator its path is parallel to the shaft of the STM tip. Also it is recommended that the tip penetrate the liquid droplet in the center to provide a uniform etching around the tip apex. After the tip and loop/droplet has been aligned, move the tip into the droplet. Initially, back polishing is performed. The correct positioning for this is too move the loop/droplet close enough to the STM tip so that the apex of the tip pierces through the far side of the droplet and the near apex region is inside the droplet. A voltage is applied between the tip and wire loop and the loop with the droplet is moved back and forth over the near apex region of the tip. This action removes material from the near apex region and eventually forms a very narrow nanowire

($< 1 \mu\text{m}$ in dia.) that supports a thicker ball that was previously the tip apex. Once the wire has been narrowed down sufficiently a front polishing process is begun.

The front polishing process removes material from the tip apex itself. Once the nanowire is formed, lower the polishing voltage and slowly remove material from the apex of the tip. To front polish, quickly move the loop/droplet down the near apex region of the tip and away from the tip apex. Eventually the nanowire that was formed in the back polishing step will continue to shrink in size until it narrows enough to become the new tip apex (which will happen very suddenly, so only apply one quick pulse [press of the “apply voltage” button] at a time) and the material that constituted the apex initially, will leave. The real trick to this is not to remove material from the nanowire before a substantial amount of the apex blob is removed. If the apex is too weighty, and the nanowire too weak to support the weight of the apex, then the nanowire will bend and the tip will be ruined. If the tip apex is ruined in this manner it may still be possible to make it into a useable STM tip by very slowly removing material off the apex by front polishing until the bend is gone. Alternatively, one could start over with the back polishing. Ideally the last pulse in front polishing will remove the last remaining blob of tip apex and leave a cleaved nanowire that is irresolvable by the resolution of the light microscope. If a tip is created that the optical microscope can not resolve then the radius of curvature at the tip apex can be assumed to be 200 nm or less. According to Dr. Allen Melmed, with experience it may be possible to guess if the tip has a radius of curvature down to the 20 nm range, depending on how blurry the tip appears.

After the tip has been created and an acceptable tip apex formed, it is necessary to clean the tip. To clean the tip, simply hold it in fresh distilled water by dipping vertically

into a beaker. Hold the tip motionless for a period of 15 to 20 seconds to allow any built up electrolyte to dissolve.

Once the tip has been made, be very careful with it. The sharp tip apex is very susceptible to damage by mechanical shock (dropping it/ or even shaking it violently). Also the tip can be damaged by electrical shock, therefore use a tip holder that is electrically conductive and won't build up a static charge that can be localized on the sharp tip. (e.g. conductive foam for ICs available at Radio Shack)

Metal Specific Tip Preparation Instructions:

Tungsten tips. (W)

The specifics for AC polishing a W wire using Dr. Melmed's procedure is; First cut a short length of wire ~1/8" longer than what the final length should be and hold it by the stainless steel pinchers. Turn the AC voltage on the variac to 35 V and quickly dip and retract the tip into a 3 M KOH solution with a carbon counter electrode. Do this to both ends of the W wire so that the entire wire is clean. Next, place the pinchers holding the tip into the coarse etch adjustment stage, and move the tip close to the electrolyte solution so that it's just touching the surface. Then put the 1/8" Plexiglas sheet under the beaker containing the electrolyte and start the etch/polish. Initially the voltage applied should be about 15 V, then after every 50 seconds, the voltage turned down about 3 V until a voltage of 6 or 7 volts is reached. At a voltage of 6-7 V let the etching proceed until it stops sparking/bubbling. At which point carefully remove the tip and pincher from the coarse etch mechanism and dip in clean distilled water. After the cleaning, look at the tip under the microscope and set up as described in the fine polishing section. For fine

polishing of W wire use the platinum wire loop as the counter electrode with a drop of KOH electrolyte on it. The voltage that should be used in the fine polishing of tungsten wire is 2-4 volts. The back polish can use the higher voltage limit and the front polish uses the lower voltage limit.

Platinum tips. (Pt)

Specifics for polishing a Pt wire is: First cut a length of wire ~1/8" longer than the desired final length and hold it in the stainless steel pinchers. The electrolyte solution that should be used with the Pt polishing is a 33% saturated solution of CaCl_2 . Prepare this solution by putting an abundance of CaCl_2 into distilled water in a polyethelyne container with a lid. Let the solution stand overnight to ensure that there is no more CaCl_2 that can be added to the water. Then take the beaker that the polishing is done in and fill 1/3 of it with the sat. CaCl_2 solution and 2/3 of it with distilled water, then mix the two together. To polish, adjust the wire so it is just touching the surface of the electrolyte solution and put the 1/8" Plexiglas sheet under the beaker, just as in the W wire etch. Next apply a voltage of ~ 40 V to the platinum wire and etch. The voltage is worked down from 40 to 20 V in 5 volt increments every 50 seconds. Once 20 V is reached, let the etching continue until there is no more sparking (as described earlier the Pt etch looks more like spark eroding). If done correctly, the last spark should generate enough heat to quickly melt the tip of the platinum wire and form a micro sphere at the very end of the wire which can be seen under the microscope. Ironically this dulling of the tip by forming a ball aids greatly in creating a good Pt STM tip when fine polishing. If the ball is not present, it is still possible to make a good STM tip, but it is more difficult. The reason

that the microball at the end of the Pt wire aids in polishing is because of the surface tension of the CaCl_2 solution. The solution typically wets the wire along the near apex up to the ball at the apex, but with the curvature of the ball at the end of the tip the solution doesn't seem to flow up and around it so the near apex region can be easily polished.

To fine polish the Pt wire, the procedure is much like the fine polishing of the W wire only the voltages are slightly higher, typically the upper limit is 7 volts with a lower limit of 4 volts. Then as described in the general fine polishing portion, back polishing is done first to create a nanowire that is then removed by the front polishing step.

3.6.5 JUDGING SHARPNESS:

Judging the sharpness of a tip under a light microscopy definitely falls under the realm of art, certainly not science. To truly get a measure of the sharpness of a tip, it has to be used in STM. However a very good estimate can be found by looking at the tip under an electron microscope, but even then the very tip of the apex is not resolvable and most likely it becomes contaminated by the electron beam hitting it, by turning hydrocarbon background gases from the SEM chamber into carbon deposited on the surface. However, with a light microscopy a rough estimate can be made to predict whether or not the tip will work well in STM.

The limit of a light microscope's resolution is dictated by the wavelength of light. This limit of resolution is generally taken to be approximately 200 nm. The resolving power of a compound microscope³² is,

$$d = \frac{(0.61 * \lambda)}{(n * \sin \alpha)} \quad (3.9)$$

Where λ is the wavelength of light used (400 nm average for visible light), n is the refractive index (1.0 for air), and α is $\frac{1}{2}$ the angle of illumination from the specimen.

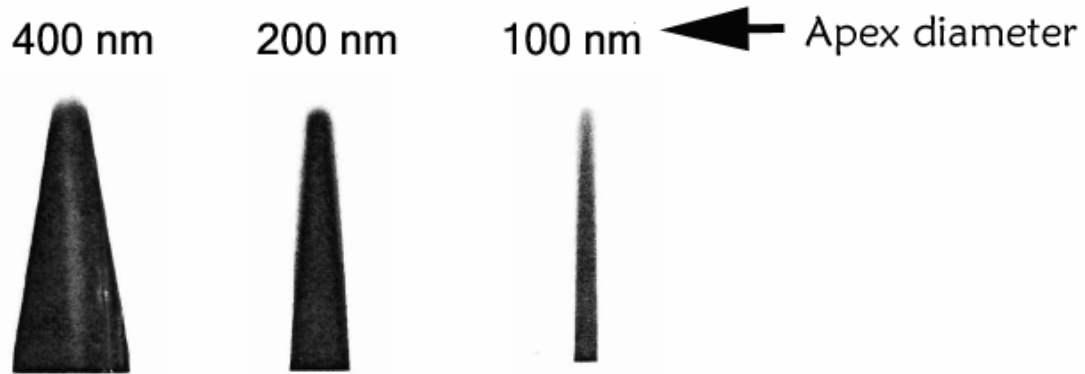


Figure 37 Picture of what various sized tips will look like under a light microscope. Showing that the resolution of the microscope starts to blur the tip at very low tip apex diameters, which is what is hopefully seen after etching the tips.

Therefore, mathematically our microscope will not be able to tell us if our tip apex is less than 200 nm. However, according to Dr. Melmed, it is still possible to guesstimate the actual sharpness of the apex by looking at how it becomes irresolvable by the microscope. Figure 37 shows images of a well resolved tip apex that is not very sharp and tips with an estimated 200 nm apex radius and an estimated 20 nm apex tip radius. These measurements are just hopeful guesses but do seem to experimentally correlate with whether the tip is good or not. When using this method of judging tip sharpness it is imperative that all optics and any glass slides be clean and free of dirt and debris.

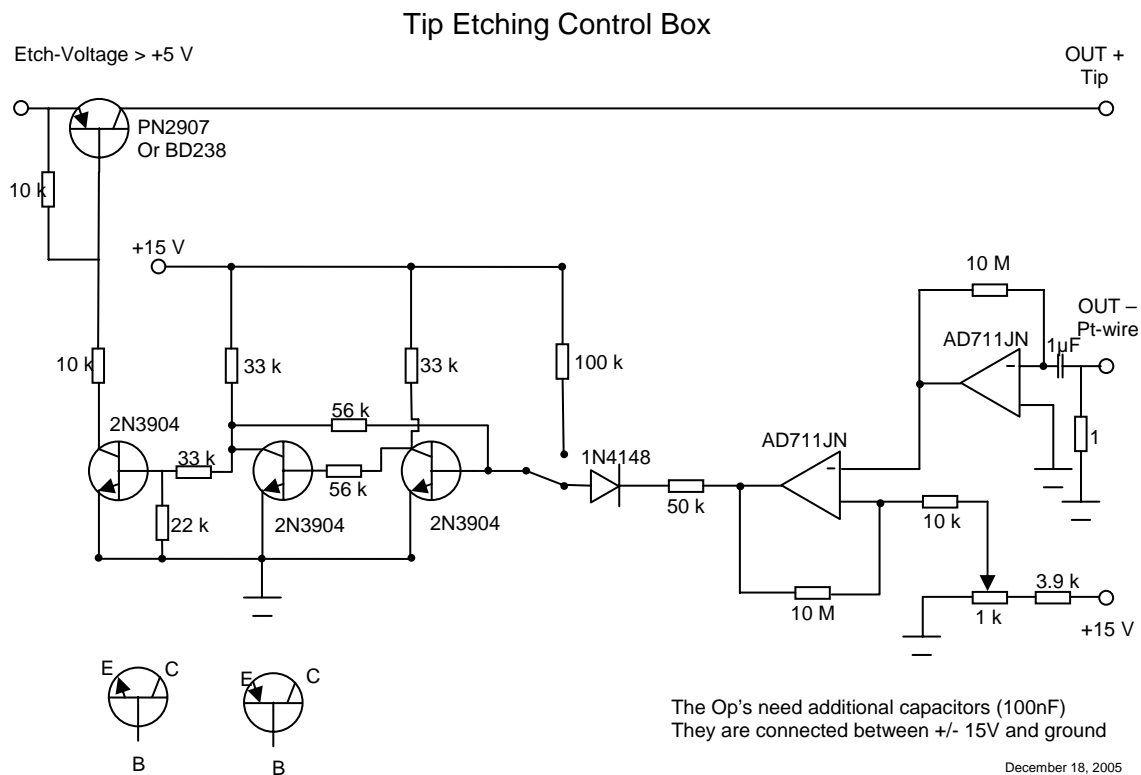
3.6.6 STM TIP STORAGE:

After good tips have been generated, it is imperative to protect them from damage before use. The tips are very delicate and can be rendered useless by impact, mechanical vibration, electrical discharge and contamination by dust or other particles. Therefore, the tips should be stored in a metal container, and the dull end stuck into a conductive foam rubber pad within the container. The metal container must also have a cover and not be too full of stored tips so that while retrieving or inserting tips others are not touched.

3.6.7 DC ETCHING:

The above writings focus on tip preparation using an AC current to etch/polish both W and Pt/Ir wire. The alternative is to etch using a DC current which only works on

Figure 38 DC etching circuit used for W wire tips.



the W wire. The DC current etch in the Harrison lab has met with mixed results, but is now the preferred method. The two major problems associated with DC etching are etching proceeds by oxidizing the metal which leaves a thick nonconductive oxide that has to be removed before tunneling can occur and the tip continues to etch until the power is turned off or the wire has been etched completely out of the electrolyte solution. Therefore, it is necessary to shut the power off at exactly the correct time or the tip that was created will no longer be useable.

The solution to these problems took many years to completely solve but it is now part of what makes very good high resolution imaging possible. The problem of when to turn off the etching power is done by a simple circuit that looks for a spike in the current which promptly stops the etch (Figure 38). The spike in current happens when the W wire that is preferentially etched at the air – solution interface has a portion of it that breaks away from the top when the weight is too much for the narrowing wire diameter to hold. When this piece breaks away and the current is stopped what is left is a tip that is extremely sharp. The design for the tip etching box came from the Möller group in Germany at the University of Essen.

The problem of removing the non-conductive oxide from the tip was solved by discussions with a fellow STM colleague at a Gordon Conference, Dr. Andreas Klust. He said that most groups rely on a tip exchange mechanism which allows them to process the tip *in situ* before tunneling. However, Dr Klust found that heating the W tips in vacuum until the tips start to glow in a secondary chamber not attached to the STM chamber is sufficient to remove the oxide layer. Also, oxide formation in air is very slow so the W tips can withstand a few hours of exposure while inserting the tip into the STM. Once the

processed tip is positioned in the STM it's ready to go! The tip annealing apparatus that I came up with is a 6 way 2-3/4" cross that attaches to the five way cross just above the turbomolecular pump on the chamber gas manifold. This allows me to insert and remove tips relatively quickly. The tips are spotwelded to a tantalum ribbon that is secured to 1/4 inch copper feedthroughs on a 2-3/4" flange. Each copper feedthrough has a wire attached that runs to a (+) or (-) output on the Kepco ATE 25-20M. When all this is connected and the electrodes are assured not to be connected to the chamber ground, the voltage and current are dialed up on the Kepco. The typical current and voltages that are used to get the Ta ribbon and W tips to glow is about 3 V with 19-20 amps (this could be fatal if the voltage is dialed up too far and the wires are touched, so be extremely careful!) Once the tips start to glow (dull orange ~900 K), dial down the Kepco current to keep the tip from being heated too much and causing a local reconstruction of the tip. After this procedure, the tips are very sharp and very clean, which is perfect for use in the STM.

Currently my preferred method of creating STM tips is the DC etch with trigger circuit and subsequent resistive heating. My preference for this method over the AC polish, cut and pull, or FIB milling, is due to its simplicity, quickness and reliable tips generated (i.e. virtually every DC etched tip should give atomic resolution STM images). The other methods can all be used to create very good tips for STM but the polishing and FIB milling are both very time consuming taking an estimated 1 hour minimum for each tip created compared to the 5 min DC etch. The cut and pull method is obviously much faster but certainly not as reliable as the DC etch.

3.6.8 AMBIENT CONDITION CLEANING METHODS FOR STM TIPS:

There are in air methods and procedures used to help make already generated tips useable for the STM by removal of contaminates and oxides. The first method is simply to wash the tips with water and/or acetone to remove any hydrocarbons and electrolyte that may have beaded up and solidified on the tip. A second method can be used to remove the oxide off etched tungsten tips is a short dip in hydrofluoric acid. This acid dip should effectively remove the oxide, but it is very dangerous to use and didn't seem to help nearly as much as I had hoped considering all the hassles involved. The third method that I had tried was a DC reverse polarity etch on the W wires to remove the oxide. This method only sporadically worked and therefore was not a method I would recommend.

3.6.9 TIP CLEANING METHODS WITHIN THE CHAMBER:

Not all *in situ* cleaning methods are possible in our STM. An example of methods used by people in other labs is electron bombardment heating of the tip to remove the oxide or cause a recrystallization of the tip metal. Another example is ion sputtering of the tip which cleans and restructures the tip.

The *in situ* tip cleaning methods available to us are: field emission, voltage pulsing, high bias scanning, and light tip crashing. The previously described resistive heating of the STM tips attached to the Ta ribbon is technically considered *in situ* but it is not a procedure that is possible to do while the tip is inserted into the STM. The field emission and other methods that fall under the “stupid tip tricks” category are all possible while the tip is inserted into the STM.

Field emission is a method that some people swear by, and is a technique that is used in both the Möller lab at Essen and in the Salmeron lab at Berkeley. After spending a morning talking with some of the scientists in Salmeron's lab I developed a detailed method and circuitry that allows us to do field emission in our chamber from the tip to the Pt crystal. A detailed procedure for field emission is discussed later in a field emission document that also addresses the theory.

A very effective method of maintaining a tip or encouraging a not so good tip to become a good tip is voltage pulsing. In this procedure I have hot keys defined in the SPM32 program that apply certain voltages over defined durations. Typically I have a $5\text{ ms} \pm 3.5\text{ V}$ pulses defined and if one polarity pulse is not doing the trick, I'll try the opposite. The voltage settings can be adjusted in the Lithography setup menu where the pulses can be assigned to hot keys. The advantage of assigning hot keys to each pulse is that the pulses can then be applied while imaging and the effect can be observed instantaneously. If you were halfway through a spectacular image and picked up an extra molecule on the tip, by pulsing the voltage there is a chance that you can remove the molecule and get the rest of the image. Sometimes, an image only works with continual pulses across the scan.

The high bias scan method of tip shaping is a kind of a hope and pray that the tip will miraculously change for the better technique, and you'll be left with a good tip. The basic idea is that at sufficient bias voltage the very close proximity of the tip to the surface causes a field emission effect that can restructure the tip apex or at least clean it of spurious molecules that have attached themselves over time. The other possibility is

that while the bias is high there is a higher likelihood of tip to surface contact which will definitely change the tip.... Hopefully in a good way.

Another tip reconstruction method that I learned by talking to the folks at Berkeley was a light tip crash method. To do this an I/Z curve is acquired that starts a few angstroms beneath the Pt surface, and is then slowly retracted to a height a few nanometers away. In doing so the hope is a nanotip will form on the STM tip and produce good images. The theoretical method for this to happen is by cold-welding the clean tip to a clean surface and as the tip is pulled away from the plane of the surface the Pt atoms stick to the tip and stretch until the tip is moved far enough away that any Pt atoms that were pulled away from the surface thin out to form a nanowire that eventually breaks, terminating in a single atom. Salmeron's group swears by this method but I have only occasionally been able to get it to work properly. For me, this tip crashing is mainly used as a last resort. A problem with it for our current STM is that the vertical thermal drift is large enough that after an initial tip approach to the surface is done the feedback loop works fairly hard to counteract the motion towards the surface. Therefore if an I/Z spectrum is acquired with the feedback loop turned off, even with the small retraction that is done in the I/Z spectroscopy the tip will move into the surface and crash hard! It is possible to do light tip crashing of the tip after the vertical drift has been eliminated, which typically is the case after one to two hours of operation. Even after the vertical drift has ceased there are other problems with lateral drift, which lasts much longer and is a function of the voltages applied to the piezo for lateral movement (hysteresis and drift). If a tip crash occurs when there is a large lateral motion, the new nanotip will be curved due to the sideways pulling of the tip, not just vertical. A good I/Z curve will show three

distinct sections; the first is a flat line of current higher than what the scale will accept which is a current of 98 nA (with the IVP-200 pre-amp and 10 X gain in the secondary amp). The second section is the important part; it is the transition from crash status to no current detected. How this transition happens is very important. If there is a nice curved structure to it (ideally one that follows the exponential decay with a work function of the Pt surface) the likelihood that the tip has a nice structure and will give good images is pretty high. However, if the curve seen is more of a delta function from high current to no current, then the tip is still no good and should probably go through another light tip crashing again. The third portion of the spectrum is when the tip has been retracted from the surface far enough that there is no detectable current, at this point the curve bottoms out and flat lines at 0 nA. A good and bad light tip crash I/Z curve can be seen in Figure 39.

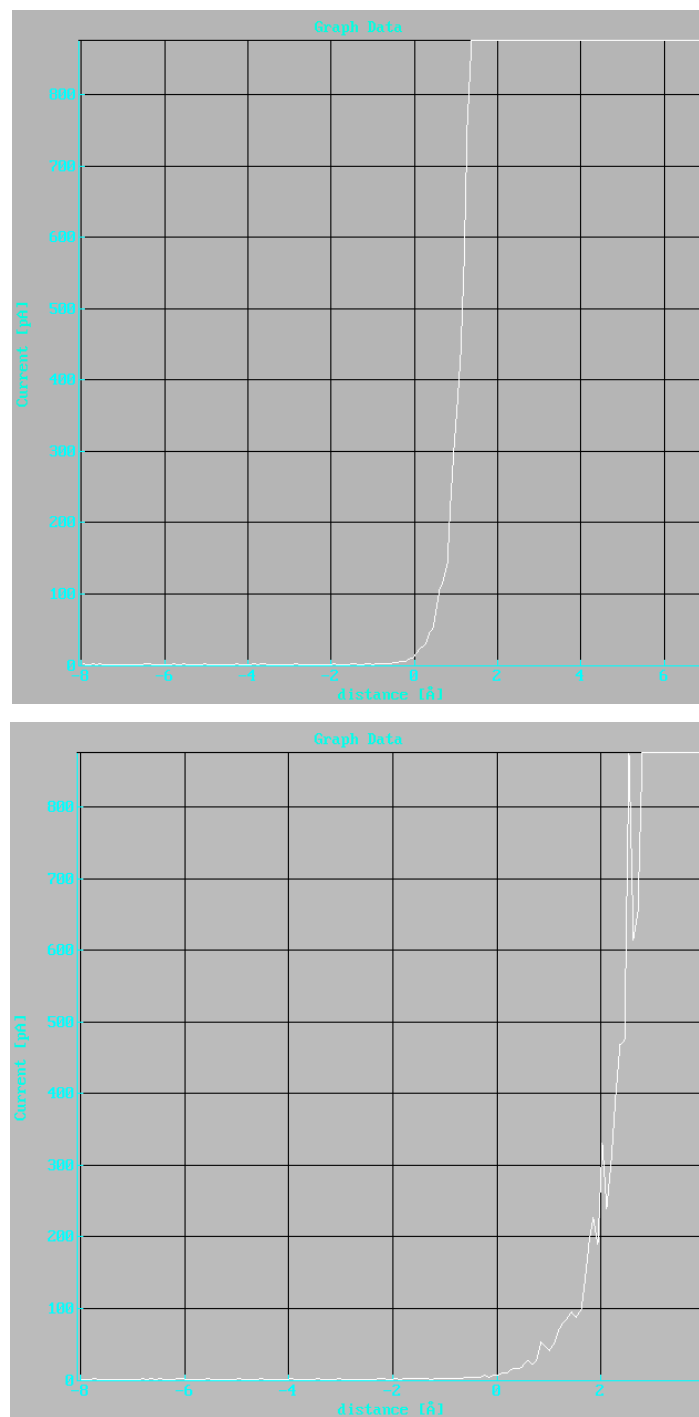
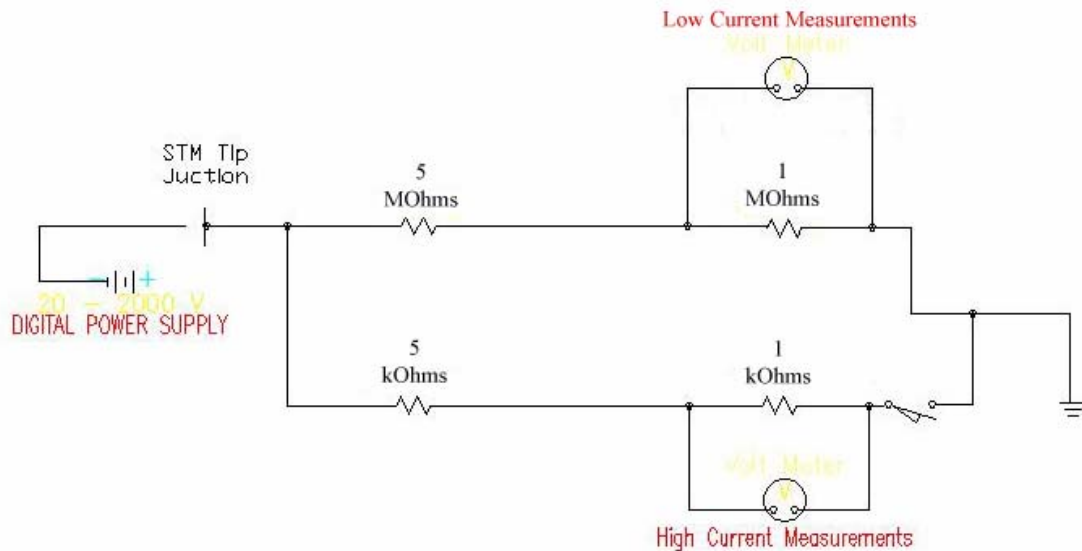


Figure 39 I/Z spectra of a good tip crash top and a poor tip crash bottom.

3.7 FIELD EMISSION:



The above electrical circuit is what allows field emission tip cleaning and sharpening to be done on both freshly etched and well used STM tips that are no longer atomically sharp. The circuit is very simple in design and variations of it are being used by STM labs throughout the world. The circuit consists of five basic components: A variable potential power supply, a capacitor (vacuum gap) which is formed by the STM tip and the crystal surface, two potential paths to ground resembling a parallel circuit, two multi-meters, and a switch that when closed allows current to flow in the lower arm of the circuit.

The variable power supply that is used for field emission is a Stanford Research Systems model PS350 high voltage power supply that has a useable range of 20 – 5000 V; 25 W. There are three items about this supply that make it perfect for use in our setup. Firstly, the potential of the supply can be set to either a positive or negative bias.

Secondly, the output voltage can be changed in small increments of 1 V if desired. Typically the incremental change is done in steps of 10 or 20 Volts at a time. Lastly, the supply has programmable current limiting capabilities and a separate programmable trip limit to protect itself and the field emission circuit. The current trip limit is set relatively high at 1.5 millamps, which allows the voltage to be quickly switched off in the event of tip to surface contact (tip crash), which can easily occur with a tip to surface distance on the order of tens to hundreds of nanometers.

The circuit itself, as stated and shown above, has two potential paths for current flow. Both paths are nearly identical in design, with the exception of total series resistance and the ability to turn the lower path off and on. The construction of the two paths allow for two regions of current flow to be measured. Initially only the high resistance side is connected and used such that the voltage drop measured across the $1\text{ M}\Omega$ resistor with a handheld multimeter registers very small current flows with a lower detection limit in the nanoamp range.

The initial measurement of the low current range is important because it is indicative of the tip conditions such as shape/size, contamination and the tip distance to the crystal. The size/shape and composition of the tip will be modified at high voltage so initially at lower voltages the tip to surface distance is the best measure of correct tip placement. If the tip is too close to the surface then there will be a current flow almost immediately when the power supply is turned on (the supply starts at 20V). In the event that there is high current flow (i.e. the current limit on the supply: 1.5 mA) then the tip is in the crystal surface and needs to be retracted to a reasonable distance. If there is a current other than the current limit upon startup, the tip is very close to the surface and

needs to be retracted as well. In the case where the tip is too close to the surface but not touching it, the tip needs to be retracted because the tip will undergo some structural changes and has a higher probability of crashing into the surface during these modifications if the tip is only a few nanometers away. The second problem with the tip being too close to the surface is that it makes it more difficult to modify the tip from electron heating effects. If the target current of 1mA that you want to achieve for field emission is done with a 300 V potential, using the power equation (3.10) yields 0.3 Watts of tip heating power. But if the tip is farther away from surface and the potential required to attain 1mA of current flow is 1500 V, there is 1.5 W of heating. That's not a lot of heat, but if that heat is spread only locally around a micron sized portion of the tip there can be dramatic effects.

$$(3.10) \quad P = I \times V$$

Conversely, if the tip is too far away from the surface, the required voltage to attain 1mA of current can be too great. Because of the design of our Besoke type STM, the tip is not removable and remains secured in the scan piezo tube. Therefore, due to the electrical breakdown limit of the materials used in the construction of the STM such as the H61 epoxy and Kaptan coated wires, the voltage applied has to be limited to 1250-1500 V. Consequently, if there is no detectable current flow with a potential less than 600 V, the tip needs to be moved closer to the crystal surface.

Once a small current has been established with a tip that is positioned an appropriate distance away from the crystal, the push button switch in the lower arm of the

circuit is used to enable the high current measurement side of the field emission box. The high current portion of the field emission box contains two resistors, a 5 kΩ and a 1 kΩ in series. Another multimeter is then connected to the circuit across the 1 kΩ resistor to take a more accurate reading of the current in the field emission gap. Without this 2nd path of lower resistance the two high resistance resistors in the 1st path start to limit the total current that is supplied to the field emission gap which give an inaccurate picture of what is really happening to the tip. The one piece of information that is crucial to enabling the high current path is: not to wait until the current is too high (>5 V on the multimeter; i.e. > 5 μA on low current monitor) before switching from the low current side of the circuit to the high current side. If the switch is made while the current is too high there will be a jump in current supplied to the field emission junction which could cause the tip to crash or break off a small portion of the tip.

The units of measure on the multimeters are in Volts not Amps. This is done so that pricey high voltage current probes do not need to be used to protect the multimeters from large voltages. The multimeters have a voltage limit of 600 V before a fuse blows or they are damaged. So, by placing a limiting resister up front and measuring the voltage drop across a second resister as in a voltage divider circuit, we can then tell the current flow in that circuit by applying Ohm's law(3.11). The measured voltage drop across the second resistor of resistance R yields the current via.

$$(3.11) \quad I = \frac{V}{R}$$

The procedure of doing field emission on a tip has been loosely described above. However, the detailed procedural steps are described below:

The first step for field emission in the STM chamber is to make a tip. This may seem to be an obvious step but without a proper tip that is relatively sharp, field emission may not work. (The procedure for etching and macroscopically cleaning the fresh tip is discussed earlier in this document.) Once the tip has been placed in the STM and the tip height set correctly, reattach the STM to the chamber and vacuum bake the valved off STM and STM manipulator assembly. After the STM has been baked out, it can be reintroduced into the main chamber. After a few hours have passed, the STM should have come to thermal equilibrium with the chamber and can be suitably used for field emission. The best way for field emission to be done is on the platinum crystal AT ROOM TEMPERATURE. If the field emission is attempted at any other temperature there will be thermal drift that will have to be adjusted for. Next attach the STM wiring harness so that a tip approach may be done. Approach the tip to the surface just as you would for a normal STM data acquisition session. After the tip is in tunneling range the tip should be physically retracted or approached to the surface with the “+” and “-“ keys on the keyboard until a reading on the Z position reads -30 to -40. It is important not to use the Z position offset knob to get to the required Z position reading because, adjustment of that knob applies a voltage to the outer beetle legs to maintain that desired position, and there has to be zero volts applied to all of the piezos. Once the Z position is set correctly, trip the “Reset / Mon. Reset” 3 way toggle switch on the lower right corner of the STM controller to “Reset”. With the toggle switch in this position all the voltages that are currently being supplied to the STM are held at that level until the reset switch is

turned off. Once the STM Z position is stable and the “Reset” switch is on, all of the wires that connect the STM controller to the STM/crystal can be removed. The removal of the wires serves to electrically isolate the STM controller so that no damage can be done in the event of an electrical short from the high voltage line to one or more of the piezo elements. With the removal of the wires as previously stated the voltages applied to the piezos have to be zero, or there is the potential for tip crash with a sudden change in potential while removing or reattaching the STM wires.

With the STM and tip in position for field emission the connections to the field emission box can be made. Start with connecting the high voltage source (Mass Spec. Multiplier supply) to the connector marked High Voltage IN. Then disconnect the STM bias BNC cable and plug it into the field emission box marked Sample. The other end of the bias cable should remain connected to the BNC feedthrough that is coupled to the Pt crystal. Next, connect a BNC cable between the field emission box connector labeled Tip and the BNC feed through connector that the RHK IVP-X00 pre-amp was previously connected to. After the coaxial cables have been connected the multimeters can be connected by the banana plug cables. The field emission box has three banana plugs situated in a row, the middle plug is the ground connection and the other two are the low current connector and the other plug with a push button switch next to it is the high current measurement connector. (Image of Field Emission Box is Figure 2)

After all the connections are made, turn on the multiplier supply and begin field emission. Initially start the voltage at 20 V (the lowest setting for the supply) then while monitoring the current on the low current circuit multimeter, increase the voltage on the supply in 10 V increments and let the current stabilize after each change, slowly working

the applied voltage up to a point where the current reaches 1 mA (ideally). Switching between the low and high current sides of the circuit should be done carefully, and should not be done if the applied voltage exceeds 500 V. When the desired current has been attained and has stabilized for about 30 seconds, then simply turn off the voltage supplies. Then disconnect the field emission box and reconnect the STM wires so the STM can be safely retracted from the Pt surface.

Operation of the multiplier high voltage supply is simple but can be initially confusing. The thing to remember about the supply is that the voltage displayed in the center meter is the voltage that you want the supply to produce, and the display meter on the left is what is currently being generated by the supply. The two displays will not be equivalent until the enter button on the front of the supply is pressed. Also the bias of the supply can be changed by turning a switch in back of the supply while the supply is turned off.

By using different applied voltages, different field emission effects can be achieved. If the power supply is negative (making the STM tip negative), true field emission occurs. The electrons are being generated at the tip and flowing to ground at the crystal. In doing so, there are intense field lines at the apex of the tip causing the tip to elongate and for atoms and molecules to migrate down the sides of the tip which reforms the surface. Also if the current and voltage are large enough then there may be a local melting and recrystallization due to heating effects. Additionally, as the electrons are traveling from the tip to ground they may encounter atoms or molecules on the surface or flying through the tunneling gap. Such encounters may result in an ionization event

leaving the atom or molecule with a positive charge that get reaccelerated back into the negative tip which causes a sputtering of tip material.

When a positive voltage is used, some of the same events occur as with negative applied voltage. Effects such as elongation of the tip due to intense field lines, sputtering of the tip from ionized atoms and molecules, and recrystallization of the tip from heating, are the same but may occur in different ways. Most notably, heating and recrystallization of the tip, the tip gets heated by electron bombardment and not resistive heating as happens when the tip is biased negative. The ionization sputtering can occur from electron-molecule collisions as before, only the species that is doing the sputtering of the tip would be from negatively charged ions. There is also the possibility that negatively charged molecules/atoms that are created by the ion pumps or ion gauge can be used for sputtering of the tip.

When using a freshly prepared, very sharp Pt/Ir tip perhaps the best method of field emission is to apply positive voltage to the tip. The reason is that a new tip should initially be very sharp and needs only to be cleaned, removing any adsorbed molecules that can interfere with the tunneling gap. The positive tip field emission can do this cleaning by electron stimulated desorption (ESD) of molecules, also there is the added benefit of electron bombardment heating, and some sputtering. However, ideally it would be best to minimize the sputtering effect and just remove adsorbed molecules.

The setup described above applies the voltage whether positive or negative always to the tip and maintains the crystal at ground. This arrangement is not the only method to perform field emission tip cleaning. It is possible to apply the high voltage (+ or -) to the crystal and make the STM tip ground. The operational details would be the

same as the cable arrangement described above. In fact this would be a preferred cable arrangement where the high voltage (i.e., 1000 V or more) didn't travel down a 0.002" diameter wire. However, the electrical connects at the crystal can be a bit flaky. Often if this cable arrangement is used then no stable field emission current is ever achieved and most of the time the tip crashes. Additionally, all the STM piezo electrodes have to be grounded so that a charge differential is not allowed to build up on the piezos which would generate STM movement.

Theory of Field emission:

The field emission current is described by Fowler-Nordstrom tunneling equations³³ and other than small correction terms is a function of the work function of the surface and the electric field applied. Typically the required electric field for field emission is $10^7 - 10^8$ V/cm which can be obtained at the surface of a very sharp tip. Field emission is a process by which a high negative potential electric field facilitates the tunneling of electrons out of a metal surface potential barrier. This process is an important one in science today with its wide spread use as a cold cathode electron source for instruments such as Scanning electron microscopes, and Auger photoelectron spectroscopy instruments. Other applications for field emission are Field emission microscopes, and Field emission displays (plasma screen TV's).

The electron tunneling probability is derived from a time independent Schrodinger equation Eq (3.12):

$$(3.12) \quad \frac{-\hbar^2}{2m} \frac{\partial^2 \Psi}{\partial x^2} + V(x)\Psi = E\Psi$$

a rewritten form of Eq. (3.12) can be seen in Eq. (3.13)

$$(3.13) \quad \frac{\partial^2 \Psi}{\partial x^2} = \frac{2m(V - E)}{\hbar^2} \Psi$$

If $(V-E)$ is taken to be independent of position in the range of x and $x+dx$ a solution to the equation can be found which yields:

$$(3.14) \quad \begin{aligned} \Psi(x + dx) &= \Psi(x) e^{-(kdx)} \\ k &= \frac{\sqrt{2m[V(x) - E]}}{\hbar} \end{aligned}$$

The above equations are the same as the previously identified tunneling equations in chapter 1. However, in the interpretation of Fowler-Nordstrom, the barrier is considered to be a triangular barrier which they then interpret as the tunneling probability of:

$$(3.14) \quad \Theta = e^{-\left(\frac{4\sqrt{2qm}}{3}\frac{\Phi_B}{\hbar}\right)^{3/2}}$$

According to Fowler-Nordstrom, the tunneling is then calculated from the product of the carrier charge, velocity and electron density available for tunneling multiplied by the tunneling probability.

$$(3.14) \quad J_n = qv_R n \Theta$$

Therefore, the tunneling current is exponentially dependent on the barrier height to the 3/2 power.

After field emission:

Once the tip is clean and sharp, it's time to get down to business. (The tip is done with field emission once a stable current of around 1 mA has been achieved for 30 seconds) After the field emission has been finished, reattach all of the STM cables back to the STM, and retract from the surface as would be the case at the end of any normal imaging session. Then clean the crystal and dose whatever molecule of interest you have. Approach the STM to the crystal surface and wait until a tunneling current is achieved.

3.8 MATLAB CODE AND INSTRUCTIONS:

When the time comes to analyze the STM data collected there are a number of tools one should have available. As described earlier there are a number of pre-written programs available to help analyze the collected data, The original RHK SPM32 program written by Frank Ogletree, is a very useful tool for analysis, but the problems using this program is, it requires the DOS operating system and therefore will not run on any operating system newer than Windows 98. Also the programs are locked to the STM acquisition computer by a hardware key interlock, therefore the hours spent in image analysis must be done exclusively at the lab computer. Another option is the new windows version of the RHK software that can run on Windows XP systems and can be installed on any computer without the hardware key for image analysis only. This XPMPro software by RHK is similar in operation to the original SPM32 program but

seems to be less stable and generally not as useful, therefore my recommendation is to use the SPM32 while in lab.

A freeware SPM analysis program available to use is WSXM from Nanotec Electronica (Madrid Spain). This program can be of great value for generating nice 3-D images and impressive colormaps for image contrast and enhancement. The WSXM program also has some nice features that are not available in the RHK software such as flooding and easy enhancement of the Z contrast range.

There are a few other freeware SPM programs out there that are of much lesser use to do STM image analysis, mainly because of the image file format. The files created by the RHK SPM32 software are .SM2 files that use the first 512 bytes of the file to include information about the image and acquisition parameters. Following the acquisition information is the image file which consisting of 8 bit color bitmap data. The new XPMPro RHK program uses a new .SM3 file format that is not readable by any of the current freeware or commercially available software as of November 2005.

One of the commercially available programs is SPIP by Image Metrology. This is a program that has been recommended by numerous people in different STM groups as a good tool to have but the cost makes it prohibitive, and an unnecessary expense given all of the freeware and mathematical programs available at the university.

Perhaps the most powerful tools available to analyze STM data are mathematical programs such as Mathematica and MatLab coupled with creative thought. Once the image has been imported into the math program any manipulation program that you have written can be applied. Some of the programs that are of good value would be the X or Y background subtraction, and image contrast adjustment.

Either Mathematica or MatLab can be used for this function. However, MatLab is the preferred math program due to its easy interface and intrinsic ability for graphical work. Included will be code that allows the creation of theoretical images of adsorbates on a Pt(111) surface (and instructions on how to create new overlattices.), and coding that allows a theoretical Pt lattice to be overlaid on the STM data to try and determine the adsorption sites of molecules.

Instructions for using the written programs are as follows.

Creation of a theoretical Pt(111) lattice with over layers:

The programs that are needed for this are: (latprep, lattice, MeBr1,MeBr2,MeBr3,MeBr4 (for creation of the four atoms in the (6 x 3) unit cell of MeBr)). Multiple other files are available that create different molecules in the unit cell.

To start, first run the MatLab program. At the prompt in MatLab type “figure”. By typing figure this creates a new graphic element window where the lattice will be created. Next type “latprep”, which generates the matrix for the sphere coordinates, sets the size of the Pt lattice, and the number of times the Pt lattice unit cell is repeated, and very importantly holds the graphic window so items will be continuously written to the window without removing what was there previously. After latprep has been used type “lattice”, lattice generates a hex array of spheres with a certain number ‘n’ repeated.

Once the lattice has been created the overlayer molecules can be formed simply by typing “MeBr1” for the first molecule in the unit cell and “MeBr2” for the second molecule and so on for the MeBr3 and MeBr4 programs. However before the overlayer is added to the Pt lattice it is recommended that the number of times the unit cell is repeated

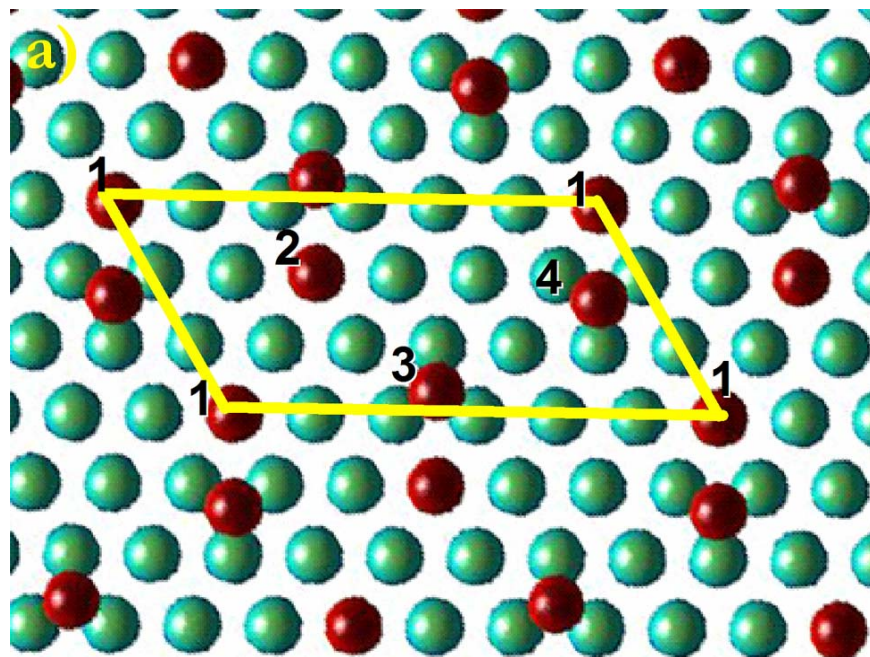
is reduced. This is done simply by setting (typing at the command prompt) “n = 2” or some lower number that you want the unit cell to be repeated.

After the lattice with overlayer has been created to make it more attractive as a figure, the commands “axis equal off” can be typed to square the figure and remove the grid. The next command should be “shading interp”, this smoothes the spheres and changes their color based on the Z height matrix. To add more of a 3-D look to the spheres the command “camlight(45,45)” should be used to move the lighting around.

All the commands dealing with the axis, shading and camlight can be modified to whatever is desired, to list the options with these commands type “help (functionname)” Another command that is useful is colormap, by typing colormap with a preset color scheme such as (jet, hsv, or winter) changes how the color interpolation of the Z matix is done, it is also possible to create a colormap from scratch to get exactly what is wanted.

Now the theoretical image is finished and within the graphic window there is the typical zoom in/zoom out, and a 3-D rotate to change the viewing angle. The example in Figure 40 shows a (6 x 3) MeBr lattice that was created using the programs listed above in MatLab.

Figure 40 Image of a theoretically generated 6×3 lattice of MeBr on the Pt(111) surface created in MatLab.



Creation of the Pt(111) lattice over a STM image:

There are many more intricacies of generating a Pt(111) lattice over a STM image than creating a lattice from scratch. Therefore this requires the user to participate more in procedure by measuring and specifying where the theory lattice should start, and calculating how many points correspond to an Angstrom in the image.

First, Start the MatLab program. Then at the command prompt type

```
"A = imread('filename here');"
```

This loads the image file into a matrix labeled "A". This matrix will then be used to generate the window with the STM image. The image file needs to be a JPEG, BMP, Tiff, or some other acceptable image file format, (to date I have not written a program to

convert the .SM2 files to a readable image file for MatLab. So, currently this step needs to be done in the SPM32 or WSXM program.) Once the image has been read into memory type “imageprep”, this creates a new figure window, writes the image file from A into that window, squares the axes and holds the graphic window.

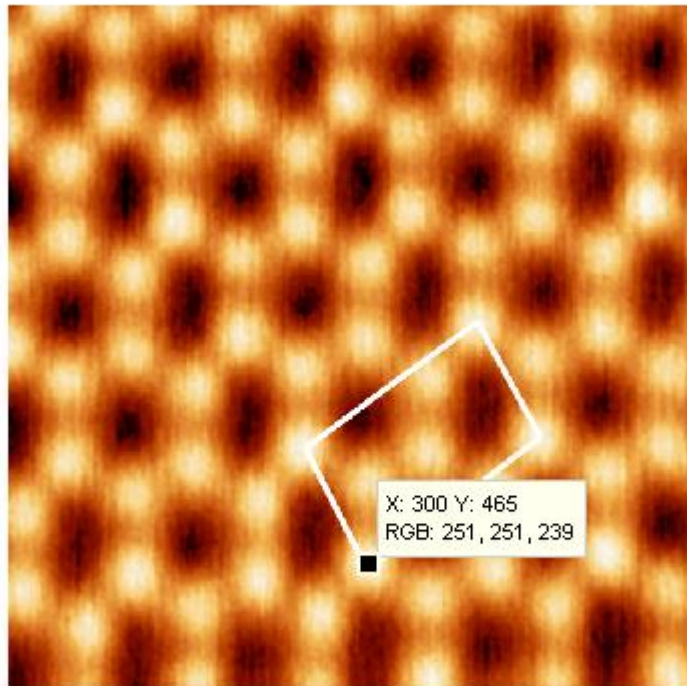
Now there are a few measurements that need to be done before the Pt(111) overlattice can be imposed on the image. First type “whos” to see how big the image file A is, typically this number is displayed like:

Name	Size	Bytes	Class
A	568x568x3	967872	uint8 array

Which states that the current image is 568 point by 568 point. The 568 points can be divided into number of points per angstrom by knowing how many angstroms the image corresponds to. In this case it is a 40 x 40 angstrom image so there are 14.2 points per angstrom, which gives 39.48 as the number of points between the Pt atoms.

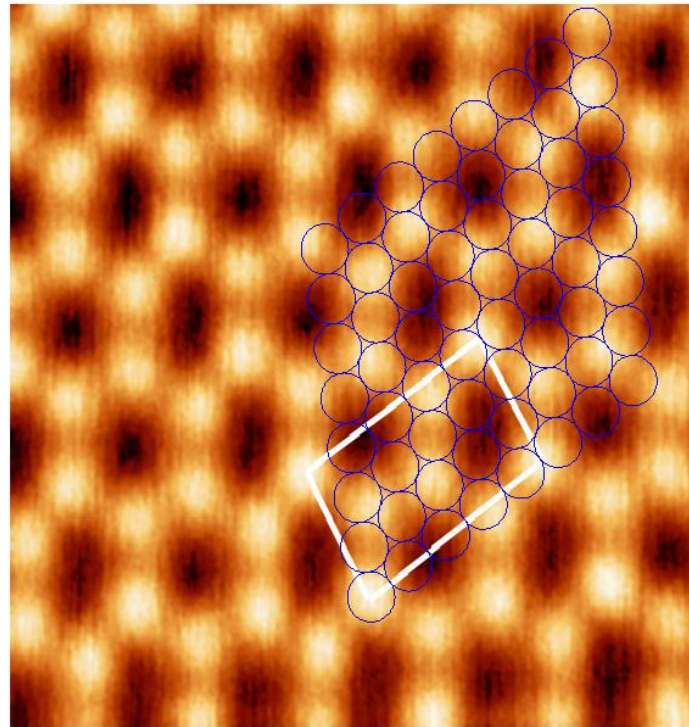
To continue with the measurements done by the user, the figure window with the STM image needs to be brought to the front and the ‘data cursor’ button at the top of the figure needs to be pressed. This changes the cursor to a cross that when clicked on part of the image, displays the coordinates of that pixel (Figure 41). The X and Y coordinates of that pixel can then be used as a starting point for the Pt(111) overlayer.

Figure 41 STM image from MatLab that shows the X and Y coordinates for a selected pixel.



To generate the Platinum lattice the command “`overlattice([X,Y],atom_size,adjusted_angle,number_of_repeats)`” needs to be typed in where the X, and Y are the starting coordinates for the theoretical lattice, the atom_size is the number of points between Pt atom centers found previously from the size of the image, the adjusted_angle is an angle number between 0 and 360 which makes the overlayer lattice conform to whatever angle from the horizontal the lattice should follow. And the number_of_repeats is how many times the Pt lattice should repeat. A final image should look like Figure 42.

Figure 42 MatLab image which shows an idealized Pt(111) lattice on a STM image of MeBr.



This procedure starting at “imageprep” needs to be run to make new figures with adjustments made to the the Pt atom spacing, adjusted angle, and starting coordinates in the overlayer command until a lattice that fits the existing data is found or it is determined that a lattice can not fit due to factors such as image drift, molecules being incommensurate, etc..

The entire procedure can be automated and made such that the overlattice can be moved simply by moving sliders or pressing buttons if the time is spent coding a nice interface. I have not done this yet, but the basic procedures for this have been written into the program and should be possible to implement in the MatLab framework.

Code for Theoretical Lattice generation:

```

latprep:
a=2.78;
n=10;
[Xs,Ys,Zs]=sphere(10);
Lat=surf(Xs,Ys,Zs);
hold

lattice:
i=0;
j=0;
Px=0;
for i = 1:n
    Y=(i-1)*a*sin(60*(2*pi)/360);
    for j = 1:n
        X=Px+(j-1)*a;
        surf(Xs+X,Ys+Y,Zs)
        j = j + 1;
    end
    Px = Px + a*cos(60*(2*pi)/360);
    i = i + 1;
end

MeBr1:
i = 0;
j = 0;
Px = 0;
Py = 0;
for i = 1:n*2
    Y = (i-1)*a*3*sin(60*(2*pi)/360);
    for j = 1:n
        X = Px + 5*(j-1)*a;
        surf(Xs+X,Ys+Y,Zs+2)
        j = j + 1;
    end
    Px = Px + 3*a*cos(60*(2*pi)/360);
    i = i +1;
end

MeBr2:
i = 0;
j = 0;
Px = 0;
Py = 0;
a60 = (60 *(2*pi)/360);
for i = 1:n*2
    Y = a*sin(a60) + Py;
    for j = 1:n
        X=a + a*cos(a60) + 5*(j-1)*a +Px;
        surf(Xs+X,Ys+Y,Zs+2)
        j= j + 1;
    end
end

```

```

Px = Px + 3*a*cos(a60);
Py = Py + 3*a*sin(a60);
i = i + 1;
end

```

MeBr3:

```

i = 0;
j = 0;
Px = 0;
Py = 0;
a60 = (60 *(2*pi)/360);
a30 = (30 *(2*pi)/360);
for i = 1:n*2
    Y = .5*a*tan(a30) + Py;
    for j = 1:n
        X=2*a + .5*a + 5*(j-1)*a +Px;
        surf(Xs+X,Ys+Y,Zs+2)
        j= j + 1;
    end
    Px = Px + 3*a*cos(a60);
    Py = Py + 3*a*sin(a60);
    i = i + 1;
end

```

MeBr4:

```

i = 0;
j = 0;
Px = 0;
Py = 0;
a60 = (60 *(2*pi)/360);
a30 = (30 *(2*pi)/360);
for i = 1:n*2
    Y = .5*a*tan(a30) + a*sin(a60) + Py;
    for j = 1:n
        X=4*a + 5*(j-1)*a +Px;
        surf(Xs+X,Ys+Y,Zs+2)
        j= j + 1;
    end
    Px = Px + 3*a*cos(a60);
    Py = Py + 3*a*sin(a60);
    i = i + 1;
end

```

The coordinates of each adsorbate molecule in the unit cell needs to be specified and inserted into a program similar to the ones above, which will cause them to be repeated at the specific position and adjusted by each change from the origin of the original unit cell.

Code for the insertion of the Pt(111) overlayer on a STM image.

```

circle:
function H=circle(center,radius,NOP,style)
%-----
% H=CIRCLE(CENTER,RADIUS,NOP,STYLE)
% This routine draws a circle with center defined as
% a vector CENTER, radius as a scalar RADIS. NOP is
% the number of points on the circle. As to STYLE,
% use it the same way as you use the routine PLOT.
% Since the handle of the object is returned, you
% use routine SET to get the best result.
%-----

THETA=linspace(0,2*pi,NOP);
RHO=ones(1,NOP)*radius;
[X,Y] = pol2cart(THETA,RHO);
X=X+center(1);
Y=Y+center(2);
H=plot(X,Y,style);
axis square;

imageprep:
figure
image(A)
axis equal off
hold

overlattice:
function H1=overlattice(center,a,angle,n)
%-----
%defintion of center is input of starting corodinates for [X,Y]
%a is defined as the interatomic spacing of the lattice
%angle is the angle of the lattice adjustment in relative position to a
%horizontal line in the graph
%n defines the number of times the lattice is repeated.
%-----
i = 0;
j = 0;
a60 = (60 *(2*pi)/360);
aa = (angle *(2*pi)/360);
Px = center(1);
Py = center(2);
for i = 1:n
    for j = 1:n
        X = (j-1)*a*cos(aa)+Px;
        Y = (j-1)*a*sin(aa)+Py;

```

```
    circle([X,Y],a/2,100,'-');
    j = j +1;
end
Px = Px + a*cos(a60+aa);
Py = Py + a*sin(a60+aa);
i = i + 1;
end
```

-
- ¹ "RHK SPM-100 User Manual"
- ² "Piezoelectricity" Walter Guyton Cady, 1st Ed. 1946 New York
- ³ Staveley Sensors Inc. Product manual for piezoelectrics.
- ⁴ J. Weaver, J. Chen, A.L. Gerrard, Surf. Sci. 592 (2005) 83
- ⁵ R. V. Lapshin, Rev. Sci. Instrum., 69 (9), (1998) 3268
- ⁶ S. Carrara, P. Facci, C. Nicolini, Rev. Sci. Instrum., 65 (9) (1994) 2860
- ⁷ V. Yu Yurov, A.N. Klimov, Rev. Sci. Instrum., 65 (5) (1994) 1551
- ⁸ "The Art of Electronics" Paul Horowitz, Winfield Hill, Cambridge University Press (1989)
- ⁹ "Lessons in Electric Circuits: Volume II -AC", Tony R. Kuphaldt 5th Ed. Open Book Project www.Ibiblio.org/obp
- ¹⁰ "Building Scientific Apparatuses" 2nd Ed. J.H. Moore, C. C. Davis, M.A. Coplan, Addison-Wesley, New York 1989
- ¹¹ "Noise Measurement" Marshall Leach, Jr. CRC Press 2000
- ¹² "Power Quality" C. Sankaran, CRC Press 2002
- ¹³ R. Roy, D. K. Agrawal, H. A. McKinstry, Ann. Rev. Mat. Sci. 19 (1989) 59-81
- ¹⁴ Staverly Sensors Inc. E. Hartford CT
- ¹⁵ L. A. Hockett, S. E. Creager Rev. Sci. Instrum. 64 (1) (1993) 263
- ¹⁶ L. Libioulle, Y. Houbion, J. M. Gilles, Rev. Sci. Instrum. 66 (1) (1995), 97
- ¹⁷ A. J. Nam, A. Teren, T. A. Lusby, A. J. Melmed, J. Vac. Sci. Tech. B 13(4), (1995) 1556
- ¹⁸ M. Fotino, Rev. Sci. Instrum. 64(1) (1993), 160
- ¹⁹ D. K. Biegelsen, F. A. Ponce, J. C. Tramontana, S. M. Koch, App. Phys. Lett. 50(11) (1987) 696
- ²⁰ D. J. Larson, K.F. Russell, A. Cerezo, J. Vac. Sci. Tech. B 18(1), (2000), 328
- ²¹ R. Taylor, R. S. Williams, V.L. Chi, G. Bishop, J. Fletcher, W. Robinett, S. Washburn, Surf. Sci. Lett. 306 (1994), L534
- ²² V. T. Bihn, J. Marien, Surf. Sci. Lett. 202 (1988), L539
- ²³ P. Sutter, PZahl, E Sutter, and J.E. Bernard, Phys Rev. Lett. 90, (2003)
- ²⁴ V. P. LaBella, D.W. Bullock, Z. Ding, C. Emery, A Vendatesan, W. F. Oliver, G. J. Salamo, P.M. Thibado, M. Mortazavi, Science, 292, (2001), 1518
- ²⁵ S. H. Pan, E. W. Hudson, J. C. Davis, App. Phys. Lett. 73(20), (1998) 2992
- ²⁶ Uwe Mick, alt.sci.nanotech archives, Oct. 28 1998
- ²⁷ Frank Ogletree, alt.sci.nanotech achieves, Dec, 2 1998
- ²⁸ A. J. Melmed, J. Vac. Sci. Technol. B 9 (2), (1991) 601
- ²⁹ M. J. Heben, M. M. Dovek, N. S. Lewis, R. M Penner, C. F. Quate, J. Microsc. 152, (1988) 651
- ³⁰ H. Lemke, T. Goddenhenrich, H. P. Bochem, U. Hartmann, C. Heiden, Rev. Sci. Instrum. 61 (1990) 2538
- ³¹ S. P. Kounaves, Platinum Metals Rev. 34, (1990), 131
- ³² B.K. Johnson, "Optics and Oprical Instruments: An Introduction", 1960 Dover Publications, New York
- ³³ R. Fowler, L. W. Nordeim, Proc. Roy. Soc. Lond. A. 119 (1928) 173

CHAPTER 4

CH₃Br STRUCTURES ON Pt(111): FERROELECTRIC SELF ASSEMBLY OF DIPOLAR AND WEAKLY ADSORBED MOLECULES

4.1 INTRODUCTION:

Although currently being phased out industrially because of its deleterious effects on the stratospheric ozone layer,¹ methyl bromide has long been used as a methylating agent in organic chemistry² and as a fumigant and biocide in agriculture. On surfaces, methyl halides are useful precursor species for delivering CH₃ radicals and halogens to surfaces³ and also as model adsorbates for studies of surface reactivity,⁴ photochemistry,⁵ and photoinduced electron-transfer chemistry.⁶ Methyl bromide has been a particularly important polyatomic adsorbate for advancing our understanding of surface photochemistry on insulators,^{7,8} semiconductors,^{9,10} and metals.^{11,12,13,14} Unfortunately, detailed structural information about adsorbed CH₃Br, that would be most helpful in rigorously interpreting and predicting its photochemical dynamics, has been largely lacking. The traditional structural probes of surface science such as low energy electron diffraction (LEED) or near edge x-ray fine structure (NEXAFS)¹⁵ are difficult to

apply to CH₃Br because of the ease by which this molecule falls apart via dissociative electron attachment whenever low energy secondary electrons are present. Consequently, structural information about adsorbed CH₃Br has been derived primarily from He beam scattering,¹⁶ photofragment angular distributions,^{9,12,13} and reflection absorption infrared spectroscopy (RAIRS).^{13,17} In this study, scanning tunneling microscopy (STM) with picoamp currents at low surface temperatures is employed to directly examine the ordering and structural behavior of CH₃Br on Pt(111) for the first time. Several ferroelectrically ordered CH₃Br structures are identified and kinetic limitations on the molecular ordering behavior are observed.

The nanoscale structure, orientation, and self-assembly of adsorbed dipolar molecules is a subject of considerable interest. Self-assembly of physisorbed CH₃Br on Si(111) – (7 x 7) followed by adsorbate photochemistry has recently been shown to chemically imprint Br photofragments on to atomically precise locations of the underlying surface.¹⁰ The resulting nanofabricated Br/Si(111) pattern is stable to 600 K but owes its existence to the initial self-assembly of physisorbed CH₃Br at 50 K. Although low temperature STM was used to directly visualize these nanopatterns, the imprinting process was made to occur over the entire ultraviolet irradiated surface and so might be useful as a practical nanofabrication technique.¹⁸ The ability to flip the orientation of adsorbed CH₃Br as a function of O coverage on O/Ru(001) surfaces has enabled fundamental studies of the steric effect in the dissociative electron attachment of electrons to an adsorbate (i.e., the electron/molecule approach geometry is important).^{14,19} He beam scattering indicates that CH₃Br antiferroelectrically orders on

C(0001) graphite, NaCl(001), and LiF(001) surfaces.¹⁶ Theoretical analysis of the surface ordering of dipolar molecules, such as CH₃Br on MgO, indicates a variety of ordered antiferroelectric, ferroelectric, and disordered phases are possible for different values of the coverage, temperature, adsorbate binding energy and dipole moment. Understanding 2-D dielectric ordering behavior is deemed important to the development of next generation non-volatile memory and electronic devices based on ferroelectric thin films.^{20,21}

Methyl bromide has a substantial dipole moment of 1.8 Debye (D) and physisorbs or very weakly chemisorbs to Pt(111) through the more polarizable Br end of the molecule. The adsorption energy falls from 0.6 eV to 0.3 eV as the coverage increases from 0 to the saturation coverage of 0.25 ± 0.02 ML.¹³ Only about a third of this energetic decrease can be attributed to dipolar repulsions, the remainder is attributed to the occupation of different adsorption sites or structures, and electronic tempering of the surface. Temperature dependent RAIRS experiments employing pre- or post-dosed CO, O₂, and CD₃Br to block and monitor different adsorption sites established that CH₃Br preferentially adsorbs on Pt(111) top sites and only at higher coverages, do multifold adsorption sites also become occupied. At submonolayer coverages, both the CH₃ photofragment angular distributions from the 193 nm photoinduced dissociative electron attachment (DEA) to physisorbed CH₃Br and RAIRS indicate that the molecules tend to lie with C-Br axis closer to the surface plane at low coverage (e.g., 42° by RAIRS at 0.1 ML) and tip towards the surface normal as the coverage increases (e.g., 30° by RAIRS at 0.18 ML). However, the results from these ensemble averaged techniques do not

quantitatively agree with one another. Both techniques indicate that CH₃Br diffusion is suppressed when adsorbed at a surface temperature of 20 K. Attainment of equilibrium across the submonolayer was presumed to be achieved by annealing to 85 K, a temperature within about 20 K of where a full monolayer would begin to desorb and a temperature that led to reproducible experimental results. As will be detailed below, even more aggressive annealing procedures are required to approximate thermal equilibrium conditions because the CH₃Br ordering/diffusion kinetics are surprisingly slow. The purpose of the current STM study is to provide a consistent microscopic picture of the CH₃Br surface behavior and ordering phenomena that can aid in the interpretation of its photochemical dynamics and RAIRS spectra.

4.2 EXPERIMENTAL:

STM experiments were performed in an ultrahigh vacuum (UHV) chamber with a working pressure of 4×10^{-11} torr maintained by a 640 l/s ion pump and a titanium sublimation pump. The Pt(111) crystal (5 mm dia x 2 mm thick) was cooled by a flexible copper braid connection to an Oxford Instruments liquid He cryostat and was heated by electron bombardment from a 2 mm coiled tungsten filament located directly behind the crystal. The sample temperature was monitored by a Eurotherm 9000 temperature controller connected to an alumel/chromel thermocouple spotwelded to the sample. The temperature could be varied from 20 K to greater than 1250 K, and was calibrated based on the thermal programmed desorption (TPD) of CO multilayers as described by Schlichting and Menzel.²² Surface analytical techniques employed in the STM chamber were: STM via a homebuilt, variable temperature, Besocke-beetle style STM driven by

RHK electronics, Auger electron spectroscopy (AES) using a cylindrical mirror analyzer, and TPD to a twice differentially pumped quadrupole mass spectrometer. Further details of the STM chamber have been described elsewhere.²³ Typical STM images were obtained with currents in the 10 – 200 pA range and sample bias voltages, V_B, were kept below ±2.5 V in order to avoid dissociative electron attachment. Image acquisition times were typically 30 seconds and the in-plane thermal drift at low temperatures was ~4 Å per minute.

RAIRS and TPD experiments were performed in a separate UHV chamber with a working pressure of 6×10^{-11} Torr maintained by a 240 l/s turbopump backed by a diffusion pump, and a titanium sublimation pump. The Pt(111) sample (15 mm dia. x 2 mm) was cooled by a Cu braid connection to a closed cycle helium refrigerator and heated by electron bombardment to achieve a temperature range from 18 K to greater than 1250 K. The RAIRS chamber¹³ has RAIRS, AES, TPD, LEED, and x-ray photoelectron spectroscopy (XPS) capabilities.

The Pt(111) samples were initially cleaned by Ar⁺ ion sputtering at 800 K followed by high temperature annealing at 1100 K for 5 minutes. After Ar⁺ sputtering, the cleanliness of the surface was checked by AES. Once the surface was free of carbon and other contaminates the subsequent day to day cleaning of the surface could typically be performed by oxidation in a $\sim 5 \times 10^{-8}$ Torr local oxygen atmosphere in front of the directed doser at 700 K for 5 minutes. Following cleaning by oxidation, a final oxygen TPD was taken and the ratio of the oxygen recombinative desorption peak (~800 K) to

the molecular oxygen desorption peak (~150 K) was used to confirm the surface cleanliness before dosing the molecules of interest.

Methyl bromide, UHP grade from Matheson Gases, was stored in a stainless steel bottle on a gas manifold that led through a leak valve to a capillary array (or cosine effusive doser) pointed directly at the sample surface. A trapped volume whose pressure could be measured with a Baratron capacitive manometer was filled with a known pressure of gas and then evacuated though a leak valve to dose the sample in a reproducible manner (ca. 2-5%). Gas exposures were calibrated using TPD of CO dosed at 20 K where the CO sticking coefficient is assumed to be unity and the CO coverage saturates at 0.50 ML.²⁴ In this study, the Pt(111) sample was typically dosed with CH₃Br at 20 K and slowly annealed to 104 K over several minutes prior to experiments at low temperature.

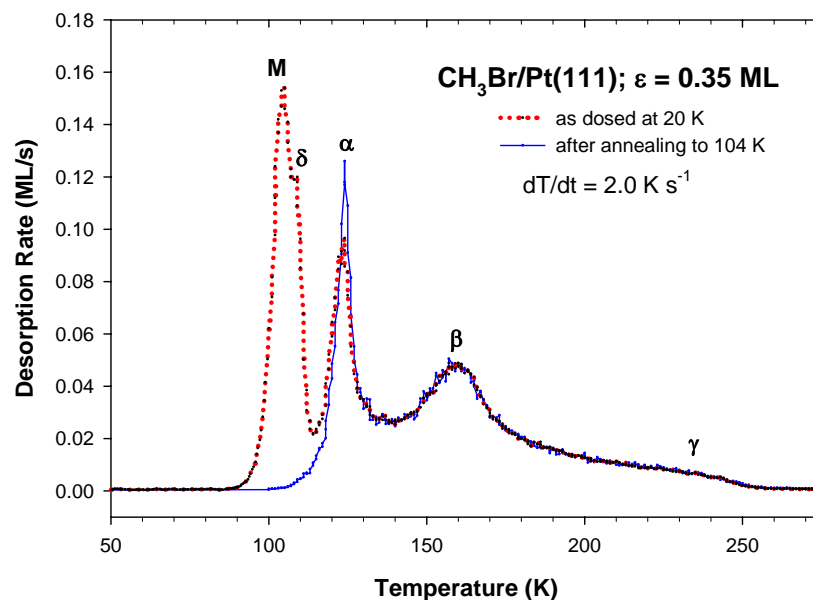
4.3 RESULTS AND DISCUSSION:

4.3.1 THERMAL PROGRAMMED DESORPTION (TPD):

The TPD spectra of Figure 1 illustrates the thermal behavior of CH₃Br on Pt(111). Briefly summarizing earlier work,¹³ small coverages of CH₃Br yield a γ TPD peak at 230 K which broadens smoothly to lower temperature with increasing coverage to yield the β TPD peak at 155 K. Additional submonolayer coverage populates the α TPD peak at 120 K which is kinetically slow to complete when CH₃Br is dosed at 20 K and the surface temperature is ramped at 2 K s⁻¹ in TPD. Further CH₃Br exposure at 20 K populates a

transitional feature, δ , at 103 K in the TPD spectrum before multilayers, M, are populated that desorb at 100 K. The 20 K sticking coefficient of CH₃Br is constant and assumed to

Figure 1 TPD spectra ($m/e = 95$ amu) of $\epsilon = 0.35$ ML exposures of CH₃Br dosed on to Pt(111) at 20 K, without and with slow annealing to 104 K over several minutes. The α , β , and γ TPD peaks of the monolayer remain following annealing and the coverage within the α peak increases slightly.



be unity up until exposures greater than 0.23 ML that lead to the appearance of the δ peak in the TPD spectra and a suddenly reduced sticking coefficient. The post-annealing TPD spectrum of Figure 1 shows that by dosing CH₃Br multilayers at 20 K and slowly annealing the CH₃Br to 104 K over several minutes it is possible to further populate and complete the α TPD peak of the CH₃Br monolayer and avoid substantially populating the surface with any residual overlayer molecules.

4.3.2 MOLECULAR ORIENTATION WITHIN THE CH₃Br MONOLAYER:

The orientation of CH₃Br within the annealed monolayer could be established by examination of the monolayer's defect structures by STM and also by the monolayer's RAIRS spectrum.

4.3.2A SCANNING TUNNELING MICROSCOPY (STM):

Initial STM images of an ordered CH₃Br monolayer were observed by dosing multilayers and annealing slowly to 95 K over several minutes to anneal away the overlayer. The resulting images obtained at 30 K showed patches of ordered structures but there was substantial non-uniform noise consistent with the presence of loosely bound molecules diffusing and aggregating randomly on the surface. Accordingly, TPD following STM images of samples prepared in this manner showed the presence of a small multilayer/δ peak at 103 K. After some experimentation with RAIRS, STM, and TPD it was found that annealing multilayers slowly to 104 K over several minutes gave the most perfectly ordered CH₃Br monolayer with a minimum of the loosely bound overlayer molecules that can degrade STM imaging.

Figure 2 shows a constant current STM topographic image of a fairly well ordered CH₃Br monolayer that contains several kinds of defect structures. The molecules appear as bright dots and the underlying Pt(111) lattice cannot be simultaneously resolved. The van der Waals size of the molecules is approximately ~3.8 Å dia x 6.4 Å long. There is a substantial surface work function drop as the CH₃Br monolayer is formed,²⁵ and an

earlier RAIRS study¹³ argues that the molecules are oriented close to the surface normal and bind with the Br end against the surface. The STM image is consistent with these expectations. Nevertheless, it is conceivable that CH₃Br could image either as a dot-like projection if the C-Br axis is oriented along the surface normal, or possibly as two distinct projections if the molecule lies in the surface plane and tunneling is enhanced through both the CH₃ and Br ends of the molecule. In the latter case, “dogbone” defects involving the loss of two bright dots as illustrated in Circle B of Figure 2 should be the minimal building block of any more complicated defects. However, as can be seen in Circle A of Figure 2 a defect involving the loss of a single bright dot is also possible and so we assign the dots to be individual molecules, probably oriented with the C-Br bond vertical to the surface normal. The orientation by STM relies on a consistently shaped molecule surface projection over a broad range of bias voltage images, where if the molecules were lying down one might expect to see a differential change in the recorded tomography as a function of the biasing voltage for tunneling into either the CH₃ or Br ends of the molecule. In practice, the topographic images were almost identical over bias voltages from +1.8 V to -1.8V. The highest resolution molecular images were obtained at very low bias voltages (\pm 50 mV) and biases greater than \pm 2.5 V may lead to fragmentation of the molecules by dissociative electron attachment.

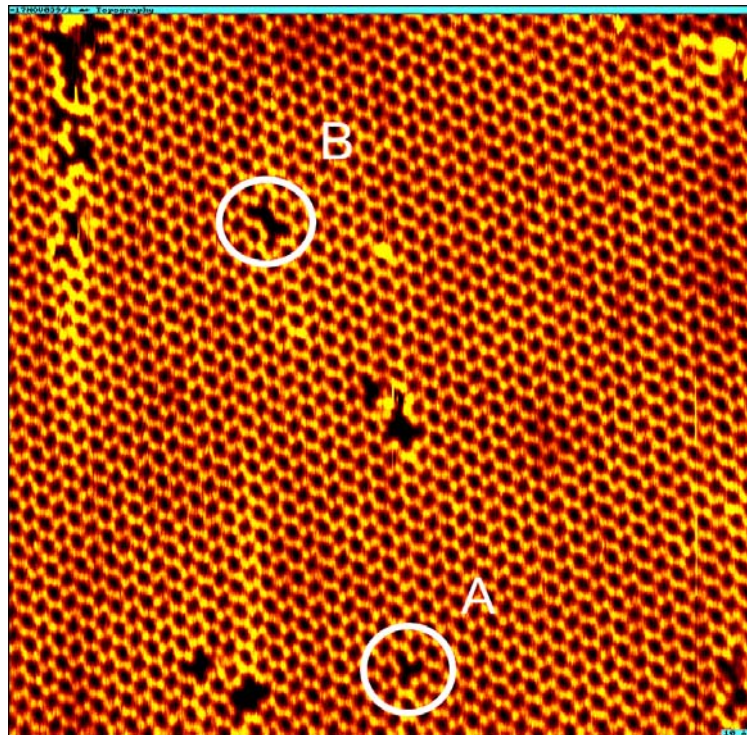


Figure 2 STM image of a CH₃Br monolayer formed by dosing multilayers and annealing to 98 K. Within the ordered monolayer there are defect structures labeled A and B. Circle A contains a single missing molecule defect, while circle B contains a "dog bone" defect corresponding to two molecules missing from the lattice (250 Å x 250 Å image, I = 100 pA, V_B = +300 mV).

4.3.2B REFLECTION ABSORPTION INFRARED SPECTROSCOPY (RAIRS):

Figure 3 compares 2 cm⁻¹ resolution RAIRS spectra for submonolayer and multilayer exposures of CH₃Br on Pt(111) dosed at 20 K and annealed to 104 K over several minutes. The multilayer annealing procedure yields the annealed TPD trace of Figure 1 and best prepares the well-ordered monolayer observed in Figure 2. Important for making assignments of the CH₃Br orientation are the v₂ and v₅ "CH₃" deformational

modes which have dipole derivatives parallel and perpendicular to the molecular C-Br axis, respectively. The presence of both the ν_2 band at 1278 cm⁻¹ and the ν_5 band at 1412 cm⁻¹ in the submonolayer RAIRS spectrum is evidence that not all molecules are lying either parallel or perpendicular to the surface normal. This follows because the infrared electric field in RAIRS on metals is directed only along the surface normal and hence only modes with a dipole derivative that has a non-zero projection on the surface normal (electric field) will be RAIRS active. Consequently, the submonolayer RAIRS spectrum indicates that at this coverage some molecules may lie down while some may stand up, or the molecular angular distribution may be peaked towards an angle tilted away from the surface normal. The disappearance of the ν_5 band in the monolayer RAIRS spectrum requires that all the molecules must be standing up and oriented along the surface normal within the monolayer.

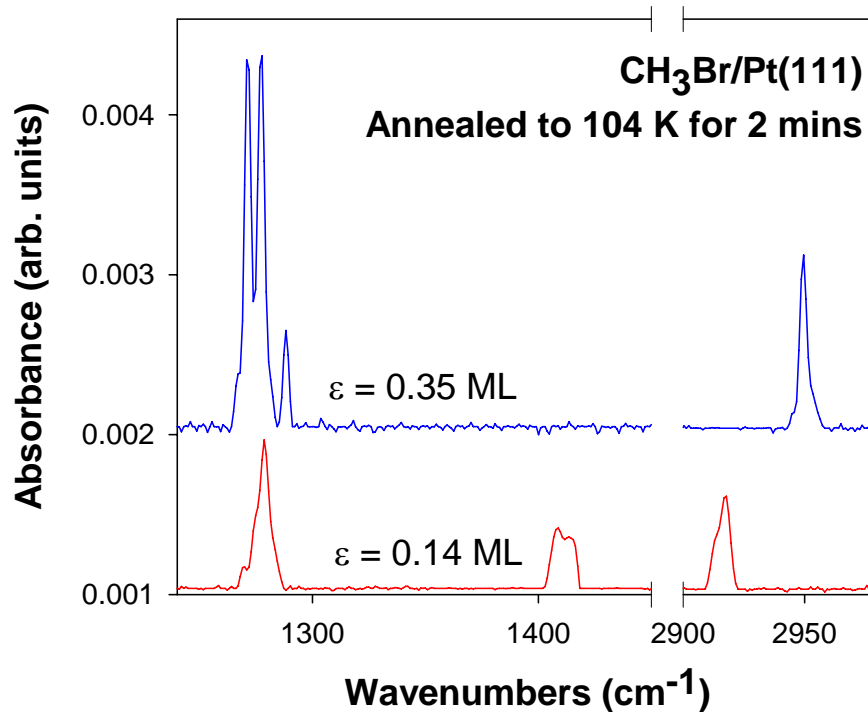


Figure 3 RAIRS spectra of a well-annealed CH₃Br submonolayer and monolayer. The absence of the v₅ mode near 1410 cm⁻¹ in the ordered monolayer spectrum requires that all molecules within the monolayer are oriented along the surface normal, unlike their behavior in submonolayers. The splitting of the monolayer v₂ band into two sharp symmetric peaks at 1270 cm⁻¹ and 1277 cm⁻¹ (3 cm⁻¹ fwhms), and a small satellite peak at 1288 cm⁻¹, provides evidence for CH₃Br adsorption at primarily two different sites or local environments, in equal measure.

The annealed monolayer RAIRS shows no evidence for overlayer molecules that would have given rise to additional absorption peaks (e.g., another v₂ peak at 1300 cm⁻¹). The splitting of the v₂ band of the monolayer into two sharp symmetric peaks at 1270

cm⁻¹ and 1277 cm⁻¹, and a small satellite peak at 1288 cm⁻¹, provides evidence for CH₃Br adsorption at primarily two different sites or local environments. The symmetric splitting indicates that the two different environments are populated in equal measure. The integrated absorbance of the smaller 1288 cm⁻¹ satellite peak is only 6% of the total for the v₂ band. Since the defect density of the Pt(111) surface has been titrated by CO RAIRS as less than 1%, it seems likely that the 6% satellite RAIRS peak does not derive from molecules adsorbed at Pt(111) defects but rather from molecules at the boundaries of ordered domains or other defects in the CH₃Br monolayer lattice. The sharpness of the v₂ band peaks with 3 cm⁻¹ full width half maximums (fwhm) argues for the structural homogeneity of the monolayer structure.

An earlier RAIRS study¹³ performed with CH₃Br annealing to 85 K and a lower 4 cm⁻¹ resolution never observed the v₅ band to disappear as a function of coverage, nor could the v₂ band splitting be completely resolved as seen in Figure 3. However, the v₂ band was clearly observed to be split at high submonolayer coverage and line shape analysis in conjunction with pre- and post-dosing of CD₃Br, CO, and O₂ made possible an assignment of the CH₃Br adsorption to different Pt(111) sites on the basis of the v₂ band peak positions. It was found that CH₃Br preferentially occupies top sites at low coverage and multifold, presumably 3-fold hollow, sites become increasingly occupied at higher coverage. Table 1 summarizes the RAIRS observations of Figure 3 and provides consistent site assignments.

Table I. RAIRS Active Modes of Methyl Bromide (cm⁻¹)

v_2 deformation (\parallel to C-Br axis); [fwhm]					v_5 deformation (\perp to C-Br axis)	C-H stretch	Exposure Annealed
Gas Phase	Multilayer	3-fold hollow	Top site	Satellite			
1305.1	1300	1270 [3 cm ⁻¹]	1277 [3 cm ⁻¹]	1288 [4 cm ⁻¹]		2958 [3 cm ⁻¹]	0.35 ML
		1268 -trace-	1278 [8 cm ⁻¹]		1412 [15 cm ⁻¹]	2922 [7 cm ⁻¹]	0.14 ML

The satellite v_2 band peak is relatively unperturbed in frequency away from CH₃Br in multilayers or in the gas-phase, suggesting that the associated molecules may be relatively loosely bound (e.g., at domain walls). The top and 3-fold hollow site v_2 peaks are increasingly perturbed in frequency and this is expected on the basis of increasing electron back donation into the molecule from the surface. The C-H stretch frequency of the tilted molecules in the submonolayer is substantially lower than that for the standing-up molecules of the monolayer and here again it may be that more efficient electron back donation into the tilted molecule lowers the C-H vibrational frequency.

4.3.3 STRUCTURE OF THE (6 x 3) CH₃Br MONOLAYER:

A high resolution, constant current STM image of the ordered CH₃Br monolayer formed by dosing multilayers and slowly annealing to 104 K over several minutes is

shown in Figure 4. The bright, gold-colored spots are assigned as standing-up molecules on the basis of their defect pattern and RAIRS spectrum as described above. The molecules are arranged in a modulated hexagonal pattern around either round or oblong depressions. The lattice's most easily seen distinguishing feature is the alternating diagonal rows of round and oblong depressions that run from top left to bottom right across the STM image. The A defects of Figure 2 can be seen to derive from removing any single molecule from the lattice and the "dogbone" B defects derive from removing any 2 molecules facing one another across a depression. The minimal repetitive unit cell for the CH₃Br monolayer can be seen to be fairly large. Although it was not possible to simultaneously resolve the CH₃Br and Pt(111) lattices, we tentatively assign the CH₃Br monolayer as a (6 x 3) pattern. The STM length scale was calibrated by separately imaging an O p(2 x 2) layer on Pt(111) at 30 K.

Figure 4 High resolution STM image of the ordered CH₃Br monolayer displayed (a) as a 2-D contour map and (b) in 3-D. The 40 Å x 40 Å image was taken at Ts = 30 K, I = 10 pA and V_B = -10 mV. Outlined in white is a proposed (6 x 3) unit cell for the molecular lattice whose unit vectors of lengths 16.8 Å and 8.5 Å have an angle of 61° between them.

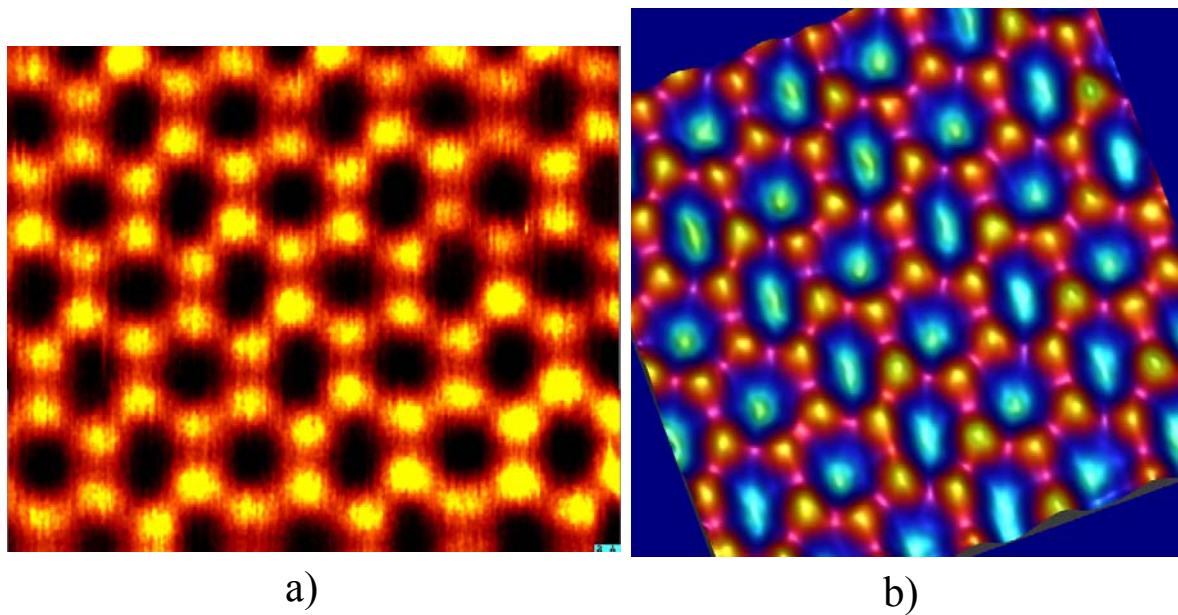


Figure 5 provides a comparison of a theoretical model of a (6 x 3) CH₃Br overlayer on Pt(111) with a corresponding high resolution STM image. Important in assigning this structural model were constraints introduced by RAIRS. We assume that the symmetric splitting of the v₂ band in the monolayer RAIRS of Figure 3 indicates that there are two kinds of CH₃Br local environments populated in equal measure. These environments are assigned to CH₃Br adsorption at Pt(111) top and 3-fold hollow sites on

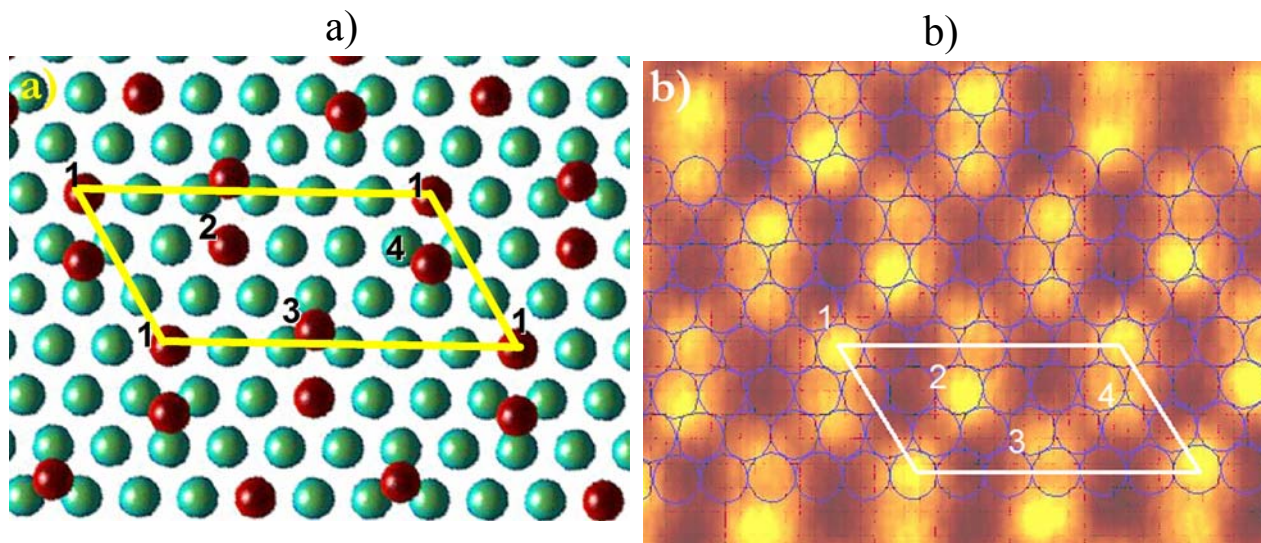


Figure 5 (a) Model of the ordered CH₃Br monolayer (red) on top of a Pt(111) atom lattice (green) **(b)** High resolution STM image of the ordered CH₃Br monolayer with a proposed grid of Pt(111) atoms overlaid. The proposed (6 x 3) unit cell and the molecules in the unit cell have labeling of 1,2,3 & 4.

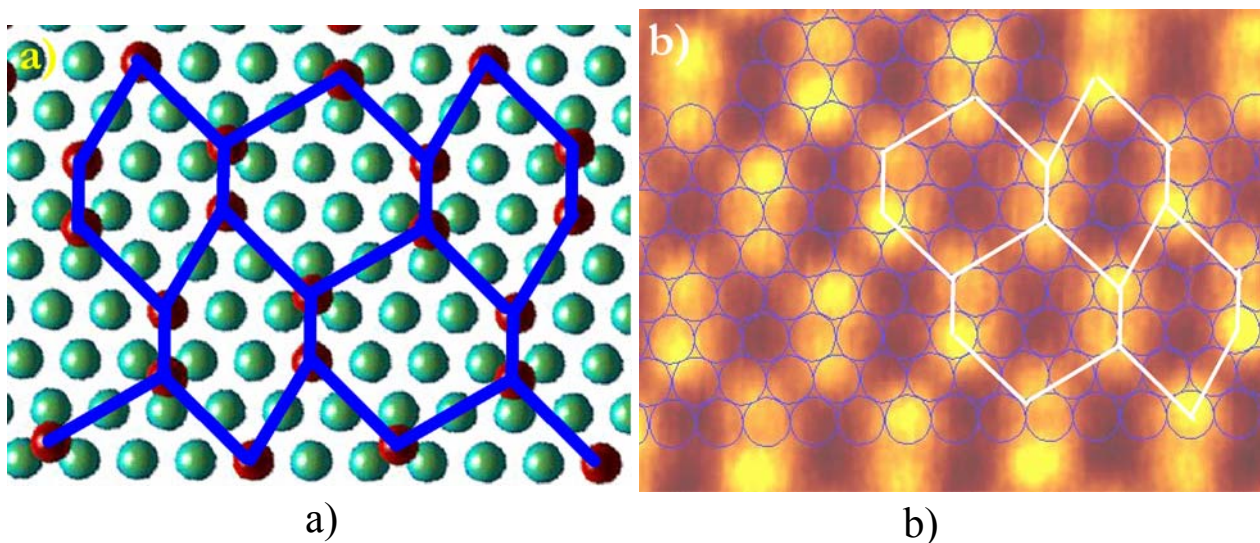
the basis of earlier RAIRS work as indicated in Table I. The proposed unit cell can be seen to contain 4 molecules, with the molecules labeled 1 and 2 being on top sites and those labeled 3 and 4 being on 3-fold hollow sites. The STM image of Figure 5(b) shows that molecules at top sites image slightly higher than those on 3-fold hollow sites. The saturation coverage of the (6 x 3) monolayer is 0.222 ML which compares to the 0.25 ± 0.02 ML value calculated by French and Harrison¹³ on the basis of TPD and the

assumption of an initial sticking coefficient of unity for both CO and CH₃Br on Pt(111) at

20 K.

Figure 6 illustrates how the (6 x 3) lattice of upright CH₃Br molecules leads to the distinctive rows of round and oblong depressions within the monolayer STM images.

Figure 6 (a) Model of the ordered CH₃Br monolayer (red) on top of a Pt(111) atom lattice (green) in which the repetitive molecular patterns framing the round and oblong depressions of the high resolution STM image of (b) are highlighted.

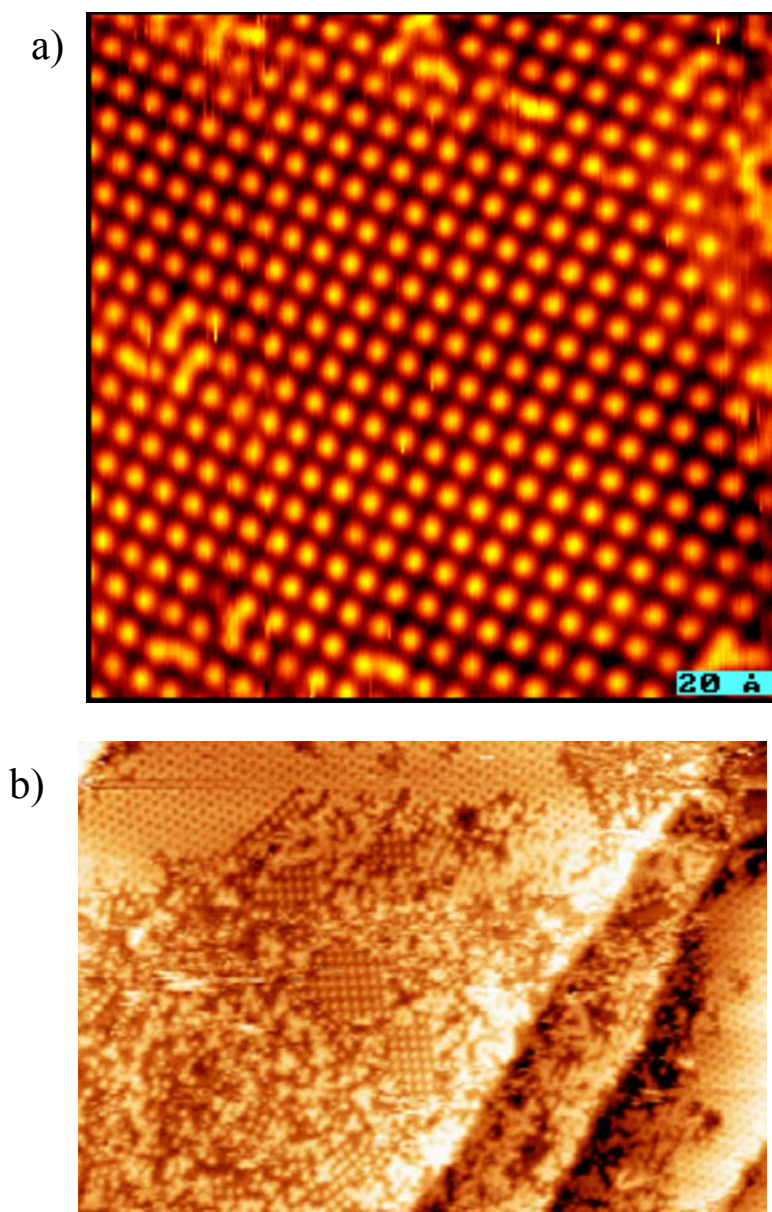


4.3.4 SUBMONOLAYER CH₃Br STRUCTURES:

When multilayers of CH₃Br were dosed at 20 K and then quickly annealed to ~115 K to remove the overlayers and some of the α submonolayer TPD peak at 120 K, it was possible to see some interesting additional structures. Figure 7(a) shows a “square” looking lattice with a nominal coverage of 0.12 ML. The average spacing between rows of molecules is 6.9 Å in one direction and 8.0 Å in the other. The angle between the rows is 82°. The existence of this low coverage “square” lattice was very rarely seen and may

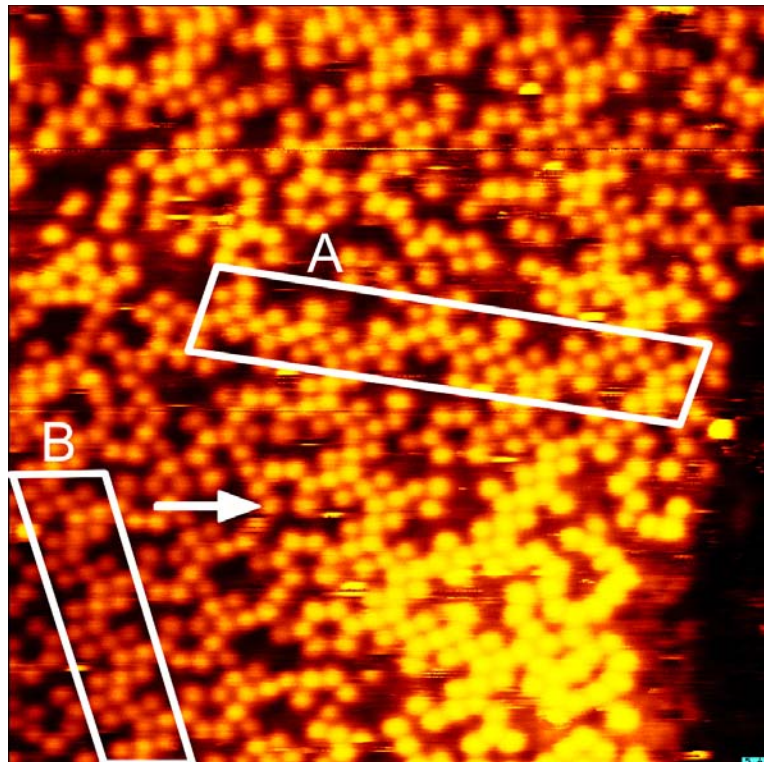
have been written off as a STM tip effect except for the image seen in Figure 7(b) which shows that the square lattice can coexist with the (6 x 3) hexagonal or “hex” looking lattice of the ordered monolayer.

Figure 7 STM image of a “square” ordered pattern of CH₃Br formed after annealing away some of the monolayer by flashing the surface temperature to ~115 K. [150 Å x 150 Å; T_s = 30 K, I = 100 pA and V_B = 250 mV] (b) STM image showing coexistence of “square” and “hex” (6 x 3) ordered structures after flashing to ~115 K. [335 Å x 500 Å; T_s = 30 K, I = 1 nA and V_B = -2.01 V]



The second sub-monolayer structure of methyl bromide molecules observed on the surface can be seen in Figure 8. In this image the surface was prepared by quickly flashing to 107 K and then annealing to 98 K for several minutes, which resulted in a complicated almost random arrangement of molecules. There are a few important items of importance to examine when looking at the image. First, there seems to be a significance of linear groups of three molecules, and that these linear groups of three

Figure 8 STM image of CH₃Br submonolayer prepared by dosing multilayers, flashing to 107 K, and annealing at 98 K for several minutes. The local coverage is 0.20 ML. Three interesting structures are noted: Box A shows an ensemble of molecules in rows containing three molecules each that begin to form a "square" lattice structure; Box B shows some three molecule rows alternately angling in and out forming a zigzag backbone; the arrow identifies a ring structure that has a small opening on one side, suggesting that the "hex" rings seen in the (6 x 3) monolayer are a stressed form that doesn't allow the molecules to occupy more favorable adsorption sites available at lower coverages [150 x 150 Å, T_s = 30 K, I_t = 200 pA, V_B = +327 mV]

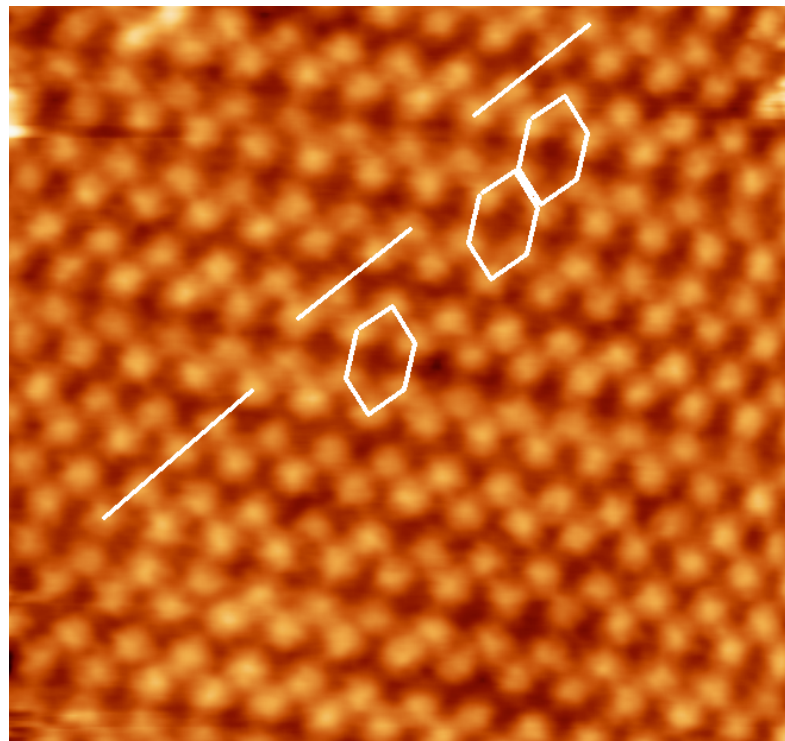


methyl bromide molecules can couple together in different ways that are outlined in box

A and box B of Figure 8. In the box labeled A, the linear groups of molecules couple in a fashion that resembles the start of a square or rectangular adsorbate lattice. The box labeled B, has a slightly different coupling of the linear group of three methyl bromide molecules, such that it starts to resemble a hexagonal adsorbate lattice. The existence of two different arrangements as seen in the image are suggestive that the substrate plays a role in the methyl bromide alignment. There must be a small but measurable difference in adsorption energies for the methyl bromide into one of the high symmetry adsorption sites on the Pt(111) lattice. This fact is further exemplified by the ring of molecules pointed out by the arrow within the image. The arrow is showing that the ring structure has a wider gap between the two molecules at the bottom of the ring than the top of the ring.

The last unique arrangement of the methyl bromide molecules was seen in Figure 9. This surface was prepared by slowly annealing the adsorbate covered surface to a temperature of 106 K which is slightly higher than the previously described ideal temperature of 104 K. Within the image of the annealed surface there are striations of two types of arrangements of molecules, there are the rows of hexagonal rings that can be assigned to the rings of the (6 x 3) monolayer lattice that are outlined in white, and rows of methyl bromide molecules that do not align to form rings. The rows of methyl bromide molecules that have been disrupted from their expected arrangement of a rings, seem to align in a high coverage square looking lattice. The calculated local coverage of the more densely packed lattice is 0.33 ML which is much higher than the monolayer coverage of 0.222 ML.

Figure 9 STM image of a CH₃Br submonolayer prepared by dosing multilayers and slowly annealing to 106 K over several minutes. The molecules form bands of “square” lattice and bands of “hex” rings. A few of the hex rings are outlined, and lines along one axis of some of the square lattice is drawn. [70 Å x 65 Å, T_s = 30 K, I = 10 pA, V_B = +195 mV]



4.4 CONCLUSIONS:

The (6 x 3) self-assembled monolayer of CH₃Br on Pt(111) was observed by STM and 2 cm⁻¹ resolution RAIRS to form a regular well-ordered pattern involving two kinds of molecules. The molecules in the (6 x 3) lattice are tentatively assigned to top and three fold hollow sites that are occupied in equal amounts leading to the symmetric and sharp splitting of the v₂ peak in RAIRS. Unlike in previous RAIRS studies of the methyl bromide covered surface, annealing to a high temperature of 104 K allowed the v₂ peak to definitively split and become very sharp (3 cm⁻¹ FWHM). Also the higher temperature annealing allowed for an orientational determination of the C-Br bond of the methyl bromide to be made with respect to the platinum surface. By the disappearance of the v₅ mode with its dipole derivative perpendicular to the C-Br bond the assumption that all of the molecules within the (6 x 3) adsorbate lattice are standing with the C-Br bond parallel to the surface normal.

In addition to the creation and imaging of a uniform monolayer of methyl bromide molecules, many sub-monolayer arrangements were revealed. The images of the full monolayer and sub-monolayer adsorbate covered surfaces should hopefully aid in theoretical work studying dipole-dipole interactions on transition metal surfaces by serving as a basis to compare against.

-
- ¹ S. E. McCauley, A. H. Goldstein, and D. J. DePaolo, Proc. Natl. Acad. Sci. U. S. A. **96** (18), 10006-10009 (1999)
 - ² S. Schmatz, "Quantum dynamics of gas-phase S(N)2 reactions, Chemphyschem **5** (5), 600-617 (2004)
 - ³ F. Zaera, "Probing catalytic reactions at surfaces," Prog. Surf. Sci. **69** (1-3), 1-98 (2001)
 - ⁴ J. L. Lin and B. E. Bent, J. Am. Chem. Soc. **115** (7), 2849-2853 (1993)
 - ⁵ X. L. Zhou, X. Y. Zhu, and J. M. White, Surface Science Reports **13** (3-6), 73-220 (1991)
 - ⁶ E. P. Marsh, T. L. Gilton, W. Meier et al., Physical Review Letters **61** (23), 2725-2728 (1988)
 - ⁷ E. B. D. Bourdon, J. P. Cowin, I. Harrison et al., J. Phys. Chem. **88** (25), 6100-6103 (1984)
 - ⁸ T. G. Lee, W. Liu, and J. C. Polanyi, Surf. Sci. **426** (2), 173-186 (1999)
 - ⁹ Q. Y. Yang, W. N. Schwarz, P. J. Lasky et al., Phys. Rev. Lett. **72** (19), 3068-3071 (1994)
 - ¹⁰ S. Dobrin, X. K. Lu, F. Y. Naumkin et al., Surf. Sci. **573** (2), L363-L368 (2004)
 - ¹¹ S. A. Costello, B. Roop, Z. M. Liu et al., J. Phys. Chem. **92** (5), 1019-1020 (1988)
 - ¹² V. A. Ukrainstsev, T. J. Long, and I. Harrison, J. Chem. Phys. **96** (5), 3957-3965 (1992)
 - ¹³ C. French and I. Harrison, Surf. Sci. **387** (1-3), 11-27 (1997)
 - ¹⁴ Y. Lilach and M. Asscher, Journal of Physical Chemistry B **108** (14), 4358-4361 (2004)
 - ¹⁵ P. J. Lasky, P. H. Lu, M. X. Yang et al., Surface Science **336** (1-2), 140-148 (1995)
 - ¹⁶ G. N. Robinson, N. Camillone, P. A. Rowntree et al., J. Chem. Phys. **96** (12), 9212-9220 (1992)
 - ¹⁷ F. Zaera, H. Hoffmann, and P. R. Griffiths, J. Electron Spectrosc. Relat. Phenom. **54**, 705-715 (1990)
 - ¹⁸ R. Osgood, Surf. Sci. **573** (2), 147-149 (2004)
 - ¹⁹ S. Jorgensen, F. Dubnikova, R. Kosloff et al., Journal Of Physical Chemistry B **108** (37), 14056-14061 (2004)
 - ²⁰ C. A. P. Dearaujo, J. D. Cuchiaro, L. D. McMillan et al., Nature **374** (6523), 627-629 (1995)
 - ²¹ D. D. Fong, G. B. Stephenson, S. K. Streiffer et al., Science **304** (5677), 1650-1653 (2004)
 - ²² H. Schlichting and D. Menzel, Rev. Sci. Instrum. **64** (7), 2013-2022 (1993)
 - ²³ H. Xu, R. Yuro, and I. Harrison, Surf. Sci. **411** (3), 303-315 (1998)
 - ²⁴ J. V. Nekrylova, C. French, A. N. Artsyukhovich et al., Surf. Sci. **295** (1-2), L987-L992 (1993)
 - ²⁵ J. M. White, in *Chemistry and Physics of Solid Surfaces VIII*, edited by R. Vanselow and R. Howe (Springer, New York)

CHAPTER 5

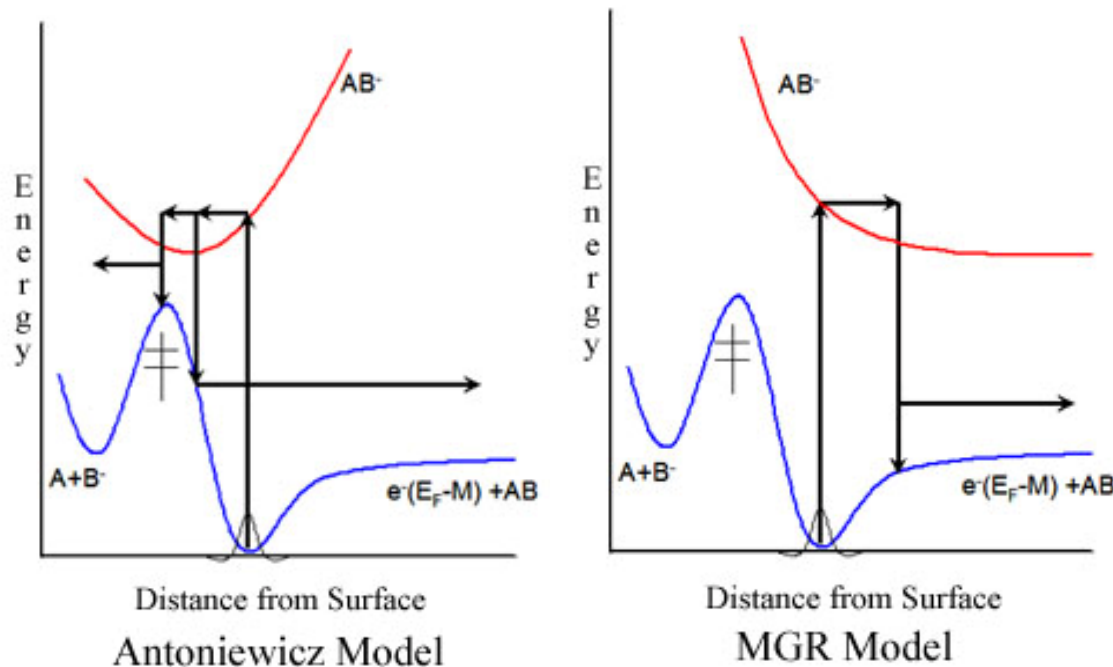
STM ANALYSIS OF CO₂ ADSORPTION ON Pt(111)

5.1 INTRODUCTION:

Carbon dioxide has become the focus of increased study since its role in the production of methanol was made clear.¹ Prior to this, CO₂ was left relatively unstudied by catalysis groups due to its strong thermodynamic stability and relative inertness. However, now that CO₂ has been shown to play a role as a chemical feedstock. It has been found to physisorb on many different transition metal surfaces^{2,3,4,5,6} and to chemisorb onto a few surfaces⁷ mainly at defect sites and on alkali promoted surfaces.^{8,9}

There are a few studies of CO₂ adsorbing on the Pt(111) surface that are of particular interest here. The first is work done by Madix et al.¹⁰ where he studies the adsorption dynamics of CO₂ molecules on a clean and partially covered surface using a molecular beam and a surface temperature of 80 K. They find that the full coverage of carbon dioxide on the Pt(111) surface falls in the range of 0.27 - 0.33 ML. The 0.33 ML coverage followed from the LEED observation of a (3 x 1) lattice when CO₂ was dosed at 80K and cooled to 32 K.

The second study was done by Zehr and Harrison,¹¹ where the estimated coverage of ¹³CO₂ was 0.30 ML. However, the focus of that paper shows how the translational and angular energy distributions of photodesorbing ¹³CO₂ are very similar to those derived from the photoreaction between CO and O. Their conclusion was that when physisorbed ¹³CO₂ is photoexcited it is attracted inwards, towards the surface, and can sample the transition state region relevant to CO photo-oxidation prior to desorption (dissociation also occurs with a 30 % probability), and so the photodesorption of ¹³CO₂ is consistent with an Antoniewicz bounce mechanism,¹² not an MGR mechanism.¹³



In this study, STM was used to investigate the physisorption of ¹³CO₂ onto the Pt(111) surface using both high and low temperature dosing schemes that gave different results. While the high temperature dosing scheme likely provides a molecular assembly that more closely resembles the thermal equilibrium configuration, the experimental conditions of low temperature dosing was done to match the photochemistry studies done

in the Harrison lab¹¹. The ordered ¹³CO₂ arrangements under different preparation schemes were used to calculate local coverages and to identify molecular configurations that gave specific adsorption peaks in RAIRS spectra.

5.2 EXPERIMENTAL:

The STM chamber has a working base pressure of 4×10^{-11} torr maintained by a 640 L/s Ion Pump and a titanium sublimation pump (TSP). The chamber contains a 5 mm dia. Pt(111) crystal that is cooled by an Oxford Instruments liquid He Ultrastat coupled to the crystal by a flexible copper braid, which can cool the crystal to a temperature of 20 K. The crystal is heated by e⁻ bombardment from a 2 mm coiled tungsten filament located directly behind the crystal, yielding a top temperature greater than 1250 K. The temperatures are acquired with an alumel/chromel type K thermocouple wire connected to a Eurotherm 900EPC that has had the temperature calibrated by TPD using the known heat of sublimation of CO multilayers in accordance with Menzel et al. The instruments available for probing the crystal and adsorbates are: a home built variable temperature beetle style STM, a single pass Auger Electron Spectrometer (AES), and a differentially pumped quadrupole mass spectrometer for TPD/TOF experiments (The possibility of LEED exists, when a LEED optic is attached to the chamber -not currently the case).

Preparation of the ¹³CO₂ covered surface was done in four ways. Two of the prepared surfaces were, full monolayer and submonolayer coverages prepared by dosing molecules while the crystal temperature was held at 30 K. The other two prepared surfaces at full and submonolayer coverages had ¹³CO₂ molecules that were dosed at a variable crystal temperature referred to throughout this paper as a “high” temperature

dose (e.g. $88 \leq T \leq 94$ K). The “high” temperature dose is used to create a uniform lattice that should leave the adsorbates in their thermodynamically stable positions by allowing molecules to adsorb and desorb freely. Interestingly, this led to higher coverages than dosing at low temperatures.

5.3 RESULTS / DISCUSSION:

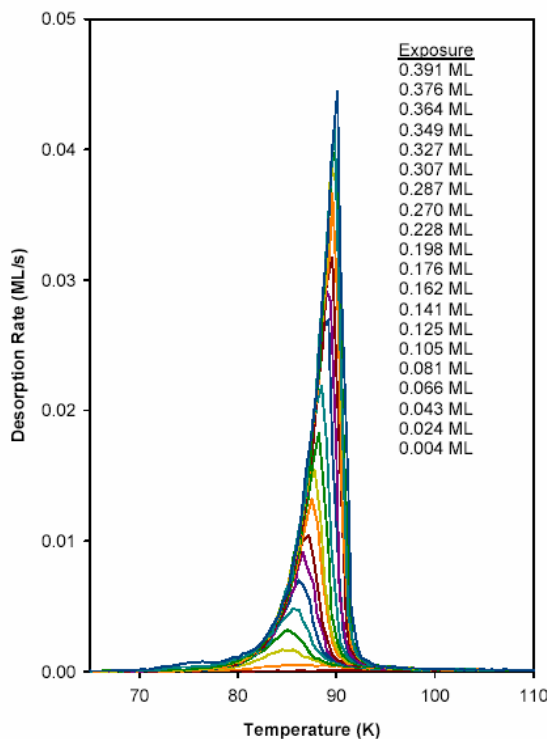
Thermal Programmed Desorption

There are three regions of desorption seen in the ¹³CO₂ TPD spectrum (Figure 1) as described by Zehr et al. The region corresponding to a coverage of less than 0.05 ML, has 1st order desorption characteristics. There is a decrease in the desorption temperature with increasing coverage up to a 0.05 ML limit. Once a coverage of 0.05 ML has been exceeded the peak desorption temperature increases to 90 K where a full monolayer coverage has been attained. Above 0.05 ML the ¹³CO₂ desorption kinetics switch from 1st order to 0th order. The switch in order is attributed to the formation of a 2-D island phase of ¹³CO₂ molecules where the interaction between the molecules suffices to drive the aggregation. The third desorption region is for multilayers with a peak desorption temperature of 75 K.

At coverages beyond the full monolayer, there is photochemical evidence molecules will move out of the monolayer to start forming 3-D islands. With this in mind the full monolayer coverage of ¹³CO₂ has been proposed by Zehr et al. to be 0.30 ML. This is slightly higher than the predicted coverage of 0.275 ML by Madix et al. The differences may arise from the method used to calculate the full coverage. Where Zehr compares the integrated area of the TPD desorption peak to a known CO coverage

desorption area peak, in contrast to Madix used molecular beam data taken at 80 K where multilayer is less likely to form. The results seen in the STM images would not exclude either coverage prediction. However, it's a more complicated than having a single coverage assignment for the monolayer. The STM images show ordered lattice structures ranging from 0.44 ML to 0.111 ML coverages with two intermediate local coverages of 0.33 ML and 0.40 ML.

Figure 1 Multiple TPD spectra showing desorption of the ¹³CO₂ changing as a function of coverage.

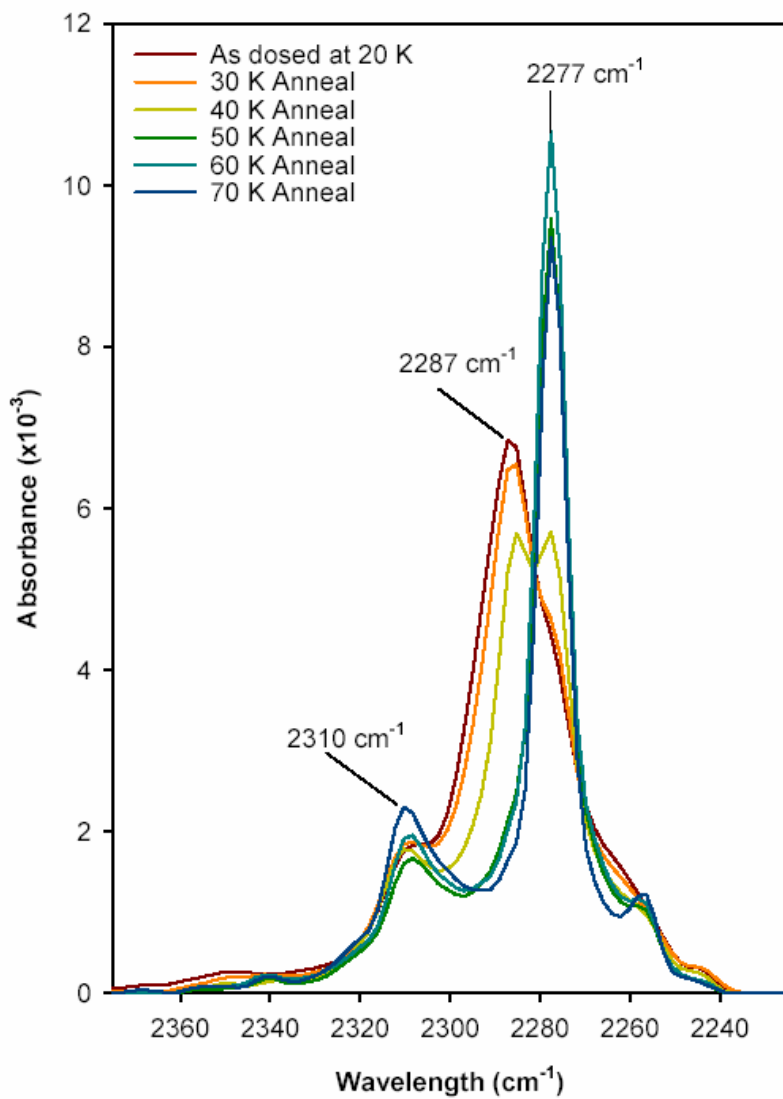


5.3.1 RAIRS:

The RAIRS spectrum shows the presence of three distinct peaks that are attributed to structural arrangements that are described in detail by Zehr et al. (Figure 2).¹¹ Briefly, the peak at 2277 cm⁻¹ closely matches the 2278 cm⁻¹ peak of individual ¹³CO₂ molecules

isolated in an Argon matrix,¹⁴ which is why the 2277 cm⁻¹ peak is attributed to singleton ¹³CO₂ molecules that are oriented, long axis of the molecule parallel to the Pt(111) surface normal. A second peak at 2310 cm⁻¹ has been attributed to a 2-D lattice of molecules that are standing upright, (parallel to the surface normal) with a coverage of 0.30 ML. This peak at 2310 cm⁻¹ seemingly does not have a dependence to the Pt(111) lattice as it has been seen while dosed on top of spacer layers of various molecules, and there seems to be no limit to its size with increasing coverage suggestive of a multilayer peak. The other peak seen in the RAIRS spectrum at 2287 cm⁻¹ occurs when the ¹³CO₂ molecules were dosed at 20 K. The peak at 2287 cm⁻¹ will disappear if the adsorbate covered surface has been annealed to 60 K or higher and was not given a designation by Zehr. The last information derived from the RAIRS spectrum of full coverage ¹³CO₂ shows that the integrated adsorption area of the peaks when compared against a known coverage of molecules, showed a much lower integrated area than expected for a 0.30 ML covered surface. Therefore, with a lower than expected integrated adsorption area most of the ¹³CO₂ molecules adsorbed onto the Pt(111) surface are expected to be oriented with their long axis parallel to the surface and therefore IR inactive.

Figure 2 RAIRS spectra of the $^{13}\text{CO}_2$ molecule as dosed to “full” coverage and annealed to various temperatures.



5.3.2 STM IMAGES:

Various methods of adsorbate preparation were used while generating the STM images to explain some of the features seen in the TPD and RAIRS spectra. The STM images show that there is a definite tendency for the ¹³CO₂ molecules to form islands. Also, there are many stable structures found within those islands, with some that can be

Figure 3 A (500 x 310) Å STM image that shows a large island of organized ¹³CO₂ molecules in the upper right corner. The rest of the surface is bare Pt, but the Pt(111) lattice is unresolved. (Imaging conditions I=100 pA, bias V= -67 mV)



attributed to the peaks found in the RAIRS spectra.

With a properly prepared submonolayer covered surface, various islands of adsorbate coverage are relatively easy to distinguish. The image in Figure 3 shows a large island of molecules that was dosed at high temperatures. The dosing scheme can be seen

in Figure 4 which shows a standard desorption TPD spectrum, with a band in blue that indicates the temperature range of the crystal over which ¹³CO₂ molecules were allowed to flow over the crystal. When the temperature was 94 K the crystal and doser were put in to position and dosing was initiated. The pressure in the chamber from the pinhole effusive doser was raised from 8×10^{-11} Torr to 6×10^{-10} Torr. The crystal temperature was then allowed to continue cooling. After the crystal temperature had cooled to 88 K the dosing valve was closed, where once again the chamber pressure dropped to 8×10^{-11} Torr (a pictorial schematic of dosing is seen in (Figure 5). With the dose as described, most of the surface was bare platinum spotted with islands of ordered ¹³CO₂ molecules.

Figure 4 High temperature dosing scheme, shown is a typical monolayer TPD desorption spectra with the highlighted temperatures in blue, were where the molecule dosing was done by starting at the high temperature and letting the crystal cool while dosing until the lower limit was reached and the gas dosing valve was turned off. (while dosing the pressure in the chamber was raised from 8×10^{-11} to 6×10^{-10} Torr.)

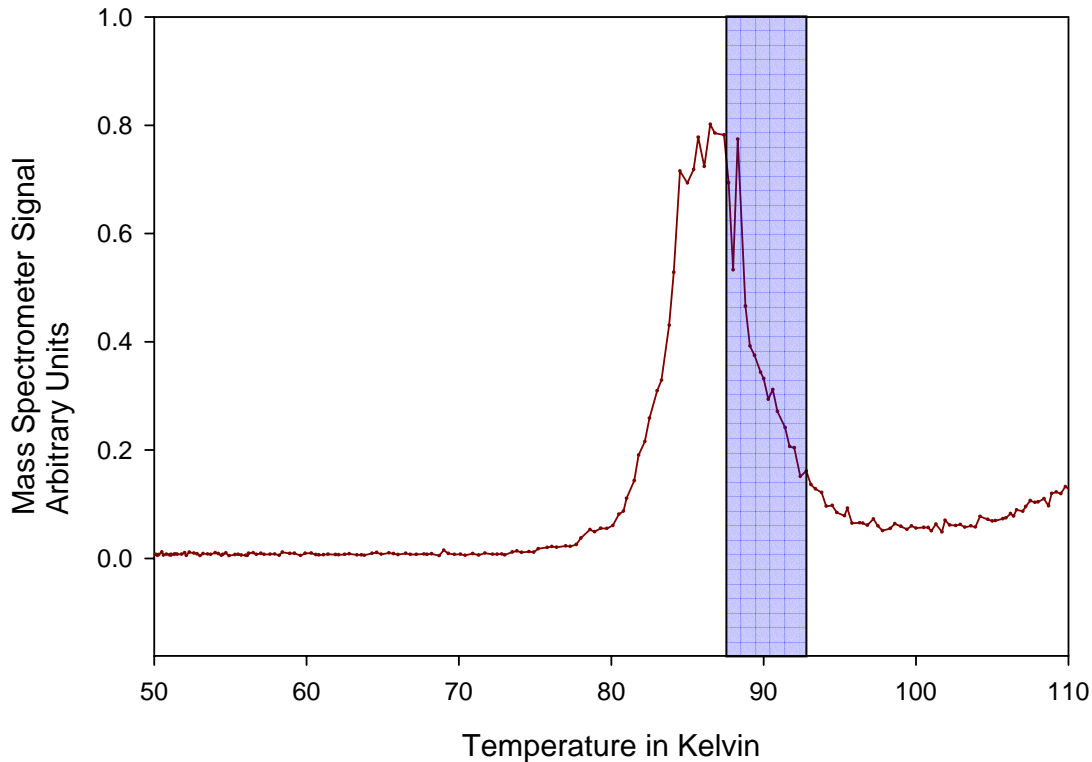
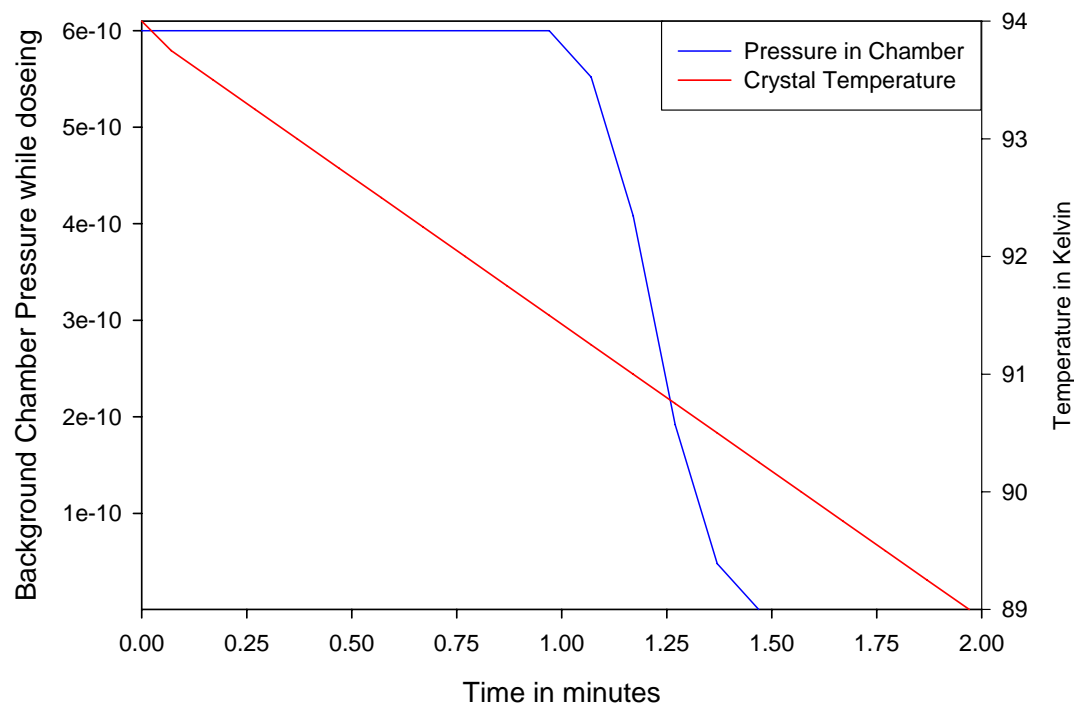


Figure 5 A model schematic diagram of the high temperature dosing of the $^{13}\text{CO}_2$ onto the Pt(111) surface. The line in blue represents the background chamber pressure while dosing, and the red line represents the crystal temperature.



The creation of a thermodynamically stable ¹³CO₂ covered surface by high temperature dosing revealed that the molecules cluster together into islands, and the predominant arrangement of molecules is a (3 x 3) lattice yielding an average local coverage of 0.33 ML. The (3 x 3) lattice can be seen in the Figure 6. This lattice has unit lattice vectors measuring 8.4 Å x 8.4 Å with a angle between them of 60°. A theoretical overlay of the Pt(111) surface can be seen in Figure 7 which fits over the adsorbates very

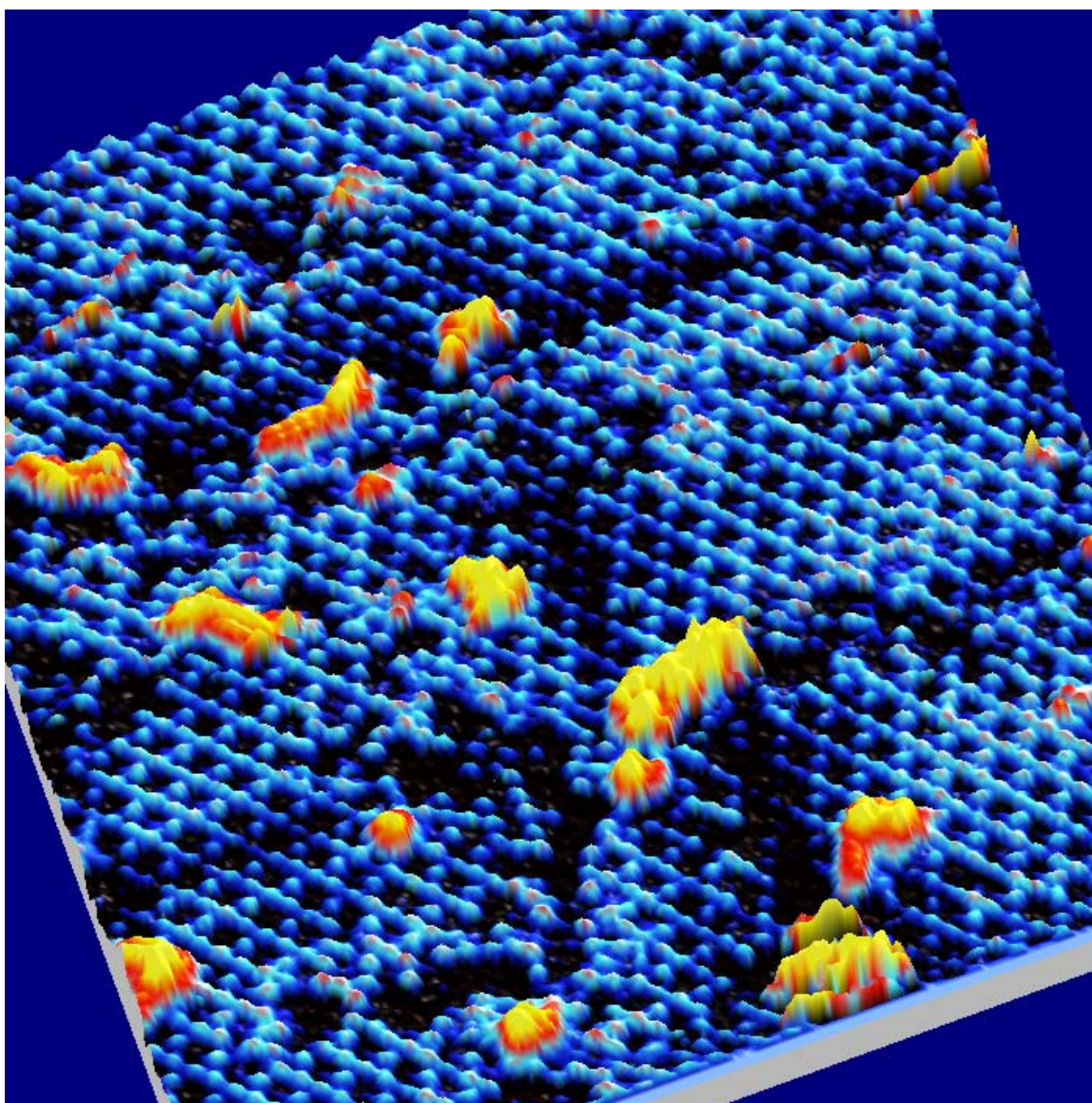


Figure 6 A (200 x 200) Å image of the ¹³CO₂ molecules in a (3 x 3) lattice. Created by the high temperature sub-monolayer coverage dose. (I=100 pA, V_b=-76 mV)

Careful examination of the (3 x 3) lattice reveals that there is a secondary sub-lattice arrangement of vertical molecules within the (3 x 3)_V horizontal unit cell. The assignment of whether the molecules are aligned vertically or horizontally comes from the assumption that a small fraction of the molecules on the surface are IR active, 1.2% estimate by Zehr, meaning that the ¹³CO₂ has its dipole derivative parallel to the surface normal. These RAIRS selection rules were put forth by Parikh and Allara¹⁵ and then summarized by Trenarry.¹⁶ As previously stated the assignment of the 2277 cm⁻¹ peak in RAIRS was attributed to isolated singletons of ¹³CO₂. The isolated singleton molecules can be seen in Figure 8. A line scan across the singletons reveal that they are on average 0.25 Å high off the platinum surface and 5 Å in diameter. A line scan across an island of the horizontal (3 x 3)_H surface Figure 9 show that the average of the adsorbates height is 0.51 Å from the surface with a circular shape of 2.5 Å diameter. Another line scan through the center of a (3 x 3)_H horizontal lattice (Figure 9), indicates that the adsorbates inside the unit cell image as 0.25 Å below the peaks of the horizontal lattice. By subtracting the height of the singletons from the height of the (3 x 3)_H horizontal lattice molecules, a height of 0.26 Å is found. The subtracted height is in agreement with the measured height of the singletons on the surface. Suggesting, the adsorbates within the (3 x 3)_V lattice are vertically oriented ¹³CO₂ molecules imaging the same as the isolated vertical singletons.

Figure 7 A small amount of the 3 x 3 lattice of ¹³CO₂ molecules shown with the Pt(111) overlaid on top of the adsorbates.

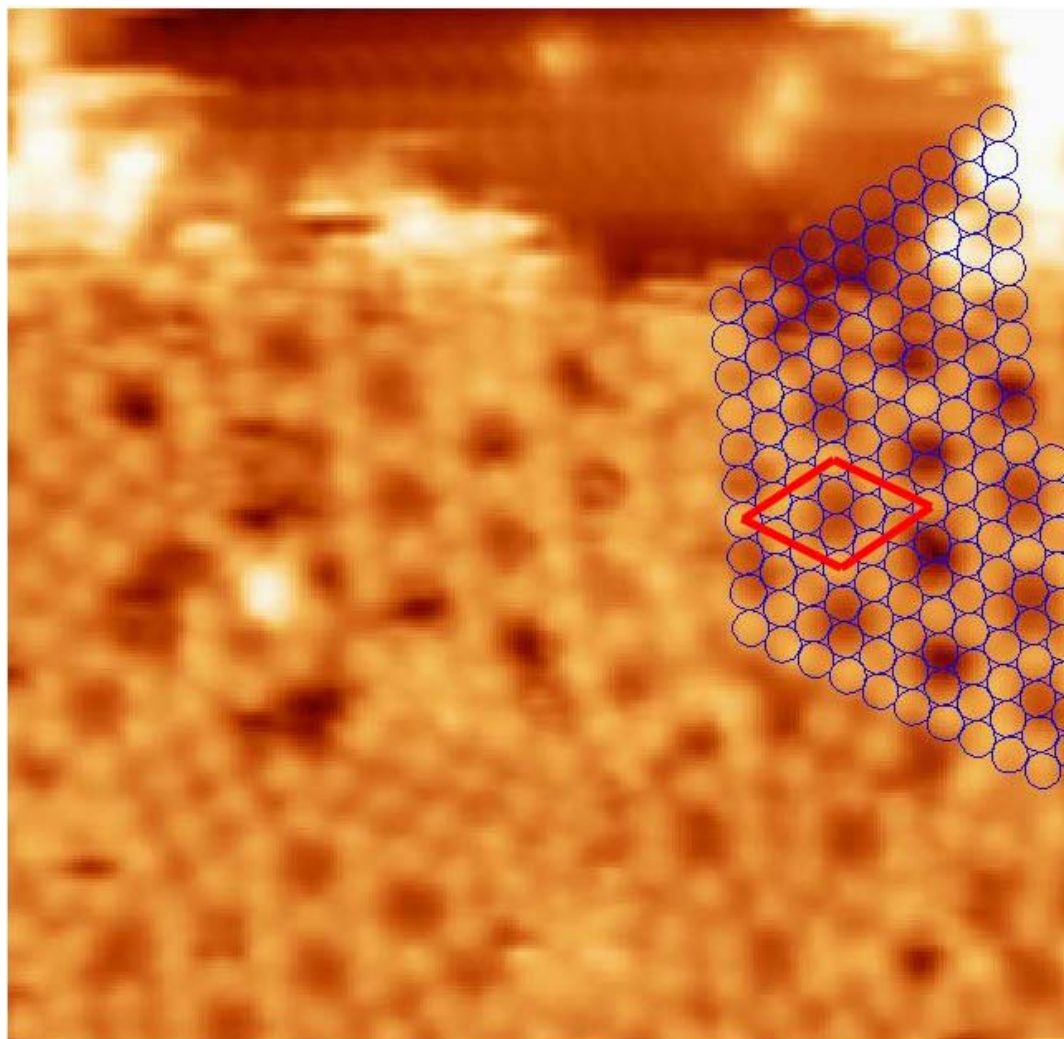


Figure 8 Image of ¹³CO₂ isolated molecules adsorbed onto the Pt(111) surface. The image is 130 x 130 Å taken at 100 pA tunneling current and -56 mV bias

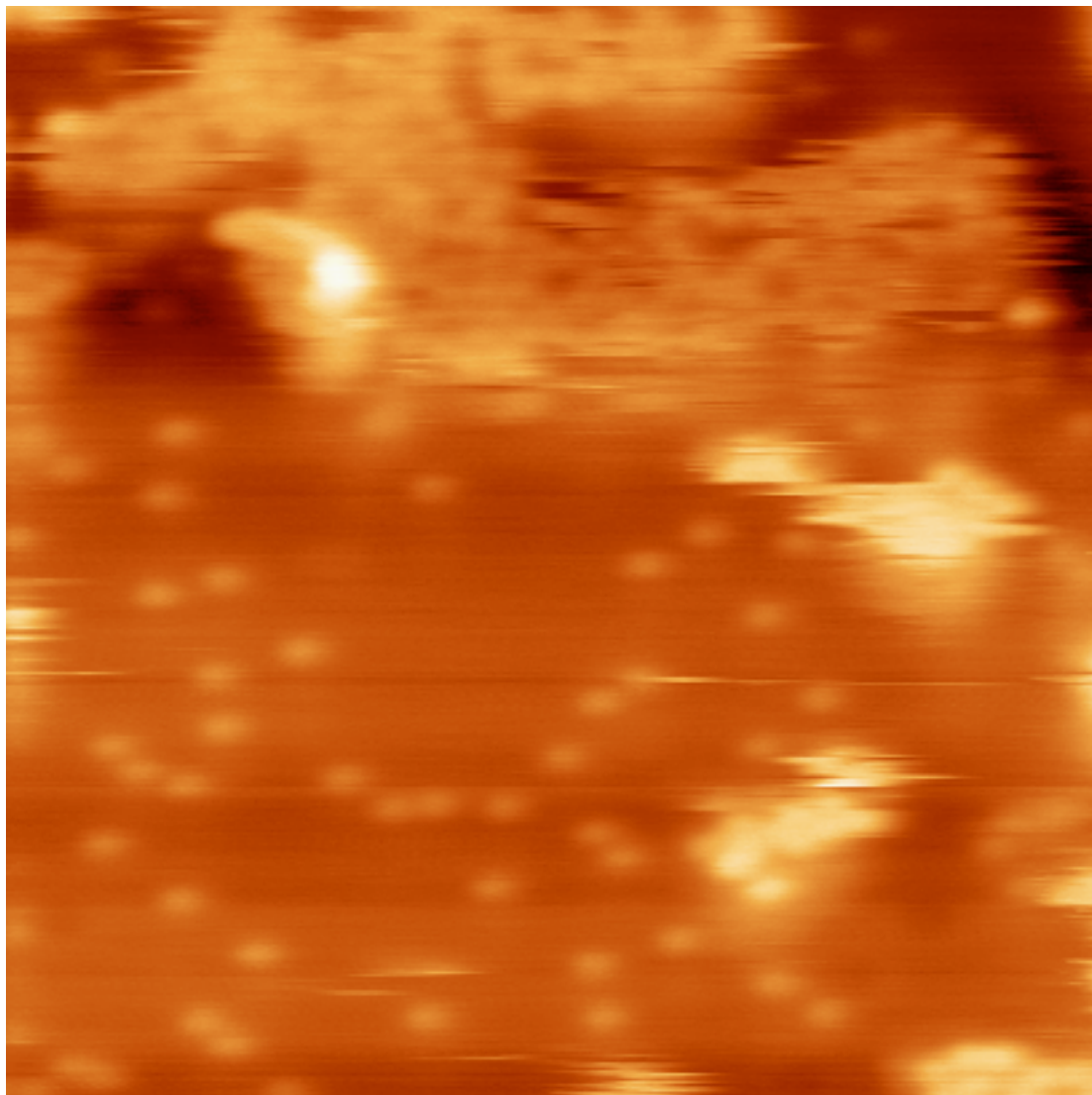
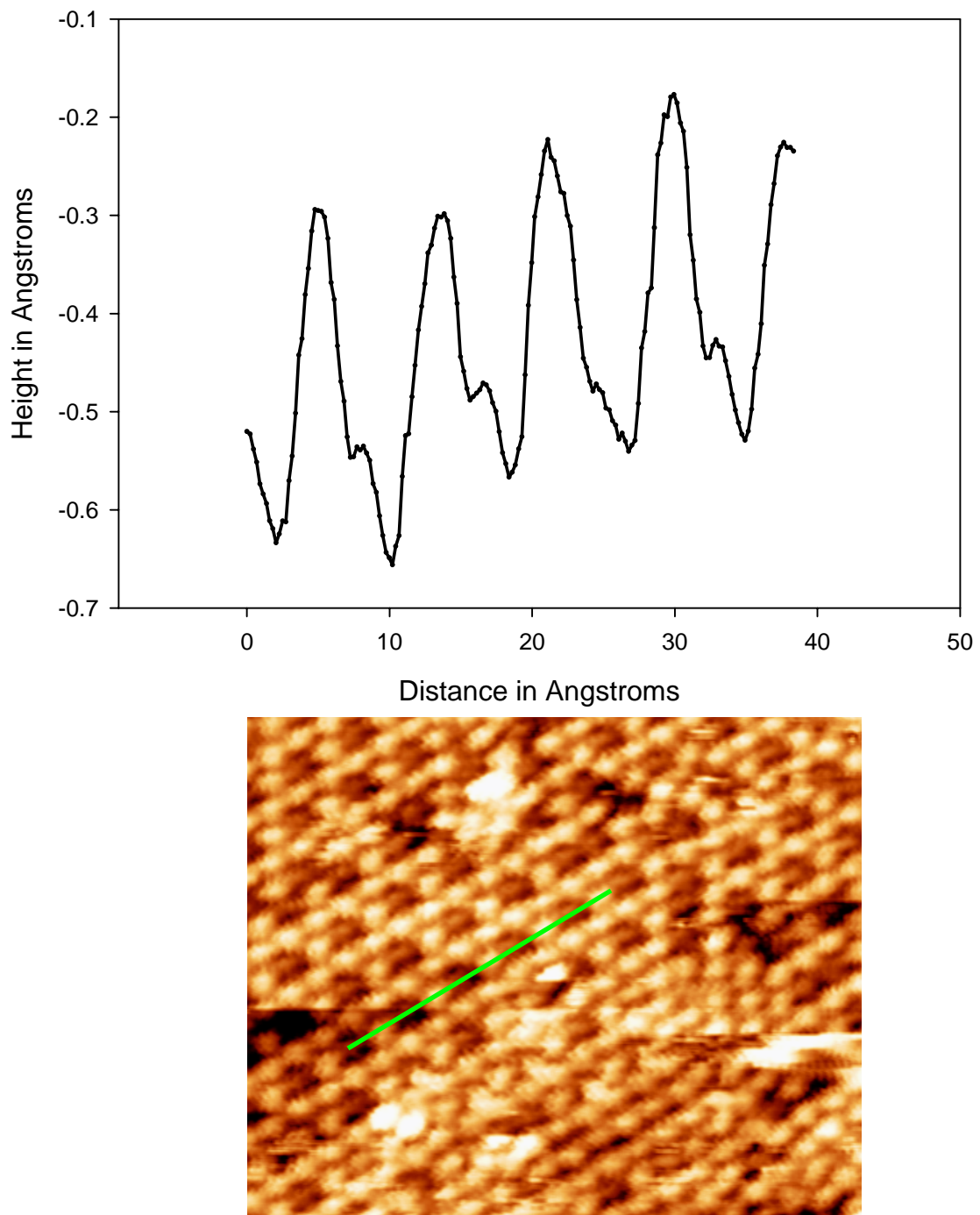
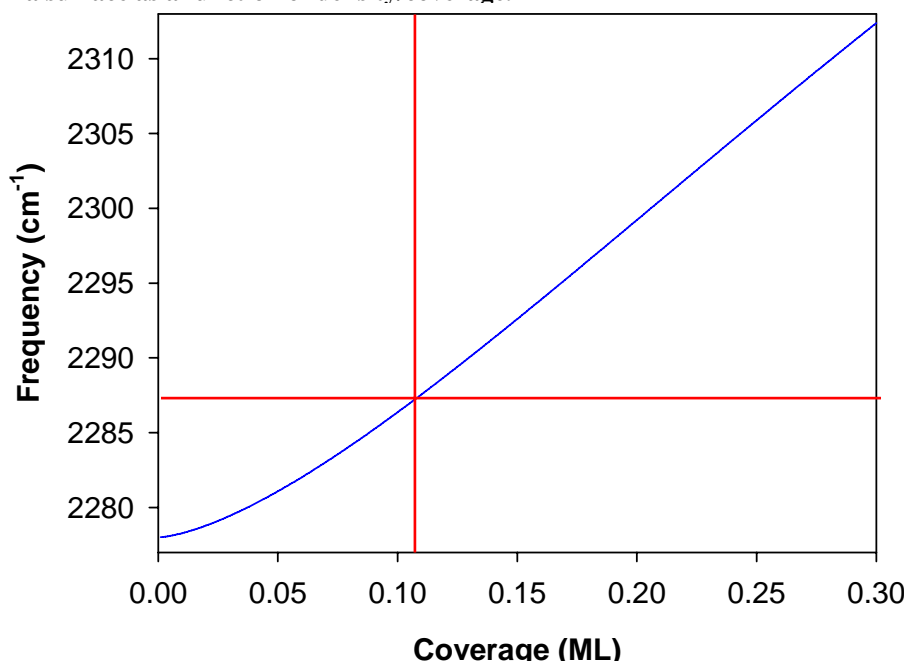


Figure 9 Line scan across the (3 x 3) lattice with an orientation that shows the interior of the large depressions seen in the lattice. (the top peaks are considered to be the horizontally oriented ¹³CO₂ molecules and the small peak in between are thought to be the ¹³CO₂ molecules oriented vertically on the Pt(111) surface.) (top graph shows the line scan, and the image of the (3 x 3) lattice below was use to generate the line scan.)



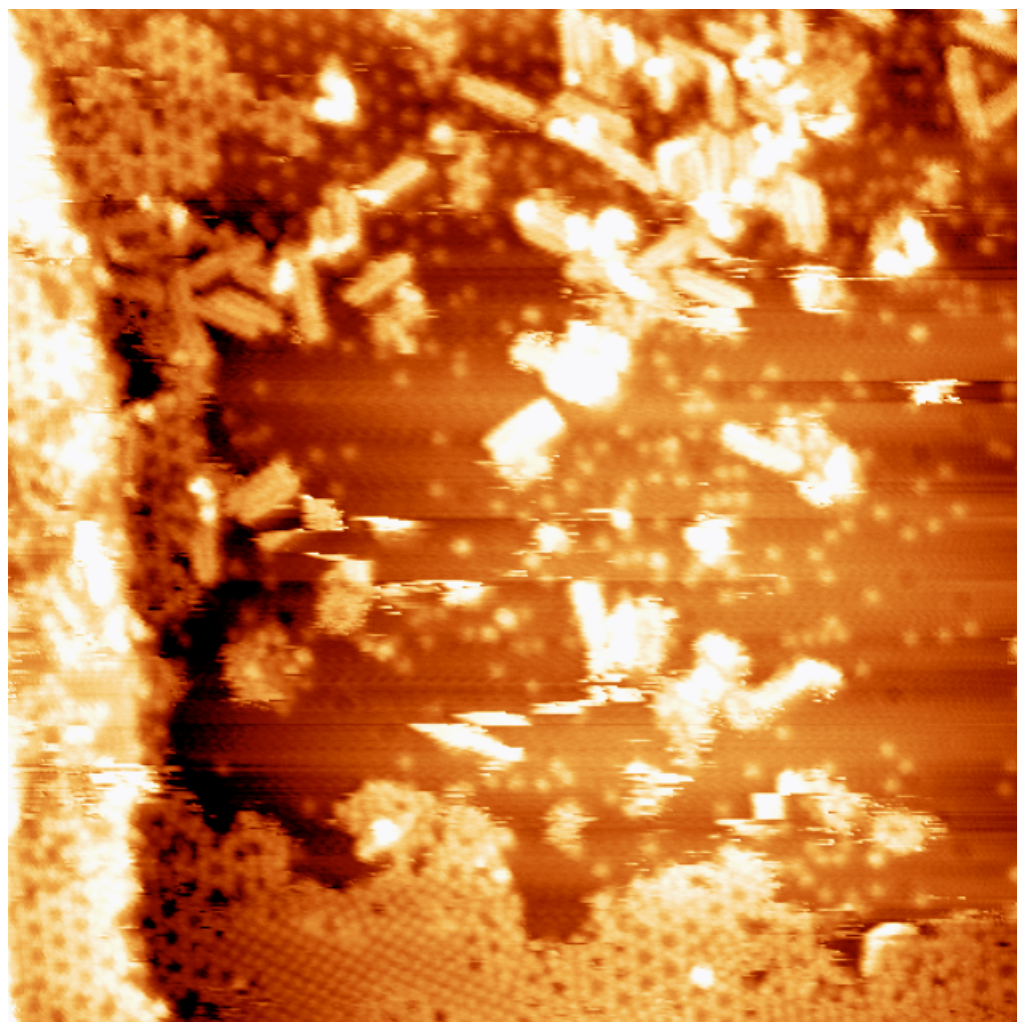
Additionally if one vertical ¹³CO₂ molecule is assumed to occupy a position within each (3 x 3)_{H+V} unit cell of the horizontal lattice, a secondary (3 x 3)_V lattice exists. If the two lattices are considered to be separate, the calculated coverage for the vertical (3 x 3)_V lattice is 0.111 ML. The coverage of vertical islands of ¹³CO₂ molecules is rather unique, because, there was no (3 x 3)_H lattice observed in the low temperature dose and annealed surfaces, only single unit cells of the (3 x 3)_{H+V} lattice that would contain isolated vertical ¹³CO₂ molecules yielding the 2277 cm⁻¹ peak in RAIRS. However if the surface was dosed cold and unannealed there was a peak at 2287 cm⁻¹ that remained unexplained by Zehr.¹¹ The analysis of shift in peak position that he did to explain the presence of the 2310 cm⁻¹ peak is actually more appropriate for explanation of the (3 x 3)_V vertical lattice. The graph in Figure 10 shows how a predicted change in the RAIRS frequency should vary as a function of coverage. The theory by Persson and Ryberg¹⁷ should be used for a 2-D

Figure 10 model of the shift in IR frequencies dependant upon the dynamic dipole coupling of molecules on a surface as a function of density/coverage.



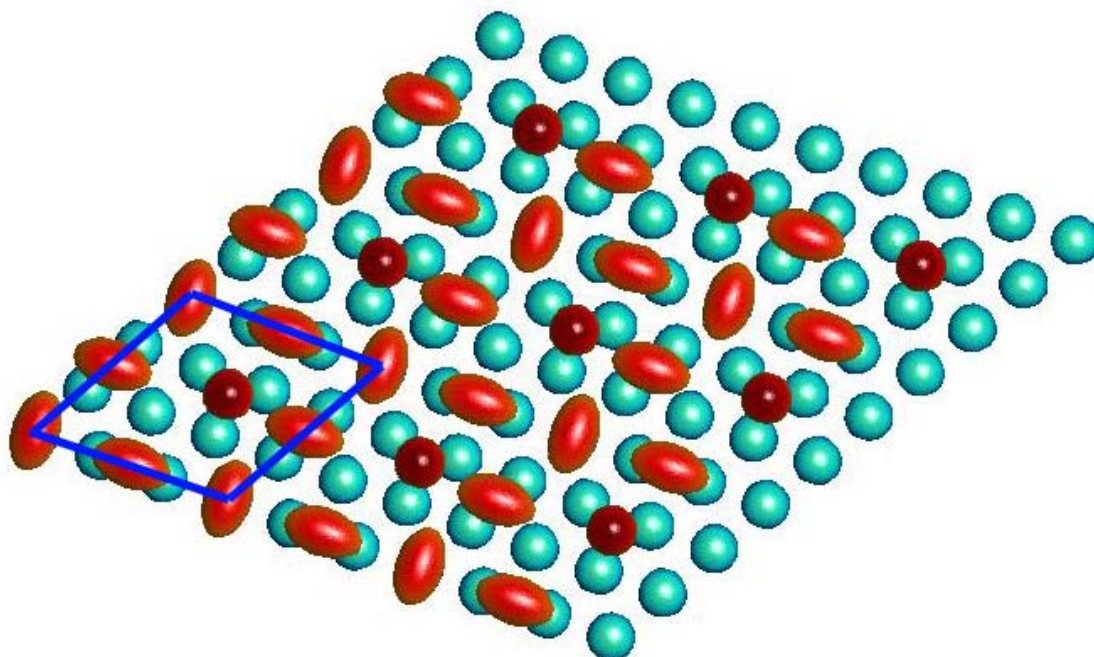
uniform lattice of only dipole coupling interactions between the molecules. The predicted frequency for a coverage of 0.111 ML would be approximately 2287 cm⁻¹ which is exactly what is seen in the low dosed surface that was unannealed. Indicating that the initial dosing of ¹³CO₂ molecules onto the surface may go into its most thermodynamically stable position of the (3 x 3)_{H+V} unit cells which is then disrupted by annealing the surface allowing for more molecules that were previously in the multilayer to slip into space on the platinum surface forcing the disruption of the (3 x 3)_{H+V} islands and elimination of the 2287 cm⁻¹ peak in RAIRS. The (3 x 3)_V lattice of vertical islands

Figure 11 300 x 300 Å image of the ¹³CO₂ covered surface showing multiple lattice arrangements of the ¹³CO₂ covered surface. I=96 pA, and -520 mV bias.



were only seen on the platinum surface by the STM at submonolayer coverages created by the high temperature dose. The vertical island of (3 x 3)_V molecules were seen to be present in the (3 x 3)_H horizontal lattice and arranged without the horizontal lattice as in Figure 11.

Figure 12 A theoretical image of the arrangement of ¹³CO₂ molecules on the Pt(111) surface in a 3 x 3 lattice.



The analysis of the (3 x 3)_{H+V} islands of molecules show that the vertical ¹³CO₂ occupies a position not exactly in the center of the (3 x 3)_H horizontal lattice. If the horizontally arranged molecules prefer to occupy top sites and bridge sites a construction can be made that would allow the adsorption of a vertical molecule into a three fold hollow site as seen in the theoretically created surface of the (3 x 3)_{H+V} ¹³CO₂ lattice (Figure 12). Analyses of the line scans across the horizontal unit cell confirm that the

molecule is shifted to one side. The scan in Figure 13 show that the small peak in between the tall peaks on one side of the scan are almost none existent and continue to get larger as the scan segments move along the unit cell. Also, this proposed configuration can account for the vertical ¹³CO₂ molecule being shifted to one side of the unit cell and still be close to the middle of the cell in one axis.

The (3 x 3)_V vertical lattice does not have to occupy every interstitial space within the horizontal lattice as seen in the line scan and image in Figure 14. The line scan suggests that there are a couple of vertical molecules missing, which leads to the assumption that the (3 x 3)_H lattice of horizontal molecules are not dependent on the presence of vertical molecules. If the (3 x 3)_{H+V} lattice of horizontal and vertical molecules are taken together it yields a relatively high coverage of molecules on the surface of 0.44 ML. With the removal of some of the vertically arranged molecules this will drop closer to the coverage of the horizontal lattice alone of 0.33 ML.

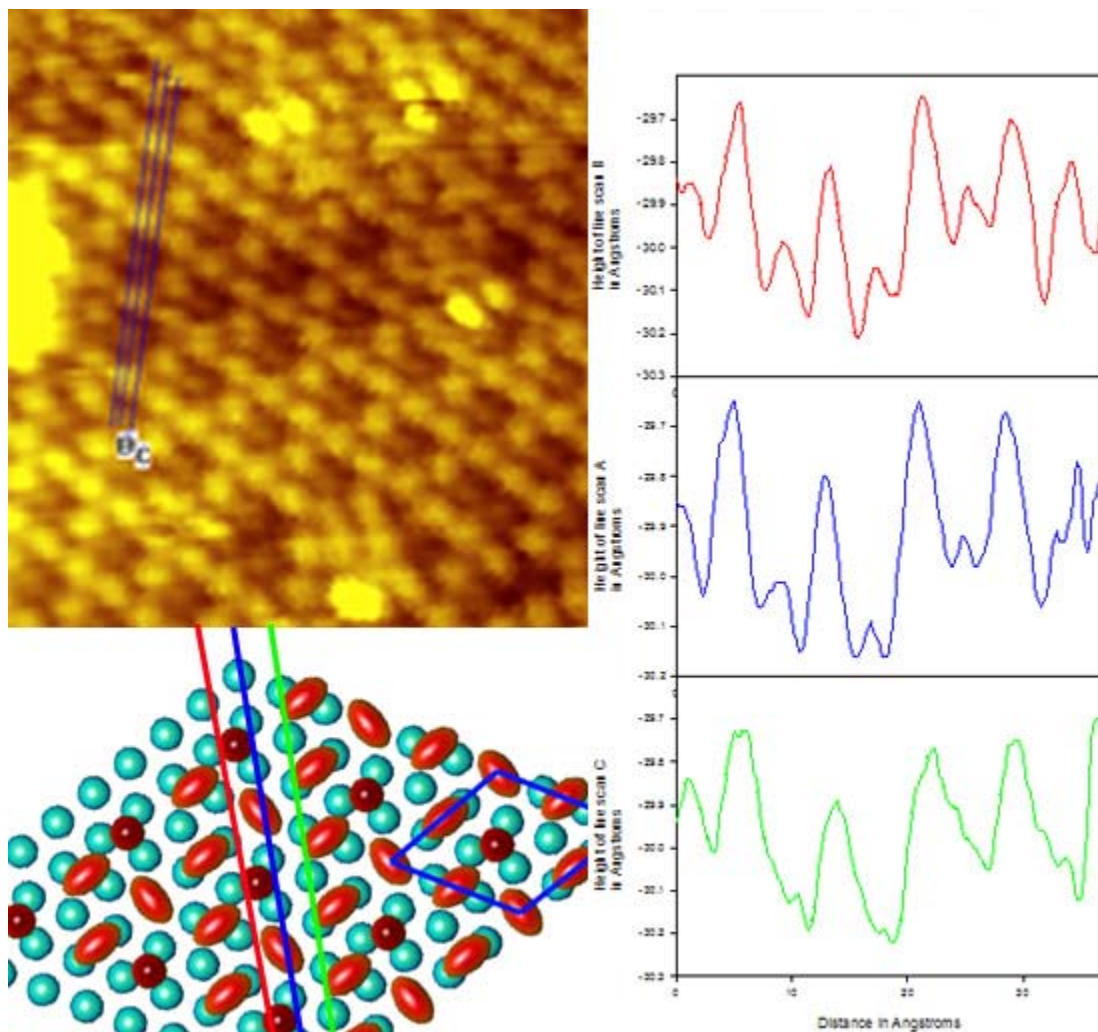
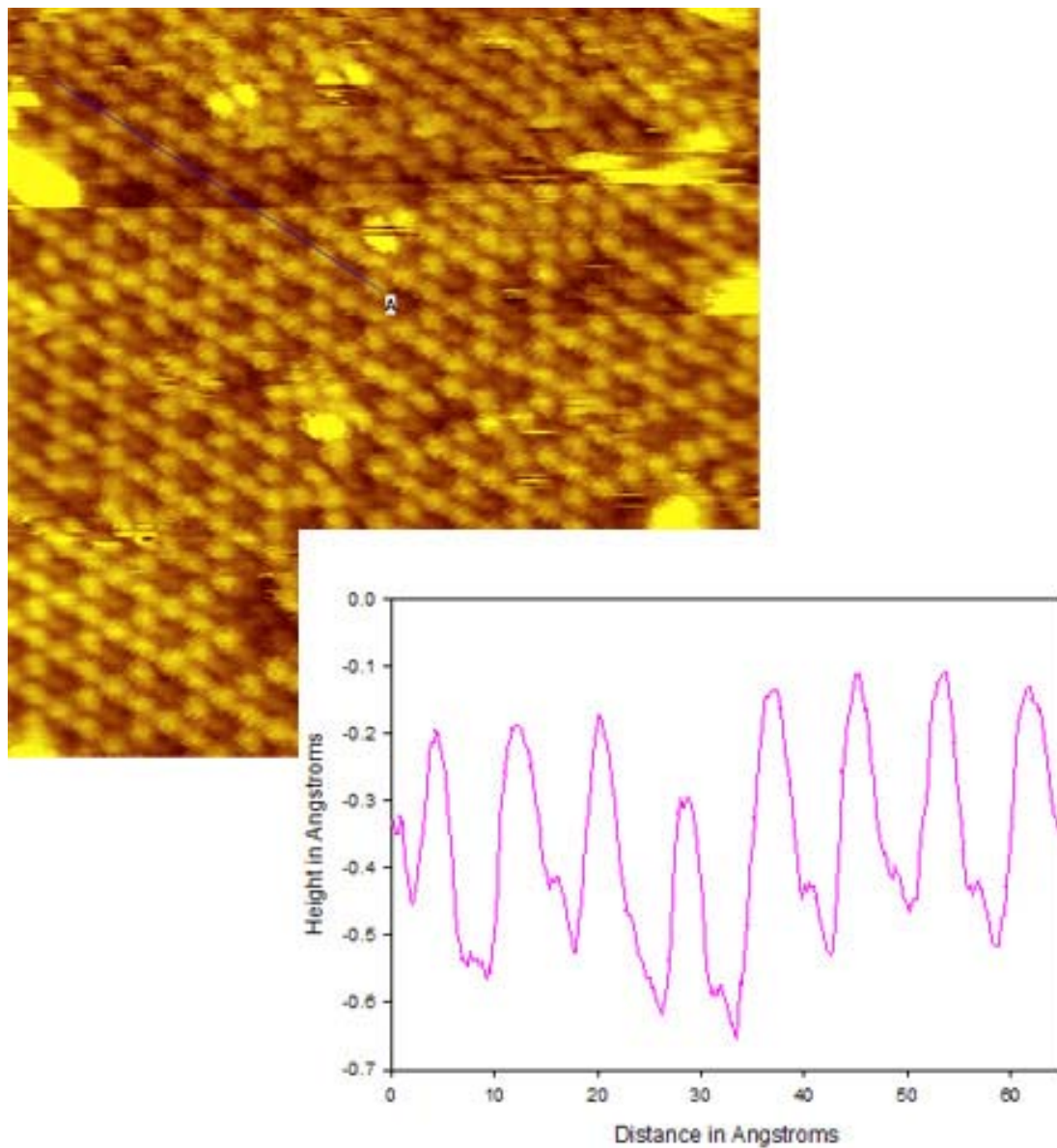


Figure 13 Representation of the offset of the vertical molecule from the center of the (3 x 3) hollow, where three line scans on the right were done at various distances into the hollow. The line scans were done on the image in the upper left corner, and the theoretical image of the (3 x 3) lattice can be seen in the lower left with lines drawn corresponding to the line scans in the STM image.

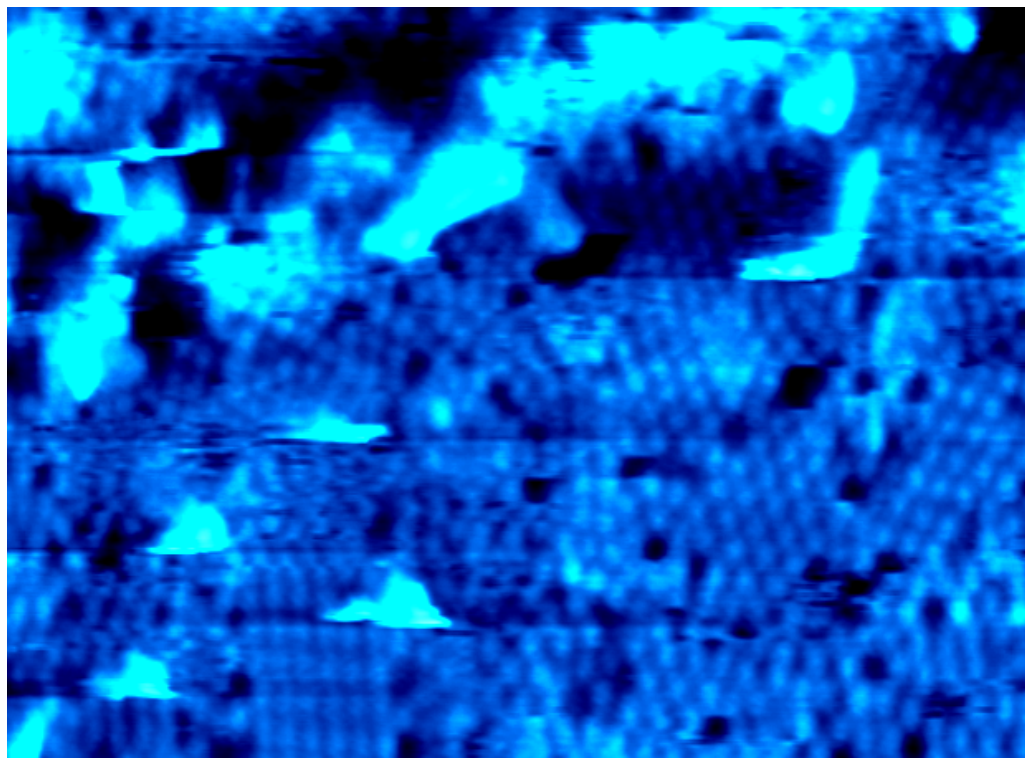
Figure 14 the Image in the upper left has a line scan across the hollows of the (3 x 3) ¹³CO₂ lattice that shows vertical molecules missing which is pointed out in the line scan in the lower right.



5.3.3 LOW TEMPERATURE DOSE:

When dosing at low temperatures and annealing the surface there are only two types of molecules that are observed on the platinum lattice, they are, the singletons and a densely packed layer of molecules that image almost identical in size to the horizontally oriented molecules after the high temperature dose. This is consistent with the RAIRS study of a dosed and annealed surface; there are singletons and a large number of

Figure 15 A (175 x 150) Å image of a “full monolayer” of ¹³CO₂ molecules created by dosing multilayers and annealing. The image shows domains of the (5 x 3) lattice with isolated depressions that are presumed to be the isolated singletons seen in the RAIRS spectrum.



molecules that are IR inactive. However, imaging of the low temperature dose and annealed surface was difficult and seldom yielded good STM images (Figure 15). The

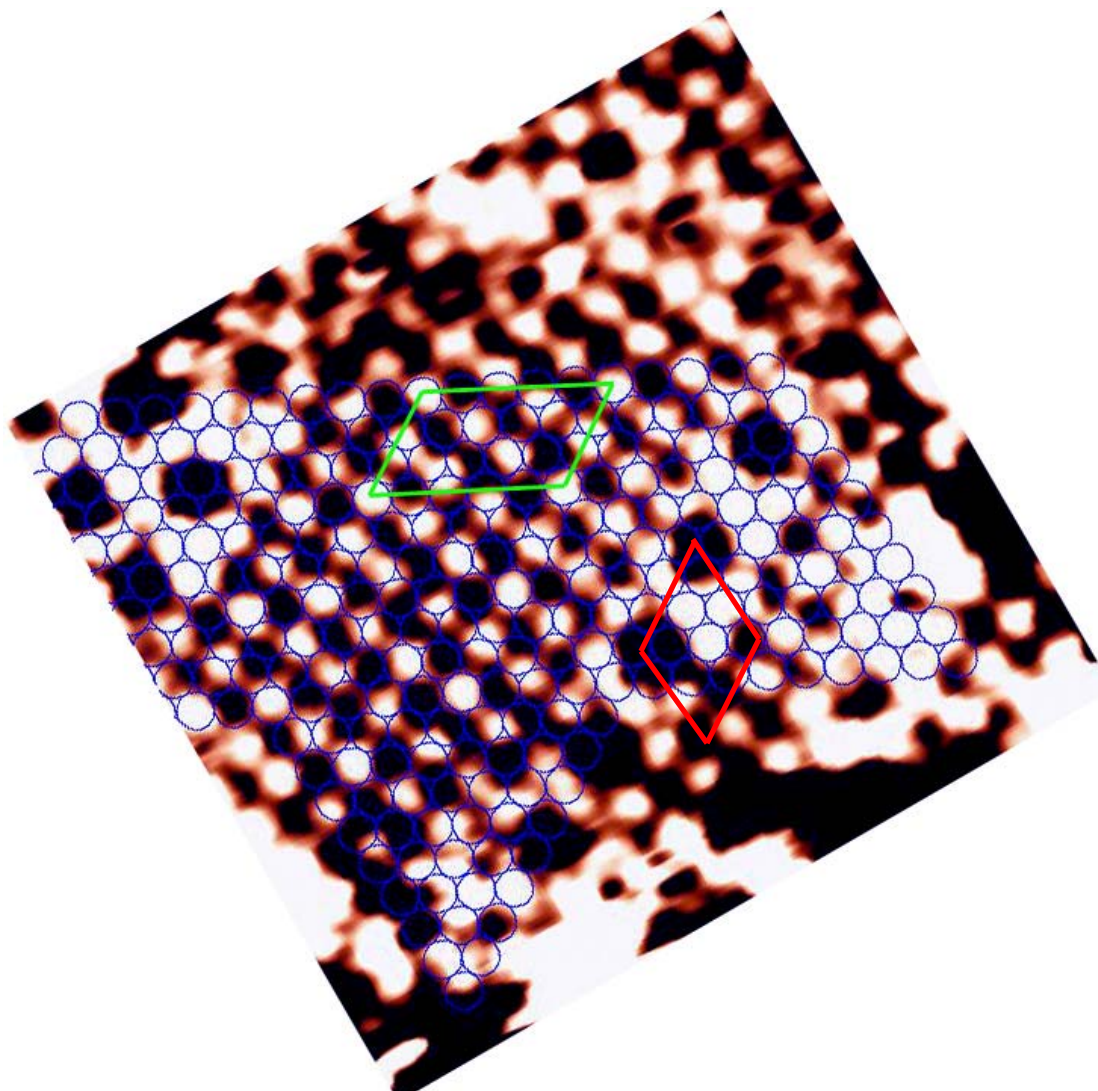


Figure 16 The image is a 65 x 65 Å surface with a theoretical Pt(111) lattice overlaid on top to determine the arrangement of ¹³CO₂ molecules on the surface. The (5 x 3) unit cell is outlined in green and the (3 x 3) unit cell is outlined in red.

surface showed numerous domains of closely packed molecules separated by the occasional ring structure that resembles the (3 x 3)_{H+V} unit cell of the high temperature dose.

By examining the same closely packed arrangement of molecules seen in the high temperature dose (lower left side of image in Figure 11), a lattice ordering assignment

was able to be made of (5 x 3). A zoomed in view of a section of the (5 x 3) lattice is shown with the Pt(111) lattice overlaid on the image (Figure 16). There are some very interesting implications of assigning the close packed surface to a (5 x 3) lattice. The first being that the local coverage is very high, yielding an amount of 0.40 MLs. Also of the 6 molecules associated with the unit cell, 4 of them are incommensurate with the underlying platinum surface. These conclusions are in partial contrast to the previous data collected by Zehr¹¹ and Madix.¹⁰ However the coverage conclusions of Zehr were based on integrated averages of TPD measurements (adjusting for mass spectrometer issues of cracking, and detectivity, etc.). The estimated coverage from Madix was done at high temperature where it was shown that the molecules will adsorb in islands of (3 x 3)_{H+V} yielding a local coverage close to what Madix suggested of anywhere from 0.33 to .275 ML. The LEED images of the ¹³CO₂ covered surface by Madix also may be suspect, because of Zehr reporting that the ¹³CO₂ molecule was able to be dissociated to leave oxygen and carbon monoxide on the surface using 194 nm photons. If the dissociation process of ¹³CO₂ is a substrate electron mediated process that can take place using 6.4 eV electrons from the surface, a 60 eV electron beam from the LEED is most certainly going to dissociate molecules as well. Additionally, Zehr reported not being able to distinguish a LEED lattice arrangement of the ¹³CO₂ covered surface, when the crystal was dosed at low temperature then annealed. Two possible explanations why there is no LEED pattern: 1)The LEED electron beam is dissociating the ¹³CO₂ molecules, or 2) a diffuse LEED pattern that is undetectable due to the multiple domain boundaries and an incommensurate number of molecules on the Pt(111).

There is the possibility that the calculated coverage of the close pack ¹³CO₂ molecules is flawed, however, prior to imaging the ¹³CO₂ lattice the STM was calibrated off of the (2 x 2) oxygen covered surface at 30 K. Therefore the dimensional measurements should be accurate to better than an angstrom. The measurements of the (5 x 3) lattice starting at one bright projection to the next nearest neighbor on two sides shows that the nearest neighbors are 4.1 Å and 4.0 Å away on average with a angle between the two of 98°. Using these measurements to formulate a coverage based on the size of the nearest neighbors and not the defined unit cell, yields a local coverage of 0.412 which is very close to the coverage of 0.40 for a (5 x 3) lattice. The calculation is done by determining a size of the nearest neighbor molecules vs. the Pt(111) as seen in Equation (5.1)

$$\theta = \frac{Pt_{Lattice_Size}}{Adsorbate_{Lattice_Size}} = \frac{2.78 \times 2.78 \times \sin(60)}{4.1 \times 4.0 \times \sin(98)} \quad (5.1)$$

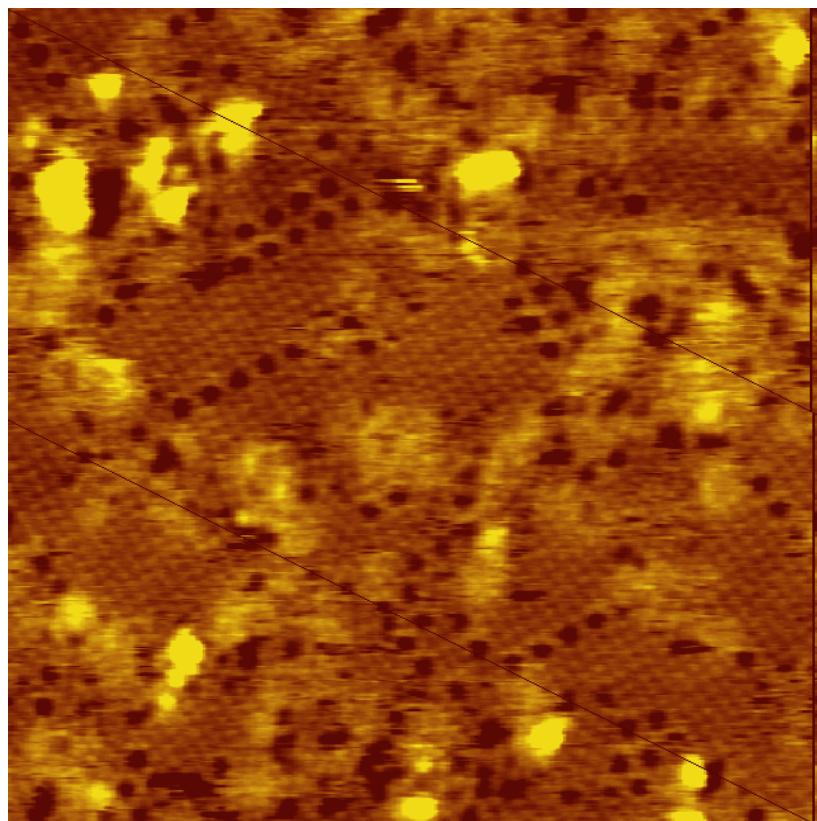
If the lengths of the nearest neighbors were to become 4.1 and 4.1 Å with a 98° angle between them then the calculated coverage would be 0.40 ML identical to the (5 x 3) unit cell.

Additional evidence that the lattice arrangement of (5 x 3) is correct, comes from the theoretical Pt(111) overlay on the ¹³CO₂ image. While trying to fit the ¹³CO₂ to the Pt(111) lattice, the overlaid lattice was extended across the image surface, and it was found that the orientation of the Pt(111) lattice that is used to align with the (5 x 3) ¹³CO₂ lattice, also aligns with the (3 x 3)_H lattice on the side of the image.

5.3.4 HIGH TEMPERATURE DOSE FULL COVERAGE:

When the ¹³CO₂ covered surface is prepared in a manner similar to the high temperature dose described earlier, but is allowed to adsorb multilayers while cooling, a well ordered surface is seen after annealing away the multilayer. The lattice that is revealed after this preparation method is mostly the (5 x 3) unit cell structure with rows of the (3 x 3)_{H+V} unit cell running throughout as seen in Figure 17 andFigure 18. This would indicate that the observed (3 x 3)_{H+V} lattice is the more stable system at sub-monolayer coverages, but when the 3-D pressure from multilayers are included in the equation, a shift in the (3 x 3)_{H+V} lattice occurs pushing the molecules closer together into

Figure 17 Full coverage dose of ¹³CO₂ by the high temperature dose method, showing large domains of the (5 x 3) lattice with single rows of the (3 x 3) lattice. The image is 250 x 250 Å taken with a 108 pA tunneling current and -78 mV bias.



the (5 x 3) lattice. This would mean that the initial dosing of molecules on the surface

might begin to form the (3 x 3)_{H+V} lattice which is the basis for the singletons observed in

the low temperature dose and anneal.

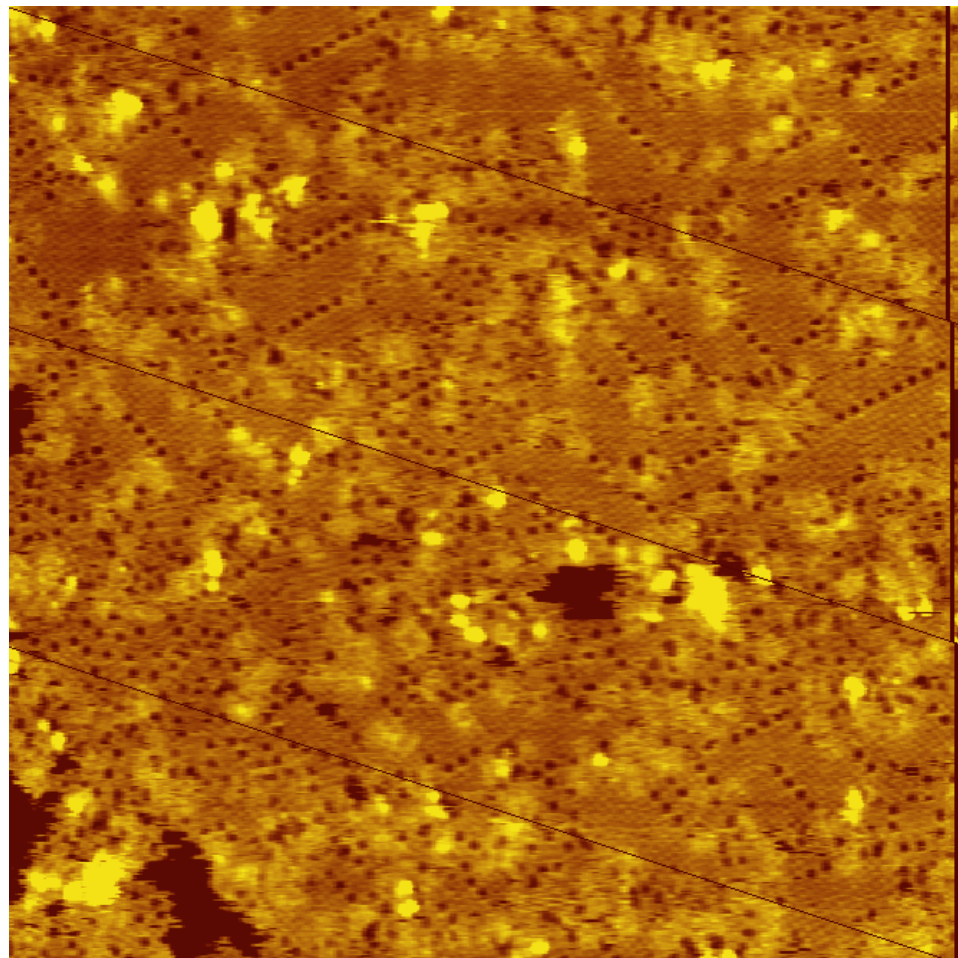


Figure 18 A larger view of the full $^{13}\text{CO}_2$ monolayer when prepared by the high temperature dose method where multilayers were allowed to adsorb. Image is 500 x 500 Å, taken with $I = 97 \text{ pA}$ and -124 mV

Summary

From the STM images there are a few conclusions that can be made. First, we can say that the ¹³CO₂ molecules form islands at sub-monolayer coverages. The tendency for these molecules to form islands is consistent with the notion that the change from zeroth order to first order desorption kinetics found in TPD is caused by the interaction of groups of molecules while in an island. Secondly, the interaction of the ¹³CO₂ molecules will form various structures that can have an effect on the observed RAIRS spectrum. There are four general lattice structures that are observed on Pt(111) surface. The highest local coverage lattice structure seen in the STM images was observed in the sub-monolayer high temperature dose which formed a (3 x 3)_{H+V} lattice with a calculated coverage of 0.44 ML, the lattice was shown to have 3 equivalent horizontal molecules in its unit cell plus 1 that images as half the height of the other molecules in the unit cell (the vertical orientation molecule), resulting in a total of 4 ¹³CO₂ molecules per unit cell. The 4th ¹³CO₂ molecule in the (3 x 3)_{H+V} lattice images differently, presumably due to its long axis parallel to the surface normal. These vertical molecules in the (3 x 3)_V lattice are seen to exist on their own without the horizontal ¹³CO₂ molecules around it, giving a local coverage of 0.111 ML. This low coverage 2-D lattice of molecules that orient vertically on the Pt(111) surface can be assigned to the RAIRS peak at 2287 cm⁻¹ which would presumably disappear with temperature and the added 3-D pressure of molecules numbering greater than full coverage, which effectively removes the (3 x 3)_{H+V} lattice of vertical molecules leaving only a few molecules still disrupting a newly created lattice to form singletons that then have a RAIRS peak of 2277 cm⁻¹. The predominant lattice

structure seen in the STM images is the (5 x 3) lattice that has a 0.40 ML local coverage formed from ¹³CO₂ molecules that orient parallel to the Pt surface. The (5 x 3) lattice is seen to be the dominate lattice formed at high coverage, with domains occasionally imaged in the high temperature sub-monolayer prepared surface. However, when the surface was dosed to a full coverage of ¹³CO₂ by the high temperature dosing method, the (5 x 3) lattice is predominate once again. This implies that the thermodynamically more favorable ¹³CO₂ molecule arrangement on the Pt(111) surface is the (3 x 3)_H horizontal lattice that allows for a molecule to be oriented parallel to the surface normal, and the more kinetically controlled arrangement is the (5 x 3) lattice.

The structural information gleamed from the STM images, combined with the data collected from the TPD and RAIRS studies suggest a very interesting and rich system of study that will hopefully aid in the understanding of the photochemistry and reactions of ¹³CO₂ molecules on the Pt(111) surface.

- ¹ P.B. Rasmussen, M. Kazuta, I. Chorkendorff, Surf. Sci. 318 (1994) 267
- ² Y. Wang, A Lafosse, K. Jacobi, J. Phys. Chem. B. 106 (2002) 5476
- ³ M. Pohl, A. Otto, Surf Sci. 406(1-3) (1998) 125
- ⁴ J.P. Camplin, S.K. Clowes, J.C. Cook, E.M. McCash, Surf. Rev. and Lett. 4(6) (1997) 1365
- ⁵ M.A. Huels, L. Parenteau, P. Cloutier, L. Sanche, J. Chem. Phys. 103(15) (1995), 6775
- ⁶ M. Sakurai, T. Okano, Y. Tuzi, J. Vac. Sci. Technol. A 5(4) (1987) 431
- ⁷ D. I. Hagen, B.E. Nieuwendaufs, G. Rovida, G.A. Somorjai, Solid-State Phys. 1976
- ⁸ A. Cupolillo, G. Chiarello, V. Formoso, D. Pacile, M. Papagno, F. Veltri, E. Colavita, L. Papagno, Phys. Rev. B 66 (2002) 233407
- ⁹ M. E. Jorgensen, P.J. Godoski, J. Onsgaard, Vacuum, 48(3-4) (1997) 299
- ¹⁰ C. L. Kao, A. Carlsson, R. J. Madix, Surf.Sci. 497 (2002) 356
- ¹¹ "Photoinduced Electron Transfer Chemistry at Surfaces: Photochemical Activation of N₂, CO₂ and CH₄ on Pt(111)" Robert Zehr Dissertation, University of Virginia, 2005
- ¹² P.R. Antoniewicz, Phys. Rev. B., 21 (1980) 3811
- ¹³ D. Menzel, R. Gomer, J. Chem. Phys., 41 (1964) 3311
- ¹⁴ M. Zhou, L. Andrews, J. Chem. Phys., 110, (1999) 2414
- ¹⁵ A.N. Parikh, D. L. Allara, J. Chem. Phys. 96, (1992) 927
- ¹⁶ M. Trenary, Ann. Rev. Phys. Chem. 51, (2000) 381-403
- ¹⁷ B.N.J. Persson, R. Ryberg, Phys. Rev.B. 24, (1981) 6954

CHAPTER 6

ATOMIC RESOLUTION IMAGING OF METHANE AND METHYL RADICAL

6.1 INTRODUCTION:

With the current rise in oil prices, many politicians and scientists are clamoring for a switch from an oil economy to a hydrogen economy. In an ideal world switching to a hydrogen economy would be good thing to do, however, just saying we should switch does not mean that it's going to happen any time soon. There are many technical hurdles that need to be overcome to allow a hydrogen economy to be brought into existence. Perhaps the first and foremost on American's minds would be how to use hydrogen to run their cars. Using a hydrogen gas cylinder is not a likely source due to the limited amount of gas held at reasonable pressures, and a tendency for hydrogen to react violently with oxygen in the atmosphere in the event of an accident. An alternative to using hydrogen gas, is to use the liquid form of hydrogen. In the liquid form, enough hydrogen could be carried in the car to make it feasible. However, liquid hydrogen has to be kept in cryogenic dewars at a temperature of 20 K, which would require a lot of added components to the car, and is now a health threat from pressure explosions, gas

explosions, and severe cold. All of these complications suggest that a hydrogen economy is not likely in the near future.

Alternatively, as Nobel prize winner George Olah suggests,¹ methane offers a multitude of unique options, through the production of methanol. The production of methanol can be done by either a recycling process with CO₂ and H₂ (shown to work), or theoretically by an oxidation of methane. Methanol has advantages of an efficient energy storage system with 3 hydrogens for 1 carbon atom and 1 oxygen atom yielding a power density twice that of gasoline, it can be blended with gasoline, and is user friendly and safe. This makes the adaptation of a methanol economy much more likely before the existence of a hydrogen economy. Once the methanol is formed it is also possible to be used for operation of automobiles by a direct-methanol fuel cell. The appeal of using methane as a feed stock for methanol synthesis is the vast abundance of methane around the earth in the form of methyl clathrates.

Because methane is abundant and most likely the next driving force in the US and world economies, it is vital for research to be done on this simplest of hydrocarbons. Potential uses of methane come from direct stripping of the hydrogen from the C atom in fuel cells, or alternatively conversion of methane into methanol for a safe and easy to transport source of energy, and uses as a chemical feed stock for reactions forming higher hydrocarbons. The problems associated with using methane to form methanol or higher chain hydrocarbons is the strength of the covalent C-H bond, which is a very strong covalent bond with an energy of dissociation of 4.48 eV. Because of the high dissociation energy, it is a very difficult molecule to activate which has been shown to require 8.3 eV energy photons and higher to photochemically dissociate the molecule in the gas phase²,

and greater than 8 eV electrons to cause dissociation of the gas phase molecules.³ By

adsorption of the methane onto a catalytic transition metal surface the energy for dissociation is reduced such that 193 nm photons can be used to dissociate the molecule on the Pt(111) surface^{4,5} as well as other transition metal surfaces. The proposed explanation for the reduced dissociation energy is that the adsorbed molecule changes from its normal T_d symmetry to a C_{3v} symmetry.⁶

The adsorption and dissociation of the methane molecules have been studied extensively by the Masumoto^{4,5,9} and Harrison^{7,8} groups. Recent research suggests that direct photodissociation of condensed phase CH₄ may be responsible. However, for the studies here we accept that the molecule can be dissociated with light, which leaves a methyl radical on the Pt(111) surface, and we look at the initial and final states of the methane / methyl radical system.

6.2 EXPERIMENTAL:

The methane and methyl radial experiments were conducted in the STM UHV chamber on a 5 mm dia. Pt(111) crystal, under pressures of 8 x 10⁻¹¹ Torr or lower, except during laser irradiation. The standard techniques of AES and TPD were used to determine the cleanliness of the crystal before experiments, and TPD used to examine the surface constituents after laser irradiation and STM imaging.

The preparation of the methane covered surface that was imaged, was done by dosing the surface with methane multilayers at a surface temperature of 28 K. Then the surface was annealed to a temperature of 58 K to remove the multilayer, leaving only the methane monolayer to be imaged. In creation of the methyl radical covered surface, the

initial surface coverage was performed the same as for imaging the methane covered surface, the crystal was overdosed with methane and annealed to 60 K, followed by irradiation of the crystal with 40,000 pulses of 5 mJ/pulse/cm², and annealing the crystal to 175 K to remove all the undissociated methane from the surface.

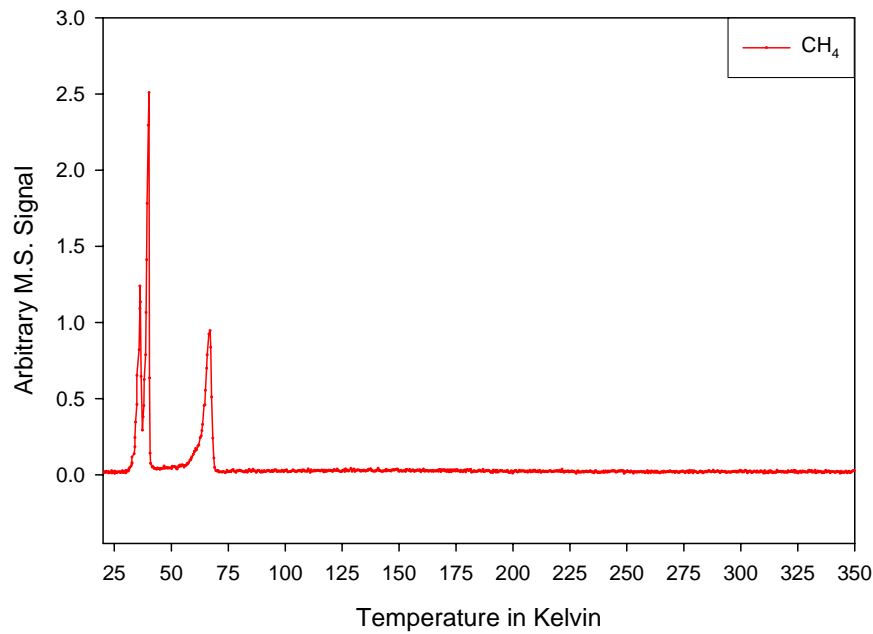
The laser used to generate the methyl radicals in these experiments is a GAM laser EX100F/125. It uses an ArF mix as the excimer gas, and has a maximum repetition rate of 125 Hz. The laser reflects off of two dielectric mirrors and passes through two apertures before entering the chamber. The laser intersects with the face of the platinum crystal at an angle of 45 degrees. The time it takes for laser irradiation of the crystal is under 5 ½ minutes with the repetition rate set to 125 Hz, however during the five minutes of irradiation the pressure in the chamber increased from 5×10^{-11} to 5×10^{-9} torr. After many irradiation experiments the increase in pressure of the chamber was reduced but still noticeable (i.e. $\Delta P = 5 \times 10^{-10}$ Torr), this was probably due to photon and electron stimulated desorption of molecules off the walls of the UHV chamber, because there is not a path for the laser to exit the chamber.

6.3 RESULTS / DISCUSSION:

6.3.1 METHANE ADSORPTION:

The adsorption of the methane molecule to the Pt(111) has three characteristic peaks in the methane TPD spectrum (Figure 1). There are two peaks associated with the multilayer desorption at temperatures below 50 K, and the last peak defined as the monolayer with a peak desorption temperature of 66 K. By TPD analysis the calculated converge of the full monolayer peak was found to be 0.33 ML.⁹

Figure 1 TPD spectrum of the multilayer CH₄ covered PT(111) surface showing two characteristic multilayer peaks below 50 K, and the monolayer peak at 66 K.



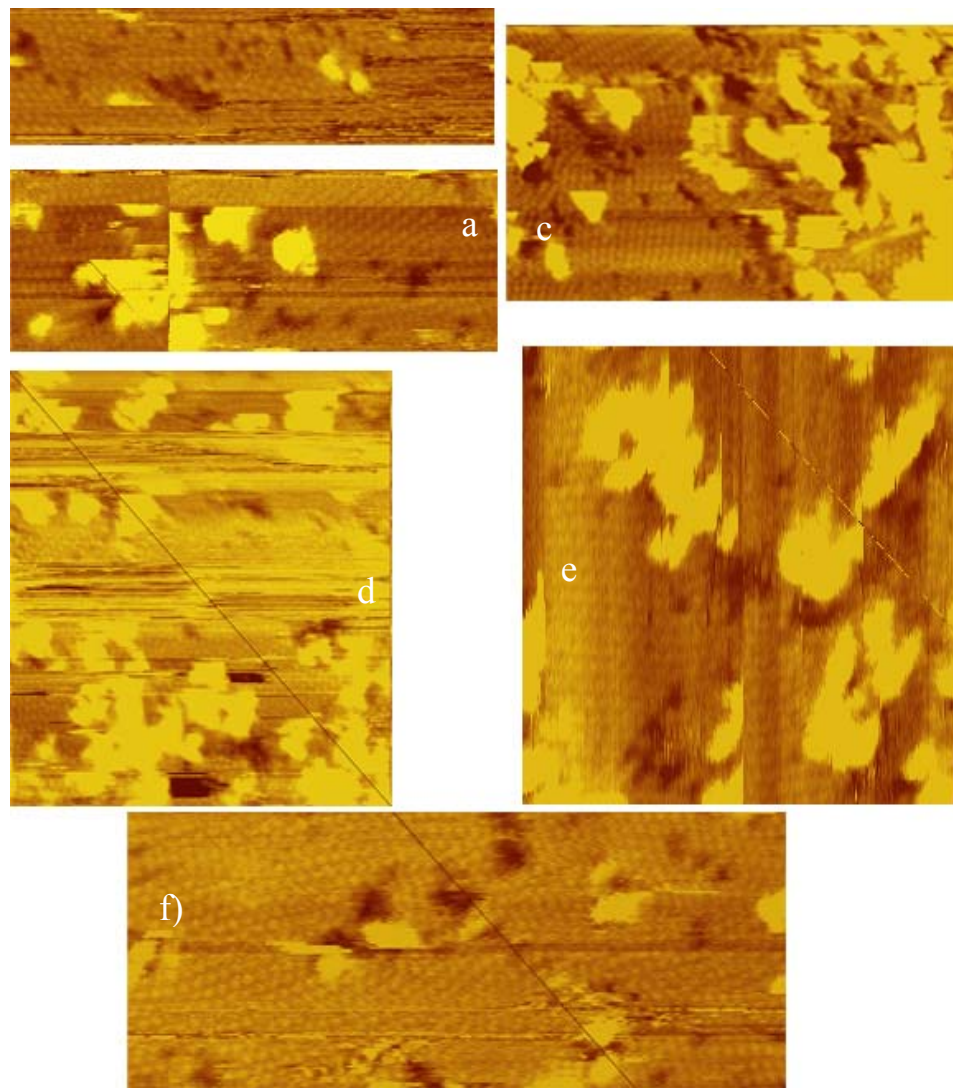


Figure 2 Clips from 6 different STM images showing the ordered arrangement of methane on the Pt(111) surface. Image a) a 60×200 Å image taken at 103 pA, and -2V bias, and shows well defined molecules as orange dots on the surface. b) is a 66×192 Å image taken at 103 pA and -2.03 V bias, c) is a 72×200 Å image taken at 107 pA and -2.09 bias, and shows some drift on the image as well as two distinct domains. d) is a 200×200 Å image taken at 53 pA and -620 mV bias, e) is a 150×150 Å image taken at 103 pA and -2 V bias, f) is a 100×200 Å image taken at 46 pA and -520 mV bias,

As stated in the experimental section a full coverage methane surface was created by overdosing until there was a multilayer peak present and then annealing to 58 K for 1

minute, where the monolayer survives but the multilayer is removed. The STM images of the methane covered surface (Figure 2) were very difficult to resolve. There were many tip changes throughout the imaging sessions, leading to poor image quality. The tip instability was most likely due to loose methane molecules on the surface or tip, because, there were no bias voltages found that helped stabilize the tip during imaging of the surface. Due to the poor image quality, it is difficult to average over a large number of methane molecules in order to determine an adsorption unit cell, however, with the small sample size, a ($\sqrt{3} \times \sqrt{3}$ R30) lattice seems to be the most likely unit cell. The assignment of a ($\sqrt{3} \times \sqrt{3}$ R30) lattice to methane adsorption yields a coverage of 0.33 ML which is in good agreement with coverage found by TPD studies.

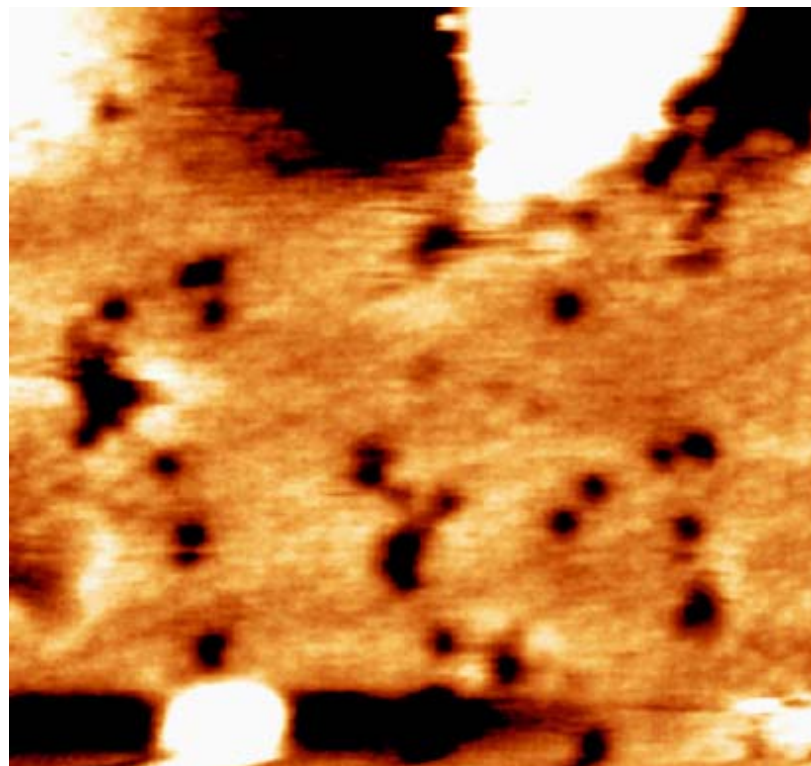


Figure 3 A 125×125 Å image of the full methane covered surface with a tunneling current of 100 pA and a bias voltage of +413 mV, The image shows nice corrugation of the methane covered surface.

Figure 4 The image is 250 Å x 250 Å, and was taken with a tunneling current of 100 pA, and a bias of -2 V. The image shows a better distinction of the methane molecules on the surface but has significant drifts throughout the image, which gives the ordered lattice a wavy look. The blue line represents the line scan found in Figure 5.

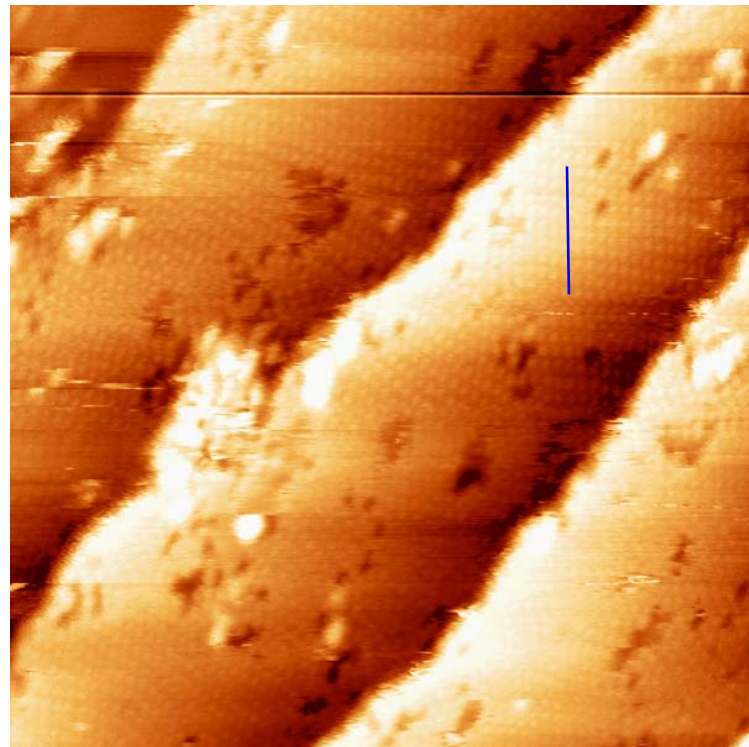
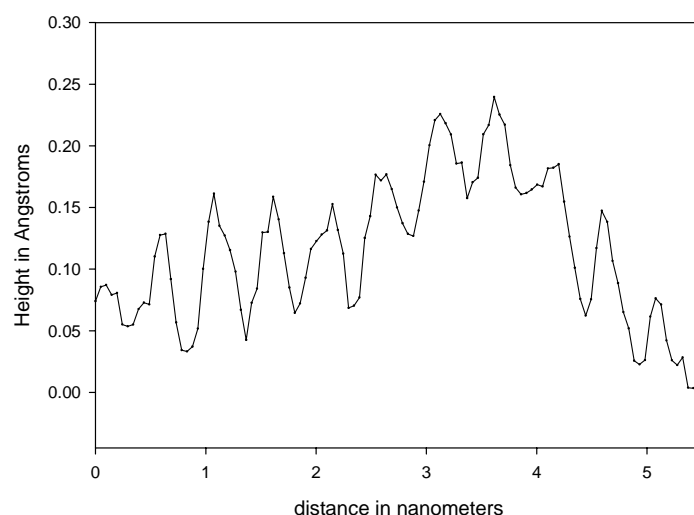


Figure 5 A line scan showing the corrugation of the methane surface, yielding an inter atomic spacing of approximately 5 Å



The interatomic lattice spacing for the methane surface is found to be approximately $5.0 \text{ \AA} \times 5.0 \text{ \AA}$ with an angle of 60° between lattice vectors. A theoretical view of the methane covered surface can be seen in Figure 6, and methane covered surface with the Pt(111) lattice overlaid on the image can be seen in Figure 7.

Figure 6 A theoretical view of the $(\sqrt{3} \times \sqrt{3} \text{ R}30)$ CH_4 arrangement on the Pt(111) surface. The $(\sqrt{3} \times \sqrt{3} \text{ R}30)$ lattice unit cell has been outlined in red.

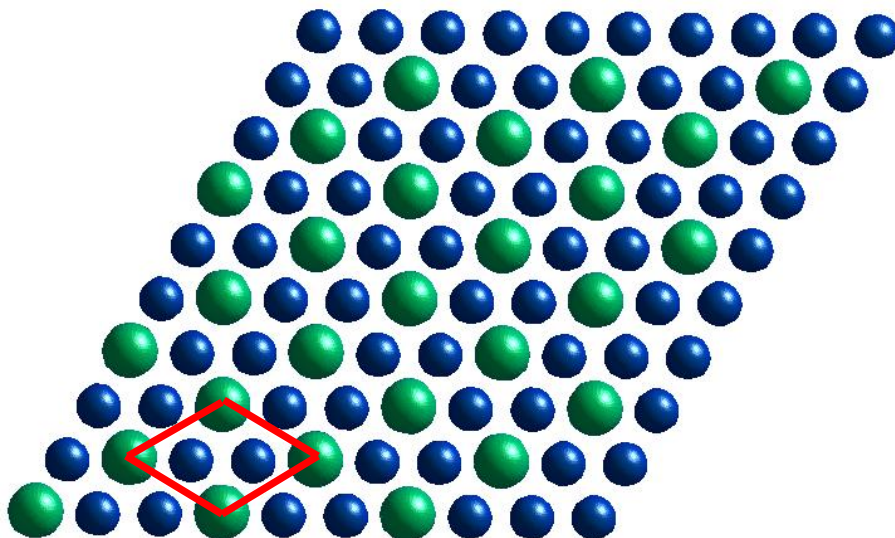
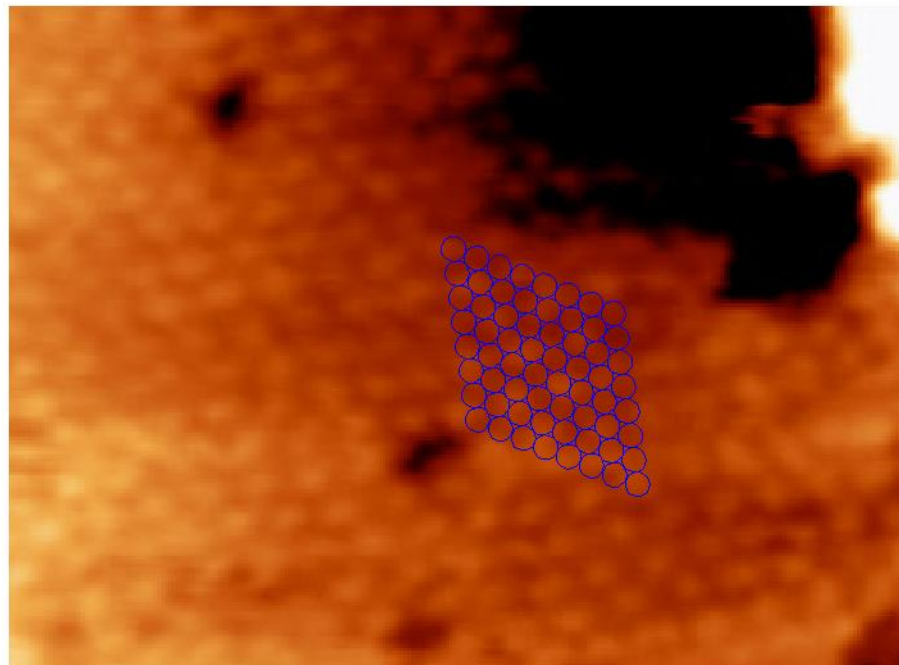


Figure 7 An STM image of the methane covered surface with an approximate area of 120 x 93 Å containing an overlay of the Pt(111) lattice



6.3.2 METHYL RADICAL FORMATION AND IMAGING:

The formation of the methyl radical was similar to the full methane coverage surface creation, in that the surface was overdosed with methane and annealed to 58 K to form a monolayer of methane. Once the methane monolayer was formed, the surface was irradiated with 193 nm laser light for 5 1/3 minutes. The repetition rate of the laser was 125 Hz and the number of pulses was 40,000 at a power of 5 mJ/pulse/cm². At this laser fluence there was no noticeable change in crystal temperature detected by the Eurotherm,

however, the pressure in the chamber did increase during irradiation to 5×10^{-10} Torr, but returned to normal once irradiation was completed. The surface was then annealed to a temperature of 175 K for 1 minute, in order to remove any undissociated methane molecules still left on the surface. The crystal was then cooled back down to a temperature of 25 K for STM imaging.

The images of the individual methyl radicals on the Pt(111) surface can be seen in the Figure 8 and Figure 9. The isolated methyl radicals seen on the Pt(111) surface image as round dots with a average diameter size of 5.5 Å. The radicals then have a projection from the surface on average of 0.40 Å.

Figure 8 A 100 x 100 Å image taken at 82 pA and a bias of 81 mV, which shows nice distinction of the methyl radical covered surface.

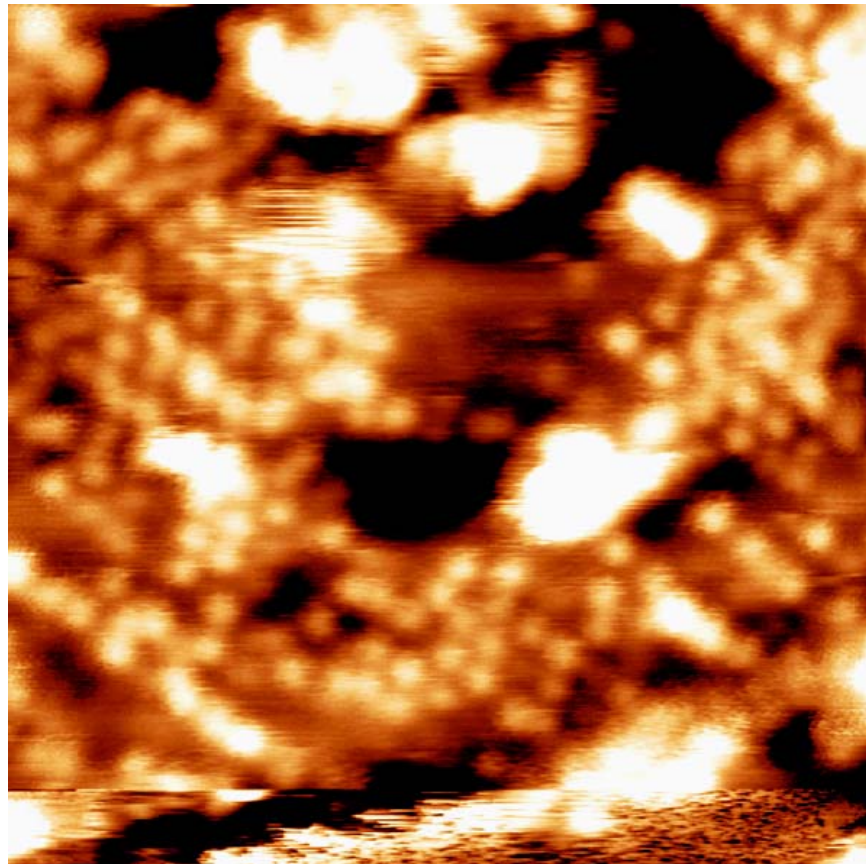
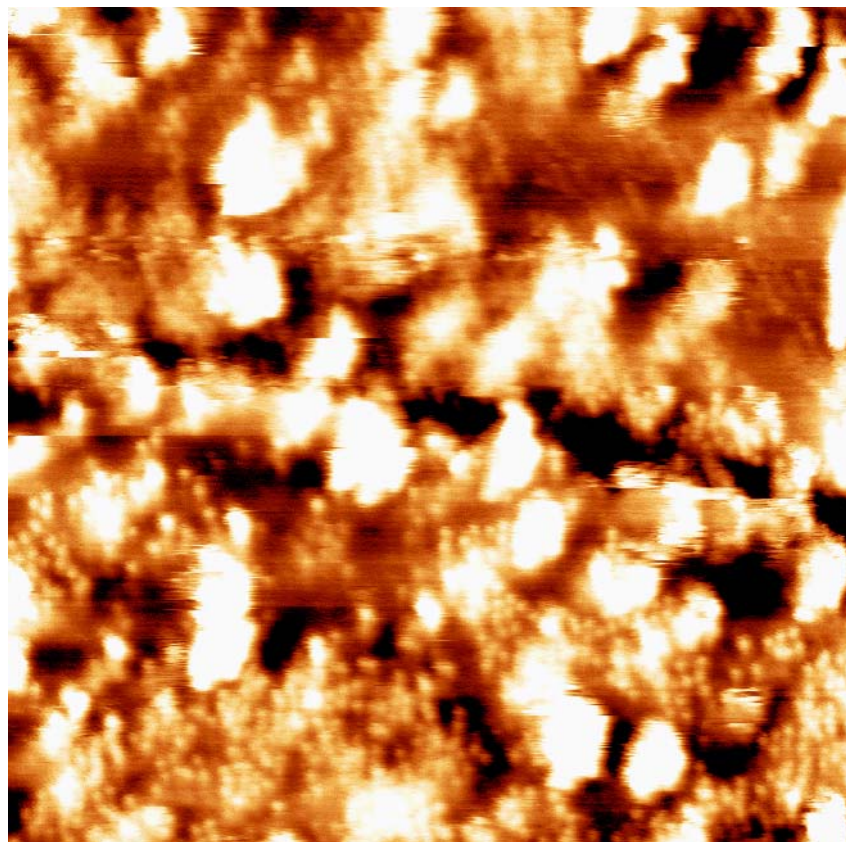


Figure 9 A 300 x 300 Å image of the CH₃ covered surface showing some random arrangement of the methyl radicals at the bottom, the image was taken at 82 pA tunneling current and 80 mV bias. The small bright projections are methyl radicals and the larger white blobs are presumably multilayers of contamination.



The surface seemed to show small areas of ordered arrangement of the methyl radicals that were poorly resolved by STM. However, the images that have some small scale ordering, seems to be in a ($\sqrt{3} \times \sqrt{3}$ R30) lattice arrangement. There have been very few papers that have used STM to image methyl radicals on metal surfaces, one group has shown that the methyl radical forms a ($\sqrt{3} \times \sqrt{3}$ R30) lattice arrangement on the Cu(111) surface.¹⁰ This study however is the first to image the methyl radical following photochemical preparation and on a non-coinage transition metal. The two other groups that have studied methyl radical by STM have used the dissociative adsorption of methyl

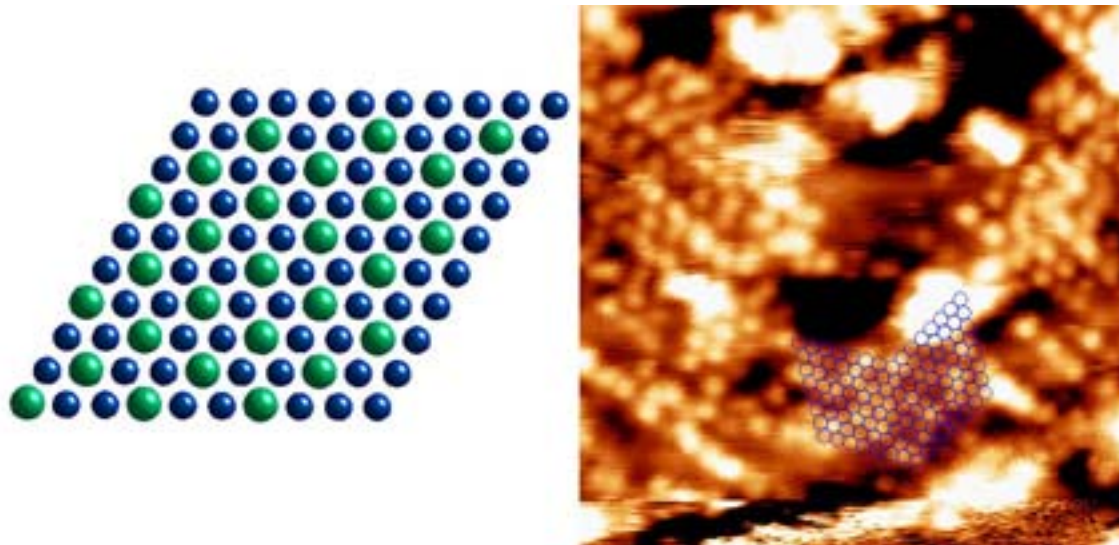
iodine to form the methyl radical imaged on Al(111),¹¹ and the other group used pyrolysis of azomethane to create methyl radical on the Cu(111) crystal at a surface temperature of 350 K.^{10,12}

There would seemingly be two possible explanations as to why the methyl radicals end up in a ($\sqrt{3} \times \sqrt{3}$ R30) lattice configuration: 1) that the ($\sqrt{3} \times \sqrt{3}$ R30) is the preferred packing of the radicals and when annealed to 175 K they find this arrangement, or 2) that the true desorption temperature of the isolated methyl radical is much higher than the annealing temperature yielding a molecule that is unable to move along the surface after photodissociation from the methane molecule and is bound to the surface where the methane was bound originally in it's ($\sqrt{3} \times \sqrt{3}$ R30) lattice. While it is difficult to determine if the methyl radicals are mobile at an annealing temperature of 175 K, the most likely answer is that they are mobile. The reasoning is; the acquired images show small clusters of molecules throughout the surface with a number of isolated molecules decorating the terrace. This would be consistent with mobile molecules that were quickly quenched and frozen in place. Additional evidence to suggest that the molecules are mobile, and that the preferred arrangement is the ($\sqrt{3} \times \sqrt{3}$ R30) lattice is, the collected images seem to show there is a preferred lattice direction on the surface, because, the molecules seem to align in one direction as seen in Figure 11. The lack of multiple small domains areas seen in the image suggest that there has been some interaction between the clusters to organize in a preferred alignment, indicating mobile molecules.

The approximate dimensions of the methyl radical unit cell are 5.1 x 5.1 Å, with a 60° between lattice vectors. The theoretical Pt(111) overlay and ($\sqrt{3} \times \sqrt{3}$ R30) lattice can be seen in Figure 10. The measured dimensions are not exactly consistent with a ($\sqrt{3} \times \sqrt{3}$

R30) lattice which is accepted to be 4.85 Å per side, however, given the drift in the images this is within a reasonable margin of error.

Figure 10 A theoretical ($\sqrt{3} \times \sqrt{3}$ R30) methyl radical covered surface on the left and a theoretical Pt(111) overlay on a methyl radical surface on the right.



The STM images were collected in the UHV chamber at a pressure of 8×10^{-11} torr, over a period of 5 hours. Even though the pressure in the chamber allows for multiple hours of experiments before a monolayer contamination of the crystal, given the length of time of the imaging there is some contamination on the crystal. Figure 12 shows the TPD analysis of the molecules adsorbed onto the crystal after the STM imaging session was finished. The TPD shows that there where a couple of small multilayer CO peaks coming from the surface which could explain some of the large bright blobs seen in the images. However, there is also a small CO chemisorbed peak observed. An integrated area analysis of the CO peak, shows that there is an approximate coverage of 0.05 ML of CO contamination possible. The CO coverage of 0.05 ML, is a high side estimate, due to the high likelihood of post-dosing the crystal with CO during TPD from heating of the

tungsten filament, crystal mount, and copper braid that all release CO into the chamber

when heated.

Figure 11 The image of a 300 x 300 Å look at the methyl radical covered surface, showing a distinct lattice direction that the molecules seem to want to order along. The image was taken with a tunneling current of 88pA and 81 mV bias.

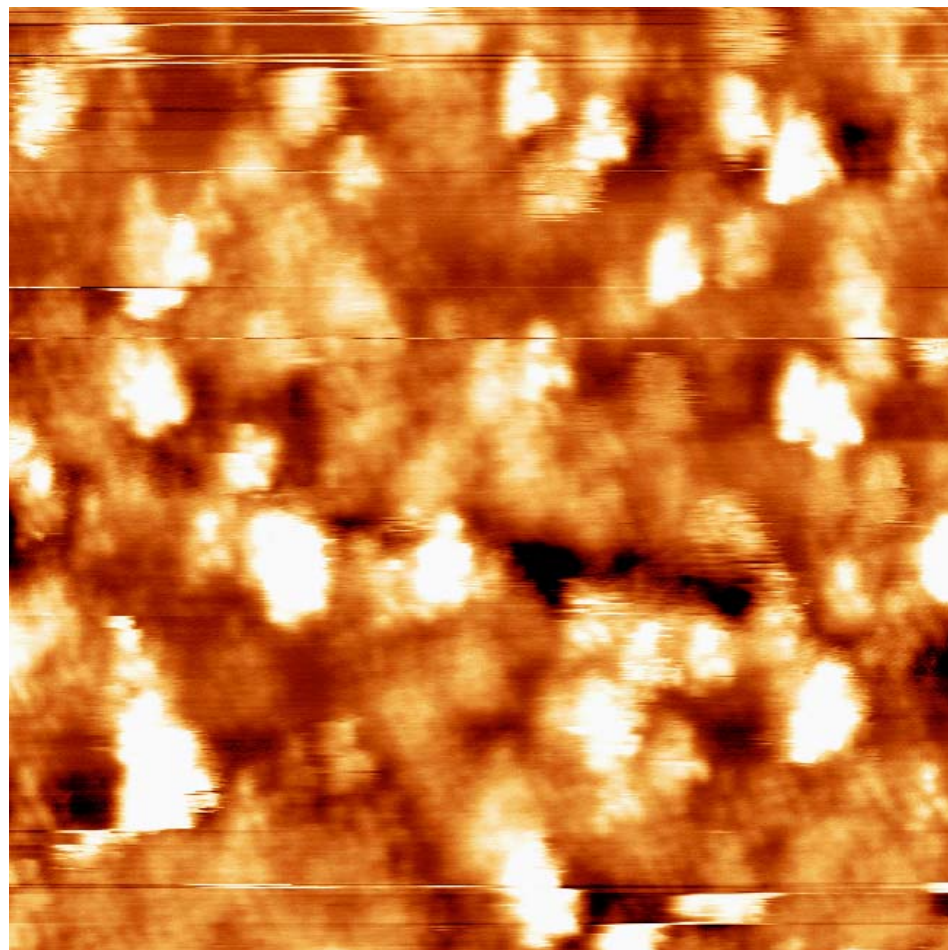
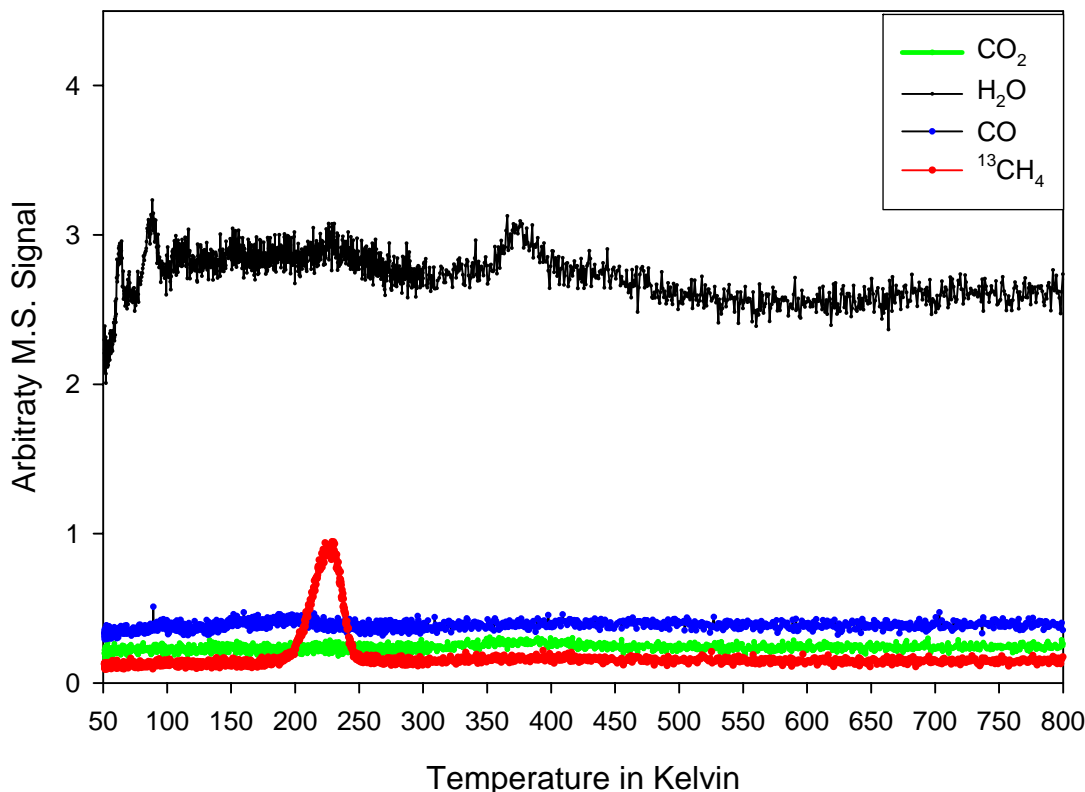


Figure 12 A post imaging TPD analysis of the methyl radical covered surface. The peaks show a substantial amount of methyl radical that have reacted with H to desorb at 200-250 K and a small peak of CO molecules coming off the surface with an estimated coverage of 0.05ML.



6.4 CONCLUSION:

The methane molecule adsorbs into an ordered lattice arrangement of ($\sqrt{3} \times \sqrt{3}$ R30) previously unseen by other surface imaging techniques. The calculated coverage of the methane unit cell is therefore 0.33 ML which is consistent with the previously determine full coverage determined by TPD.

To the best of the author's knowledge this is the first time that the methyl radical has been imaged on the platinum surface and the first time that a methyl radical has been

imaged by STM from photodissociation of a methane molecule. The methyl radical adsorbs strongly to the Pt(111) surface as its desorption temperature in TPD is higher than its recombination with H desorption temperature of 200-250 K, making it an easier molecule to image. The isolated molecule itself forms a 5.5 Å dia. round projection from the surface with an average height off the surface of 0.4 Å.

While it is difficult to say that the methyl radical has a preferred ordering arrangement on the Pt(111)surface, small groups of molecules seem to prefer the same ($\sqrt{3} \times \sqrt{3}$ R30) lattice arrangement as found in the methane examination. The observed clustering of the methyl radicals are most likely due to the molecule being mobile at the 175 K annealing temperature and forming its own preferred lattice.

¹ George A. Olah, Angewandte Chemie International Ed. Vol 44, 18, (2005) 2636-2639

² R. W. Ditchburn, Proc. Roy. Soc. A229, (1955) 44.

³ L.G. Christophorou, D.L. MacCorkle, and A.A. Christououlides, “Electon-Molecules Interaction and their Applications”, Editor, L.G. Christophorou (1984), New York

⁴ Y. A. Grudkov, K. Wantanabe, K. Sawabe, Y. Matsumoto, Chem. Phys. Lett. 227 (1994) 243.

⁵ Y. Matsumoto, Y. A. Grudkov, K. Wantanabe, K. Sawabe, J. Chem. Phy. 105 (1996) 4775

⁶ J. Yoshinobu, H. Ogasawara, M. Kawi, Phys. Rev. Lett. 75 (1995) 2176

⁷ “Photoinduced Electron Transfer Chemistry at Surfaces: Photochemical Activation of N₂, CO₂, and CH₄ on Pt(111)” Robert Zehr Dissertation, University of Virginia, 2005

⁸ V.A. Ukrainstev, T. J. Long, T. Gowl, I. Harrison, J. Chem. Phys., 96, (1992) 9114

⁹ K. Wantanabe, M. C. Lin, Y. A. Grudkov, Y. Mastumoto, J. Chem. Phys. 104(15), (1996) 5974

¹⁰ Y. L. Chan, W. W. Pai, T. J. Chuang, J. Phys. Chem. B, 108 (2004) 815-818

¹¹ S. Mezhenny, D. C. Sorescu, P. Maksymovych, J. T. Yates Jr., J. Am. Chem. Soc. 124 (2002) 14202

¹² R. Wellmann, A. Bottcher, M. Kappes, U. Kohl, H. Niehus, Surf. Sci. 542(1-2) (2003) 81

CHAPTER 7

IDENTIFICATION OF PHOTOACTIVE DIATOMIC NITROGEN ADSORBATES

7.1 INTRODUCTION:

Adsorption of molecular nitrogen onto transition metal surfaces has been a hot bed of activity for research,^{1,2} due in part to its interesting behavior and also the drive to find a better method of cracking the triple bond of N₂.³ Some theoretical^{4,5} and experimental^{6,7,8} studies show that a fraction of the diatomic molecules can be lightly adsorbed onto transition metal surfaces in a chemisorbed state that leads to lowering of the LUMO in the nitrogen molecule. Once the molecule has been chemisorbed to the surface it is then possible to electronically excite the molecule that gets accelerated into the surface, neutralizes and bounces off the surface leading to photoinduced desorption. The majority of the molecules that are adsorbed onto the Pt(111) surface at low temperatures are in a physisorbed state that is not photoactive. The molecules that are chemisorbed to the Pt(111) surface have been determined to align vertically to the surface based on the presence of a peak in the RAIRS spectrum.

An interesting analysis of the adsorption sites of the chemisorbed nitrogen molecules have been done by Yates^{7,6} and Norskov. The experimental work revolves

around examining the RAIRS spectrum under the conditions of high temperature (88K)

and high pressure (flowing N₂ over the surface), and also co-dosing CO molecules used to block the step edge and defect sites. The theoretical work revolved around studying the adsorption energies of a (111) surface [terrace] and a (112) surface [terrace (111) with steps]. Both of the analyses show that there is little to no binding of the nitrogen molecules to the terrace sites under normal conditions, but that adsorption of diatomic nitrogen onto the step edge was preferred, and that the N₂ uptake of the surface depends on the concentration of the step sites. Nitrogen is short lived in its physisorbed state on the terrace at 88 K, so, if the time it takes to travel the distance to a step edge is longer than the lifetime of the physisorbed state on the terrace, the molecule would desorb before it found a step edge to bind to. Norskov's theoretical work using generalized gradient approximation (GGA) density functional theory (DFT) work agreed with this and found that the binding of the molecules to the top side of the step edge is stabilized by a binding energy of -.67 eV using the Perdew and Wang 91 (PW91) density functional.

With all the information collected about molecular nitrogen binding in a chemisorbed fashion to the top side of the step edge little work has been done examining the chemisorbed nitrogen molecules to the terrace sites of the Pt(111) surface. A theoretical pinwheel structure that fits the data has been suggested, but is only a best approximation. So, while the adsorption of the chemisorbed diatomic nitrogen molecules to step edges and site defects are agreed with in this paper, the previously proposed structure of pinwheels adsorbing onto the terrace is in conflict with the STM images presented here.

7.2 EXPERIMENTAL:

The reported experimental results here were done under UHV conditions with a chamber pressure of less than 8×10^{-11} torr. The chamber is equipped with multiple surface analytic techniques for measurement of the crystal conditions before and after the experiment. The chamber, crystal, and existing available analytic techniques have been described previously. However, the analytical technique used in this study is the variable temperature scanning tunneling microscope.

The adsorbed nitrogen on the Pt(111) surface, was isotopically labeled $^{15}\text{N}_2$ gas purchased from Matheson with an isotopic abundance of 99.9%. The use of an isotopically labeled gas was done so the dosed labeled nitrogen could be distinguished from the traditional carbon monoxide and diatomic nitrogen typically present in the chamber. The gas was dosed onto the Pt(111) crystal by a point source doser with a trapped volume and leak valve, where the trapped volume of gas has previously been calibrated against a standard of CO, for a repeatable coverage amount dosed.

The experiments described here were performed with a Besocke style STM at a surface temperature of 25 K. At this low surface temperature, some of the chemisorbed molecules should move slow enough that allows for imaging.

7.3 RESULTS/DISCUSSION:

The binding of molecular nitrogen to the Pt(111) surface has been shown to have multiple desorption peaks in the TPD spectra (Figure 1). The origins of which have been attributed to a multilayer peak at 28 K, the monolayer peak starting at 52 K with

coverages below 0.07 ML and with increased dosing forms a peak at full coverage

saturation with a peak temperature of 45 K having an approximate coverage of 0.41 ML.

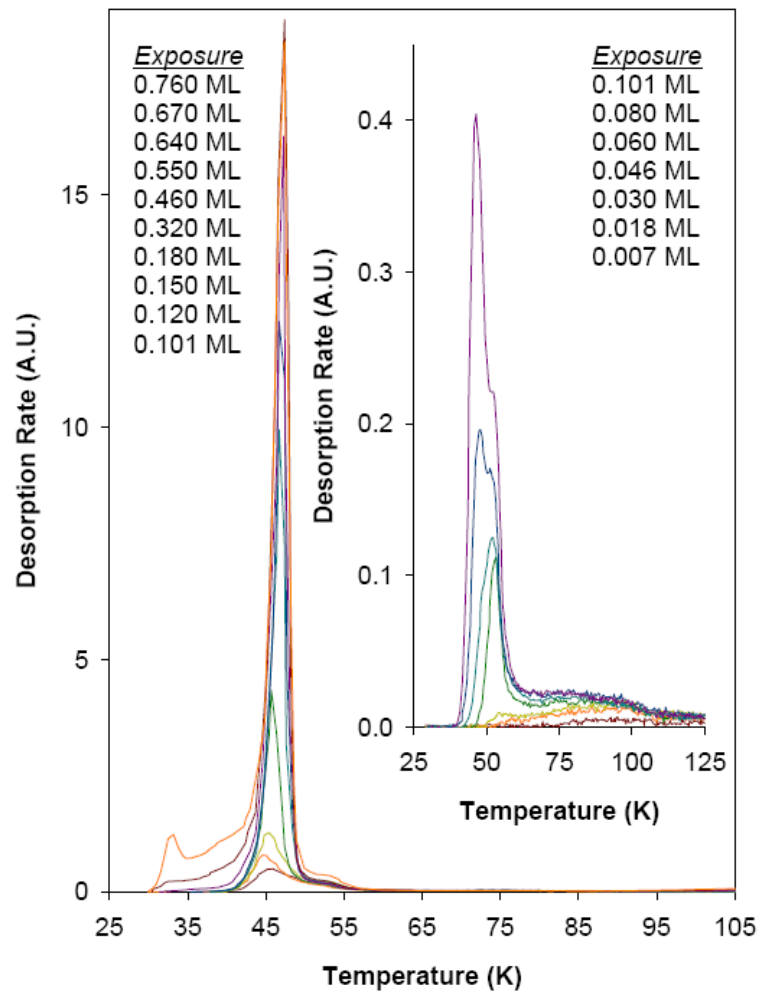


Figure 1 TPD spectra of the diatomic nitrogen molecule desorption from a Pt(111) lattice at a number of gas exposures.

Higher in temperature there is a broad peak from 65 to 110 K that is attributed to molecules adsorbing onto step edges and site defects. The molecules that attached to the step edge and site defects contribute not at all or negligibly to the observed photoactivity of the adsorbed nitrogen molecules. However, they seem to interact with the Pt(111) surface significantly, such that the desorption in TPD occurs at a much higher temperature than the monolayer molecular nitrogen. The tighter binding of the diatomic nitrogen to the platinum step edge has been seen and verified by Tripa et al. examining the effect of the size of the terrace to saturation coverage at 88 K. Additionally, Norskov has theoretical evidence that the nitrogen molecules which are more tightly bound will bind to the top side of the platinum step edge. These results are in good agreement with the STM images reported here. By STM we are able to see that there is a significant amount of molecules that bind to the top side of the platinum step edge (Figure 2). An easier method of distinguishing that the nitrogen molecules are bound to the top side of the platinum step is to do a line scan across the step edge seen in Figure 3, which clearly shows a protrusion from the surface just before the termination of the terrace.

The image in Figure 2, was created by overdosing the platinum surface with diatomic nitrogen until a multi layer peak was observed and then the surface was annealed to 35 K to remove the multilayer. The annealing was done while monitoring the molecular emission of labeled N₂ with the mass spectrometer, and continued until the observed level returned to the original baseline level seen before annealing (approximately 4 minutes). By annealing to 35 K, only the multilayer molecules should have desorbed leaving the monolayer behind.

Figure 2 STM image showing a 1-D row of nitrogen molecules adsorbed along the platinum step edge. The molecules are imaging as bright dots. The image is 175 x 150 Å taken at 102 pA tunneling current and +68 mV crystal bias.

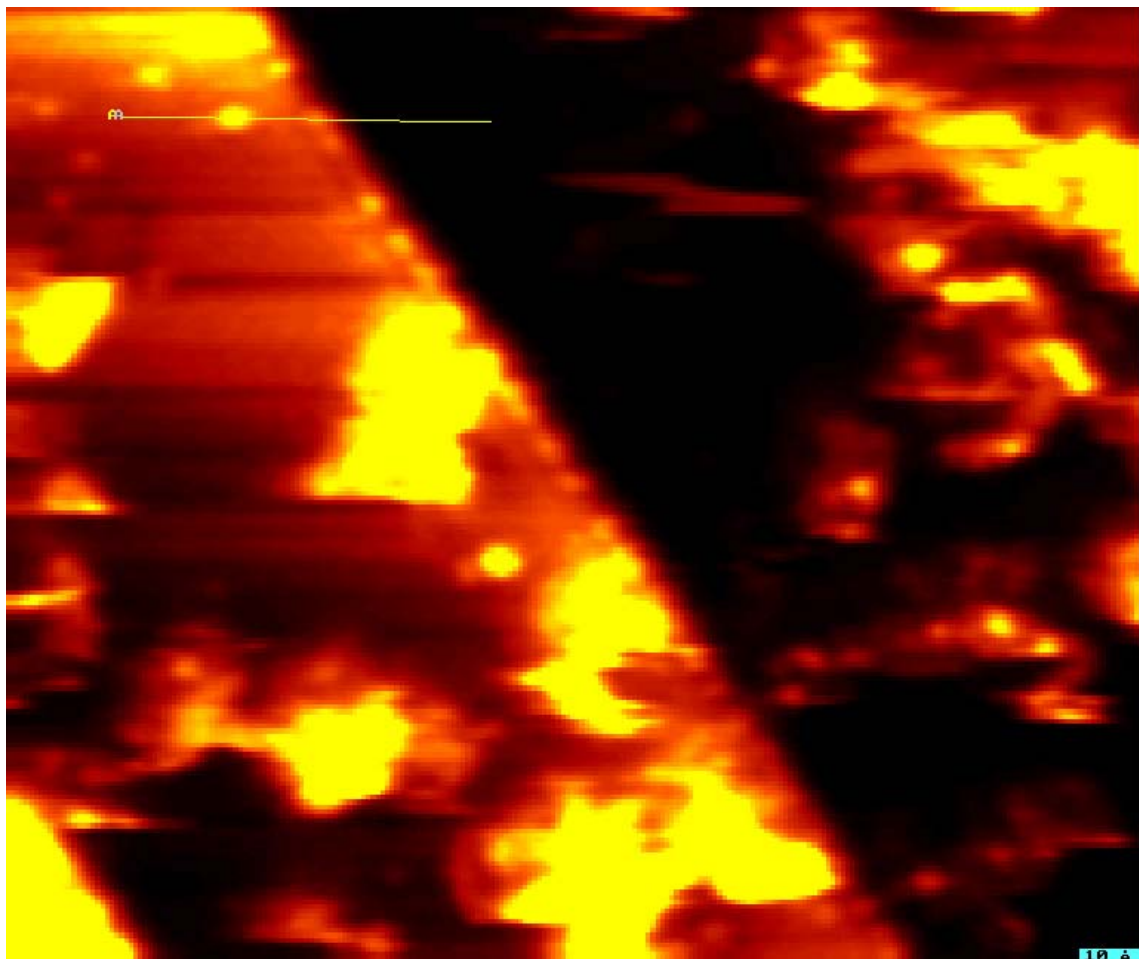
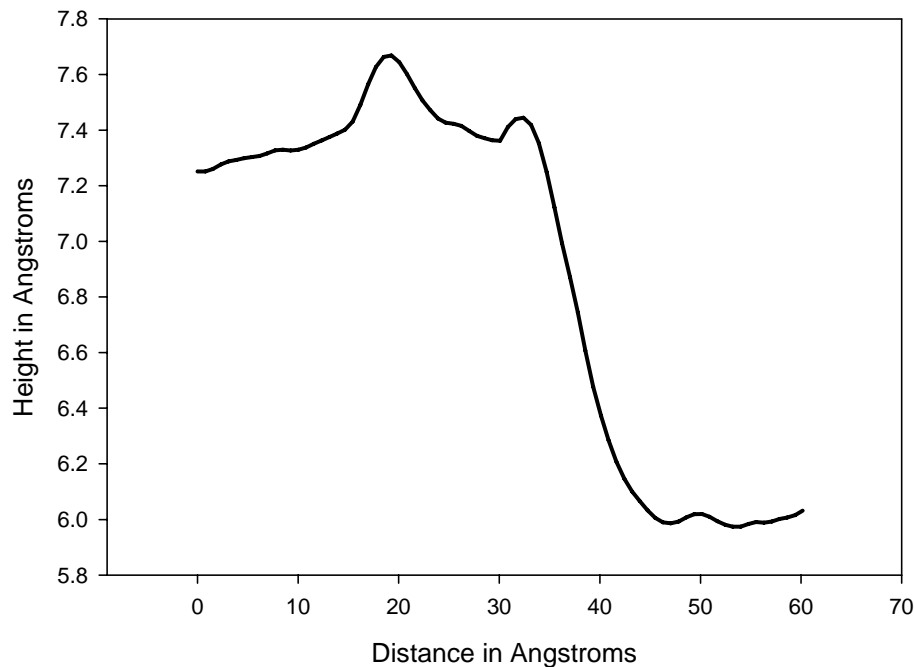


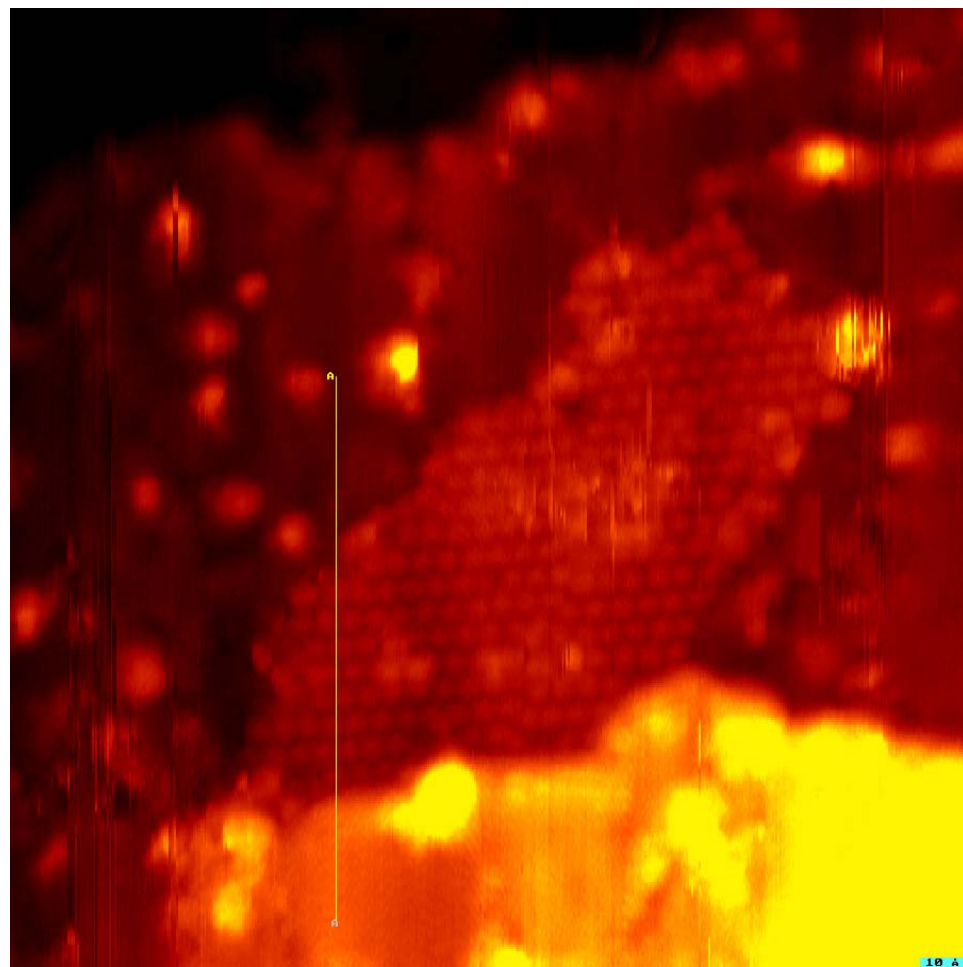
Figure 3 Line scan across the platinum terrace showing a bound molecule possible to a site defect and then a molecule bound to the top side of the Pt(111) step edge.



After preparing the surface in this manner, many STM images were taken. Most of the images were not able to resolve molecules due to many disturbances in the tunneling current. The tunneling current was extremely noisy, most likely for two reasons: 1) not all of the multilayer molecules were removed off the surface by annealing or, 2) at the surface temperatures of 25 K where these images were taken, most of the monolayer nitrogen molecules are still mobile on the flat surface and are in place for a much shorter time scale than that needed for an STM image (typically 1 minute).

However, despite the difficulties in imaging the diatomic nitrogen covered surface, multiple images were found that showed molecules adsorbed to the top side of the terrace steps on the platinum surface, and a few images were collected over a few different preparations of the surface that showed molecules in a condensed islands growing off the lower side of the step edge (Figure 4). As described previously there are a number of adsorbed nitrogen molecules that have been identified as photoactive. It was also shown that the adsorbed molecules on the step edge contributed negligibly to the photoactivity. It was also described that at coverages greater than 0.18 ML, zeroth order desorption was seen, indicating that a condensed island phase of molecules existed that continually replenished the 2-D lattice gas phase that would desorb from the surface. To accommodate the notion of a small number of molecules binding vertically to the Pt(111) surface that are photoactive and fit into a island lattice, a theoretically proposed arrangement was take from the arrangement of nitrogen on a Cu(110) surface. The arrangement proposed by Zeppenfeld was a pinwheel structure where one molecule was aligned vertically in the center and contained 6 horizontal molecules around it. The pinwheel structure was then borrowed by Zehr to explain the arrangement of N₂ on Pt(111). However, the observation of this condensed island of molecules on the surface casts doubt over the proposed arrangement of a pinwheel structure. Because the only ordered arrangements seen by STM was this (2 x 2) and the 1-D line of molecules bound

Figure 4 A STM image of the 2 x 2 condensed island phase of diatomic nitrogen molecules on the platinum surface. Image conditions are: 200 x 200 Å, tunneling current 0 100 pA, bias voltage of +495 mV



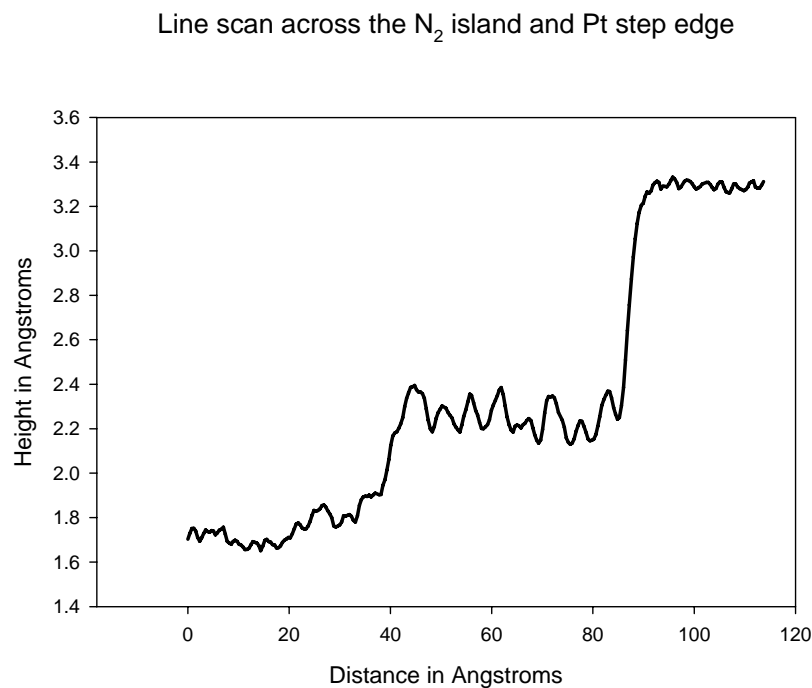
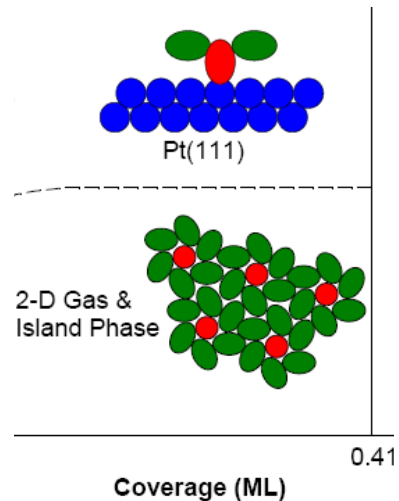


Figure 5 A line scan across the surface of the 2 x 2 island phase of diatomic nitrogen.

Figure 6 Previously proposed condensed island arrangement for N₂ on Pt(111).



to the step edge. It is entirely possible that the condensed island is comprised entirely of vertically oriented chemisorbed N₂ molecules, and because these molecules are lightly chemisorbed, they provide just enough binding to the surface at a temperature of 25 K to keep them from moving over the time scale of the STM image acquisition. Conversely the physisorbed molecules that have essentially no binding to the surface can move about on the surface faster than the image time. The size of the (2 x 2) diatomic nitrogen lattice is 5.5 Å x 5.5 Å with a 60° angle between the sides of the unit cell (Figure 7). The dimensions of the measured (2 x 2) unit cell are almost identical to the expected size of 5.56 Å². Therefore if the nitrogen molecules are assumed to be bound to top sites a theoretical image would look like Figure 8.

Figure 7 Image of the nitrogen 2 x 2 lattice with a

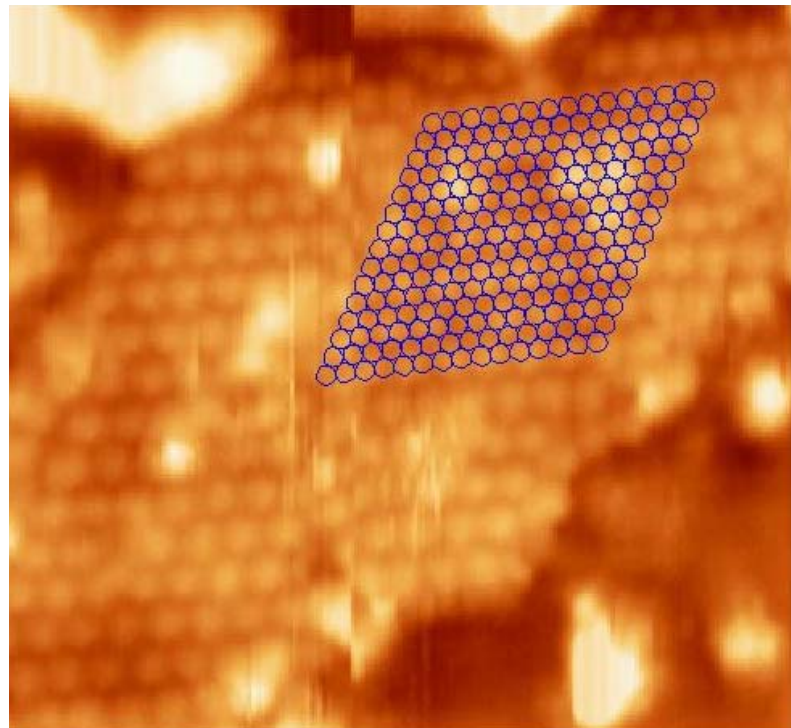
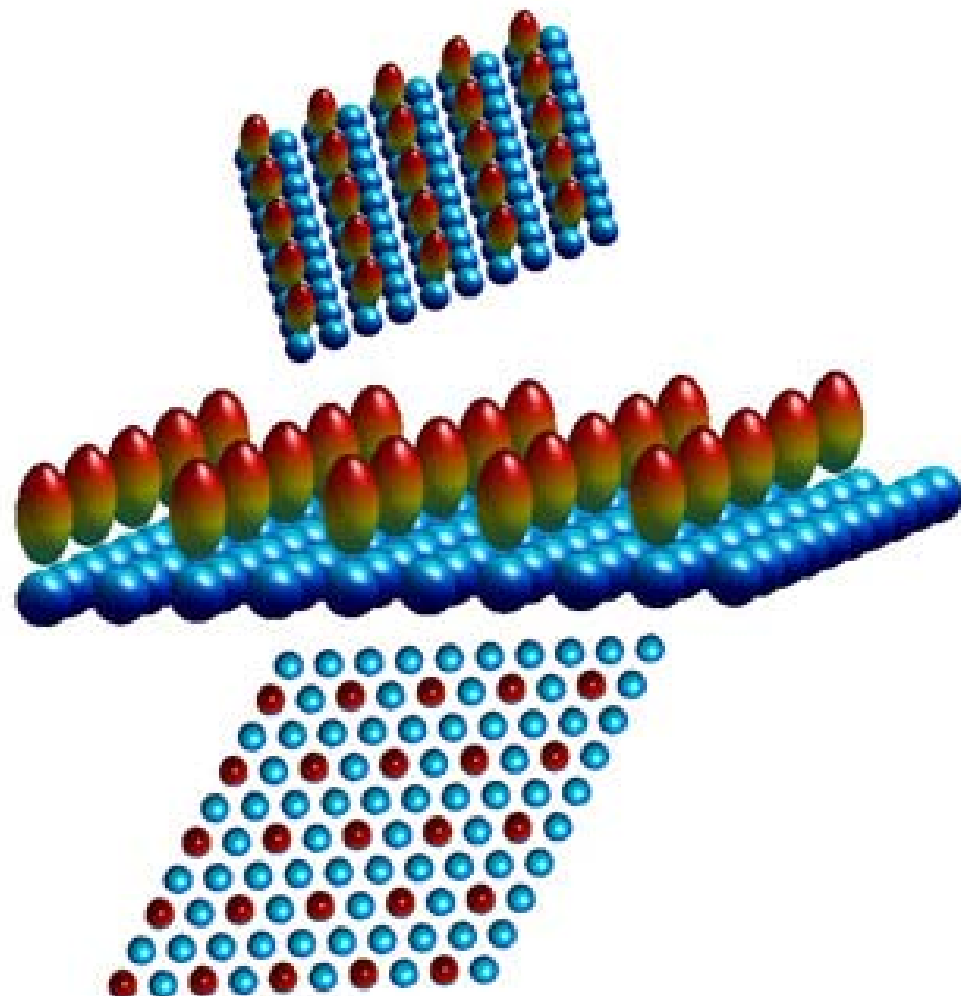


Figure 8 A theoretical image of diatomic nitrogen molecules adsorbed onto a Pt(111) lattice in a 2 x 2 configuration.



7.4 CONCLUSIONS:

The diatomic nitrogen binding to the Pt(111) surface has been examined with initial evidence suggesting that there are two stable adsorption species observable by STM. The first is adsorption on to the top side of the step edge platinum terrace, which is consistent with theoretical conclusions, and easily seen in STM. The second arrangement is proposed to identify the chemisorbed N₂ that can lead to photoactivity. The increased binding of the vertically oriented species lends itself to photoactivity due to the lowered electron affinity level of the LUMO. Secondly, the ability to remain bound to the surface without diffusional movement over the time span of STM data acquisition allowing the (2 x 2) lattice to be imaged by the STM.

¹ A. Marmier, C. Ramseyer, P.N.M. Hoang, C. Girardet, J. Goerge, P. Zeppenfeld, M. Buchel, R. David, G. Comsa. Surf. Sci. 383, (1997) 321-339

² T. Zambelli, J. Trost, J. Wintterlin, G. Ertl. Phys. Rev. Lett. 76(5) (1996) 795

³ R.C. Egeberg, S. Dahl, A. Logadottir, J.H. Larsen, J.K. Norskov, I. Chorkendorff, Surf. Sci. 491(1-2) (2001) 183

⁴ C. E. Tripa, T.S. Zubkov, J.T. Yates Jr., M. Mavrikakis, J.K. Norskov, J. Chem. Phys, 111(18), (1999) 8651

⁵ J. L. Whitten, J. Phys. Chem. A 105, (2001) 7091-7095

⁶ T S. Zubkov, C. E. Tripa, J. T. Yates Jr. J. Phys. Chem B. 105 (2001) 3733-3740

⁷ C. Emil, Tripa, T. S. Zubkov, J. T. Yates Jr. J. Phys. Chem. B 105 (2001) 3724-3732

⁸ R. Zehr, A Solodukhin, B. C. Haynie, C. French, I. Harrison J. Phys. Chem. B 104 (2000) 3094-3106

CHAPTER 8

FUTURE EXPERIMENTS:

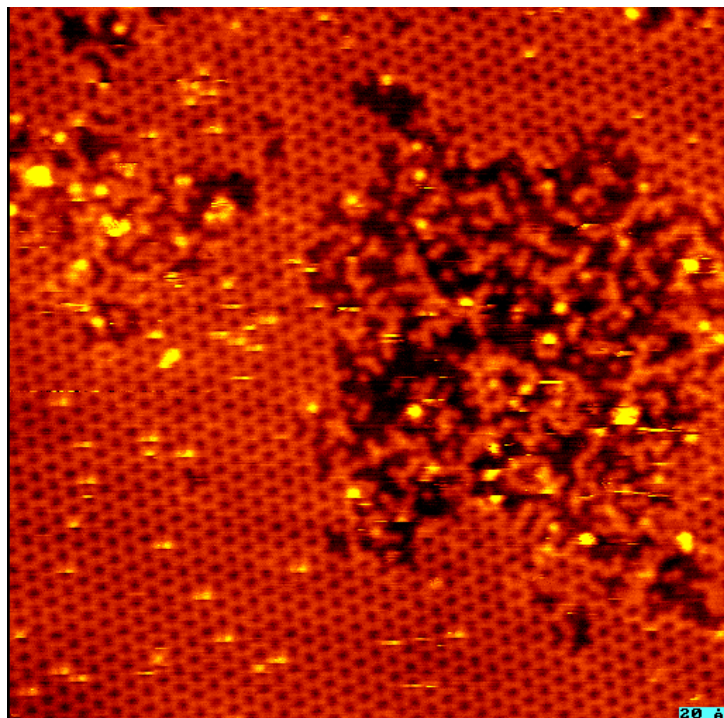
Discussed here are some partial experiments that produced some data that might be interesting to follow up on. Those include: an electronically driven rearrangement of bromine atoms on the Pt(111) surface following molecular dosing when seen by LEED. A second study would be electron induced dissociation of CH₃Br molecules on Pt(111) underneath an STM tip using both positive and negative sample biases. Co-dosing molecules on top of an ordered CH₃Br covered surface and looking for disruption in ordered monolayers or ordering in the overlayer based on the strong dipolar electric fields might be interesting. Finally, use real-time Kelvin probe based work function measurements might be helpful in producing a recipe for creating the various sub-monolayer structures of CH₃Br.

Previously, Dr. Xu had conducted an STM study of Br on Pt(111),^{1,2} and found both a (3 x 3) and a ($\sqrt{3} \times \sqrt{3}$ R30) lattice of Br atoms adsorbed onto the surface. An interesting find because earlier studies of halides on Pt(111) by LEED observed a ($\sqrt{3} \times \sqrt{3}$ R30) lattice for most of the halides, but not for bromine.^{3,4} A (3 x 3) Br atom lattice previously seen by LEED was the expected result. However, the image that was generated by our LEED showed a ($\sqrt{3} \times \sqrt{3}$ R30) lattice which quickly disappeared and

was replaced by the expected (3 x 3) lattice. This result was not followed upon but by dosing at lower temperature (i.e., 20 K) it may be possible to observe the ($\sqrt{3} \times \sqrt{3}$ R30) lattice for longer periods of time. The kinetics of the electron stimulated rearrangement by the LEED electrons at various electron potentials could then be examined and subjected to Arrhenius analysis.

Dr. Xu was reportedly able to dissociate single MeBr molecules with biases of +2.2 volt electrons and higher, and also with -2.2 volt electrons and lower. This can be seen in Figure 1 where the CH₃Br covered surface was imaged and then zoomed in to a scan an area of 100 x 100 Å at a bias voltage of +2.5 V. After the

Figure 1 a 250 x 250 Å image of a MeBr covered surface that shows a 100 x 100 Å area of disruption done by scanning a 100 x 100 Å area of the surface with a tunneling current of 1 nA and +2.5 V. The images seen here was collected after disruption of the area with a tunneling current of 1 nA and bias voltage of +250 mV



scan was complete the scan range was expanded to 250 x 250 Å and the bias was reduced. The result was a roughly 100 x 100 Å square disruption in the CH₃Br lattice

Later STM studies to analyze this dissociation phenomenon in a systematic way met with mixed results. The idea was to scan the surface as a function of tunneling current and bias voltage looking for a quantitative amount of dissociated molecules under

each condition. The results were inconclusive, leaving either no molecules dissociated or the entire area. This may mean that the disruption of the MeBr surface is not a function of bias voltage, but a tip effect where something jumps on to the tip and is dragged around the sample pushing all the molecules away and not dissociating them. The question of whether e- induced dissociation was observed was not answered. It maybe a difficult or even impossible problem to answer with the present STM. This is because our STM has a warm tip where molecules can adsorb and desorb easily. This experiment should be tried with the new isothermal STM where the tip is kept as cold as the surface providing limited molecular mobility that might interfere with the STM measurements.

Another STM experiment that could be done is to post-dose molecules onto the ordered CH₃Br covered surface. Indraneel Somanta has done initial work examining the RAIRS spectrum of MeBr covered surfaces after post-dosing of molecules like oxygen, carbon monoxide, and xenon, which shows a spectrum of peaks with a reduction in the splitting of the v₂ mode assigned as occupying top and three fold hollow sites and to possibly eliminate the satellite peak in this mode.

The last experiment that should be considered is work function analysis of the sub-monolayer structures seen in the MeBr STM images. By performing macroscopic work function measurements if may be possible to develop a recipe for creation of these secondary structures on a real-time basis as opposed to the testing of one experimental condition a day using STM. Once a reliable method of creating the sub-monolayer ordered structure surfaces is found, the prepared surfaces could be studied in the photochemistry chamber by RAIRS and LI-TOF to test dynamical models of adsorbate photochemistry.

¹ H. Xu, R. Yuro, and I. Harrison, Surface Science 411 (1998) 303

² H. Xu, I. Harrison, J Phys Chem B 103, 51 (1999) 11233

³ W. Erley Surf. Sci. 94 (1980) 281.

⁴ E. Bertel, K Schwaha, F. P. Netzer, Surf. Sci. 83 (1979) 439

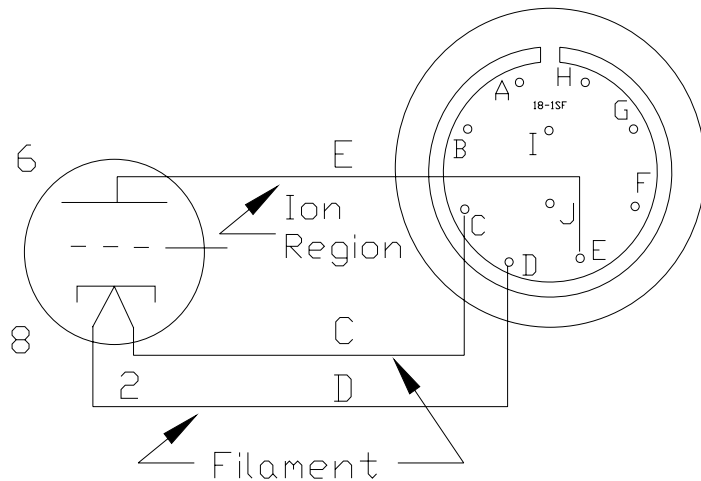
APPENDIX**A)****Mass Spec Emission Control Test:**

The condition of the emission regulation circuit in the Ionizer Controller box for the mass spectrometer may need to be tested occasionally. When switching from the original Extrel Ionizer Controller box to the present one this test was necessary due to unknown conditions of the new controller box acquired from Toronto.(I didn't particularly want to burn out the ionizer filament while under UHV chamber conditions.) Therefore, it was thought that by connecting a vacuum tube to the Ionizer control the emission regulation could be tested. Simple in concept, use the two filament power pins to power the filament in the vacuum tube, and connect the collector pin on the tube to the emission detection pin on the ionizer control to detect a current flow.

This idea was tried with all of the vacuum tubes that were available in the Harrison lab, with no success. It was possible to get the filament to glow and even adjust the luminescence intensity of the filaments by running in voltage regulation mode but while in emission regulation the filament would continue to grow brighter until a maximum power of the ionizer controller was reached.

After contacting ABB (formerly Extrel) they confirmed that the proposed test was a good one and one that they use to test questionable controllers as well. However, they use a 5U4 vacuum tube for testing.

Unable to find a 5U4 vacuum tube we were able to buy a newer equivalent tube of 5U4G from a local photography/electronics store (Pro Camera Inc.) where the owner was a vacuum tube collector. Once the new tube was used, the emission control of the ionizer worked exactly as expected. When the collector pin on the tube was connected to the E pin on the ionizer cable there was a current detected which was able to be adjusted by dialing the emission control knob on the ionizer controller front panel. However, once the collector pin on the tube was disconnected the filament increased in intensity until the power limit of the ionizer control was reached, acting like there was no current detected as was expected.



The connections are shown above; For the filament, pin C from the ionizer control cable is connected to pin 2 on the vacuum tube, and pin D from the IC is connected to pin 8 on the tube. If the emission control portion of the IC is to be tested connect pin E from

the IC cable to pin 6 on the vacuum tube, and run the ionizer controller just as you would when connected to the mass spec.

B)**Construction of a new STM head: Materials List**

Materials that are needed to construct an STM head.

- 1.) Piezoelectric ceramics
 - a. From - Staverly Sensors Inc. E. Hartford Ct.
 - b. Type - EBL # 2 (nickel plated)
 - c. Dimensions – 1” length x 1/8” diameter x 0.020 wall thickness.
- 2.) Macor nonporous machineable glass/ceramic
 - a. From - McMaster-Carr (purchased new before machining)
 - i. Dimensions – 1/8” thick rod
- 3.) Stainless Steel Hypodermic tube stock
 - a. From – McMaster-Carr
 - i. 22 Gauge tube for holding the STM head
 - ii. 24 Gauge tube for the tunneling current tip holder.
 - iii. 23 Gauge tube (it's possible use for either purpose, to hold the head or the tips. It's just nice to have around.)
- 4.) Copper wire
 - a. From – California Fine Wire
 - i. Kapton coated (polyamine)
 1. 0.010” dia. About 30 ft. needed
 2. 0.002” dia About 20 ft. needed
 - ii. Razor blade, glass microscope slide, and cigarette lighter. (used to remove the kapton coating on the wire.)
- 5.) Thermocouple wires
 - a. From – California Fine Wire
 - i. 0.005” dia. bare wire, both Alumel and Chromel
- 6.) Sapphire/Ruby balls
 - a. From – Swiss Jewel Co.
 - i. 1/8” dia.
 - b. (1/8” Tungsten Carbide ball came from McMaster-Carr)
- 7.) Silver Solder & Flux
 - a. Eutecrod 157 with flux
 - i. From - Eutectic Corp.
 1. Free of Cd, Pb, Zc, and Sb
 2. Melting point 220 C
 3. Used for Surgical Instruments

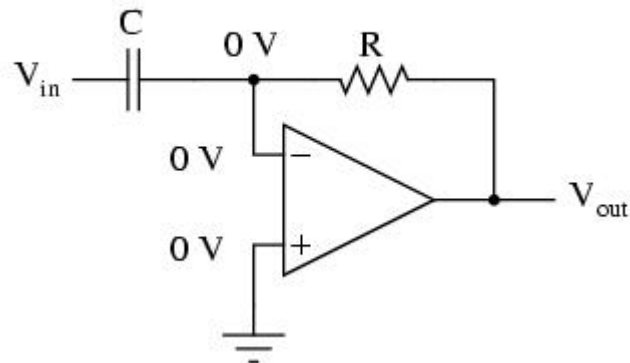
- b. Silver solder & flux from National Welding Supply in Richmod, Va.
 - i. Repackaged by National Welding Supply – it is a J.W. Harris equivalent of the Eutecrod 157.
 - ii. Free of Cd, Pb, Zn, and Sb
 - iii. Contain approximately 96 % Sn and 4 % Ag
 - iv. (packaged with its own flux)
- 8.) Epoxy
 - a. From – Epoxy Technology, Billerica, MA
 - b. Conductive epoxy
 - i. Product name – H35-175MP
 - c. Non-conductive epoxy
 - i. Product name – H61
- 9.) STM Head material
 - a. Potential materials
 - i. Aluminum - Easy to machine and clean, but large difference in the thermal expansion coefficient between Al and the piezoelectric ceramic.
 - ii. Macor - Harder to do fine detail machining, very fragile when completed, However it has approximately the same coefficient of thermal expansion as the piezoelectric ceramic.
 - iii. Super Invar - Very difficult to machine (Rodger in the machine shop will complain about it for the next 5 years.) But has a zero coefficient of Thermal expansion.
- 10.) Microshield/ Microshield remover
 - a. From – SPI-Chem, West Chester, PA (www.2spi.com)

C)**Short explanation of the tip etching box**

To start the etching process one has to press the Button on the etching box and hold it down for a couple of seconds (see Figure C.1 schematic). This causes the first transistor after the switch to open. As it opens you get a low potential on the base of the second transistor, causing this one to close. Now you have a high potential on the 56 k resistor that goes back to the base of the first transistor holding this one open. You also have a high potential on the base of the third transistor opening this one up as well. This lowers the potential on the base of the PNP-transistor referenced to the etching Voltage causing this one to open and therefore applying the **positive voltage to the tungsten wire**.

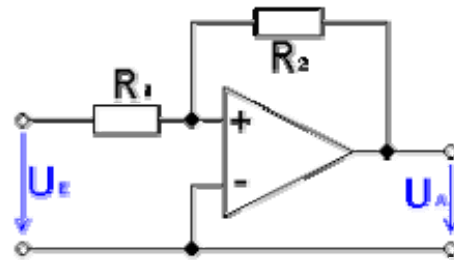
To switch everything off you have to know when the etching process should be finished, this is when the tungsten wire tears apart. This leads to a sharp drop of the current. This can be detected by a small OP-Amp circuit.

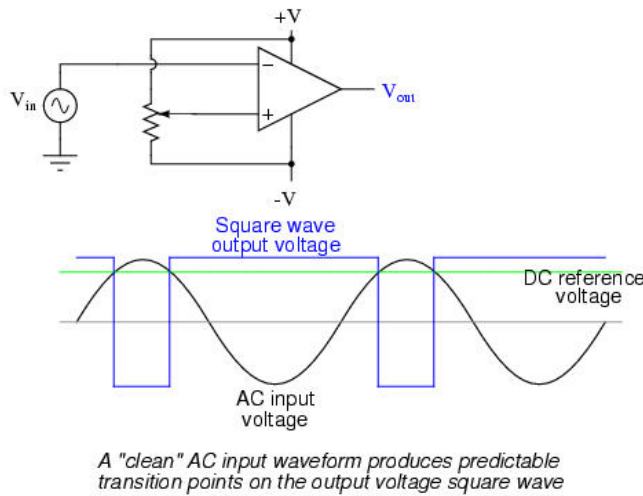
The first OP-Amp works as a differentiator. This means a signal proportional to the change in voltage on the input is given to the output. As the etching is completed you will have a sharp change, hence you get a high voltage output.

Differentiator

This output signal is fed into the second OP-Amp, the second OP-Amp works as a Schmitt-Trigger.

The principle of a Schmitt Trigger is as follows. Any signal below a certain threshold is ignored, signals higher than the threshold (here DC reference voltage) lead to max output voltage.





The potentiometer in the etching box sets the trigger level (threshold). You need to adjust this trigger level quite often. Therefore the potentiometer is accessible from the outside of the etching box, marked as “**Gain**”. If the gain is set to low, the etching box will switch off the voltage between anode and cathode before the tip is finished. Ideally the gain setting is set so that the voltage will turn off as the bottom part of the wire hanging in the solution falls off.

The high output voltage of the OP-Amp causes the first OP-Amp after the switch to close, opening up the second one closing down the third. Now the 10 k resistor between the base and emitter of the PNP-transistor both are at the same potential, thus closing the transistor, and stopping the etching process.

Using a fresh 3M KOH solution, a reasonable value for the etching voltage is between 7-8 V. If you go to higher voltages, you get shorter but apparently less sharp tips. Using lower voltages leads to longer tips that may be less stable in the STM.

Tip Etching Control Box

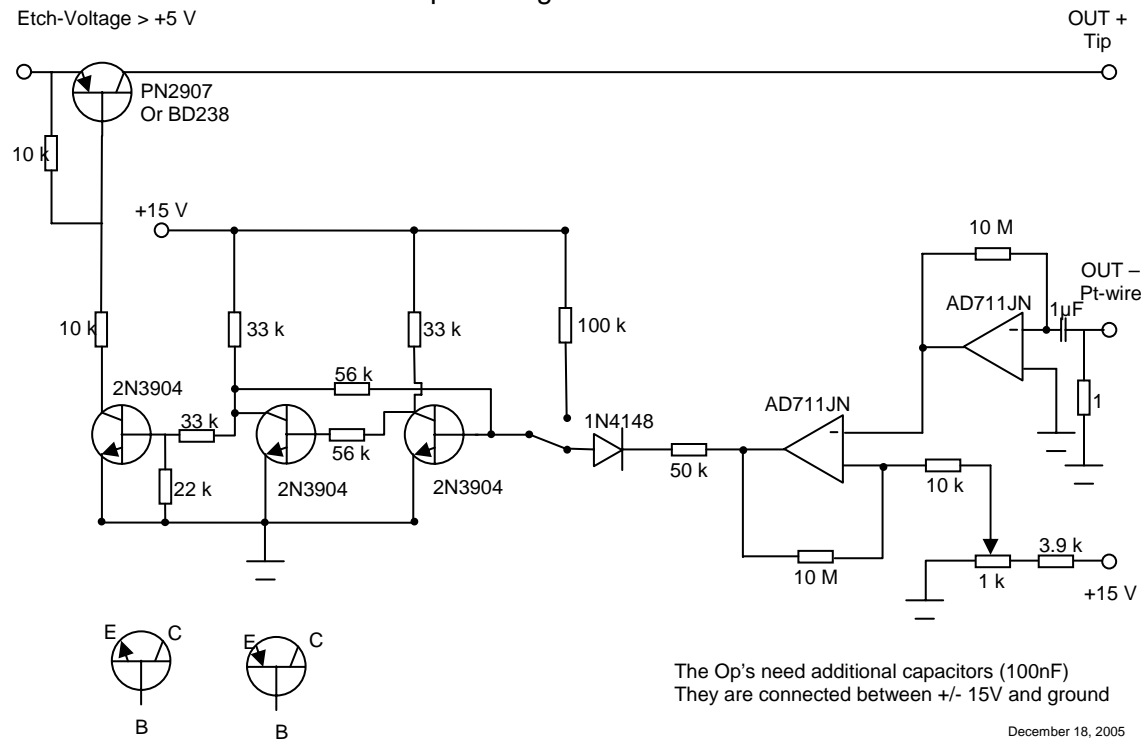


Figure C.1 The electronic schematics for the DC tip etching.

D)

Ion Pump Reconstruction / Operation

Our UHV chamber is pumped almost exclusively by Ion Pumps. Therefore knowledge of how ion pumps work, their day to day operation and an understanding of how to do periodic maintenance is important. This document will provide the relevant information necessary to operate and maintain our ion pumps.

Figure 1

An ion pump consists of a large number of individual Penning cells. The individual cell was designed and used by Penning in 1937 (Figure 1) originally as a pressure measurement device. To his credit he noted the ability of these cells to cause a pumping action, but apparently left it as a curiosity. It wasn't until much later that Hall (1958) utilized the pumping action of these cells by combining a number of these cells together to develop the first ion pump.



Ion pumps are a type of sputtering/gettering pump that removes material from the vacuum in a number of ways (Figure 2). The first way is simply gas adsorption to the surfaces of the pump elements after a dissociation/ionization event. Secondly, pumping occurs through gettering by freshly sputtered cathode material. A third method is burial of adsorbed gases by sputtered cathode material. The fourth and fifth pumping mechanisms are; ion and fast neutral burial. With ion burial a molecule is ionized in the anode region and is then accelerated into the cathode. With fast neutrals, the ion that was

created undergoes a surface charge transfer which causes them to be reflected to another surface for implantation and thus removal from the vacuum chamber.

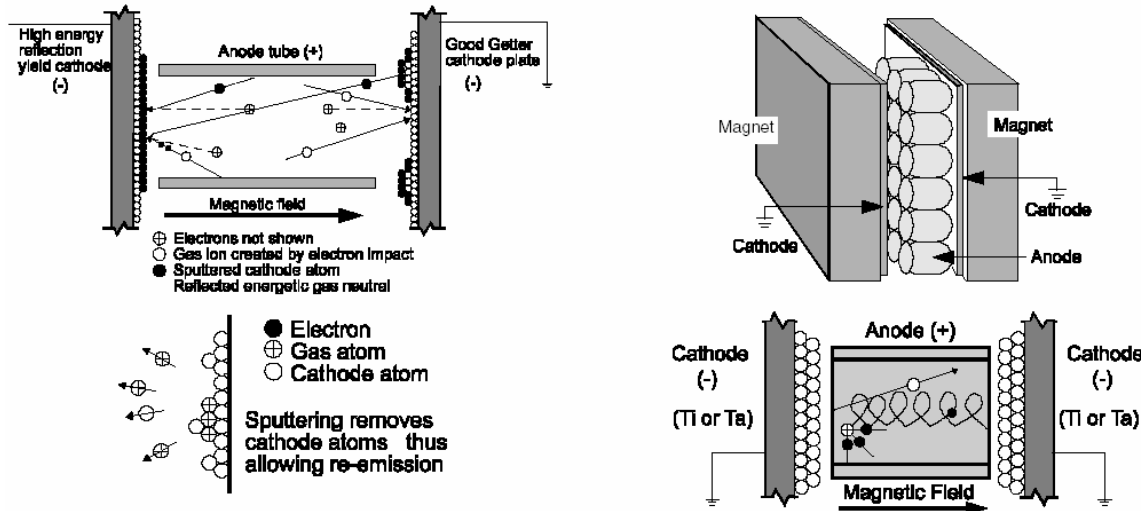


Figure 2 Ion pump, pumping mechanisms

The pumping speed of the ion pumps scale with the number of Penning cells present. Therefore a simple 2 L/s pump may contain only one Penning cell like Figure 1 while our 640 L/s pump contains 16 banks of pump elements like Figure 3 that each contains 72 cylindrical penning cells in a square lattice pattern. The square lattice also inadvertently creates 55 small star/diamond shaped Penning cells that are not necessarily intended to pump, but examination of the divots in the cathode elements suggests that they are capable of some pumping action on their own.

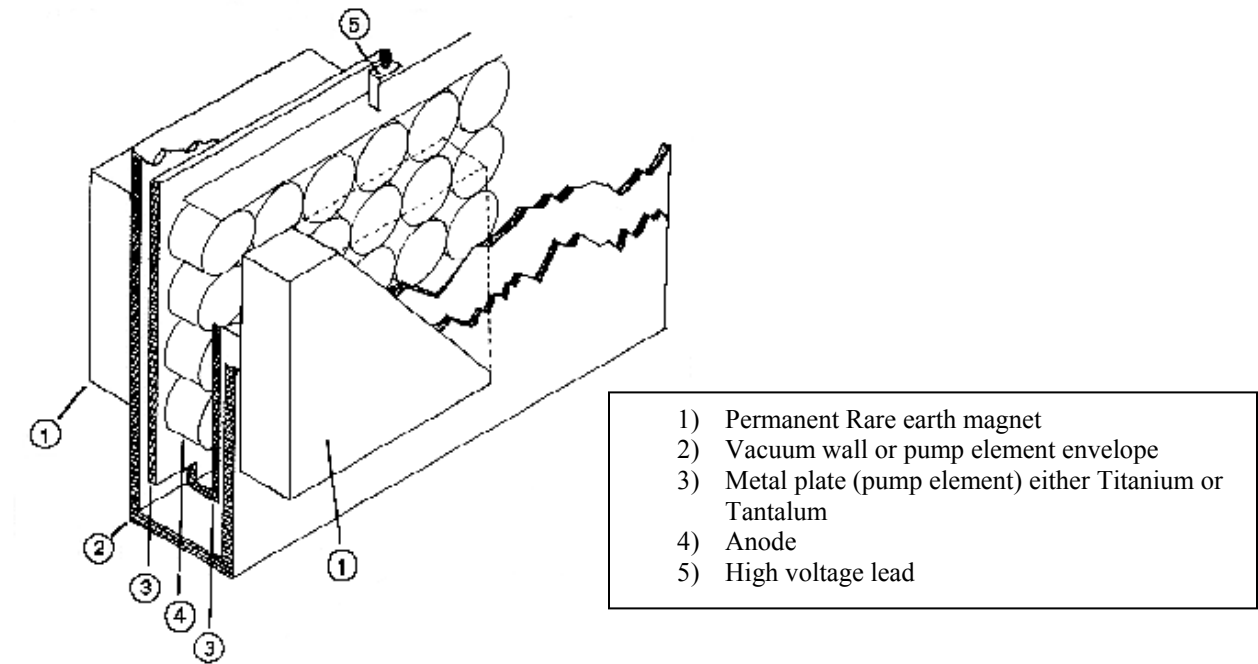


Figure 3 Ion Pump element

The Ion pumps consist of five component pieces Figure 3: The anode with attached high voltage lead, cathode (metal plate), vacuum wall, and two permanent magnets located outside the vacuum chamber walls. The ion pump uses high voltage (+6000V) applied to an anode that has cathode plates on either side at ground potential. This creates electrons as a cold cathode electron source. Once the electrons are in the vacuum, they fall down an electric potential between the two cathode elements. Then the permanent magnets apply an axial magnetic field that forces the electrons into a circular (helical) orbit inside the anode cells. If the magnets were not present, there would be little to no ionization events occurring. The reason is that the free electrons would travel in a

straight line from the cathode to the anode. This means the time spent by the electron in the vacuum is very limited and this limits the probability of causing an ionization event to occur. When the magnets cause the electrons to spiral in the anode, it greatly increases the path length of the electrons which increases the likelihood that the electron will interact with a molecule in the vacuum and cause an ionization event.

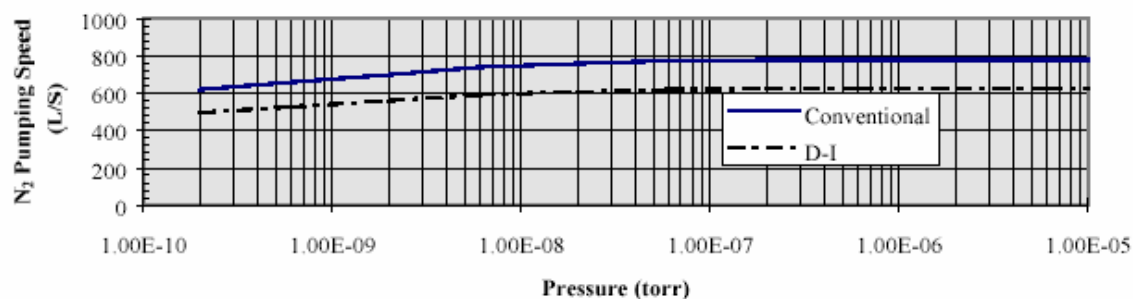
The magnets are an integral part of the ion pump, and much work has gone into optimizing the strength, material, orientation and temperature characteristics of the ion pump magnetic fields. Currently, the magnets in our ion pumps are rare earth ceramic (barium ferrite) magnets that produce fields of 1 to 2 kGauss (or 0.1 – 0.2 tesla). Increasing the magnetic fields beyond this range results in a decrease in the pumping speed. The same paper that studied the effects of magnetic field strength on pumping speed also studied the orientation effects of the magnetic field by varying the angle of the magnet from 0 to 12° from the normal axis of the anode. As expected the pumping speed drops as the angle from the normal increases. Perhaps, the most readily apparent effect to us with our ion pump is temperature. While baking the chamber the temperature of the ion pump must increase with the rest of the chamber. The barium ferrite magnets exhibit a reversible field loss of 0.2% per degree Celsius, and a 7% irreversible loss above 350° C. At temperatures greater than 85° C the pumping speed of the ion pumps decline with increasing temperature. The ion pump can then have difficulties pumping due to magnetic field loss and increased gas load from baking out.

Most ion pumps are very similar in design consisting of a cylindrical anode and a cathode plate; however there are many variations on a theme when it comes to ion pumps used for pumping inert gases such as argon. Due to argon present in the atmosphere, and

the extensive use of it for sputtering in UHV chambers, there has to be a method of removal from the chamber as well. Conventional ion pumps use two titanium cathode plates for pumping, which works well for reactive gases. However, a conventional ion pump will reach a base pressure to which it can not go below, simply because it can not pump argon efficiently; typically argon pumping speeds are 1 to 2% of the active gas speed. This inefficient pumping leaves the chamber with a high partial pressure of argon. With what little argon the ion pump does remove, quickly saturating the cathodes which then start to re-release Argon back into the chamber by what is termed "argon instability". Since argon is pumped exclusively by implantation and burial, the continuous sputtering of material off the cathode causes Argon to eventually be unburied. To prevent this, our ion pumps use one titanium plate and one tantalum plate which is termed a differential ion pump. With this design the recoil energy of the scattered neutral inert gas is increased and it is not implanted in the same spot on the cathode that the rest of the ions are focused into. The recoil energy depends solely on the relative atomic weights of the gas atom and cathode material.

The working operational pressure range of a typical ion pump runs from 10^{-4} torr to 10^{-12} torr. If an ion pump is started in a pressure that is too high, the electrons that are

Figure 4 Pumping speed vs. Pressure of Ion pumps



created at the cold cathode element can't build up enough energy to cause an ionization event to occur which means there is no pumping. Conversely, if the pressure is too low, the ion pump has a difficult time pumping (see Figure 4). The cold cathode electron emission is not sufficient to continuously run the ion pump, it is mostly used to initiate the ionization of a few molecules that can then accelerate into the cathode which while sputtering Ti/Ta atoms also creates secondary electrons which then propagate the ionization/pumping process. This "autocatalytic" cycle continues until a steady state electron creation exists. When steady state pumping occurs the electron impact density on the anode is roughly 10^{10} electrons/cm². When starting the ion pump the initial voltages applied are relatively low perhaps 1000 to 3000V however the voltage ramps up as needed to maintain the previously stated steady state electron density and eventually tops out at 6000V.

The various gases in a vacuum chamber can have very different pumping methods, speeds and effects. As previously explained Argon is a problem in terms of pumping speed and retention in the cathode element but can be greatly improved by a change in pump design. The organic gases tend to be easily pumped by simple chemisorption after being dissociated by a high energy electron. Other active gases such as oxygen and nitrogen will react with the fresh titanium deposited on the anode surface and also by ion implantation. The one gas that has the potential to be a real problem is hydrogen. It is initially pumped by adsorption and ion burial. Once the hydrogen is captured, it can diffuse into the bulk and form a hydride for permanent removal. However, continual pumping of hydrogen can cause the titanium plates to warp, and release gas as the cathode plates heat up. The good news is that there seems to be no rate

limit to the pumping until the cathode surface is covered by other molecules that eliminate the abilities of hydrogen to diffuse into the bulk. This is easily solved by pumping on active gases such as Oxygen or Nitrogen to break up and sputter a new cathode surface. (One unique observation about starting the ion pumps on our system at pressures $\geq 10^{-6}$ torr, is that a glow discharge can be seen in the ion pump. This discharge heats the cathodes and releases hydrogen gas but should rapidly diminish as the ion pump continues to pump. If the glow discharge does not extinguish quickly, this may be a symptom of contamination problems.)

All ion pumps have an average rated useable lifetime giving to them by the manufacturer. This lifetime can vary with the gases pumped, but mostly it scales inversely with the pressures it sees. At a working pressure of 10^{-4} the ion pump will last only a few tens of hours before it will not operate properly. Whereas at the pressures we operate our UHV chamber at, the rated lifetime is on the order of hundreds of thousands to millions of hours operation. So for true UHV operation there is little that needs to be done to maintain these ion pumps. That is not to say that there are no problems that can arise with a UHV ion pump, but for the most part they should not need to be rebuilt in its, or our, lifetime.

The problems arising with UHV ion pumps can be; reduced pumping speeds due to Hydrogen saturation, Argon saturation, or hydrocarbon chamber contamination. The hydrogen problem has been discussed previously and is fixed by pumping on a reactive gas for a short time. The Argon problem can be solved in two ways. First the pressure in the chamber can be increased to 5×10^{-5} torr with oxygen and left to pump for 10 to 12 hours. This sputters enough cathode material to completely give a new cathode surface

for the Argon to be implanted into. The second method for Argon recovery is to remove the cathode plates from the pump and bead blast them so that the first few microns of cathode material is removed leaving a new surface. The solution for hydrocarbon contamination is hopefully just simple time and temperature, a long high temperature bake is probably the best thing, then deal with pump saturation issues once the pressure is mostly recovered.

When an ion pump fails, it is usually by either gas saturation, or electrical breakdown. Gas saturation has been addressed above, and can be fixed in situ or by removal of the cathode plates. One item to be mentioned about the cathode plate removal is that bead blasting is not the only physical way to fix the pump. The simplest method is simply flip the plates so that the pumping action is being done on the untouched surface of the cathode. With electrical failure the pump has usually pumped too much hydrogen and other reactive gases which cause the cathode material to start flaking and cause shorts. To recover from this type of breakdown, simply disassemble the ion pump's pumping elements and completely clean them.

A complete physical cleaning of the ion pump elements consists of wiping off using a Kimwipe, excess material from the cathode plates, the anode surfaces and wiping clean the vacuum walls that enclose the pumping elements (Keep everything UHV clean, wear gloves). Special attention needs to be paid to the ceramic spacers that isolate the high voltage anode from the ground potential of the cathodes and rest of the pump. The most likely cause of electrical breakdown is that the flakes of titanium turn to a powder that falls down onto these ceramic spacers, coating them and causing a short.

The disassembly of an ion pump is relatively simple; it requires 3 wrenches 1/4, 3/8, and a 5/16 also a Philips head screwdriver. The first step is to vent the ion pump and remove one of the flanges to gain access to the pump elements. Once it is possible to get your hand into the pump, use the ¼ inch wrench to remove the nuts from the high voltage anode leads. The ¼ inch nuts hold a power strip down, making an electrical connection from the electrical feedthrough to all the pump elements. It is recommended that you remove all the connections to this power strip and remove it from the vacuum chamber. After the power strip has been removed it is easy to gain access to the pumping elements, so use the 3/8 inch wrench to unbolt the pump elements from the vacuum pump walls. Next gently work the elements out of the vacuum envelopes. (Repair one pump element at a time!)

Once the pumping element is out of the pump, use a 5/16 inch wrench on the nut at the top middle of each cathode plate and a screwdriver on the other side to separate the cathode from its holder. There are four bolts that have to be removed before the cathode and anode completely separate. Once the bolts are removed the housing/holder will separate from the cathode and anode, then you should have a total of 5 component pieces. Examine the condition of the cathode and anode carefully. If there is debris inside the cylinders of the anode clean them out with a Kimwipe and your glove covered finger. Be sure to remove all of the loose material off the anode and cathode. Next, gently tap the anode/cathode holders to remove the loose debris. Then test the resistance across the ceramic spacers at multiple points on the ceramic to make sure there is no chance of shorting by material that has plated on to the ceramic (because more than likely the ceramic will no longer be the bright white clean piece it was when it started its life. It will

look dark and maybe even shiny in some places.) If the ceramic is too contaminated and provides anything less than infinite resistance across it, CLEAN it, or replace it. The plated titanium can be removed by soaking it in a sulfuric acid / nitric acid (an aqua regia solution can be used) bath for a while. If you really want to get aggressive with it a boiling sulfuric acid solution with hydrogen peroxide (piranha solution) will digest the titanium and any other metal on the ceramic and then start to digest the ceramic so only use this as a last resort, and for short periods of time. Most likely if a piranha solution is needed it is best to buy replacement pieces from either Duniway Stockroom, or directly from Gamma Vacuum (which is the new incarnation of PHI).

If the cathode material is excessively worn, the plate may be flipped to expose a new pumping surface. Towards the end of the effective life of the cathode plate it would be possible to mill off one end of the plate making it slightly shorter and drill a new hole for the bolt to attach the cathode to the holder. This change effectively moves the point where sputtering occurs on the plate to a new area which should act almost like a new plate. There may be some initial outgassing of material but should be eliminated quickly. Effectively by making these periodic changes, it is theoretically possible to extend the lifetime of these ion pumps to infinity. However, if the cathode is just too far gone or is just too contaminated by hydrocarbons/argon etc. new plates are easily obtained. But, due to the expense of tantalum moving the plate around is the best way to fix these pumps.

Once all the components are clean and free of debris, reassemble the pump element and test the resistance across the anode to the cathode, it better be infinite! Clean all the elements and replace them back the way they were and test the resistance from anode to the cathode and pump wall (this better still be infinite). Next, reattach the power

strip to the anode high voltage leads. Please be careful when tightening the nut down on the electrical vacuum feed through! This is a small threaded rod that is free standing in the vacuum chamber and is only supported by being attached to the ceramic isolator/vacuum seal, it is very possible to over torque this nut and break the ceramic seal, making good contact is all that is necessary DON'T OVER TIGHTEN.

Now that everything is cleaned and reassembled rough the pump back down. It may be a good idea to let the turbo-molecular pump on it overnight just to give it a good starting pressure. But, once the ion pump is under vacuum it is certainly possible to start it up. Most likely the initial start up of the pump is going to liberate a lot of gas and the ion pump will not be able to keep up with itself so continue to pump on it with the turbo-molecular pump. After a while, the cathode should have enough material sputtered away that it will start to get into a rhythm of its own and pump more and more. The ion pump controller will more than likely let the pump run for a period of time and then shut it down on its own. This is a safety feature to keep the pump from overheating and warping the cathodes. You will find that the first time the pump starts after an hour of pumping the sides may become noticeably warm which is due to the glow discharge happening in the pump, but after the ion pump is turned off and allowed to cool once again, more than likely the pump should start up fine the next time now that it has been out gassed.

Recommended Reading Material:

- 1) "A User's Guide to Vacuum Technology" John F. O'Hanlon, 1989
- 2) Physical Electronics Ion Pump Users manual
- 3) "Getter and Getter – Ion Vacuum Pumps" Georgii Saksaganskii 1994
- 4) "High Vacuum Technology" Marshed, Hablanian, 1990
- 5) "Ultra High Vacuum Practice" G. F. Weston, 1985

Bake out procedure

A thorough bakeout of the STM surface science chamber is critical for attaining good ultra high vacuum (UHV) and working pressures in the mid 10^{-11} torr range necessary to keep the surface clean over extended STM imaging experiments. The bakeout is used to drive off water and adventitious hydrocarbons that have adsorbed onto the inside walls and surfaces of the chamber when it was opened to air. For an effective bakeout, the entire chamber needs to attain and maintain a temperature of 400 K for at least 24 hours. The higher the temperature that the chamber can attain the shorter the bakeout time required due to the Arrhenius form of the desorption rate constants. Ideally the chamber might be baked out at 500 K or higher. However, given all of the Viton, silver solder, and Teflon in the STM chamber, a maximum bakeout temperature of 423 K (150° C) should not be exceeded. Above 150° C Teflon and Viton become very outgassy materials, and the Viton starts to take a compression set which reduces its vibration dampening abilities. A temperature of 400 K is our usual temperature for baking. If there are contamination problems a higher temperature bake may be necessary, but here you may want to remove the damageable components (i.e. STM, Manipulator....). Remember that the amount of material that desorbs off the walls is exponential in temperature and linear in time!

To effectively bake out the chamber all parts need to be heated and maintain a temperature that does not differ much from the average bakeout temperature. If there are significant spatial deviations in temperature the chamber essentially performs a trap to trap distillation, where most of the material that was desorbed from a hot surface

becomes reabsorbed onto a relatively cooler surface. This can become a difficult problem with a spherical chamber and limited abilities to uniformly wrap and heat sections of the chamber. Specifically non-uniform bakeout temperatures can easily limit the ultimate working pressure that can be attained. To remedy this problem on the STM chamber Tobias Kuntsmann and I designed and built a bake out box that evenly heats the entire chamber. (There were some complications in measuring and constructing the box that left some gaps and uneven joints that are simply patched with insulation.)

There are 13 parts to the bake out box and the assembly starts at the bottom. First make sure that there is an array of $\frac{1}{4}$ -20 socket cap screws, screwed into the table that are approximately $\frac{1}{2}$ inch protruding from the table top. The bottom panels will sit on these bolts to allow air circulation between the bake out box and the optics table. This is done because the optics table can handle a maximum temperature of 60° C due to the glue used for construction of the honeycomb dampening network inside the table. Once the bottom panels are installed the side panels are installed one at a time and bolted together. The box is a sort of jig-saw puzzle that will only go together one way. A final assemble picture can be seen in image Figure 5.

Figure 5 Images of the bakeout box assembled around the STM chamber.

The bakeout box has two heating elements in it that are easy to recognize, they were the remnants of an electric table top stove. These heating elements are a very efficient way of heating the bake out box, and the oven heating elements are wired such that they plug into a 120 V variac for simple use. It is possible to wire them to use a 220V

variac to get more heat, but not necessary. There are four additional heating elements that are used along with the stove top heaters: the ion pump heaters, two on the mass spectrometer, and one on the main ion pump. The mass spectrometer and its ion pump heaters were designed into the bake out box to efficiently utilize the heat generated by the pump heaters. The fourth heater is an infra red lamp heater that is inside the chamber. The fifth heating element was a last minute addition to give just a bit more heating power to the bake out box. It is a 1000 W heating plate that is bolted to the inside of one of the bake out box panels and is wired to be plugged into a 120 V variac.

With all of the heating elements spread around the chamber there may not be need for additional circulation of the air inside the box but to make everything heat evenly there was a convection fan from an oven that was installed on the top panel that circulates the air around the bake out box. The fan is wired, so that it can be plugged directly into a 110 V wall socket.

Monitoring the progress in temperature is done by installing a few thermocouple probes around the bake out box to make sure everything is heating evenly. To monitor the temperature there are two thermocouples inside the chamber; 1) attached to the STM support stalk, and 2) the thermocouple attached to the Pt crystal. Then I also install a thermocouple that makes contact with a window flange near the center of the chamber and another thermocouple that sits in mid air to monitor the air temperature inside the box. The thermocouple that is attached to the Pt crystal is typically what is used to measure the final temperature of the chamber because it has the longest time constant for heating up. The crystal temperature is monitored by the computer, the other

thermocouples are periodically tested by a multimeter to spot check the conditions of the bake out box.

Before bakeout starts all nonessential and certainly any non-bakeable wiring needs to be removed. The only wires that should still be connected are the thermocouple wires, the ion pump wires heating and power wires, the power wire for the IR lamp heater, and the wires for the ion gauge.

Once the bake out has been started the heating process takes about 24 hours to come to temperature. This is not to say that the temperature in the chamber can't be raised to 400 K in a matter of a few hours. It takes time for the ion pump to keep up with the amount of gas that is being desorbed off the walls. With uniform heating of the chamber the temperature has to be gradually turned up a little at a time. With each increase of voltage to the heating elements the thermocouples will each monitor an increase in temperature with time. The order of temperature increase is typically first the air monitoring temperature thermocouple followed by the thermocouple connected to the flange and then the STM thermocouple and finally the crystal thermocouple. Each increase in voltage can be monitored by both the temperature reported by the thermocouples, and by the pressure monitored by the ion gauge and ion pump controller. If a pressure of greater than 3×10^5 torr is reported on the ion pump controller for an extended period of time the ion pump will shut down to cool, which stops the pumping. Therefore monitoring the ion pump pressure reading along with the temperature is critical. Note: the ion pump pumping speed drops as the temperature increases, so with an increased outgassing rate the pressure can easily runaway if the temperature is raised too quickly.

Once the chamber temperature is at 400 K the chamber continues to bake until the pressure reading drops to an acceptable level (typically I expect to reach 5×10^{-8} torr while hot). However, monitoring the pump down curve (Pressure vs. Time) will indicate if the desired pressure will take another 5 hours or 5 years of baking. To monitor the bake out process I wrote a Labview program that monitors both the chamber pressure and crystal temperature as a function of time. A typical bake out process should look like Figure 6 (Use of this program is very useful for monitoring the bake out progression from home, because it is set up to broadcast to a web server that can be monitored from anywhere in the world over the internet.)

The bake out of the chamber is done occasionally and generally only after the chamber has been vented to atmosphere. However, the STM is typically baked out once a week to replace the STM tip (ideally once a month). To bake out the STM the bake out box is not needed. The STM section can be wrapped with two heating tapes and baked out into the manifold turbomolecular pump. Typically the pressure of the STM bake out comes down to the low 10^{-7} 's or high 10^{-8} 's torr pressure while hot. It generally can be heated and baked to its ultimate pressure within 12 hours.

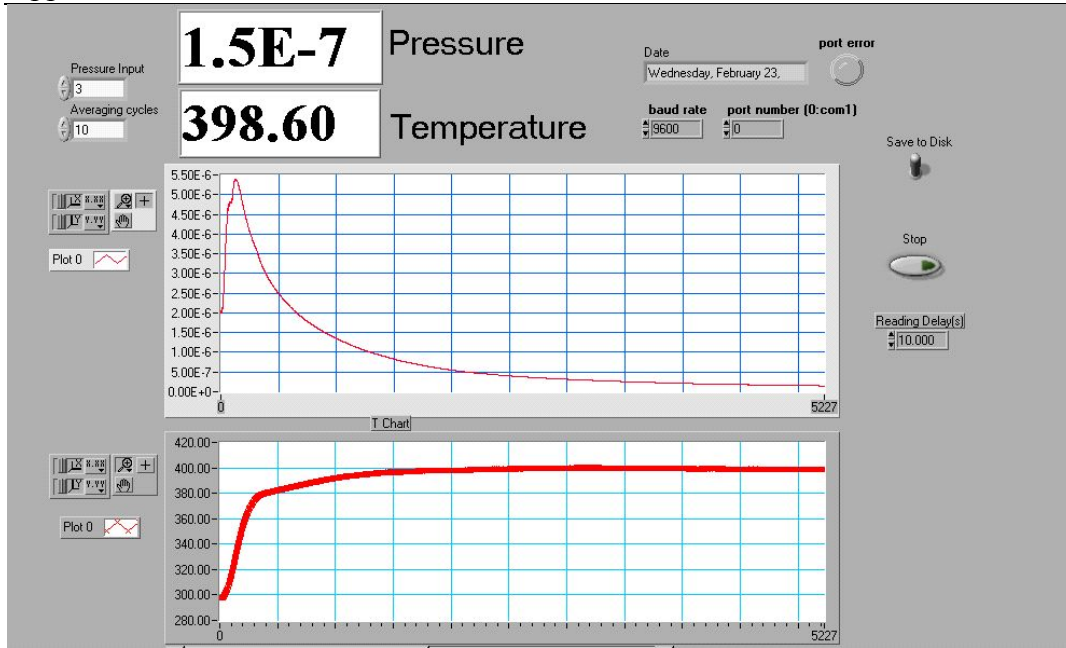
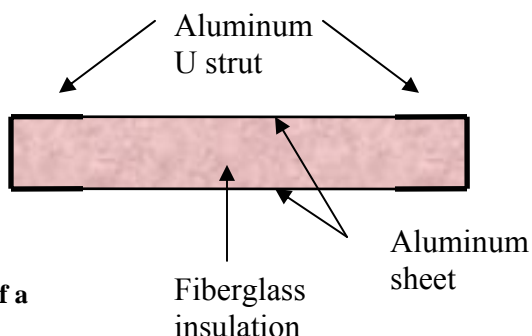


Figure 6 Screen capture of the bakeout program in Labview, showing a nice bakeout curve in pressure and temperature.

Construction of a bake out box is simple. The sides of each panel are made from aluminum 1" U strut, and the faces of each panel are made of 1/32" aluminum sheets. The U strut is cut to length and laid out together to form the framework, making sure that the open end of the U is facing into the center of the panel. Next, the aluminum sheet that has been cut to the correct dimensions is placed on the top of the U strut framework and a drill is used to drill holes through the aluminum sheet and U strut. After the holes have been drilled a rivet gun is used to attach the sheet to the U strut. The partial assembly is then flipped over so insulation can be stuffed into the interior space. The insulation is a standard fiberglass insulation that can be found at Lowe's. (The insulation is most effective if it isn't packed down tightly.) Once the insulation has been placed in the panel, repeat the procedure for attaching the aluminum sheet to the U strut. An image of the panel and assembly can be seen in Figure 7.

Bake Out Box Numbered Panels <i>(Panels are numbered in assembly order and require the number on the panel to face the outside of the bake out box)</i>		
Panel Pieces #	Panel description	If heater is attached, Typical variac setting used
1	Bottom Front	
2	Bottom Back	
3	Right side	
4	Back Lower Side	
5	Ion Pump Side	
6	Ion Pump Top	
7	Back Side	
8	Front	90 V
9	Left Side	
10	Lower Back Left Side	
11	Upper Back Left Side	30 – 40 V
12	Bottom Left Front	
13	Top	90 V
14	Upper Back Left Side Ion Pump	
Other Variac settings for heaters		
	Ion Pump Heaters	90 V
	IR Lamp	12-15 V
	Typical Heat Tape settings (if used)	26-28 V



**Figure 7 cross section of a
bakeout box panel**

F)

Shaker STM construction:

The Shaker STM idea was originally conceived by Mugele¹ in conjunction with Rolf Möller's lab at Essen Germany. I first became aware about it through discussions with Torsten Wagner, and then a more detailed description from Tobias Kuntsmann² both from the University of Essen in Rolf Möller's lab. At Essen they had constructed one, and were very excited about its design. Meanwhile, in the summer of 2004 I visited

Miguel Salmeron's lab at the University of California Berkeley and discussed many STM issues with the students and post-docs there³. One discussion led to the knowledge that they had switched from a beetle STM design to the shaker design and have been generating amazing images with it.

Details of Salmeron's shaker STM construction were similar to those recently described by Möller and Koel (see Figure 8). The basic set up is a single piezo tube that

houses a tip holder tube that moves in and out along the long axis of the piezo tube. The tip holder may be a

dumbbell shaped piece that slides on rails and held in place by magnets, as described by Möller and Koel, or

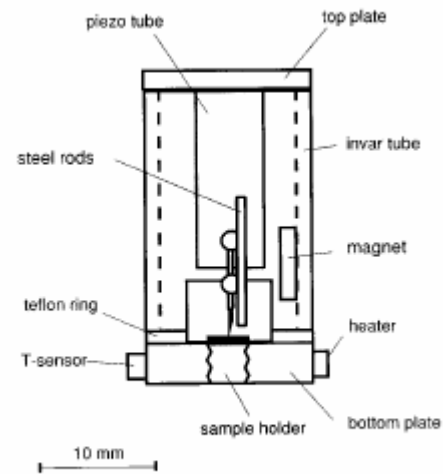
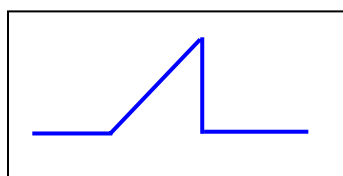


Figure 8 Mugele Shaker STM

**Figure 9 Approach waveform
for a beetle STM**



may be a tube that slides on SiN balls with the tube held in place by a Pt wire using spring tension applied to the tube as Salmeron's group does (The Salmeron's design is like the design described in this document). In all cases the difficulty is in setting the force that holds the tip holder in place. If the force is too large the tip holder will not slide and if it's too loose then the rigidity of the system is reduced. As described by Mugele onset of sliding is determined by the relationship between the static and dynamic forces on the tube tip. The eq. (1.1)

$$a > \left(\frac{\mu_{static} F_{normal}}{m} \right) \quad (1.1)$$

depicts the conditions between the static and dynamic forces that need to be met in order for the tube to move. On the left side of the equation there is the dynamical force that has had the mass divided out, leaving the acceleration of the tube to be the crucial factor. Then on the right side is the static forces that need to be overcome divided by the mass of the tube. If the acceleration is larger than the right side of the equation then movement will occur. In our case the force normal had two components associated with it, 1) the force of gravity holding the tube in place being the STM is mounted horizontally, and 2) the force applied by the spring wire.

The action by which the tip tube moves within the piezo is like a beetle STM when it moves along a ramp; both use a slip-stick motion. Papers and conversations suggest that the slip-stick motion of the shaker design is not as straight forward as the beetle design. Where as in a beetle STM, movement is created by application of a simple sawtooth waveform Figure 9 the shaker plans requires a more parabolic waveform with sharp rates of change on the sides of the approach waveform Figure 10.



Figure 10
Approach
waveform for a
Shaker STM

The body around the piezo tube in our “Shaker” STM is made from a single piece of copper that yields a very rigid construction and an isothermal STM and tip (Figure 11). The rigidity of the STM is a function of a single piezo tube tightly bonded to a single piece of metal used in the STM body and, having that piezo/body very securely attach the crystal mount with SmCo rare earth magnets (an estimated 5 oz force per magnet at a distance of 0.010 inches, with a total of 6 magnets holding a STM that weights 2 oz. total). Another advantage with the STM held tightly to the crystal mount is a strong coupling of the STM temperature to the crystal mount temperature and therefore the crystal. Advantages of an isothermal system are; the long term lateral thermal drift of the beetle design can be minimized, also, because the tip is surrounded by material at a low temperature the tip should cool to the same temperature as the crystal and copper body by radiative heat loss and heat conduction from the tip to the shaker body. Once the tip is cooled to a very low stable temperature, repeatable and reliable scanning tunneling spectroscopes become more likely since the motion of atoms or other molecules adsorbed onto the tip are greatly diminished.

The construction process of a shaker STM is straight forward. No exotic materials are used to fabricate the Shaker STM. Due to the variation of thermal expansion of each material there is an inherent advantage to using as few different materials as possible. Therefore the Shaker STM is almost made exclusively of copper with a small amount of Vespel, stainless steel, silicon nitride, and of course the piezoelectric material Figure 11.

The mount holds the platinum crystal and what the SmCo magnets pin the STM to is made of Nickel, and according to the machine shop was the most difficult piece to fabricate. All assembly plans for the shaker STM can be found at the end of this document.

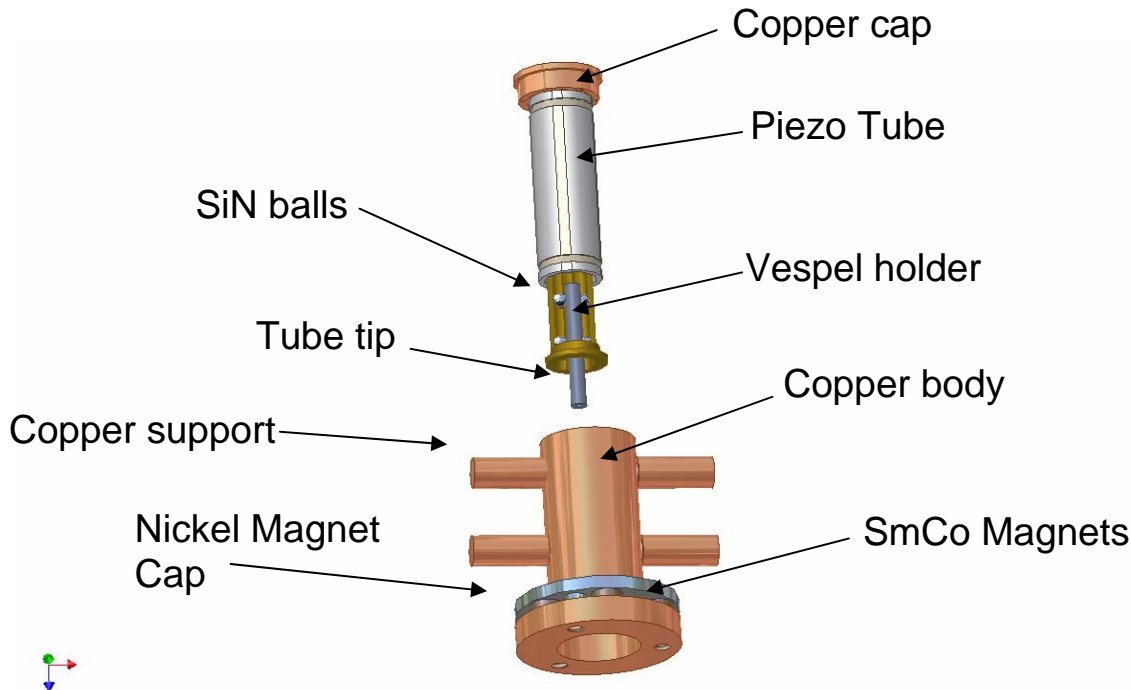


Figure 11 Shaker STM exploded view

The specifics for the Shaker STM assembly are as follows: The first step is to clean all pieces and fit all parts together sequentially; this insures that all parts will go together correctly and should not contain any surprises later during final assembly. First, start on the assembly of the Vespel piece; epoxy the SiN balls into the grooves along the axis of the Vespel. The first set of balls should be aligned at 0.125" from the face of the Vespel piece. The second set should be fixed at 0.125" from the rear face of the Vespel piece, which leaves a distance of 0.25" between the sets of SiN balls. To attach the balls to the Vespel, first thin the epoxy with acetone so it is the consistency of whole milk.

Then add a drop of the thinned epoxy to the place on the Vespel that the SiN balls will attach too. Next, very carefully place the SiN ball in the epoxy droplet, and press in to make a solid connection. Add the second SiN ball in the same manner and align the two balls so that a line formed by connecting the centers of the two balls is perpendicular to the long axis of the Vespel piece. Before heating to cure the epoxy, check and double check to make sure there are no drops of epoxy or attached debris to the surface of the SiN balls that the tip tube slides along, if there is, remove the balls and thoroughly clean the SiN balls and the Vespel. Once the pieces pass inspection, heat to cure the epoxy at a temperature of 180° C for 120 min. After the first set of SiN balls have been attached and cured repeat the same procedure for attaching the second set.

Once the SiN balls are securely attached, the Pt spring wire must be epoxied into place. This step is by far the most difficult step in the shaker STM assembly. In future revisions, attachment of this wire could be made more convenient by using a very thin strip of Pt ribbon instead of wire, or by designing a hole for the wire to epoxy into on the top rim of the Vespel piece. However, for this step in the construction, I used a bent piece of stainless steel wire as a spring and fulcrum to hold the wire in place against the Vespel and used the top of a pair of tweezers to hold the other end of the wire up. This was a very crude method that worked for me, but I would recommend some creative thought here to find out what works best for you. Once the Pt wire was set in the correct position, a drop of the thinned epoxy was dabbed onto the wire and Vespel, and then cured. Key points to be very very aware of while making the Pt wire attachment is: Make sure that the wire is the correct length (~0.3"), long enough that the slight bend in the wire can meet and hold the tip holder at about mid-distance between the sets of SiN balls, And

more importantly that the wire runs exactly down the center of the Vespel piece! If the wire is not centered, when the tip tube is in place the wire will not hold the tube down against the SiN balls, instead it will push it to one side or another which makes the whole STM useless, SO BE CAREFUL!! See Figure 12 for correct alignment.

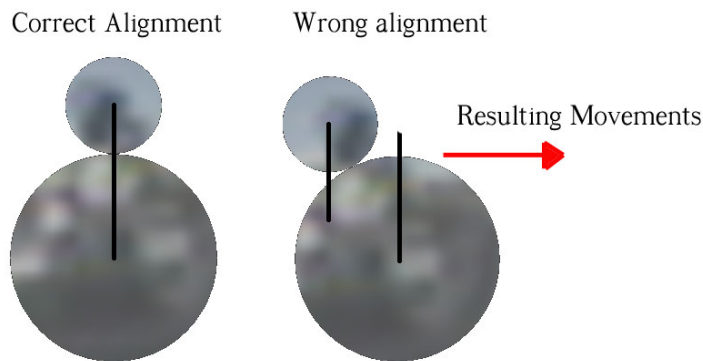


Figure 12. Correct and Incorrect alignment of the Pt spring wire against the tip tube holder. When the Pt wire presses down on the tube incorrectly the tip holder will be pushed laterally and be an obstacle for correct tip operation.

Once the Pt wire has been attached correctly, the tunneling current wire needs to be soldered onto the Pt spring wire. In this way the Pt wire serves a duel purpose, one to

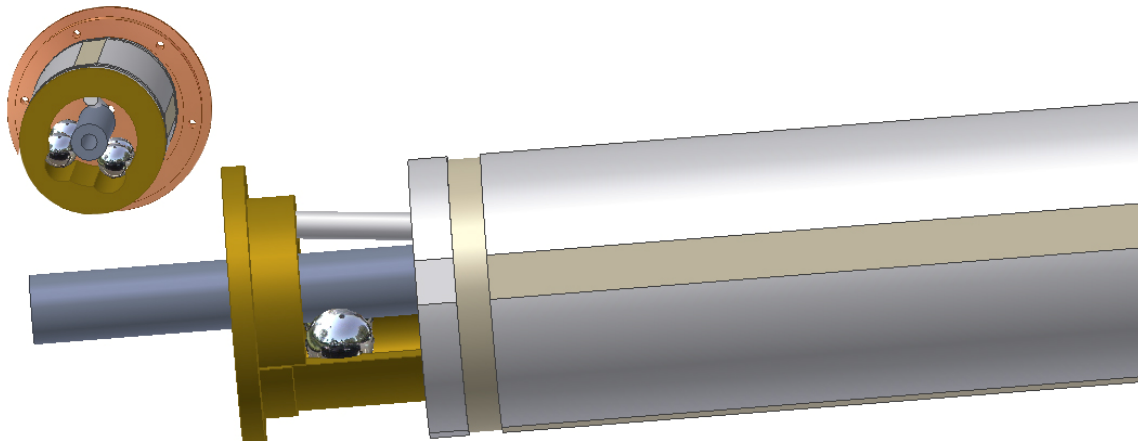


Figure 13 Alignment of the Pt spring wire and Vespel holder with respect to the piezo outer quadrant electrodes.

hold the tip tube in place, secondly to make an electrical connection to the STM tip. Once the 0.002" inch diameter kapton coated wire is soldered to the Pt wire, test the continuity of the soldering connection. Then run the tunneling wire through the Piezo tube and epoxy the Vespel piece into position in the piezo tube. The correct orientation of the Vespel piece in the Piezo tube would be, to have the Pt spring wire located at the top of the Vespel piece in line with a break in the nickel plating on the PZT that form the boundaries of two electrodes Figure 13. In this orientation the Vespel liner, which is resting on half of the curvature of the PZT, will not favor or hinder the movement in one axis vs. another, and will be distributed across both an X and Y electrode. Secondly the Vespel piece has to be epoxied into the end of the piezo tube that has the nickel plating remaining on the open face of the piezo so that the electrode wraps around from the outside to the inside. On the other open face of the piezo tube, the wrap around part of the electrode has been removed to prevent the possibility of the interior wall of the piezo grounding to the copper cap that the piezo is attached to in the next step.

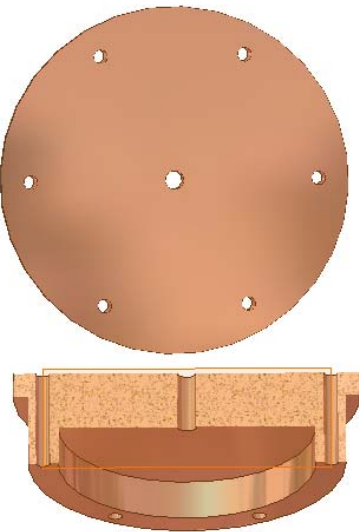


Figure 14 Copper cap which fits into the copper Shaker body, and the Piezo tube epoxies into. The piezo movement wires wires run through the outer holes in the top of the cap and the tunneling current wire is run through the center hole.

After the Vespel piece has been epoxied

into the piezo tube, thread the tunneling current wire through the hole at the center of the copper cap Figure 14. Align the piezo tube electrodes so that two of the holes on opposite sides on the rim of the copper cap are in line with two of the breaks between the X and Y electrodes on the piezo. This orientation allows for a straight and easy path for wires soldered to the electrodes to exit the back of the STM through the copper cap with holes near the centers of each electrode, additionally a wire can be attached to the Z scan electrode which

wraps around to the interior, so a grounding wire can be run along the break between the electrodes to minimize electrical crosstalk Figure 16. Once the piezo is oriented in the copper cap, attach it with the non conductive epoxy and cure it. After the epoxy has cured, solder the wires onto each electrode in the arrangement described above, but minimize the amount of solder used to attach the wires so that there is no chance the solder balls up on the electrode and creates a large protrusion that would ground the electrode to the wall of the STM body.

The next step is to attach the piezo/copper cap assembly into the copper shaker body. The orientation of the piezo assembly should be such that the bottom of the Vespel part is set towards the bottom of the shaker body. This allows the tip tube to be held down by gravity against the SiN balls in addition to the Pt spring wire. The copper cap can be attached to the copper body by either silver solder or epoxy. The differences between the epoxy and solder is that epoxy is easy to apply, but

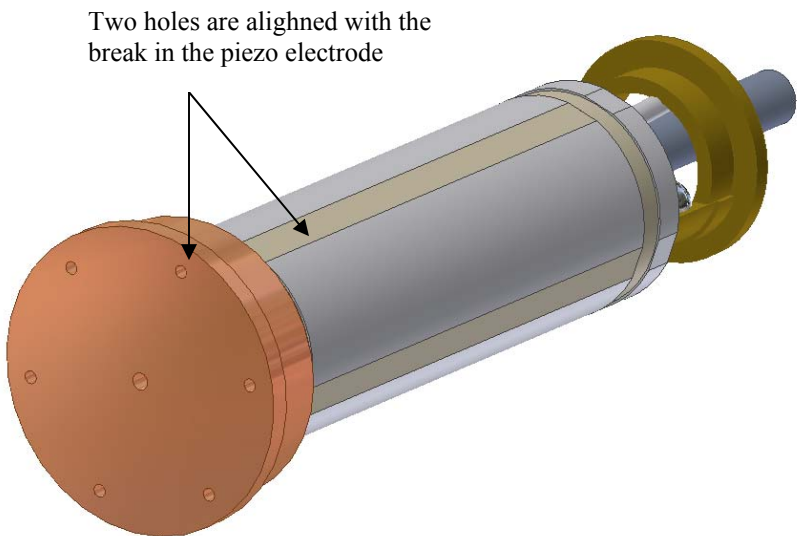
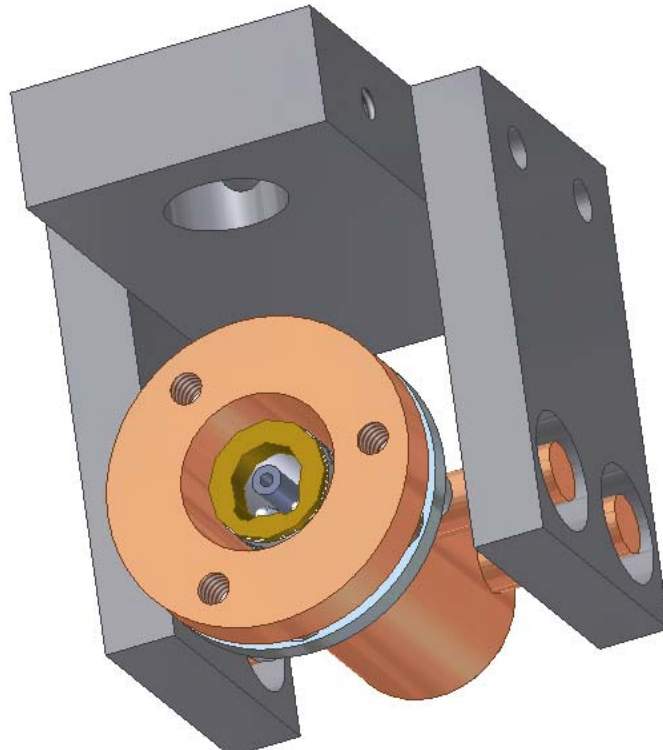


Figure 16 Shows the alignment for wiring the piezo with the least amount of crosstalk possible.

Figure 15 Final assembly image of the Shaker STM and holder.



permanent, whereas the silver solder is difficult to smoothly apply and remove because of the rapid heat conduction of the copper, but still possible to remove.

With the piezo set into the shaker body, the copper support rod can now be screwed into place. After the support rods have been secured into place all electrical connection need to be tested, to establish there are no electrical shorts between the electrodes on the piezo to the copper body. Next, start to position the SmCo magnets in place around the base of the shaker body. The orientation of the first magnet is of no consequence but after that the poles need to be placed in an alternating arrangement. Alternating the poles of the magnets help to minimize stray magnetic fields and maximizes magnetic fields locally. Now with the magnets set into the copper body ease the shaker STM onto something magnetic, this step is important before the nickel magnetic washer cap is to be placed down around the shaker STM. Next place the Ni washer cap down around the STM and over the SmCo magnets, the Ni washer is used to cap the magnetic fields created by the magnets. With the Ni cap in place, use the stainless steel screws to hold it down and in place. To reduce mass, if cooling is a problem, the stainless steel screws can be omitted because the nickel washer is held very tightly by the magnets themselves.

After the STM is assembled the holder can be built around it. Start by screwing one side of the stainless steel holder into the top holder and then place one set of the copper support rod off of the STM into the holes in the stainless steel side holder. Next place the second stainless steel side holder into position on the opposite side of the shaker STM and screw into the top holder as was done on the other side of the shaker. This forms a cage that the STM body can not be removed from with out removal of a side

holder but will allow the STM to be completely free from contact with the holder or UHV chamber once held by the crystal mount Figure 15.

The wiring of the STM is very simple. In the present version there are two possible wiring conventions. Both use the same connection paths but are wired differently at the STM controller. Therefore, the wire connections from the STM to the Teflon ring should be as seen in Figure 18. The convention as to what axis on the STM is X or Y doesn't matter, what does matter is that along one axis there is +X and -X components, and perpendicular to that axis is +Y and -Y components. In this configuration the STM can use the same wiring harness as the beetle STM and leave all connections on the back of the SPM 100 the same as that used for the Beetle STM operation. The change comes in how the jumpers are set in the SPM 100 controller. The difference in the two settings are that the inner electrode on the piezo can be grounded, like how our beetle head is wired, or the inner piezo electrode can be biased to be used as the Z scan and/or Z offset. There are problems with both configurations and the operator will need to choose what best suits their needs.

The problem with keeping the inner electrode grounded is that all voltages for piezo movements are applied to the outer four electrodes from one power operational amplifier, this can easily cause the output of the operational amplifier power stage to saturate due to multiple sources trying to drive the piezo, causing inaccurate movement and therefore a high possibility of tip crash. If the Z motion voltages are not applied to the X and Y electrodes, there can be a problem of inaccurate movement due to op-amp saturation, but this is typically not an issue for our operation due to the very small scan sizes (i.e. small voltage changes) unless care is not used when adjusting the X-Y offset.

Additionally if the Z voltages are applied to the piezo interior and not the X and Y electrodes the chance of tip crash due to limited movement is greatly reduced.

However, the main issue with putting a voltage on the inner piezo electrode is noise. When the inner electrode is grounded, it acts as a Faraday cage and shields the tunneling current wire from spurious noise. When there is an oscillating voltage applied to the inner electrode, there can be capacitive coupling onto the tunneling current wire that increases linearly as a function of

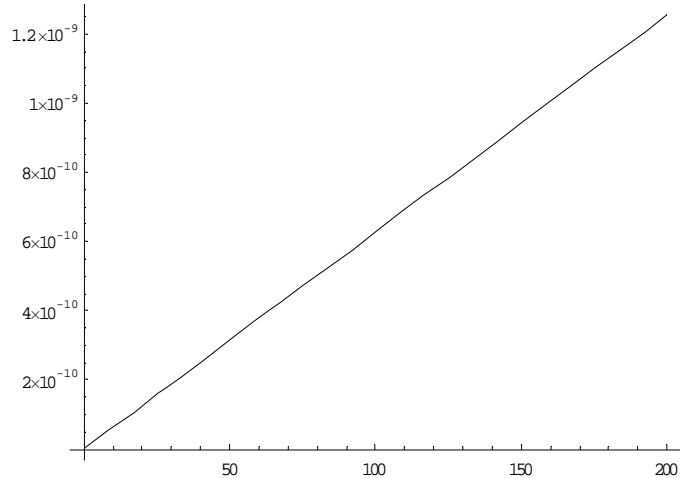


Figure 17 Plot of worst case scenario tunneling current noise in Amps vs. frequency in Hertz. (Calculation assuming a capacitance of .01 pF and 100 V applied to the inner piezo electrode.)

frequency (Figure 17). To minimize the capacitive coupling, a Z offset circuit separate from the Z scan can be used to make coarse changes to the tip position by applying the voltage to the inner electrode. Because the Z offset should vary at a much lower frequency than the Z scan signal, the capacitive coupling onto the tunneling current wire should be minimal, leaving the inner electrode to continue acting as a “modified” faraday cage.

The correct jumper setting in the RHK SPM-100 controller would be: For a grounded inner piezo electrode (i.e. possible op-amp saturation and tip crash, with low noise)

Board 1:

SW1: jumpers 1&2

SW2: jumpers 1&2

SW3: jumpers 1&2

Board 2:

SW1: jumpers 1&2

SW2: jumpers 1&2

SW3: jumpers 1&2

Board 3:

SW1: jumpers 2&3

SW2: jumpers 1&2

SW3: jumpers 1&2

Board 4:

SW1: jumpers 3&4

SW2: jumpers 3&4

For a Z offset applied to the inner piezo electrode and the Z Scan applied to the X and Y electrodes (i.e. possible Op-Amp saturation, lower potential for tip crash, acceptable noise).

Board 1:

SW1: jumpers 1&2

SW2: jumpers 1&2

SW3: jumpers 1&2

Board 2:

SW1: jumpers 2&3

SW2: jumpers 1&2

SW3: jumpers 1&2

Board 3:

SW1: jumpers 2&3

SW2: jumpers 2&3

SW3: jumpers 1&2

Board 4:

SW1: jumpers 3&4

SW2: jumpers 3&4

In either configuration there has to be a coarse approach mechanism used to get the STM tip into tunneling range. The shaker STM approaches just like its name. There is an applied waveform to the electrodes of the piezo, which creates movement such that the tube tip gets shaken into and out of position with a slip stick motion. In both configurations the shaking waveform will be applied to the Z Offset electrode (whether that voltage is applied to the inner piezo electrode or distributed across the four outer electrodes). As described earlier in Figure 10, the optimal Shaker approach waveform is a parabolic one with sharp voltage direction changes at the edges. Unfortunately, this optimal approach waveform can not be created in the RHK electronics/software. The best that we are able to due with the RHK is a fast large sawtooth waveform with slightly rounded corners (adjusted by the inertial filter). With the approach waveform applied to the inner piezo electrode implementing a “tip retract” mode approach is relatively simple. The voltages applied to the Z offset motion of the inner electrode need to be such that the distance the tip holder slides towards the crystal surface is less than the Z scan range motion. This configuration allows the Z scan to move the tip as far towards the surface as the piezo can move it and check to see if the tip is in tunneling range or not. If there is no tunneling current the Z scan voltage is removed to zero and a single approach waveform

is applied to the Z offset electrode which move the tip towards the crystal surface where the Z scan motion can check to see if the tip is within tunneling range or not again. This cycle is repeated numerous times until a tunneling current is detected. The “tip retract” approach mode is the safest way to approach a tip to the surface, with a trade off being that it is the slowest as well. Another mode of approach would be to just to apply the approach waveform until the tip holds a tunneling current without the intermediate tunneling current check (not recommended). If the Z offset voltage is being applied to the outer piezo electrodes with the Z scan voltage, the previously describe “tip retract” approach will still work, but more time would be needed between the tunneling current check and the approach waveform cycles than if the voltages were being applied to different electrodes so that the voltages can be fully removed from the piezo electrodes before the next movement is initiated.

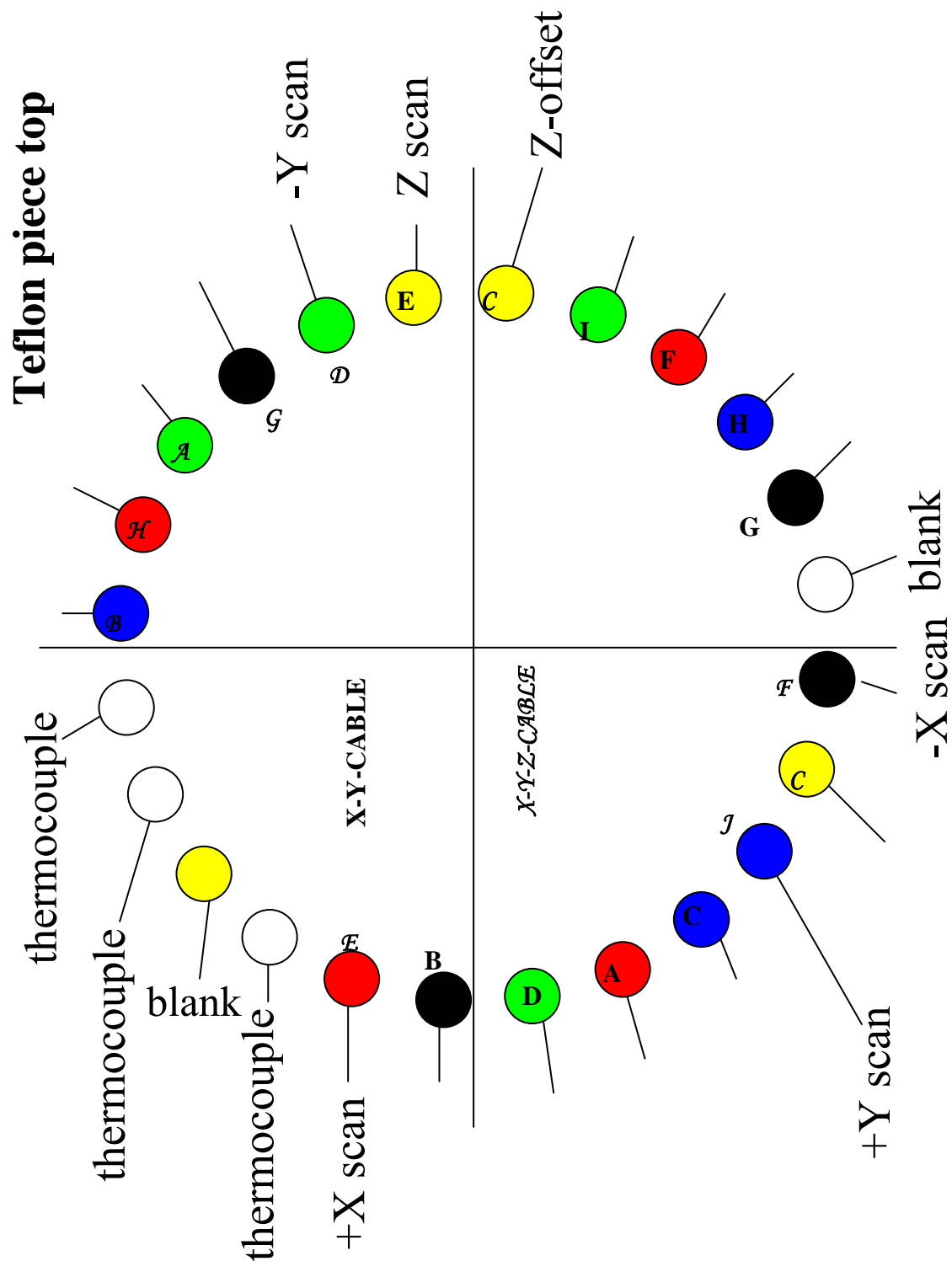
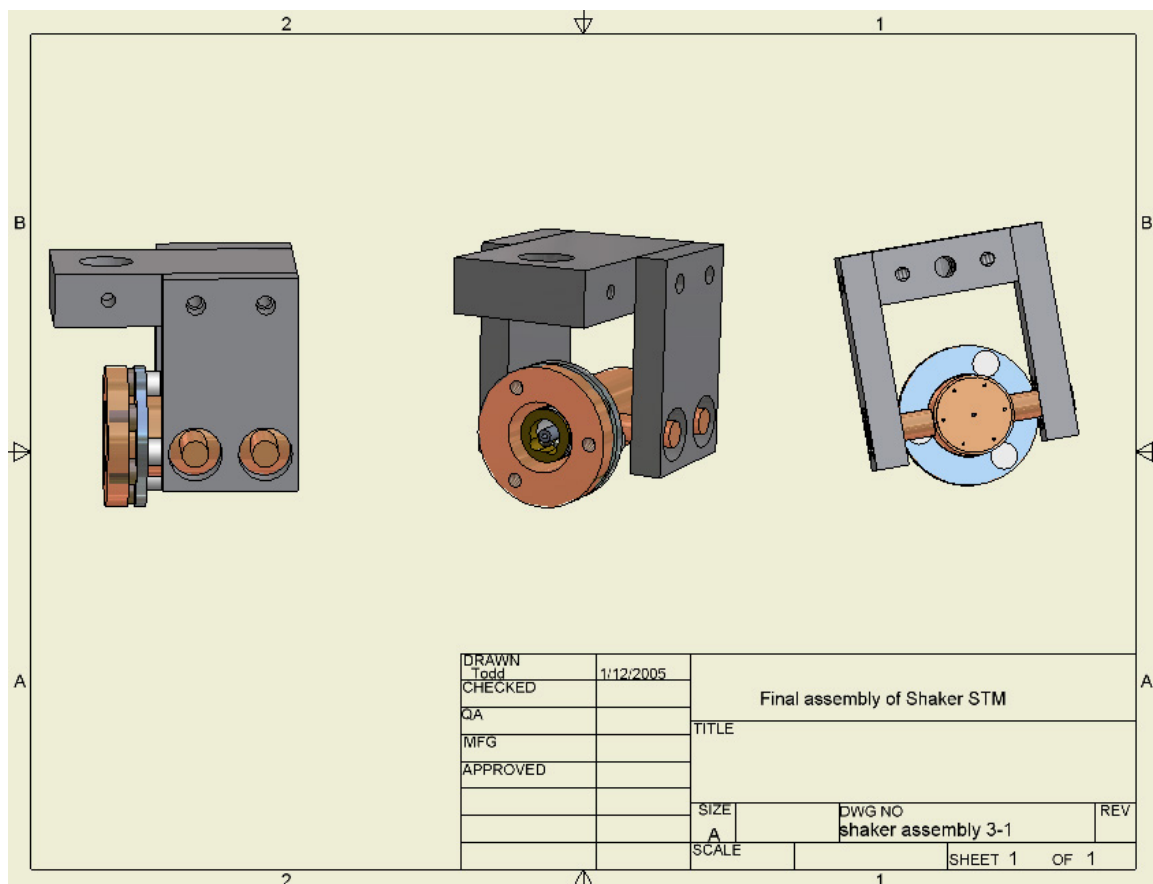
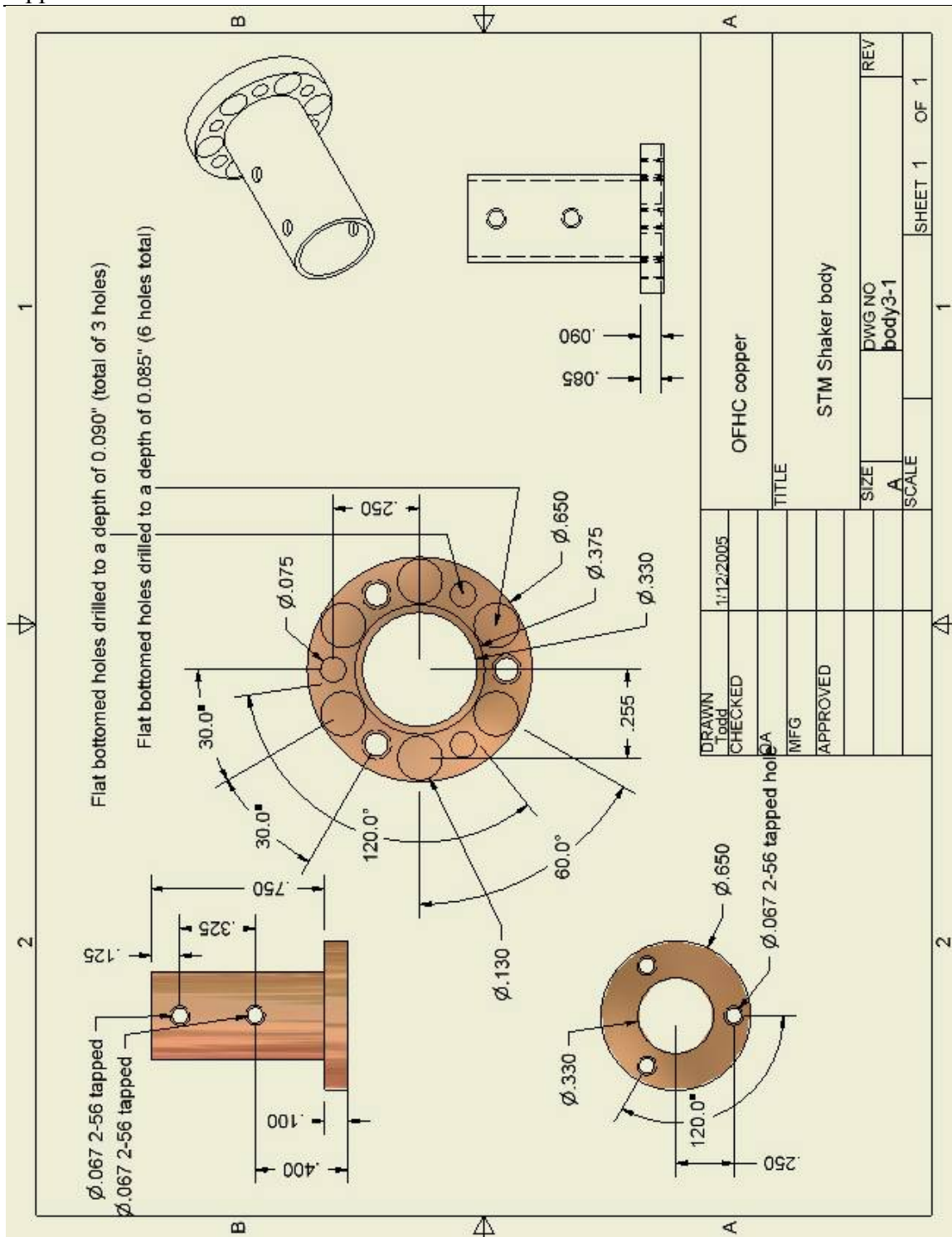


Figure 18 Wiring configuration for the Teflon ring on the STM support stalk, Showing connections for the +/- X and Y connections and the connection for the inner piezo electrode labeled here as Z offset.

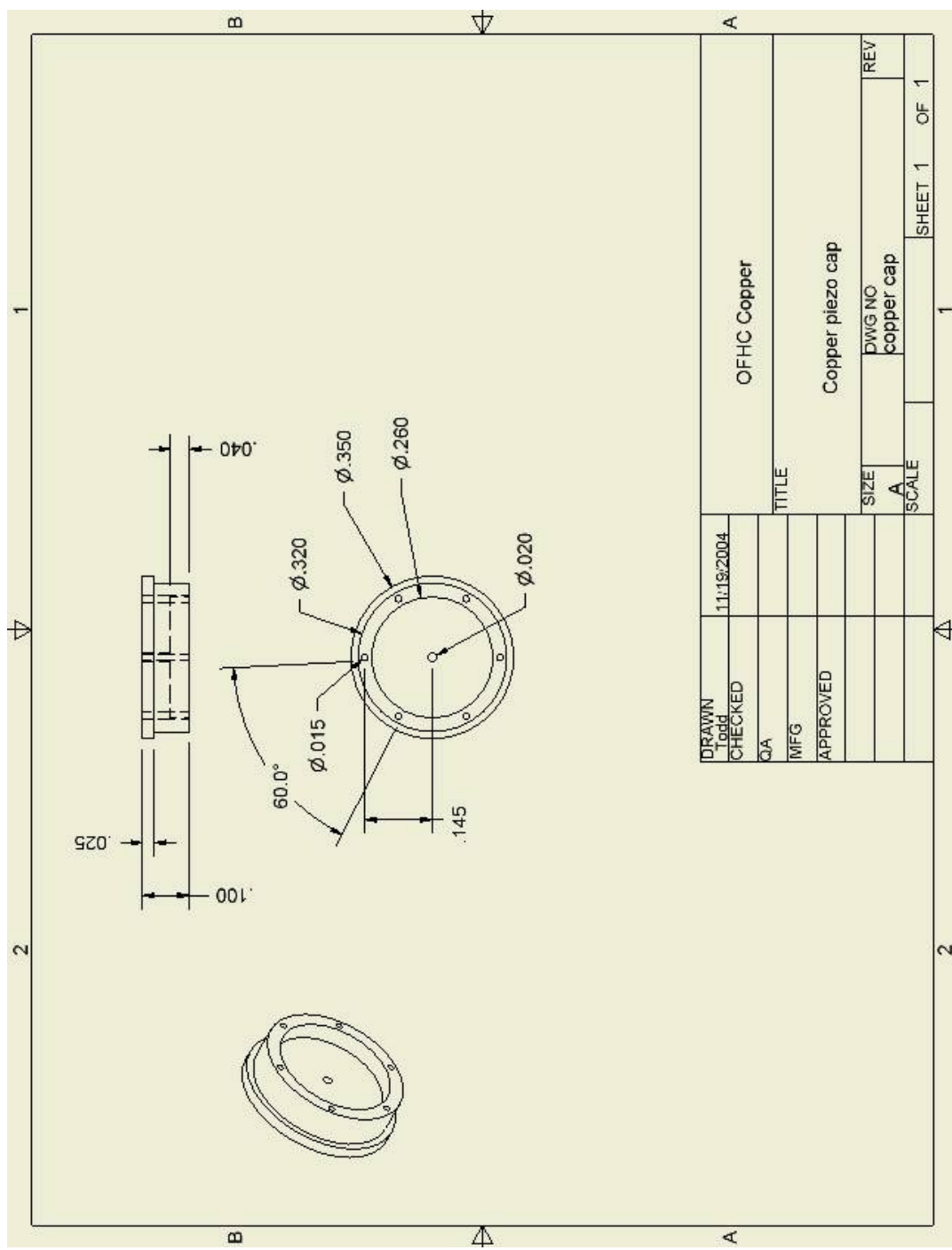
Construction blueprints:



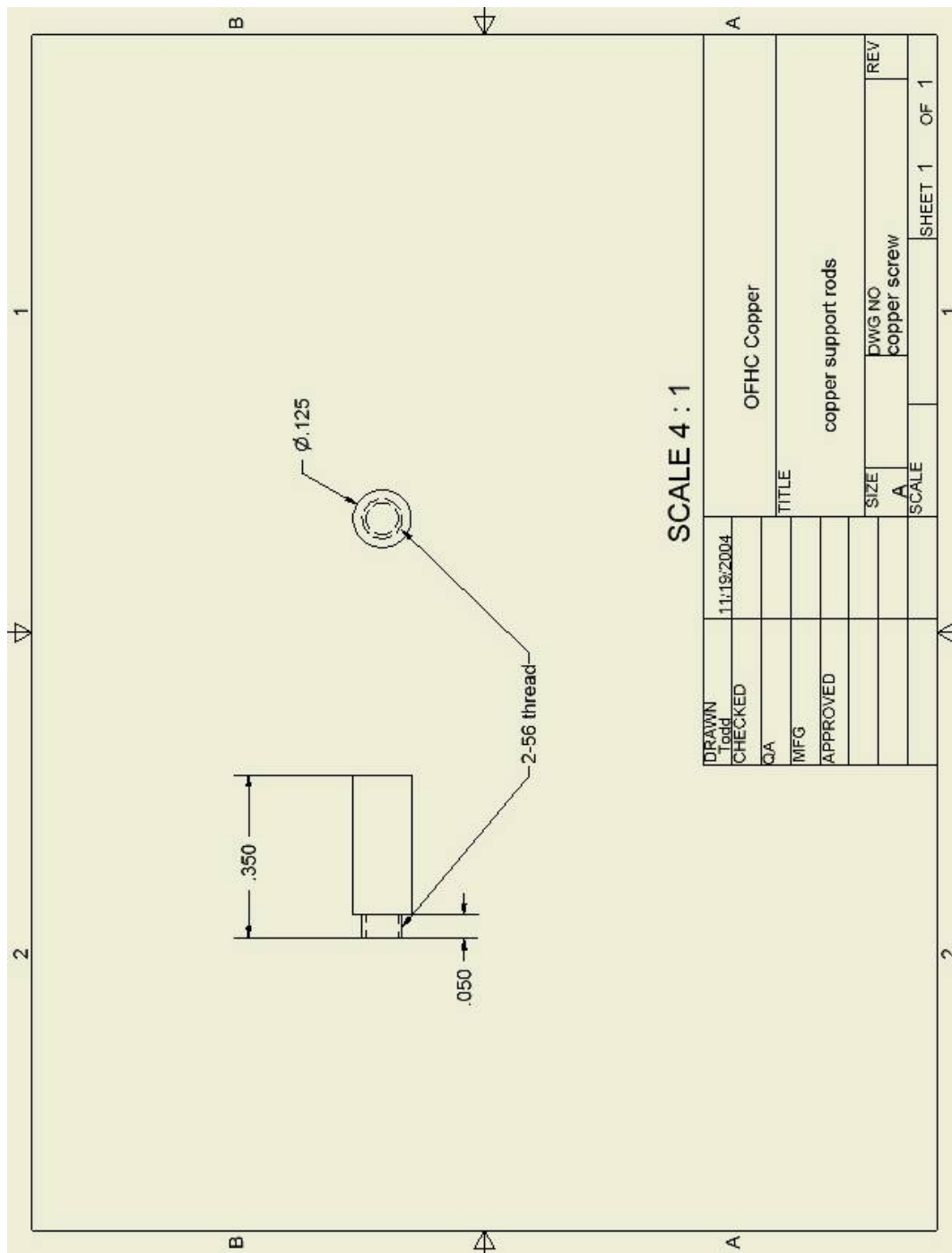
A final assembly view of the Shaker STM in its holder. The holder is attached to the STM support stalk by inserting the stalk into the hole at the top of the holder and a 2-56 thread screw press against the stalk holding it in place.

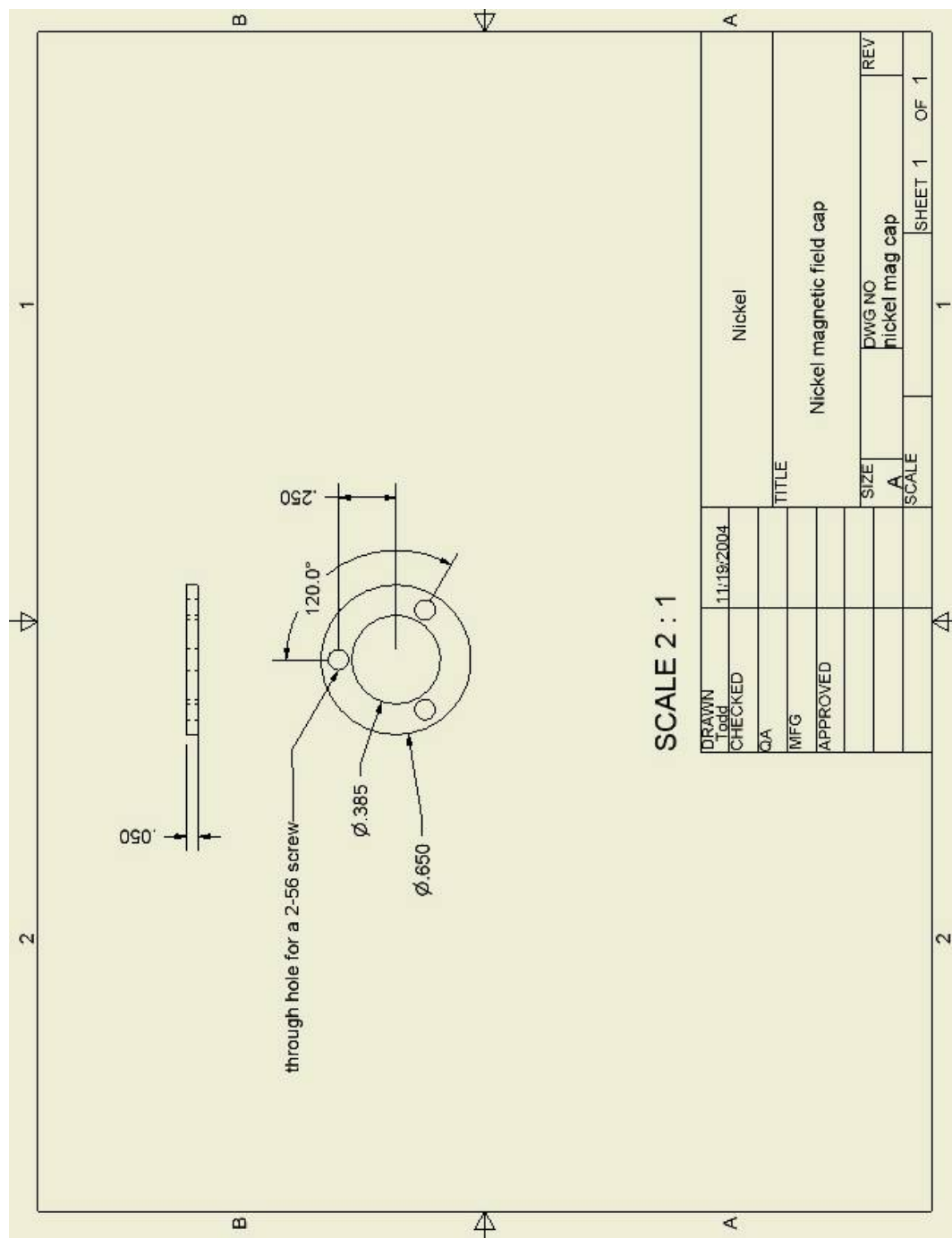


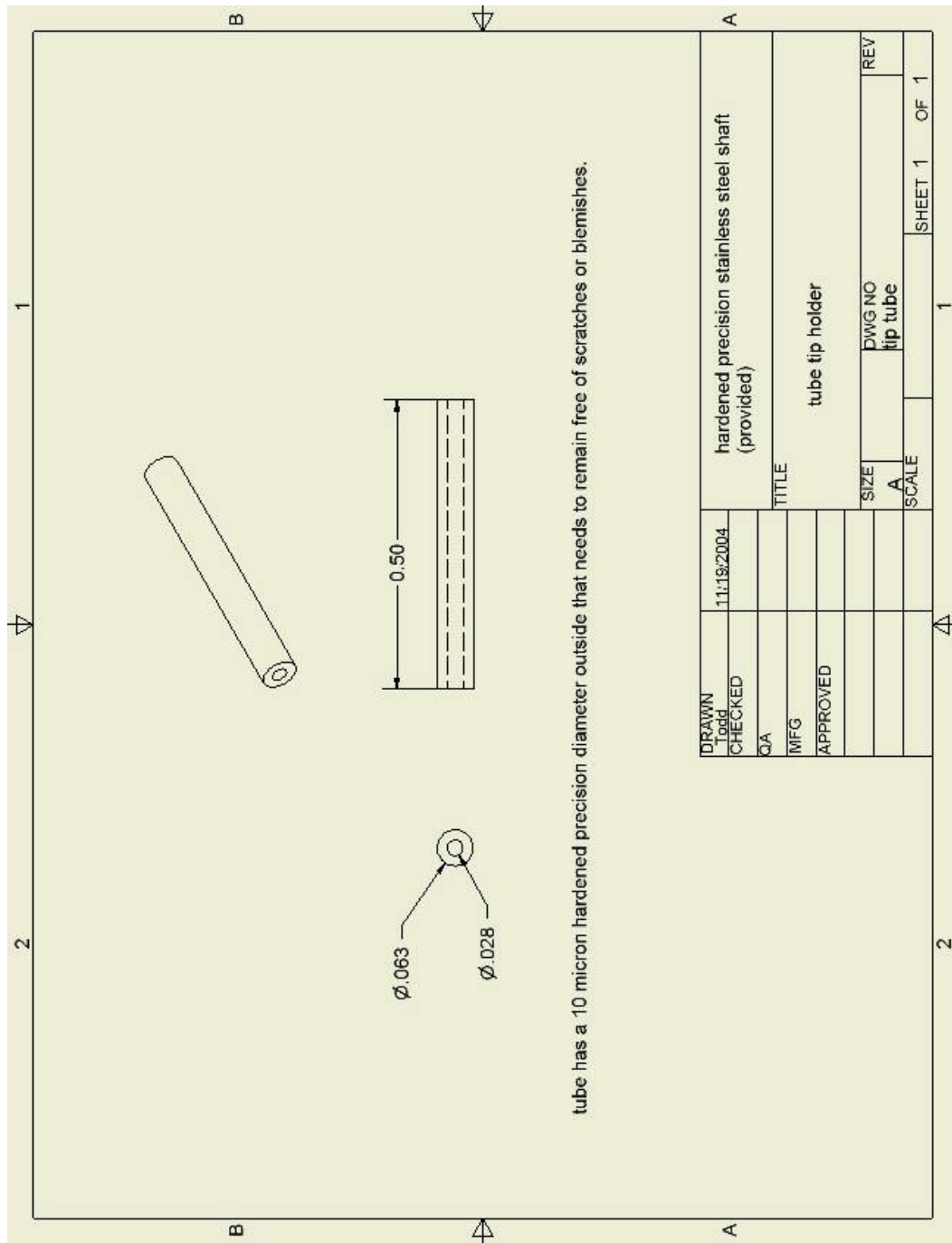
The body of the Shaker STM is made from a single piece of copper.

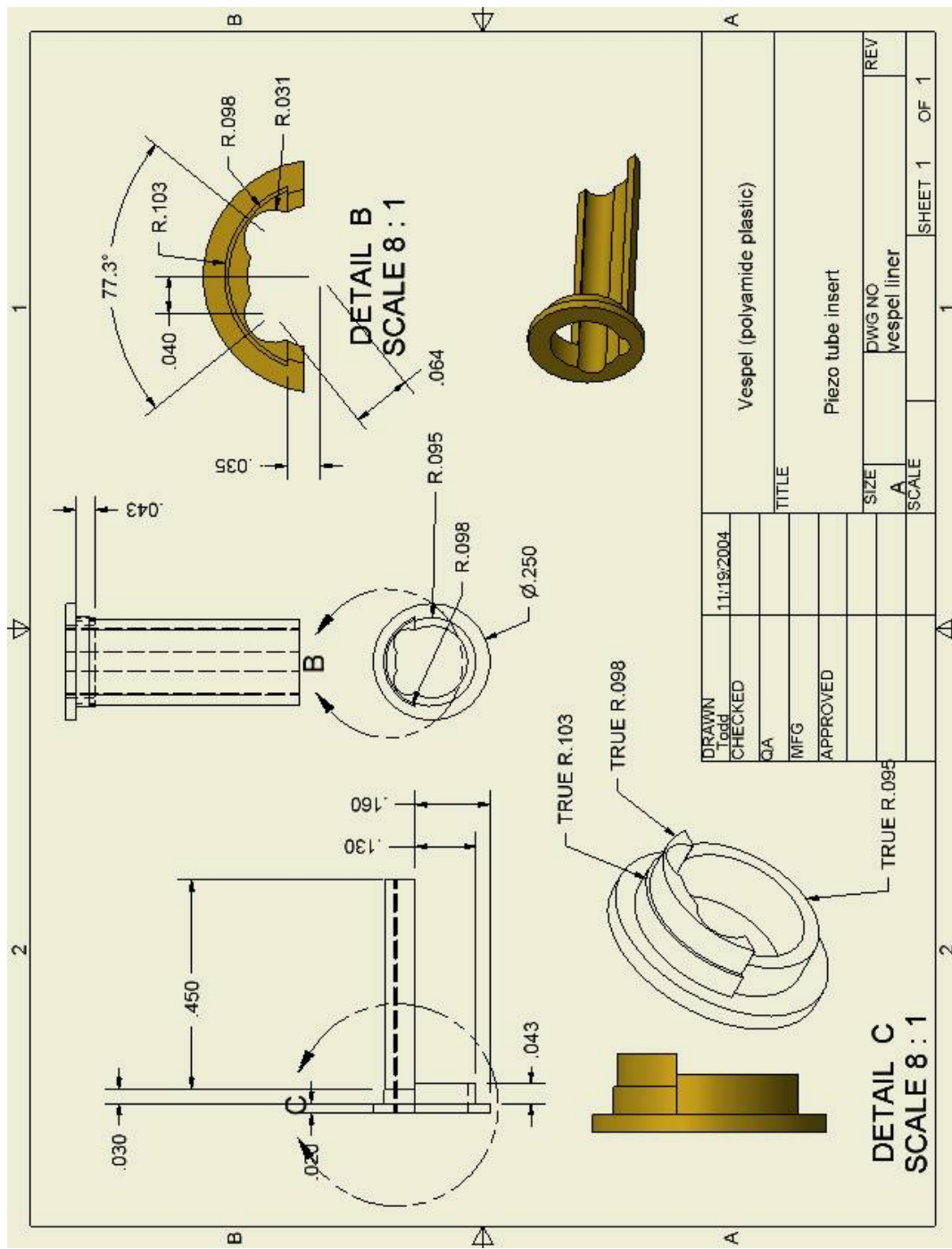


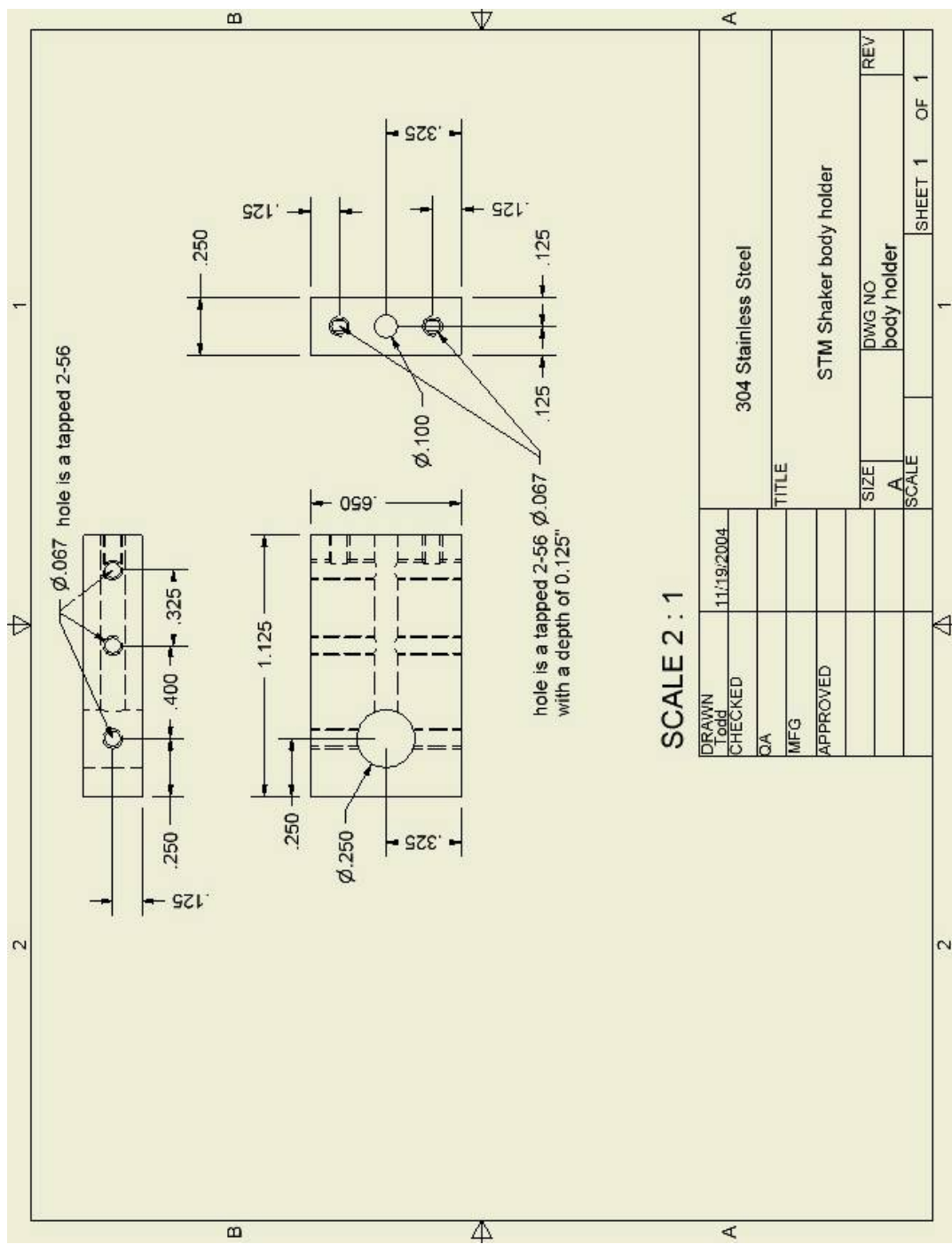
The copper cap is made from a single piece of copper. The cap fits into the back end of the copper shaker body, and holds the piezo tube in its interior hollow space.

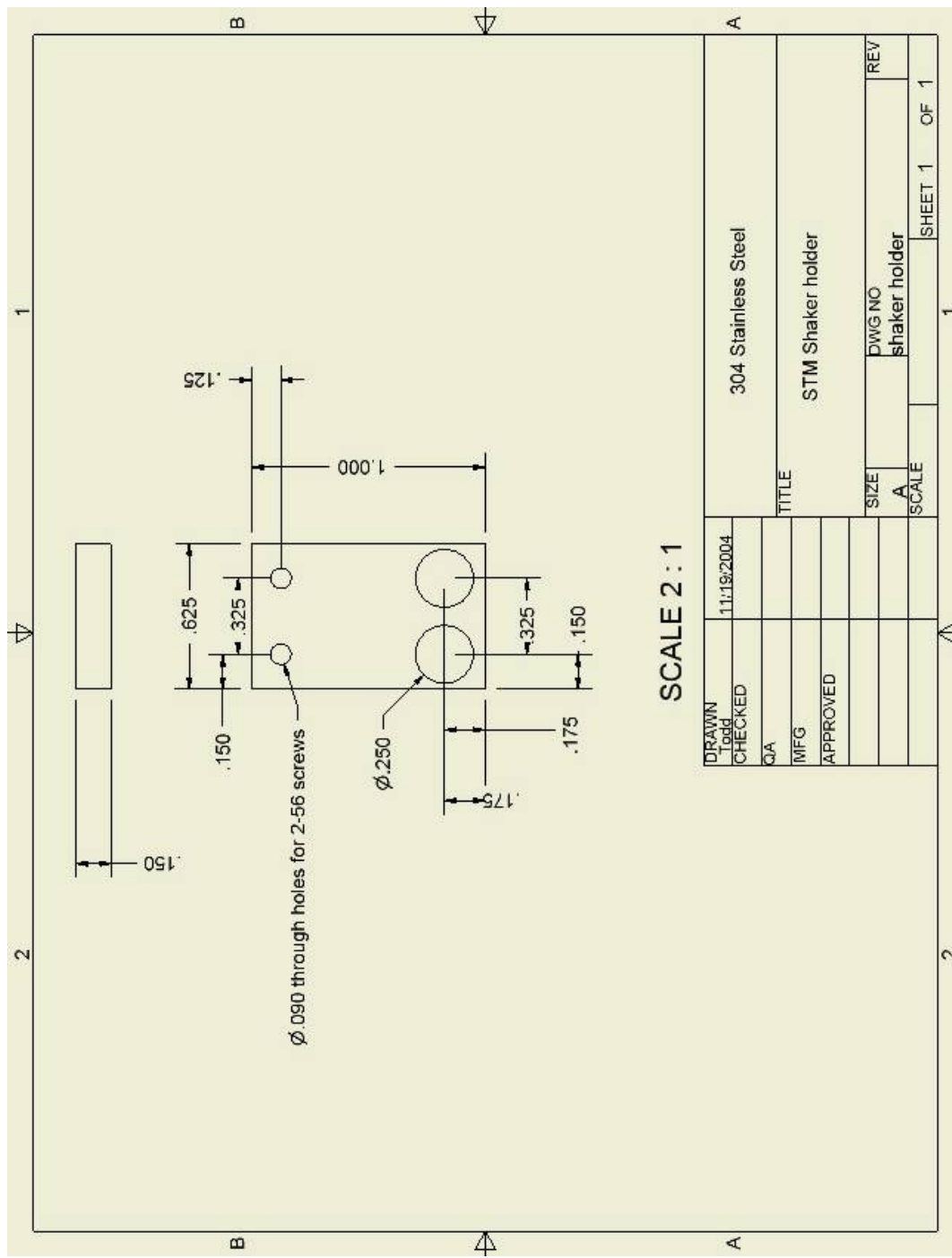


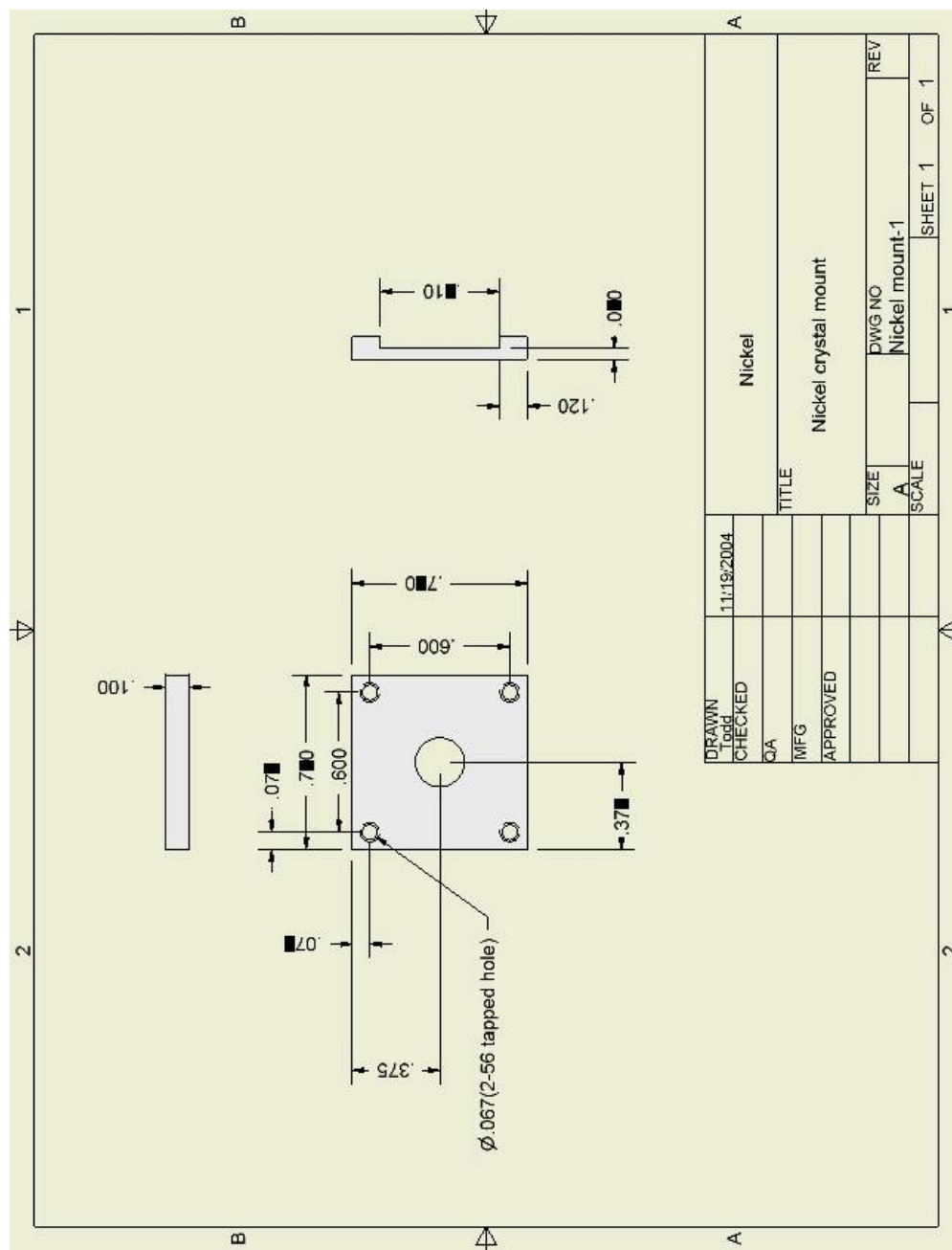












¹ F. Mugele, C. Kloos, P. Leiderer, and R. Moller, Rev. Sci. Instrum. **67** (7), 2557 (1996).

² T. Kuntsmann (Personal communication (email)).

³ E. Fomaine. (Personal communications)

G)**SPM-32 Parameter file settings**

SPM 32 2003.40 Program Configuration File

[CONFIGURE
SYSTEM]*****

[SPM 100:Hardware]

Configure SPM-100 Electronics

<1458> Electronics type ::(1) RHK SPM-100 version 8 DSP scan control
<1459> VSCAN-100 DSP upgrade installed ::ON
<1460> RHK AIM Interface ::(0) None installed
<1461> Offsets summed with scan ::ON
<1462> RHK Aux1/Aux2 installed ::ON

[SPM 100:DSP]

DSP Scan Board

<1471> Serial number ::0
<1472> SPM-100 IP ::128.143.18.13
<1473> SPM-100 Scan Code ::RHK.COF
<1474> Reboot DSP scan program ::OFF
<1475> Restart DSP communication ::OFF
<1476> Retract tip during DSP initialize ::ON
<1477> DSP timeout ::6.0000e+01 s
<478> Debug status ::(2) Extended Debugging output to file
<1479> Do not halt on error ::OFF

[SPM 100:DSP STAT]

DSP Status

[SPM 100:Gains]

SPM-100 Gain Calibration

<1463> X scan volts/monitor volt ::1.3000e+01 V
<1464> Y scan volts/monitor volt ::1.3000e+01 V
<1465> Z scan volts/monitor volt ::1.3000e+01 V
<1466> X offset volts/monitor volt ::1.3000e+01 V
<1467> Y offset volts/monitor volt ::1.3000e+01 V
<1468> Z offset volts/monitor volt ::1.3000e+01 V
<1469> Sample bias per monitor volt ::1.0000e+00 V
<1470> STM current per monitor volt ::1.0000e-10 A

[Head:Scanner]

Description/Offsets	
<1431>	Scan head description ::RHK UHV-STM
<1432>	X motion per piezo volt ::1.4860e-08 m
<1433>	Y motion per piezo volt ::1.7174e-08 m
<1434>	Z linear motion per piezo volt ::2.1200e-09 m
<1435>	Offsets summed with scan ::ON
<1436>	X analog offset per piezo volt ::4.0000e-08 m
<1437>	Y analog offset per piezo volt ::4.0000e-08 m
<1438>	Z analog offset per piezo volt ::5.0000e-09 m

[Head:Feedback]

Positioning Feedback	
<1439>	Enable positioning feedback ::OFF
<1449>	Position sensors connected ::OFF
<1441>	Time constant ::2.0000e-01 s
<1442>	Bandwidth ::5.0000e+00 Hz
Calibration	
<1443>	Automatic sensor calibration ::OFF
<1444>	Automatic re-calibration ::OFF
<1445>	X (image/true) size ratio ::1.0000e+00
<1446>	Y (image/true) size ratio ::1.0000e+00
<1447>	XY angle correction ::0.0000e+00

[Head:Adv. Feedback]

Advanced Positioning Feedback	
<1448>	X detector offset ::0.0000e+00 V
<1449>	Y detector offset ::0.0000e+00 V
<1450>	X detector sensitivity ::1.0000e-05 m/V
<1451>	Y detector sensitivity ::1.0000e-05 m/V
Detector Cross Coupling	
<1452>	Y contribution to X ::0.0000e+00 m/V
<1453>	X contribution to Y ::0.0000e+00 m/V
Detector Nonlinearity Corrections	
<1454>	X detector square sensitivity ::0.0000e+00 m/V^2
<1455>	X detector cube sensitivity ::0.0000e+00 m/V^3
<1456>	Y detector square sensitivity ::0.0000e+00 m/V^2
<1457>	Y detector cube sensitivity ::0.0000e+00 m/V^3

[PC]

Configure PC Cards	
<1480>	A/D Card type ::(1) DT-2821-F 150 kHz
<1481>	Base address (hex) ::240
<1482>	DAC 1 range ::(0) -10 to +10 Volts
<1483>	DAC 2 range ::(0) -10 to +10 Volts
<1484>	Input test limit ::3000000

<1485> DT-2817 TTL Card installed ::OFF
<1486> TTL card base address (hex) ::228
<1487> RHK AFM-100 installed ::OFF
<1488> PC-TIO-10 counter installed ::OFF
<1489> Counter base address (hex) ::1A0

[SYSTEM

SETTINGS]*****
**

[Pref]

User Preferences

<1304> Use Angstroms ::ON
<1305> Scale bar ::ON
<1306> Preserve zoom ::ON
<1307> Rotate mode ::(2) Solid
<1308> Interactive windows ::(0) Mouse select
<1309> Data acquisition delay ::1.5000e+00 s
<1310> Debug messages ::(0) Off
<1311> Pop acquisition pages ::ON
<1312> Pop status windows ::OFF
<1313> Pop scan area window ::OFF
<1314> Parameter increment ::5.0000e+00

[File]

File Control

<1067> Default disk ::D:
<1068> Default path ::\NEW\NEWFOL~1\DATA\
<1069> Default comment ::dosed CO and annealed to 220K imaged @ 3"
<1070> Open files in index only ::OFF
<1071> Read auto name ::ON
 root ::DEMO5_
 index ::11
 ext ::SM2
<1075> Save auto name ::ON
 root ::29JUL
 index ::035
 ext ::SM2
<1079> autoincrement ext ::ON
<1080> Comment question ::OFF
<1081> Auto Input page limit ::200
 Index plot display
<1082> Index plots in color ::ON
<1847> Index smoothing ::ON
<1848> smooth mode ::(4) 11 point

<1083> Index plot mode ::(2) line slope subtract
<1085> Index plot size ::(0) minimum

[Output:Type]

Output Mode

<1043> Graphical output type ::(1) PCX File (.PCX)
<1044> Remove window frames ::OFF
<1045> Save with white background ::OFF
<1046> Postscript mode ::(1) Landscape full page

[Output:Files]

Output Files

<1054> Default disk ::D:
<1055> Default path ::\
<1056> Overwrite graphics files ::OFF
<1057> Autoname output ::ON
<1058> root ::OUT
<1059> index ::21
<1060> Autoprint Output ::OFF
<1061> Auto delete after print ::OFF
<1062> Print command ::copy /B
<1063> Print command trailer ::LPT1:

[Output:Direct]

Direct Image Output

<1047> Image X size ::500
<1048> Image Y size ::500
<1049> Background color ::(15) White
<1050> Display rotated ::OFF
<1051> Batch filter ::OFF
<1052> Filter direction ::(0) ¶
<1053> Filter Z units ::m

[Output:Sheet]

Output Spreadsheet

<1064> Spreadsheet delimiter ::(0) TAB
<1065> Spreadsheet no header ::OFF
<1066> Spreadsheet column tags ::ON

[I/O:Define]

Define Inputs

<1367> SPM Acquisition mode ::(0) STM
<1368> User label ::User
<1369> User units ::V
<1370> units/monitor volt ::1.0000e+00 V

<1371> Lock-in/Aux label ::Aux
<1372> Lock-in/Aux units ::V
<1373> units/input volt ::1.0000e+00 V
<1374> Aux 1 label ::Aux 1
<1375> Aux 1 units ::V
<1376> units/input volt ::1.0000e+00 V
<1377> Aux 2 label ::Aux 2
<1378> Aux 2 units ::V
<1379> units/input volt ::1.0000e+00 V
<1380> DSP A/D 1 label ::DSP 1
<1382> DSP A/D 1 units ::V
<1383> units/input volt ::1.0000e+00 V
<1384> DSP A/D 2 label ::DSP 2
<1385> DSP A/D 2 units ::V
<1386> units/input volt ::1.0000e+00 V

[I/O:Ctrl]**Hardware Controls****[I/O:DAC]****DAC Assignments****[I/O:LOCKS]****Locked I/O Channels**

<1086> DAC 1 ::(1) Waveform Approach primary
<1087> DAC 2 ::(0) DAC unlocked
<1088> DSP DAC ::(0) DAC unlocked
<1089> DSP AD 1 ::(0) unlocked
<1090> DSP AD 2 ::(0) unlocked

[Aux FB]**Aux Feedback**

<1277> Enable Aux Feedback ::OFF
<1278> Time Constant ::1.0000e+01 s
<1279> Setpoint ::0.0000e+00 V
<1280> Change output value ::OFF

Aux Feedback Configuration

<1281> Aux feedback mode ::(0) User defined
<1282> Aux feedback Z offset invert ::OFF
<1283> Disable aux feedback during imaging ::OFF
<1284> Re-enable aux feedback at startup ::ON
<1285> units/input volt ::1.0000e+00 V
<1286> units/output volt ::1.0000e+00 V
<1287> feedback units ::V

Aux Monitor

<1288> Monitor mode ::(0) Disabled
<1289> Monitor Maximum ::5.0000e+00 V
<1290> Monitor Minimum ::-5.0000e+00 V
<1291> Pen up/down output ::OFF
<1292> units/monitor volt ::1.0000e+00 V
<1293> monitor units ::V

[Screen]

Screen/Mouse Preferences
<1315> Resolution ::(3) 1280 x 1024
<1316> disable VESA protected mode ::OFF
<1317> VESA graphics ::OFF
<1318> Mouse sensitivity ::0
<1319> Menu close range ::50
<1320> CONTROL is left button ::ON
<1321> Click delay ::3.5000e-01 s

[APPROACH

CONTROL]*****
**

[Main]

Approach Control
<1611> Approach system ::(0) Kinetic Waveform
<1612> Approach mode ::(0) Tip Retract
<1613> approach threshold ::-2.0000e+01
<1614> feedback delay ::1.0000e+00 s
<1615> signal threshold ::5.0000e-10 A
<1616> test delay ::1.0000e-02 s
<1617> approach steps ::2
<1618> adjust steps ::1
<1619> retract steps ::1500
Tip Control
<1620> tip back in motion ::ON
<1621> tip retract mode ::(1) TTL-Feedback
<1622> tip retract delay ::1.0000e-04 s
<1623> tip restore delay ::1.0000e-04 s
<1624> tip back after approach ::OFF
Secondary Approach Test
<1625> Channel ::(3) Aux 1
<1626> Secondary condition ::(0) Disabled
<1627> Secondary Max ::1.0000e+00 V
<1628> Secondary Min ::-1.0000e+00 V

[Kinetic:Wave1]

	Primary Waveform
<1630>	Waveform ::(0) Sawtooth
<1631>	Approach amplitude ::1.9990e-06 m
<1632>	Retract amplitude ::1.9990e-06 m
<1633>	Fast approach ::2.0000e-07 m
<1634>	Fast retract ::2.0000e-07 m
<1635>	Adjust amplitude ::1.0000e-07 m
<1636>	Period ::1.0000e-02 s
<1637>	Cycle delay ::0.0000e+00 s
<1638>	Filter period ::0.0000e+00 s
<1639>	Assymmetry ::0.0000e+00
<1640>	Signal test ::OFF
<1641>	output channel ::(1) DAC 1
<1642>	motion per D/A volt ::1.0000e-07 m
<1643>	Waveform polarity ::(1) Bipolar allowed

[Kinetic:Wave2]

	Secondary Waveform
<1644>	Waveform ::(0) Sawtooth
<1645>	Approach amplitude ::1.0000e-07 m
<1646>	Retract amplitude ::2.0000e-07 m
<1647>	Fast approach ::2.0000e-07 m
<1648>	Fast retract ::2.0000e-07 m
<1649>	Adjust amplitude ::1.0000e-07 m
<1650>	Period ::1.0000e-02 s
<1651>	Filter period ::0.0000e+00 s
<1652>	Offset from primary ::0.0000e+00 s
<1653>	Assymmetry ::0.0000e+00
<1654>	output channel ::(2) DAC 2
<1655>	motion per D/A volt ::1.0000e-07 m
<1656>	Waveform polarity ::(1) Bipolar allowed

[Kinetic:Nano]

	Nanonics Translation
<1657>	Waveform ::(0) Sawtooth
<1658>	Amplitude ::1.0000e-07 m
<1659>	Period ::1.0000e-02 s
<1660>	Assymmetry ::0.0000e+00
<1661>	output channel ::(1) DAC 1
<1662>	motion per D/A volt ::1.0000e-07 m
<1663>	Invert X motion ::OFF
<1664>	Invert Y motion ::OFF

[Kinetic:View]

[Motors:Step]**Stepper Motor**

<1665> CW tip approach ::ON
<1666> step time ::2.0000e-02 s
<1667> use half steps ::ON
<1668> 2 phase motor ::OFF
<1669> coil energized at rest ::ON
<1670> control line 4 ::(0) Not used
<1671> control line 5 ::(0) Not used

[Motors:Inch]**Inchworm(tm)/TTL Control**

<1690> pulse width ::1.0000e-04 s
<1691> fast pulse width ::1.0000e-05 s
<1692> reverse direction ::OFF
<1693> pre-set direction ::OFF
<1694> HI enable/LO stop-hold ::OFF
 For IWC-100 Only
<1695> reverse reposition ::OFF
<1696> back-off step count ::0

[Motors:Walker]**Piezo Walker**

<1672> Step Period ::2.0000e-02 s
<1673> active time ::1.0000e-03 s
<1674> Active High ::ON
<1675> Pre-motion delay ::0.0000e+00 s
<1676> Post-motion delay ::0.0000e+00 s
<1873> Invert approach motion ::OFF
<1712> Walker DAC channel ::(0) NO CONNECTION

[Motors:PMC-MSCU]**RHK PMC/Omicron MSCU Control**

<1701> Step Voltage ::400 V
<1702> Step Rate ::1000 Hz
<1703> Move channel ::1
<1704> Move steps ::0
 Technical Parameters
<1705> Control mode ::(0) TTL control
<1706> MSCU Connected ::OFF
<1707> MSCU COM Port ::1
<1708> Approach channel ::1
<1709> Invert approach motion ::OFF
<1710> Open XYZ control ::OFF
<1711> Steps per click ::10

Legacy Parameters

<1712> PMC/MSCU control channel ::(0) NO CONNECTION
<1713> Single step time ::1.0500e-01 s

[Motors:Slide]

Microslide(tm) Control

<1697> Z+ tip approach ::ON
<1698> Slider step time ::5.0000e-03 s
<1699> Direction switch time ::7.5000e-02 s
<1700> Use 'debounce' mode ::OFF

[Motors:Phi]

Phi UHV STM Motor

<1686> tip approach hi ::OFF
<1687> start pulse ::1.0000e-06 s
<1688> stop pulse ::0.0000e+00 s
<1689> fast step delay ::1.0000e-02 s

[Motors:DC]

DC Approach Motor

<1683> approach time ::5.0000e-01 s
<1684> adjust time ::5.0000e-01 s
<1685> retract time ::1.0000e-04 s

[Tip Ramp]

Analog Ramp Tip Control
Tip Retract and Approach

<1677> advance ramp speed ::1.0000e-06 m/s
<1678> retract ramp speed ::1.0000e-06 m/s
<1679> tip retract position ::0.0000e+00 m
<1680> tip standby position ::0.0000e+00 m
<1681> motion per D/A volt ::1.0000e-07 m/V
<1682> Offset piezo ::OFF
<1884> Z control DAC ::(0) NO CONNECTION
 Open Loop Approach::
<1685> approach test ramp speed ::1.0000e-04 m/s
<1686> use distance limits ::OFF
<1687> retract limit ::1.0000e-06 m
<1688> advance limit ::-1.0000e-06 m
 Tip Retract/Signal options
<1882> Offset step mode ::OFF
<1883> Offset step count ::2

[IMAGE

CONTROL]*****
**

[Scan:Size]

Scan Control

<1322> Scan size ::1.5000e-08 m
<1323> image pixels ::(6) 512 x 512
<1324> Image aspect ratio ::1.0000e+00
<1325> Move speed ::2.0000e-07 m/s
<1326> Scan speed ::2.0000e-07 m/s
<1327> Line time ::0.0000e+00 s
<1328> X offset ::-6.4186e-09 m
<1329> Y offset ::-1.6355e-09 m
<1330> Scan Rotation ::0.0000e+00

[Scan:Options]

Scan Options

<1331> Scan count ::0
<1332> Fast image mode ::OFF
<1333> Scan direction ::(0) X scan
<1334> Scan delay ::1.0000e-01 s
<1335> Alternating slow scan ::ON
<1336> Slow scan disabled ::OFF
Save/Display Options
<1337> Autoscale Image ::OFF
<1338> Line display ::ON
<1339> Page save mode ::(1) Screen and disk
<1340> Scan Autosave ::ON
<1341> Save Contrast ::OFF

[Scan:Advanced]

Range Control Options

<1344> Reset Range ::OFF
<1345> Test Range at Startup ::OFF
<1346> Set Range Tip Retract ::ON
Advanced Scan Options
<1347> Standby action ::(4) free scan
<1348> Scan type ::(0) linear
<1349> Image shift increment ::1.0000e+01
<1350> Image rotation increment ::5.0000e+00

[Input]

Image Input Data

<1351> Record one scan direction ::OFF

<1352> Topography::ON
<1353> A/D range ::(0) ñ 10 V
<1354> Current ::OFF
<1355> A/D range ::(0) ñ 10 V
<1356> Aux ::OFF
<1357> A/D range ::(0) ñ 10 V
<1358> Aux 1 ::OFF
<1359> A/D range ::(0) ñ 10 V
<1360> Aux 2 ::OFF
<1361> A/D range ::(0) ñ 10 V
<1362> A1 rate ::OFF
<1363> A2 rate ::OFF

[Spec]

Image Spectroscopy
<1427> Spectroscopy mode ::(0) None
<1428> Multi volt mode ::(0) None
<1429> Image Out Spectroscopy ::OFF
<1430> Spec Location ::(3) 8 x 8

[Drift]

Image Drift Correction
<1273> Reset drift correction ::OFF
<1274> Enable drift correction ::OFF
<1275> Reference radius ::7
<1276> Search range ::10

[Setup:Sim]

Simulated SPM-100-8 Acquisition
SPM-100 CONTROLS
<1387> Z position gain ::(6) x64
<1388> Z offset ::5.0000e+00
<1389> bias adjust ::1.5000e+00
<1390> bias range ::(1) ñ 1 V
<1301> bias polarity ::(1) -
<1392> current setpoint ::9.0000e-01
SIMULATED IMAGE
<1393> lattice angle ::1.5000e+01 ø
<1394> x origin ::5.0000e-09 m
<1395> y origin ::5.0000e-09 m
<1396> x slope ::2.0000e+00 ø
<1397> y slope ::1.0000e+00 ø

[Setup:Count]

Pulse Counting

<1584> Count interval ::1.0000e-02 s
<1585> Monitor Rates ::ON
<1586> Channel A1 label ::A1 rate
<1587> Channel A1 units ::Hz
<1588> A1 units/input count ::1.0000e+00 Hz
<1589> Channel A2 label ::A2 rate
<1590> Channel A2 units ::Hz
<1591> A2 units/input count ::1.0000e+00 Hz

[Setup:AFM]

AFM Control

<1505> Lever k value ::5.0000e-01 N/m
<1506> Deflection sensitivity ::0.0000e+00 V/m
<1507> Lateral sensitivity ::0.0000e+00 N/V

RHK AFM-100 Parameters

<1508> Normalize AFM PSD ::ON
<1509> Mux 1 Data ::(0) Normal Force
<1510> Mux 2 Data ::(1) Lateral Force
<1511> Laser current gain ::1.0000e-02 A/V
<1512> PSD threshold ::5.0000e-01 V
<1513> Laser power multiplier ::1.0000e+01
<1514> Photocurrent/Laser mW ::1.5000e-04 A
<1515> Error output gain ::5.0000e+01
<1516> Ext signal label ::Force gradient
<1617> Ext signal units ::N/m
<1518> Ext signal/input volt ::1.0000e+00 N/m
<1519> Mux 1 input ::(1) Aux/Lockin
<1520> Mux 2 input ::(0) OFF

D.I. Bioscope Parameters

<1521> Bioscope A-B Signal x8 ::OFF

[Setup:GPIB]

Configure GPIB

<1492> GPIB Enabled ::OFF
<1493> GPIB path ::c:\gpib
<1494> GPIB address ::1
<1495> Device is SCPI compliant ::ON
<1496> GPIB Initialize ::(0) none
<1497> Init script file ::init.txt
<1498> GPIB Status check enabled ::OFF
<1499> Status script file ::f3
<1500> Spectroscopy script file ::f2
<1501> Spectroscopy control ::(0) Feedback on
<1502> Spectroscopy data limit (kB) ::2
<1503> Spectrum delay ::1.0000e-02 s

<1504> Stabilization interval ::1.0000e-02 s

[POINT

SPECTROSCOPY]*****

START OF PARAMETER SET*****

[Spectra:Control]

General Control

<1874> choose type ::(0) I/Z
<1832> Spectra location ::(0) Present position
<1091> Control Loop ::(1) Feedback off
<1092> Monitor test ::(0) Disabled
<1093> Variable gap mode ::OFF
<1875> Type name ::I/Z

Output Range

<1094> initial value ::-8.4999e-09 m
<1812> final value ::4.9998e-09 m
<1833> alternate scan direction ::OFF
<1095> output increment ::2.5232e-11 m
<1096> Samples/point ::1
<1099> pre-sample delay ::0.0000e+00 s
<1101> Spectra to acquire ::1

Timing

<1097> sweep rate ::1.5000e-08 m/s
<1098> setup rate ::1.0000e-09 m/s
<1100> spectrum delay ::1.0000e-03 s

Data

<1102> Page save mode ::(2) Disk only
<1813> spectrum autosave ::OFF

[Spectra:Input/Output]

Spectrum Input & Output

Inputs

<1105> Channels to acquire ::1
<1106> Channel 1 ::(1) Current
<1107> range 1 ::(0) ñ 10 V
<1108> Channel 2 ::(3) Aux 1
<1109> range 2 ::(0) ñ 10 V
<1110> Channel 3 ::(4) Aux 2
<1111> range 3 ::(0) ñ 10 V

Output

<1112> output DAC ::(3) DSP DAC
<1113> STM Bias Mode ::OFF
<1114> output units per D/A volt ::2.1200e-09 m

<1115> Spectrum units ::m

[Spectra:Adv. Modes]

Advanced Modes

<1831> Graphics updates ::(0) Continuous (inline)
<1116> Handshaking ::OFF
<1117> Stabilize feedback ::OFF
<1118> Stabilization interval ::5.0000e-02 s
 Monitor Mode
<1119> Monitor response ::(1) Stop spectrum group
<1834> Monitor warning message ::ON
<1120> Monitor test ::(0) Disabled
<1121> Monitor channel ::(1) Current
<1122> Monitor max ::1.0000e-09 A
 Variable Gap Mode::
<1124> Z offset before spectrum ::0.0000e+00 m
<1125> Z change per bias volt ::2.0000e-10 m
<1126> Z attenuation length ::1.0000e-10 m
<1127> Z change per D/A volt ::1.0000e-07 m

[Spectra:SpecWin]

Spectrum display window

<1814> window color ::(8) Grey
<1815> display mode ::(1) stack lines
<1830> display cycles ::0
<1816> x channel ::-1
<1821> x line mode ::(1) auto DC
<1817> line 0 mode ::(1) auto DC
<1818> line 1 mode ::(1) auto DC
<1819> line 2 mode ::(1) auto DC
<1820> line 3 mode ::(1) auto DC
<1822> line 0 color ::(14) Yellow
<1823> line 1 color ::(15) White
<1824> line 2 color ::(1) Blue
<1825> line 3 color ::(4) Red
<1826> line 0 color2 ::(7) Off White
<1827> line 1 color2 ::(7) Off White
<1828> line 2 color2 ::(9) Light Blue
<1829> line 3 color2 ::(6) Brown
<1835> line 0 bold ::OFF
<1836> line 1 bold ::OFF
<1837> line 2 bold ::OFF
<1838> line 3 bold ::OFF
<1839> line 0 bold2 ::OFF
<1840> line 1 bold2 ::OFF

```
<1841>    line 2 bold2 ::OFF
<1842>    line 3 bold2 ::OFF
<1167>    high pass attenuation constant ::2.0000e+00
<1876>    END OF PARAMETER SET*****
```

START OF PARAMETER SET*****

[Spectra:Control]

General Control

```
<1874>    choose type ::(0) I/Z
<1832>    Spectra location ::(0) Present position
<1091>    Control Loop ::(1) Feedback off
<1092>    Monitor test ::(0) Disabled
<1093>    Variable gap mode ::OFF
<1875>    Type name ::Spectrum 2
          Output Range
<1094>    initial value ::0.0000e+00 V
<1812>    final value ::1.0010e+00 V
<1833>    alternate scan direction ::OFF
<1095>    output increment ::4.8828e-03 V
<1096>    Samples/point ::10
<1099>    pre-sample delay ::0.0000e+00 s
<1101>    Spectra to acquire ::2
```

Timing

```
<1097>    sweep rate ::2.0000e+01 V/s
<1098>    setup rate ::5.0000e+01 V/s
<1100>    spectrum delay ::1.0000e-03 s
```

Data

```
<1102>    Page save mode ::(2) Disk only
<1813>    spectrum autosave ::OFF
```

[Spectra:Input/Output]

Spectrum Input & Output

Inputs

```
<1105>    Channels to acquire ::1
<1106>    Channel 1 ::(2) Aux
          range 1 ::(0) ñ 10 V
<1108>    Channel 2 ::(3) Aux 1
          range 2 ::(0) ñ 10 V
<1110>    Channel 3 ::(4) Aux 2
          range 3 ::(0) ñ 10 V
```

Output

```
<1112>    output DAC ::(0) NO CONNECTION
<1113>    STM Bias Mode ::OFF
<1114>    output units per D/A volt ::1.0000e+00 V
<1115>    Spectrum units ::V
```

[Spectra:Adv. Modes]

Advanced Modes

<1831> Graphics updates ::(0) Continuous (inline)
<1116> Handshaking ::OFF
<1117> Stabilize feedback ::OFF
<1118> Stabilization interval ::5.0000e-02 s
 Monitor Mode
<1119> Monitor response ::(1) Stop spectrum group
<1834> Monitor warning message ::ON
<1120> Monitor test ::(0) Disabled
<1121> Monitor channel ::(1) Current
<1122> Monitor max ::0.0000e+00 A
 Variable Gap Mode::
<1124> Z offset before spectrum ::0.0000e+00 m
<1125> Z change per bias volt ::2.0000e-10 m
<1126> Z attenuation length ::1.0000e-10 m
<1127> Z change per D/A volt ::1.0000e-07 m

[Spectra:SpecWin]

Spectrum display window

<1814> window color ::(3) Cyan
<1815> display mode ::(1) stack lines
<1830> display cycles ::0
<1816> x channel ::-1
<1821> x line mode ::(0) DC
<1817> line 0 mode ::(1) auto DC
<1818> line 1 mode ::(1) auto DC
<1819> line 2 mode ::(1) auto DC
<1820> line 3 mode ::(1) auto DC
<1822> line 0 color ::(14) Yellow
<1823> line 1 color ::(15) White
<1824> line 2 color ::(1) Blue
<1825> line 3 color ::(4) Red
<1826> line 0 color2 ::(7) Off White
<1827> line 1 color2 ::(7) Off White
<1828> line 2 color2 ::(9) Light Blue
<1829> line 3 color2 ::(6) Brown
<1835> line 0 bold ::OFF
<1836> line 1 bold ::OFF
<1837> line 2 bold ::OFF
<1838> line 3 bold ::OFF
<1839> line 0 bold2 ::OFF
<1840> line 1 bold2 ::OFF
<1841> line 2 bold2 ::OFF

<1842> line 3 bold2 ::OFF
<1167> high pass attenuation constant ::2.0000e+00
<1876> END OF PARAMETER SET*****

START OF PARAMETER SET*****

[Spectra:Control]

General Control

<1874> choose type ::(0) I/Z
<1832> Spectra location ::(0) Present position
<1091> Control Loop ::(1) Feedback off
<1092> Monitor test ::(0) Disabled
<1093> Variable gap mode ::OFF
<1875> Type name ::Spectrum 3

Output Range

<1094> initial value ::0.0000e+00 V
<1812> final value ::1.0010e+00 V
<1833> alternate scan direction ::OFF
<1095> output increment ::4.8828e-03 V
<1096> Samples/point ::10
<1099> pre-sample delay ::0.0000e+00 s
<1101> Spectra to acquire ::2

Timing

<1097> sweep rate ::2.0000e+01 V/s
<1098> setup rate ::5.0000e+01 V/s
<1100> spectrum delay ::1.0000e-03 s

Data

<1102> Page save mode ::(2) Disk only
<1813> spectrum autosave ::OFF

[Spectra:Input/Output]

Spectrum Input & Output

Inputs

<1105> Channels to acquire ::1
<1106> Channel 1 ::(2) Aux
<1107> range 1 ::(0) ñ 10 V
<1108> Channel 2 ::(3) Aux 1
<1109> range 2 ::(0) ñ 10 V
<1110> Channel 3 ::(4) Aux 2
<1111> range 3 ::(0) ñ 10 V

Output

<1112> output DAC ::(0) NO CONNECTION
<1113> STM Bias Mode ::OFF
<1114> output units per D/A volt ::1.0000e+00 V
<1115> Spectrum units ::V

[Spectra:Adv. Modes]

Advanced Modes

<1831> Graphics updates ::(0) Continuous (inline)
<1116> Handshaking ::OFF
<1117> Stabilize feedback ::OFF
<1118> Stabilization interval ::5.0000e-02 s

Monitor Mode

<1119> Monitor response ::(1) Stop spectrum group
<1834> Monitor warning message ::ON
<1120> Monitor test ::(0) Disabled
<1121> Monitor channel ::(1) Current
<1122> Monitor max ::0.0000e+00 A

Variable Gap Mode::

<1124> Z offset before spectrum ::0.0000e+00 m
<1125> Z change per bias volt ::2.0000e-10 m
<1126> Z attenuation length ::1.0000e-10 m
<1127> Z change per D/A volt ::1.0000e-07 m

[Spectra:SpecWin]

Spectrum display window

<1814> window color ::(0) Black
<1815> display mode ::(1) stack lines
<1830> display cycles ::0
<1816> x channel ::-1
<1821> x line mode ::(0) DC
<1817> line 0 mode ::(1) auto DC
<1818> line 1 mode ::(1) auto DC
<1819> line 2 mode ::(1) auto DC
<1820> line 3 mode ::(1) auto DC
<1822> line 0 color ::(14) Yellow
<1823> line 1 color ::(15) White
<1824> line 2 color ::(1) Blue
<1825> line 3 color ::(4) Red
<1826> line 0 color2 ::(7) Off White
<1827> line 1 color2 ::(7) Off White
<1828> line 2 color2 ::(9) Light Blue
<1829> line 3 color2 ::(6) Brown
<1835> line 0 bold ::OFF
<1836> line 1 bold ::OFF
<1837> line 2 bold ::OFF
<1838> line 3 bold ::OFF
<1839> line 0 bold2 ::OFF
<1840> line 1 bold2 ::OFF
<1841> line 2 bold2 ::OFF
<1842> line 3 bold2 ::OFF

<1167> high pass attenuation constant ::2.0000e+00
<1876> END OF PARAMETER SET*****

START OF PARAMETER SET*****

[Spectra:Control]

General Control

<1874> choose type ::(0) I/Z
<1832> Spectra location ::(0) Present position
<1091> Control Loop ::(1) Feedback off
<1092> Monitor test ::(0) Disabled
<1093> Variable gap mode ::OFF
<1875> Type name ::Spectrum 4

Output Range

<1094> initial value ::0.0000e+00 V
<1812> final value ::1.0010e+00 V
<1833> alternate scan direction ::OFF
<1095> output increment ::4.8828e-03 V
<1096> Samples/point ::10
<1099> pre-sample delay ::0.0000e+00 s
<1101> Spectra to acquire ::2

Timing

<1097> sweep rate ::2.0000e+01 V/s
<1098> setup rate ::5.0000e+01 V/s
<1100> spectrum delay ::1.0000e-03 s

Data

<1102> Page save mode ::(2) Disk only
<1813> spectrum autosave ::OFF

[Spectra:Input/Output]

Spectrum Input & Output
Inputs

<1105> Channels to acquire ::1
<1106> Channel 1 ::(2) Aux
<1107> range 1 ::(0) ñ 10 V
<1108> Channel 2 ::(3) Aux 1
<1109> range 2 ::(0) ñ 10 V
<1110> Channel 3 ::(4) Aux 2
<1111> range 3 ::(0) ñ 10 V

Output

<1112> output DAC ::(0) NO CONNECTION
<1113> STM Bias Mode ::OFF
<1114> output units per D/A volt ::1.0000e+00 V
<1115> Spectrum units ::V

[Spectra:Adv. Modes]

Advanced Modes

<1831>	Graphics updates ::(0) Continuous (inline)
<1116>	Handshaking ::OFF
<1117>	Stabilize feedback ::OFF
<1118>	Stabilization interval ::5.0000e-02 s
Monitor Mode	
<1119>	Monitor response ::(1) Stop spectrum group
<1834>	Monitor warning message ::ON
<1120>	Monitor test ::(0) Disabled
<1121>	Monitor channel ::(1) Current
<1122>	Monitor max ::0.0000e+00 A
Variable Gap Mode::	
<1124>	Z offset before spectrum ::0.0000e+00 m
<1125>	Z change per bias volt ::2.0000e-10 m
<1126>	Z attenuation length ::1.0000e-10 m
<1127>	Z change per D/A volt ::1.0000e-07 m

[Spectra:SpecWin]

Spectrum display window	
<1814>	window color ::(9) Light Blue
<1815>	display mode ::(1) stack lines
<1830>	display cycles ::0
<1816>	x channel ::-1
<1821>	x line mode ::(0) DC
<1817>	line 0 mode ::(1) auto DC
<1818>	line 1 mode ::(1) auto DC
<1819>	line 2 mode ::(1) auto DC
<1820>	line 3 mode ::(1) auto DC
<1822>	line 0 color ::(14) Yellow
<1823>	line 1 color ::(15) White
<1824>	line 2 color ::(1) Blue
<1825>	line 3 color ::(4) Red
<1826>	line 0 color2 ::(7) Off White
<1827>	line 1 color2 ::(7) Off White
<1828>	line 2 color2 ::(9) Light Blue
<1829>	line 3 color2 ::(6) Brown
<1835>	line 0 bold ::OFF
<1836>	line 1 bold ::OFF
<1837>	line 2 bold ::OFF
<1838>	line 3 bold ::OFF
<1839>	line 0 bold2 ::OFF
<1840>	line 1 bold2 ::OFF
<1841>	line 2 bold2 ::OFF
<1842>	line 3 bold2 ::OFF
<1167>	high pass attenuation constant ::2.0000e+00

<1876> END OF PARAMETER SET*****

[FFT]

Noise Power Spectrum

<1260> Data source ::(0) Topography
<1261> Control status ::(0) Feedback on
<1262> Data range ::(0) ñ 10 V
<1263> Sampling rate ::(6) 10 kHz
<1264> Points to sum ::(0) 1
<1266> Points to acquire ::(5) 32 k
<1268> spectrum delay ::0.0000e+00 s
<1269> Spectra to acquire ::2
<1270> Display mode ::(0) linear
<1271> Convert acceleration to height ::OFF
<1272> Page save mode ::(0) Save to screen

[Scope]

Scope/Linetest Save

<1001> Scope data save mode ::(0) Save to screen
<1002> Scope Autosave ::OFF
<1003> Line test data save mode ::(0) Save to screen
<1004> Line Test Autosave ::OFF
<1005> High pass range ::1.5000e+01

[Datalog:Control]

Data Log Control

<1163> Sampling interval ::5.4900e-02 s
<1164> Interrupt acceleration factor ::1
<1165> Total acquisition time ::9.9973e+01 s
<1166> Total acquisition periods ::1.9793e+01
<1168> Enable output ::OFF
<1169> Display/Save output ::ON
<1170> Autosave ::OFF
<1171> Page save mode ::(0) Save to screen

[Datalog:Input]

Datalog Inputs

<1172> Topography::OFF
<1173> A/D range ::(0) ñ 10 V
<1174> Current ::OFF
<1175> A/D range ::(0) ñ 10 V
<1176> Aux ::OFF
<1177> A/D range ::(0) ñ 10 V
<1178> Aux 1 ::OFF
<1179> A/D range ::(0) ñ 10 V

<1180> Aux 2 ::OFF
 <1181> A/D range ::(0) ñ 10 V
 <1182> A1 rate ::OFF
 <1183> A2 rate ::OFF

[Datalog:Output]

Datalog Outputs

<1184> Waveform ::(0) Sine
 <1185> Wave period ::5.0508e+00 s
 <1186> initial phase ::4.0000e+00
 <1187> High limit ::4.9951e-01 V
 <1188> Low limit ::-9.7656e-04 V
 <1189> Data points per output step ::1
 <1190> Output label ::Volts
 <1191> Output units ::V
 <1192> units/output volt ::-5.0000e-01 V
 <1193> offset ::1.0000e+00 V
 <1194> Output DAC ::(0) NO CONNECTION

[IMAGE

SPECTROSCOPY]*****

[Multi]

Image Multivolt

<1574> Image voltage count ::2
 <1575> Voltage change delay ::1.0000e-03 s
 <1576> First page voltage ::1.0014e+00 V
 <1577> Second page voltage ::-1.0006e+00 V
 <1578> Third page voltage ::1.0000e+00 V
 <1579> Fourth page voltage ::-1.0000e+00 V
 <1580> Standby voltage ::0.0000e+00 V
 <1581> STM Bias Mode ::ON
 <1582> output volts per D/A volt ::1.0000e+00 V
 <1583> Output DAC ::(0) NO CONNECTION

[CITS:Control]

CITS Control

<1522> pre-sample delay ::1.0000e-04 s
 <1523> loop pre-stabilize delay ::1.0000e-03 s
 <1524> loop post-stabilize delay ::1.0000e-03 s
 <1525> Control Loop ::(1) Feedback off
 <1526> STM Bias Mode ::ON
 <1527> CITS output ::ON
 <1528> CITS image size ::(0) 1:1

<1529> CITS Handshaking ::OFF

[CITS:CITS In/Out]

	CITS Input/Output
<1539>	CITS voltage count ::1
<1881>	First voltage ::1.0014e+00 V
<1880>	Second voltage ::1.0000e+00 V
<1879>	Third voltage ::1.0000e+00 V
<1878>	Fourth voltage ::1.0000e+00 V
<1540>	Standby voltage ::0.0000e+00 V
<1877>	setup rate ::0.0000e+00 V/s
<1541>	output channel ::(0) NO CONNECTION
<1542>	Topgraphy::OFF
<1543>	Current ::OFF
<1544>	Aux ::OFF
<1545>	Aux 1 ::OFF
<1546>	Aux 2 ::OFF
<1547>	A1 rate ::OFF
<1548>	A2 rate ::OFF

[In/Out:Control]

	Image In/Out Control
<1549>	Data mode ::(0) input only
<1550>	Ramp mode ::(0) line by line
<1551>	Ramp high limit ::1.0000e+00 V
<1552>	Ramp low limit ::0.0000e+00 V
<1553>	Ramp standby value ::0.0000e+00 V
<1554>	Ramp type ::(0) low to high
<1555>	Update after ::(1) 2
<1556>	Handshaking ::OFF
<1557>	Image count ::10
<1778>	Output change delay ::5.0000e-03 s
<1559>	Output label ::voltage
<1560>	Output units ::V
<1561>	units/output volt ::1.0000e+00 V
<1562>	offset ::0.0000e+00 V
<1563>	Output DAC ::(1) DAC 1
<1564>	Output ramp speed ::0.0000e+00

[In/Out:Channels]

	Image In/Out Channels
<1565>	Topgraphy::OFF
<1566>	Current ::OFF
<1567>	Aux ::OFF
<1568>	Aux 1 ::OFF

<1569> Aux 2 ::OFF
 <1570> A1 rate ::OFF
 <1571> A2 rate ::OFF
 <1572> record output ::OFF
 <1573> record time ::OFF

[Handshake]

Spectroscopy Handshaking
Output Signal::

<1531> Handshake output channel ::(0) NO CONNECTION
 <1532> Handshake ready voltage ::5.0000e+00 V
 <1533> Handshake standby voltage ::0.0000e+00 V
 Input Conditions::
 <1535> Handshake input channel ::(0) Aux/lock-in
 <1536> Handshake threshold ::0.0000e+00 V
 <1537> Handshake condition ::(0) above threshold
 <1538> Handshake timeout ::1.0000e+01 s

[MANIPULATION]*****
**

[Tip Move:Move]

Tip Manipulation

<1213> tip Move speed ::0.0000e+00 m/s
 <1214> tip Drag speed ::1.0000e-06 m/s
 <1215> tip Move delay ::1.0000e-03 s
 <1216> tip Drag delay ::0.0000e+00 s
 Output 1
 <1217> Bias modulate ::OFF
 <1218> Move level ::0.0000e+00 V
 <1219> Drag level ::5.0000e-01 V
 Output 2
 <1220> Setpoint modulate ::OFF
 <1221> Move level ::0.0000e+00 A
 <1222> Drag level ::1.0000e-08 A
 <1235> Mark path ::OFF

[Tip Move:Define]

Define Tip Manipulation
Output 1

<1223> output channel ::(0) NO CONNECTION
 <1224> Use STM bias mode ::OFF
 <1225> label ::Bias modulate
 <1226> units ::V
 <1227> units/output volt ::1.0000e+00 V

<1228> offset ::0.0000e+00 V
 Output 2
<1229> output channel ::(0) NO CONNECTION
<1230> label ::Setpoint modulate
<1231> units ::A
<1232> units/output volt ::1.0000e-08 A
<1233> offset ::0.0000e+00 A

[TipTrack]

SPM Tip Feature Tracking

<1811> Tracking ready to go ::OFF
<1252> tracking channel ::(0) Topography
<1253> object height ::1.0000e-09 m
<1254> object width ::1.0000e-09 m
<1255> tracking time constant ::2.0000e-02 s
<1256> orbit rate ::5.0000e+02 Hz
<1257> phase lag ::0.0000e+00
<1258> repositioning orbits ::0

[Lith]

Lithography Control

<1195> output channel ::(1) DAC 1
<1196> Image spectroscopy pulse ::(0) pulse 1
 Pulse Type 1
<1197> Lithography 'on' voltage ::5.0000e+00 V
<1198> Lithography 'off' voltage ::0.0000e+00 V
<1199> Use bias voltage ::OFF
<1200> Voltage on ::1.0000e-03 s
<1201> Delay ::5.0000e-04 s
<1202> Repeat count ::1
<1203> Control Loop ::(1) Feedback off
<1204> Handshaking ::OFF
 Pulse Type 2
<1205> Lithography 'on' voltage ::5.0000e+00 V
<1206> Lithography 'off' voltage ::0.0000e+00 V
<1207> Use bias voltage ::OFF
<1208> Voltage on ::1.0000e-03 s
<1209> Delay ::5.0000e-04 s
<1210> Repeat count ::1
<1211> Control Loop ::(1) Feedback off
<1212> Handshaking ::OFF

[ANALYSIS

PROCESSING]*****

&

[Analysis]

Analysis Modes

<1402> Correlation feature size ::1
<1403> Dual scan cross sections ::OFF
<1404> Related page cross sections ::ON
<1405> Default cross section points ::(1) 5
<1406> Slope Image points ::(4) 11 point
<1407> Histogram Bar Graph ::OFF
<1408> 2D histogram grid ::(1) 64 x 64
<1409> A + cB scale ::1.0000e+00
<1410> XY average mode ::(1) local maxima
<1411> Local min/max range ::1

[FFT]

Fourier Processing

<1714> FFT Window Mapping ::(1) limited
<1715> Power display min feature size ::1.0000e-10 m

[Proc]

Process Control

<1412> Page process mode ::(0) cursor pick
<1413> Background Subtract messages ::OFF
<1414> Background Zero mode ::(0) center
<1415> Resample cropped images ::ON
<1416> Step flatten threshold ::9.0000e-01
<1417> Step flatten smooth ::(0) 3 point
<1418> Rescale all related pages ::OFF
<1419> fast scan smoothing ::(4) 11 point
<1420> high pass smooth ::5.0000e+00
<1421> line smoothing ::(4) 11 point
<1422> line derivative ::(4) 11 point

[User]

User Filter

<1423> User routine ::myprog.exe
<1424> User arguments ::1 50 test
<1425> User file ::temp.sm2
<1426> Analysis only ::OFF

[Slice]

Spectrum Slice

Slice Controls

[PLOT

CONTROL]*****
**

[Topview]

Topview Preferences

<1006> Plots per row ::6
<1007> Display rotated ::OFF
<1008> Cursor display ::(0) none
<1845> Scan smoothing ::ON
<1846> smooth mode ::(4) 11 point
<1010> Data mode ::(0) raw
<1011> Color map mode ::(1) limited
<1012> Display in color ::(1) Full color
<1013> Z exclude ::1.0000e+00
<1014> Low Z limit ::-1.0000e-06 X
<1015> High Z limit ::1.0000e-06 X
<1016> Z offset ::0.0000e+00 X
<1017> Z offset mode ::(0) absolute
<1018> Light source tilt ::3.0000e+01
<1019> Light source rotate ::1.5000e+01
<1020> High pass range ::1.5000e+01

[3-D]

3-D Preferences

<1037> plot size ::(3) 256 x 256
<1038> tilt ::3.0000e+01
<1039> rotate ::2.0000e+01
<1040> z scale ::1.0000e+00
<1041> mode ::(3) fill
<1042> line skip ::1

[X-Y]

X-Y Graph Preferences

<1024> Plots per row ::2
<1025> X axis logarithmic ::OFF
<1026> Y axis logarithmic ::OFF
<1027> plot first n lines, n= ::8
<1028> line 1 color ::(15) White
<1029> line 2 color ::(1) Blue
<1030> line 3 color ::(2) Green
<1031> line 4 color ::(3) Cyan
<1032> line 5 color ::(4) Red
<1033> line 6 color ::(0) Black
<1034> line 7 color ::(0) Black

<1035> line 8 color ::(0) Black

[Chart]

 Chart Preferences

<1021> Default chart size ::(2) 128 x 128
<1022> Chart z scale ::1.0000e+00
<1023> Chart line skip ::1

[ELECTROCHEMISTRY]*****

[Main]

 Main Control

<1128> EC Control Active ::OFF
<1129> Picostat Control Mode ::(1) Galvanostat
 Channels to record:::
<1131> Iec ::OFF
<1132> Vec ::OFF
<1133> AUXec ::OFF
<1134> STM Tip I ::OFF
 Plot & Storage mode
<1135> EC Plot mode ::(1) Plot vs. EC setpoint
<1136> Autosave ::OFF
<1137> Page save mode ::(0) Save to screen

[Expt]

 Sample/Experiment Conditions

<1138> Ref Electrode type ::Pt
<1139> Ref Electrode potential (vs NHE) ::0.0000e+00 V
<1140> Sample (WE) area ::0.0000e+00 cm²
 Experiment Limits::
<1142> Upper Potential Limit ::1.0000e+01 V
<1143> Lower Potential Limit ::-1.0000e+01 V
<1144> Upper Current Limit ::0.0000e+00 V
<1145> Lower Current Limit ::0.0000e+00 V
<1146> Voltage Control Increment ::1.0000e-03 V
<1147> Non-voltage Control Percentage ::5.0000e+00

[Config]

 Configure Interface

<1148> Potentiostat ::(0) AIM-MI PicoStat
<1149> Control DAC ::(0) NO CONNECTION
<1150> WE Current (Iec) Data Input ::(0) Not Used
<1151> WE Potential (Vec) Data Input ::(0) Not Used
<1152> WE Potential control gain ::1.0000e+00 V/V

<1153> Potential Control offset ::0.0000e+00 V
 Generic Settings
<1154> Sample (WE) Iec gain ::1.0000e-06 A/V
<1155> Sample (WE) Vec gain ::1.0000e+00 V/V
<1156> WE Current control gain ::1.0000e-06 A/V

[Adv Config]

 Advanced Configuration

<1157> Data update rate ::5
<1158> Aux EC Data Input ::(0) Not Used
<1159> Aux EC data label ::AUXec
<1160> Aux EC data units ::V
<1161> units/monitor volt ::1.0000e+00 V
<1162> offset ::0.0000e+00 V

[INDIRECT

 PARAMETERS]*****

[Hardware & Config:SPM-100]

 SPM-100 settings

<1843> x scan size ratio ::3.4059e-02
<1844> y scan size ratio ::3.4455e-02

[Interactive Window:ImageWin]

 Image Acquisition display windows

<1849> window 0 source ::0
<1850> window 1 source ::0
<1851> window 2 source ::0
<1852> window 3 source ::0
<1853> window 0 scale mode ::(1) line ëZ subtract
<1854> window 1 scale mode ::(1) line ëZ subtract
<1855> window 2 scale mode ::(1) line ëZ subtract
<1856> window 3 scale mode ::(1) line ëZ subtract
<1857> window 0 smooth mode ::(4) 11 point
<1858> window 1 smooth mode ::(4) 11 point
<1859> window 2 smooth mode ::(4) 11 point
<1860> window 3 smooth mode ::(4) 11 point
<1861> window 0 smooth ::ON
<1862> window 1 smooth ::ON
<1863> window 2 smooth ::ON
<1864> window 3 smooth ::ON
<1865> window 0 color ::0
<1866> window 1 color ::1
<1867> window 2 color ::1

```
<1868>      window 3 color ::1
<1869>      window 0 reopen ::1
<1870>      window 1 reopen ::0
<1871>      window 2 reopen ::0
<1872>      window 3 reopen ::0
```

Acquisition Parameters

```
14,51;newscope: -6, 6, 1, 3
14,52;scope1: 0, -29, 0, 1, 0
14,53;scope2: 1, 0, 0, 4, 0
14,54;scope3: 2, 0, 0, 2, 0
14,55;scope4: 1, 0, 0, 15, 0
14,61;newline: -8, 0, 1, 8
14,62;line1: 0, -5, 0, 1, 0
14,63;line2: 1, -5, 0, 4, 0
14,64;line3: 2, -5, 0, 2, 0
14,65;line4: 1, -5, 0, 15, 0
14,66;scope color2: 9, 12, 10, 7, 9, 12, 10, 7
14,67;imageline: -26, 0, 1, 8
14,68;image1: 0, -30, 0, 1, 0
14,69;image2: 1, 0, 0, 4, 0
14,70;image3: 2, 0, 0, 2, 0
14,71;image4: 1, 0, 0, 15, 0
14,74;realtime: 0, 0, 0, 0, 1, 0, 1, 1, 1, 1, 1, 1
14,75;realtime2: 1, 0, 0, 0
14,82;log channels: 0, 0, 0, 0, 0, 0, 0, 0, 0, 0, 0, 0, 0, 0
14,83;log param: 0, 9.9973e+01, 5.4900e-02, 1.9793e+01, 0, 1, 0, 0, 1
14,85;log colors: 14, 15, 1, 4, 2, 5, 0, 0, 0, 8
14,86;log modes: 1, 1, 1, 1, 1, 1, 0, 0, 1, 2.0000e+00
14,87;log output: 0, 5.0508e+00, 4.0000e+00, 4.9951e-01, -9.7656e-04, 1, -5.0000e-01,
               1.0000e+00, 0
14,88;Volts
14,89;V
```

Plot and Display Options

```
17,08;Color values: 29, 0, 18, 19
17,08;Color values: 40, 63, 63, 0
17,08;Color values: 41, 50, 50, 50
17,08;Color values: 42, 0, 0, 63
17,08;Color values: 43, 0, 0, 0
17,08;Color values: 31, 0, 32, 32
17,08;Color values: 32, 0, 0, 0
17,08;Color values: 19, 50, 35, 20
17,08;Color values: 18, 0, 0, 0
17,08;Color values: 20, 60, 60, 60
```

17,08;Color values: 21, 0, 50, 50
17,08;Color values: 24, 0, 0, 45
17,08;Color values: 35, 47, 47, 47
17,08;Color values: 36, 0, 0, 0
17,08;Color values: 33, 40, 40, 40
17,08;Color values: 34, 0, 63, 47
17,08;Color values: 38, 0, 0, 0
17,08;Color values: 39, 0, 63, 63
17,12;Window values: 1, 0, 18, 626, 456, 398
17,12;Window values: 2, 0, 861, 569, 208, 298
17,12;Window values: 3, 0, 240, 391, 240, 522
17,12;Window values: 4, 0, 959, 353, 272, 222
17,12;Window values: 5, 1, 486, 232, 280, 490
17,12;Window values: 6, 1, 998, 708, 248, 266
17,12;Window values: 7, 0, 696, 405, 256, 222
17,12;Window values: 8, 0, 941, 706, 232, 318
17,12;Window values: 9, 0, 294, 90, 280, 330
17,12;Window values: 10, 0, 542, 786, 248, 158
17,12;Window values: 11, 0, 280, 132, 744, 339
17,12;Window values: 12, 1, 95, 725, 584, 299
17,12;Window values: 20, 0, 387, 360, 365, 664
17,12;Window values: 23, 0, 654, 696, 264, 160
17,12;Window values: 25, 1, 458, 34, 272, 144
17,12;Window values: 29, 0, 100, 100, 300, 326
17,12;Window values: 34, 1, 3, 497, 141, 50
17,12;Window values: 52, 1, 0, 36, 405, 682
17,12;Window values: 56, 0, 281, 67, 280, 372
17,12;Window values: 59, 0, 372, 472, 536, 80
17,12;Window values: 60, 0, 499, 752, 472, 128
17,12;Window values: 66, 1, 748, 34, 514, 545
17,12;Window values: 67, 0, 0, 32, 152, 183
17,14;Graph colors: 15 1 2 3 4 0 0 0
17,15;version: 2.0034e+03
17,24;Transform: 0.0000e+00, 1.0000e+00, 0.0000e+00, 1.0000e+00, 1.0000e+00,
1.0000e+00
17,27;Groups: 1, 0, 0, 0, 0, 0, 0, 0, 0
17,28;Groups2: 0, 0, 1, 0, 0, 0, 0, 0, 0
17,30;Groups3: 0, 0, 3, 0
17,31;Groups4: 0, 0, 2, 0, 0, 0, 0, 0, 0, 0

Process Options

18,01;Fourier mode: 0, 1, 1
18,02;Fourier levels: 1.0000e-10, 1.0000e-08, 5.0000e-01, 2.0000e+00
18,03;Fourier notch: 0, 0, 1, 1
18,04;Fourier notch freq: 1.0000e+09, 1.0000e+09, 1.0000e-10, 0

18,05;Autocorrelate: 5.0000e+01, 0, 1, 0, 1, 1, 1, 1.0000e+00, 1, 1

18,10;Fourier MFM: 0, 0.0000e+00, 0, 3, 3, 4

Electrochem stuff

24,03;ECHEM control 0, 0, 0, 0, 0, 0, 0, 0, 0, 0

24,04;ECHEM volts 1.0000e+00, -5.0000e-01, 1.0000e+01, -1.0000e+01, 4.9411e-02,
0.0000e+00

24,05;ECHEM mode 0, 0.0000e+00, 0, 0.0000e+00, 1, 1, 0, 5, 1.0000e-03, 5.0000e+00

24,06;Pt

24,07;ECHEM gains 1.0000e+00, 1.0000e-06, 1.0000e+00, 1.0000e-06, 1.0000e+00,
0.0000e+00

24,08;AUXec

24,09;V

24,10;ECHEM mode2 0, 0, 1, 0.0000e+00, 1.0000e+00, 0.0000e+00, 0, 1

24,11;ec colors: 14, 15, 1, 4, 2, 5, 0, 0, 0, 3

24,12;ec modes: 1, 1, 1, 1, 1, 0, 0, 1, 2, 0

24,13;ECHEM offsets 0.0000e+00, 0.0000e+00, 0.0000e+00, 0.0000e+00, 0.0000e+00

24,14;ECHEM gal 0.0000e+00, 0.0000e+00, 0.0000e+00, 0.0000e+00, 0.0000e+00,
0.0000e+00, 0.0000e+00